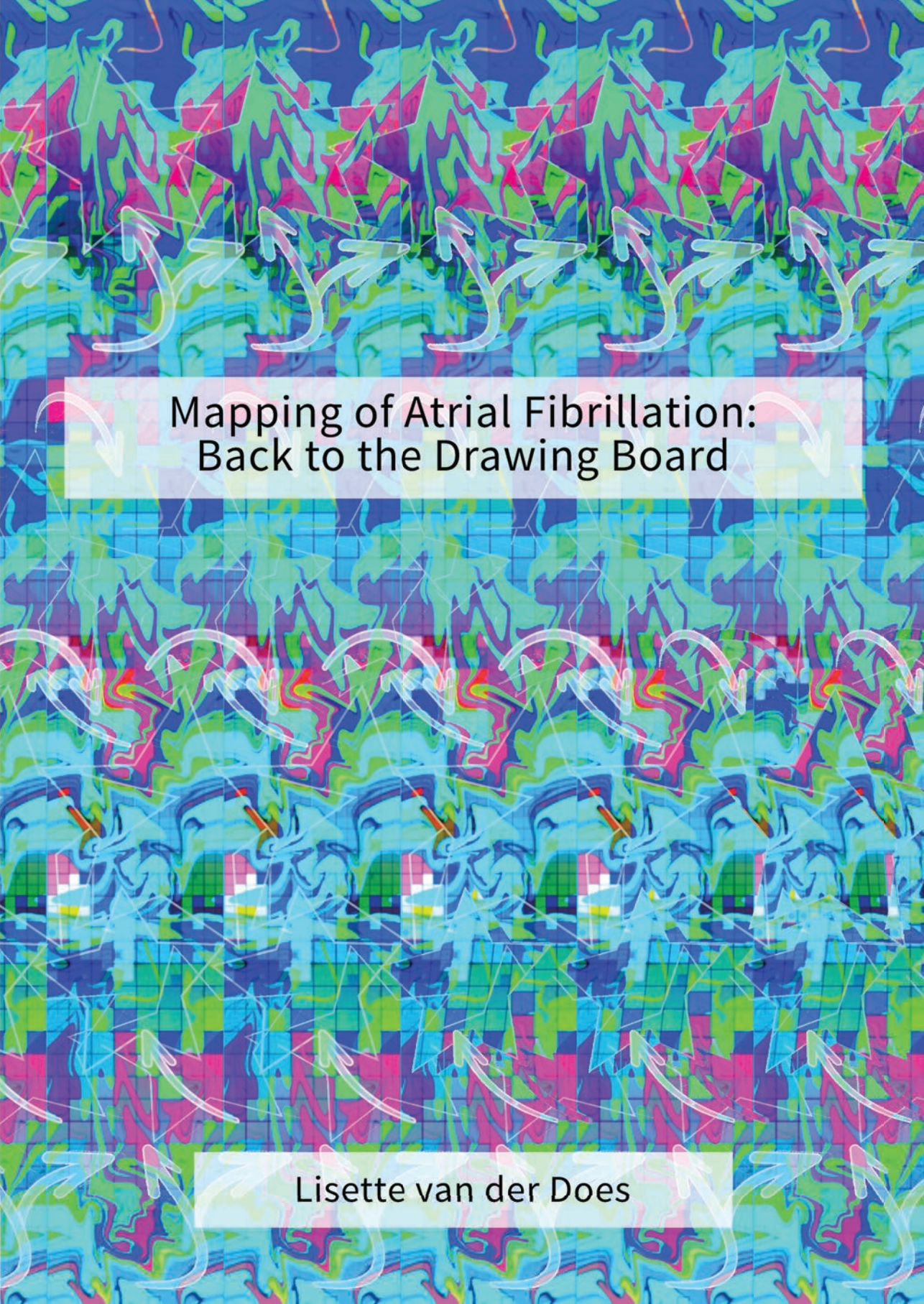

Mapping of Atrial Fibrillation: Back to the Drawing Board

Lisette van der Does

Mapping of Atrial Fibrillation:
Back to the Drawing Board

Lisette van der Does

Colofon

Author: Lisette van der Does
Cover design: Gary W. Priester
Layout and printing: Optima Grafische Communicatie
ISBN: 978 94 6361 494 8

Mapping of Atrial Fibrillation: Back to the Drawing Board
Mappen van atriumfibrilleren: terug naar de tekentafel

Proefschrift

ter verkrijging van de graad van doctor aan de
Erasmus Universiteit Rotterdam
op gezag van de
rector magnificus

Prof. dr. F.A. van der Duijn Schouten

en volgens besluit van het College voor Promoties.
De openbare verdediging zal plaatsvinden op

dinsdag 2 februari 2021 om 13:30 uur

Jacoba Maaike Elisabeth van der Does
geboren te Son en Breugel

Erasmus University Rotterdam

PROMOTIECOMMISSIE

Promotoren:	Prof. dr. N.M.S. de Groot
	Prof. dr. F. Zijlstra
Overige leden:	Prof. dr. A.J.J.C. Bogers
	Prof. dr. B.J.J.M. Brundel
	Prof. dr. ir. A.F.W. van der Steen

Financial support by the Dutch Heart Foundation for the publication of this thesis is gratefully acknowledged.

CONTENTS

* equal authorship

1

General Introduction

Lisette van der Does

GENERAL INTRODUCTION

The most common heart arrhythmia atrial fibrillation (AF) is concurrently one of the least understood and most difficult arrhythmia to cure. AF affects about 33.5 million people worldwide and is not confined to any age limit.[1] However, incidence of AF does increase rapidly with age. For persons of 40 years and older, risk of developing AF during their life is 25%.[2] Pharmacological treatment often has intolerable side effects or recurrences of AF occur despite drug therapy. Invasive treatment is more successful than conservative therapies, nonetheless, even invasive therapy still frequently fails. This chapter introduces AF including current knowledge of its etiology, prognosis and treatment options and discusses the challenges restricting optimal treatment.

Atrial fibrillation: a chaotic heart rhythm with short- and long-term consequences

During a normal heart rhythm, electrical activation of the heart starts in the sinus node located in the right atrium. From the sinus node, electricity propagates in a relatively fixed expansive pattern through the myocardium of both atria. The rate of sinus rhythm ranges between 60 per minute in rest to 200 per minute during exercise. During AF, electricity propagates through the atria in a very chaotic manner with an atrial activation frequency between 300-400 times per minute. Atrial rate is filtered between the atria and the ventricles at the AV-node, but ventricular rate can still reach up to 200 per minute during AF. The high atrial frequency and chaotic electrical conduction results in a higher resting heart rate and an irregular heart rhythm. Symptoms patients can experience during AF include fast and/or irregular palpitations, dizziness, fatigue, shortness of breath (on exertion), sweating and/or chest pain. These symptoms may hinder normal daily activities or sleep significantly. Some patients do not have any symptoms of AF and AF is diagnosed coincidentally, so-called silent AF. Hemodynamic compromise during AF rarely occurs, in most such cases another severe underlying heart disease is present, and therefore short-term prognosis is very good. However, long-term negative consequences of AF include heart failure due to rapid heart rates and the risk of cerebral vascular accidents due to blood stasis mainly in the left atrial appendage forming blood clots that can travel to the brain.[3, 4] Patients with additional risk factors for stroke such as age ≥65 years, previous stroke, heart failure, peripheral vascular disease, diabetes or hypertension are therefore required to use oral anticoagulants.[5, 6] For symptomatic patients, initially a rhythm control strategy is usually chosen aimed at maintaining sinus rhythm. On the one hand, by antiarrhythmic drug therapy combined with medicine controlling heart rate during an AF episode and on the other hand by electrical cardioversions restoring sinus rhythm in case medication fails. Unfortunately, medications have hindering side effects in 10-30% of the patients such as nausea, stomach ache, dizziness or fategue.[7] In addition, AF episodes recur in 65%

of patients while on medication and in 68% within 1 year after cardioversion.[7, 8] Since 20 years, there are also invasive treatments available that aim to terminate and prevent AF by freezing or burning parts of atrial tissue which then become electrically inactive (ablation). After one year, 36% of patients have a recurrence which is a significant improvement over other therapies, but failure rate increases to 47% after 3-years.[9] Multiple ablation procedures for AF improve outcomes and finally result in 20% failure[9], this means ablation therapy still fails in many patients.

Expression, progression and risk factors of atrial fibrillation

The success of therapies and symptomatic burden of AF depends on the clinical expression profile of AF. AF has a wide spectrum of clinical expressions from an occasional short self-limiting episode with years in between to permanent AF. AF expression has been defined in 3 clinical profiles according to the duration of AF[10]:

1. Paroxysmal AF: AF that terminates spontaneously or with intervention within 7 days of onset
2. Persistent AF: continuous AF that sustains beyond 7 days
3. Long-standing persistent AF: continuous AF longer than 12 months duration

Especially the difference between paroxysmal and persistent AF is of clinical significance as success rates of therapies decrease in patients with persistent atrial fibrillation. Ablation therapy for example is 13% less successful in patients with persistent AF than in patients with paroxysmal AF.[5] Patient with paroxysmal AF can also progress to persistent AF. Of patients that initially present with paroxysmal AF 8-15% progresses to persistent AF in the first year and 25% after 5 years.[11] Symptoms of AF can be so indistinct or absent in total that diagnosis may be delayed and patients present with persistent AF at time of diagnosis.

Multiple risk factors for AF have been identified.[12, 13] Some risk factors for AF are modifiable; those include smoking, alcohol consumption, hypertension, diabetes and a sedentary lifestyle. Although too much endurance exercise (>1500-2000 hours of high intensity/ lifetime) also has an increased risk of development of AF in men.[14-16] In short, a healthy lifestyle without excessive endurance training decreases the risk of AF. Other non-modifiable risk factors include advancing age and genetically determined risk factors. Men are 1.5 times more likely to develop AF than women. Caucasian people also have an increased risk over people of African, Asian or Hispanic descent.[13, 17] Furthermore, other structural heart diseases increase the risk of AF. Many structural heart diseases, whether congenital or valvular heart disease or cardiomyopathies, directly or indirectly cause structural changes to atrial tissue which in turn increase susceptibility for AF.[12, 18, 19]

Electrical and structural remodeling in atrial fibrillation

The progressive course of AF is not only caused by increasing tissue remodeling of ongoing underlying heart diseases or other comorbidities, but presence of AF itself triggers structural and functional changes of atrial tissue.[20, 21] When a cardiac cell is electrically activated called depolarization, different ion channels at the borders of the cell open consecutively which cause a flux of electrically charged ions in and out of the cell and the release of calcium that leads to muscle contraction. The ion flux on the outside and inside of the cell (through intercellular connections named gap junctions) depolarizes neighboring cells as well. High depolarization rates of cardiac cells during AF result in intracellular calcium overload and induce stress at the level of the endoplasmic reticulum (important for protein synthesis and distribution within the cell).[21, 22] Multiple structural changes within the cell occur in response such as down regulation of ion channels and gap junctions, dysfunctional protein synthesis and distribution, and cell enlargement ultimately lead to changes and dysfunction of electrical conduction (electrical remodeling). These functional changes in the electrical conduction and excitation include shortening of the action potential duration, delayed depolarizations, intercellular disconnection and symphatic discharges influencing ion channels.[21] The longer AF is present the more structural and functional changes are observed.[23, 24] The electrical changes have been shown to recover in time but the more time AF was present the longer it takes for cells to recover.[24-27] Structural remodeling due to AF may even be (partly) irreversible.[26] Electrical conduction patterns that follow remodeling and sustain AF are still mainly unknown and may in fact differ between patients and may even change in time within a patient due to ongoing remodeling.

Mechanisms of atrial fibrillation

In 1998 it was discovered that paroxysmal AF is mostly triggered by spontaneous electrical activity originating from the pulmonary veins.[28] Therefore, isolating the pulmonary veins from the remaining atrial tissue successfully cures AF in a high number of patients with paroxysmal AF and is now the corner stone of AF ablation therapy. However, in persistent AF other underlying mechanisms seem to take over.[29, 30] In the past, different hypotheses about the electrophysiological mechanisms underlying persistent AF have been proposed. These theories can be divided into two main categories: 1) self-sustaining multiple wavelets and 2) (focal) drivers with fibrillatory conduction.[31-33] The multiple-wavelets theory consists of a constant presence of multiple wavelets finding different pathways with non-refractory (excitable) tissue and endlessly continue circulating through the atria. The other theory is that a specific area in the atria excites at such a high rate causing fibrillatory conduction in the remainder of the atria. Fibrillatory conduction is discontinuous conduction of waves due to an activation rate near the refractory period (time in which a cell is recovered and can be reactivated) resulting in wave breaks when encountering tissue that is still unexcitable. The heterogeneity of fibrillatory conduction and thus the state

of recovery in atrial tissue is based on concepts of anisotropy (conduction speed differs between longitudinal and transversal excitation direction of cardiac cells) and structural discontinuities slowing conduction. Drivers have been proposed to present various phenomena: (multiple) site(s) of micro- or macro-re-entry, ectopic activity or rotors e.g. spiral waves (Figure 1). Over the past years different studies have shown support for either main category and thus these mechanisms remain a controversial topic.[29, 33-38]

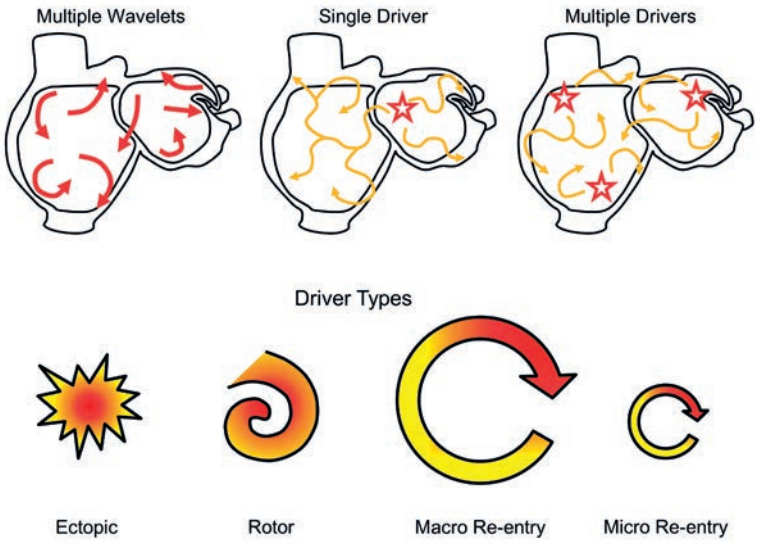

Figure 1. Proposed mechanisms for persistence of atrial fibrillation.
Multiple wavelets theory: multiple (small) waves of electrical activity are simultaneously circling the atria and continue to encounter recovered excitable atrial tissue. Single and multiple driver theories: one site or multiple sites in the atria excite at a high rate, waves continuing to the remainder of the atria from such site(s) conduct in chaotic patterns due to the high frequency and different conduction properties throughout the atria (fibrillatory conduction). Removing the driver(s) would stop atrial fibrillation. Drivers have been proposed as different mechanisms: 1) spontaneous depolarizing atrial cells from an ectopic site, 2) highly curved wave with very slow conduction at its core which thereby maintains itself as a continuing spiral of electrical activity to the remainder of the atria (rotor), 3) a large pathway of electrical activity covering a large part of the atria that keeps circling due to recovery of cells at its tail (re-entry), 4) a small pathway of (micro)re-entry in a small part of the atria.

In 2010 it was demonstrated that breakthrough waves occur frequently during persistent AF.[29] Breakthrough waves are waves of electrical activity that appear suddenly at a focal point and conduct radially from there, like a stone in water creating waves. A new proposal was made that dissociation of electrical conduction within the atrial wall was the cause for these breakthroughs and for persistence of AF. A wave of electrical activation traveling on only one side of the atrial wall due to electrical dissociation of the layers can create a new (breakthrough) wave at the other side when there is a pathway for electrical con-

duction between the layers (Figure 2). The random pattern in which these breakthrough waves appeared during persistent AF did not resemble a driver. Therefore it was proposed that multiple wavelets, combined with epi-endocardial dissociation increasing the total surface for waves to conduct, explain persistence of AF.[29] To record and visualize these atrial activation patterns a technique called electroanatomical mapping is used. Mapping of atrial activation is a tool that can help distinguish between these various mechanisms sustaining AF.

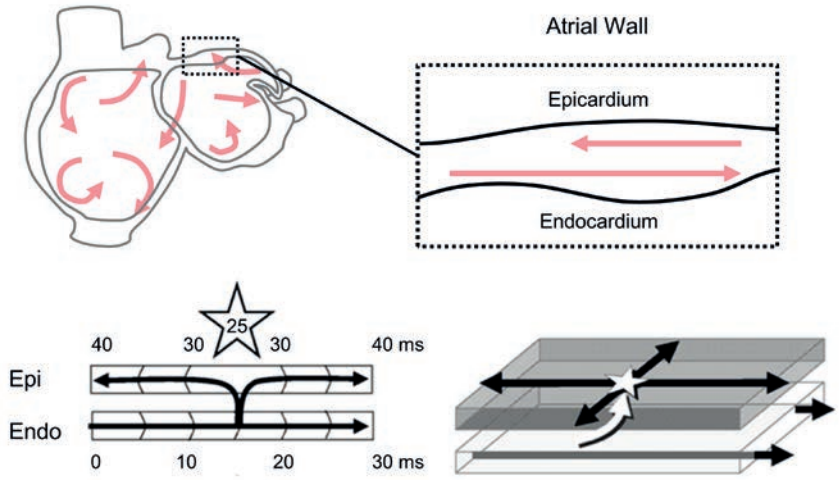

Figure 2. Theory of endo-epicardial dissociation maintaining multiple wavelets.
It was proposed that electrical dissociation between the epicardial and endocardial layers of the atrial wall are the cause for epicardial breakthrough waves. A wave traveling only on the endocardial side that is able to break through where the endocardial and epicardial layers are connected results in a new wave of electrical activity in the epicardial layer (white star).

Mapping of atrial fibrillation

Electroanatomical mapping constructs a graphic (anatomical) representation of electrical activity measured by electrograms recorded -mostly- from the surface of the heart (Figure 3). The two ways to record these electrograms are from the endocardial (in-) or epicardial (out-) side of the heart. The endocardial surface of the atria can be accessed via catheters introduced in the femoral vein and advanced upwards in the inferior caval vein to reach the right atrium, the left atrium is reached by transseptal puncture.

Standard electrophysiological catheters contain between 4-20 consecutive electrodes that record electrograms (Figure 4, left). Maps are created by software able to detect the location of the catheter in space and linking the successively recorded electrograms from different locations in the atria. Newer catheter techniques include an inflatable balloon

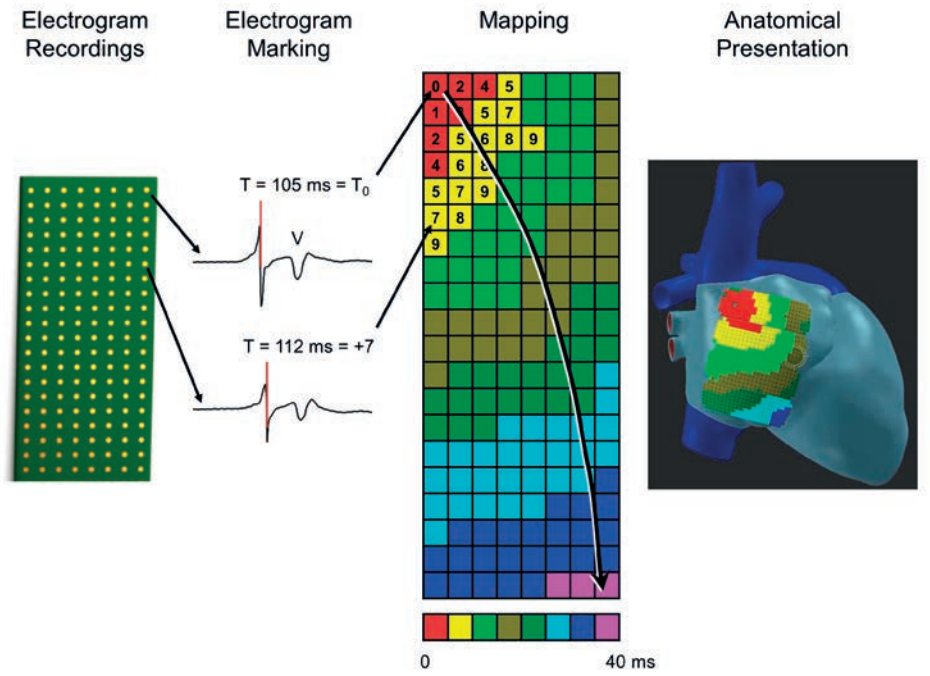

Figure 3. Demonstration of electroanatomical mapping.
An electrode array is placed directly on the surface of the atrium and records an electrogram of local electrical activity at each electrode site. Electrograms are marked at the local atrial activation time e.g. the steepest negative slope for unipolar electrograms (V = ventricular activation). The first local activation time is set as T_0 and all others are relatively measured to this time. Each activation time is placed in a map according to the site of the electrogram in the array (mapping). The activation pattern(s) can then be presented on an anatomical model of the atrium and this provides an overview of the atrial electrical activation pattern (from red to blue).

with 64 electrodes arranged in several spines (Figure 4, middle). The advantage of endocardial mapping is the minimal invasiveness of the procedure and the ability to include the interatrial septum. Epicardial mapping, on the contrary, requires thoracotomy (e.g. cardiac surgery) and is usually only performed if thoracotomy is indicated for repair of structural cardiac diseases. However, during cardiac surgery there is enough space for multi-electrode arrays that record electrograms from 192-256 sites simultaneously (Figure 4, right). In mapping of AF this could be of utmost importance as spatial patterns of activation are very irregular during AF and differ between consecutive recordings. Until now, epicardial atrial mapping was limited to a few areas of interest and high-resolution mapping of the entire epicardial surface had not been performed.

The electrodes on catheters or arrays record extracellular potential changes of 10,000 cardiac cells together residing underneath and surrounding the electrode. A continuous

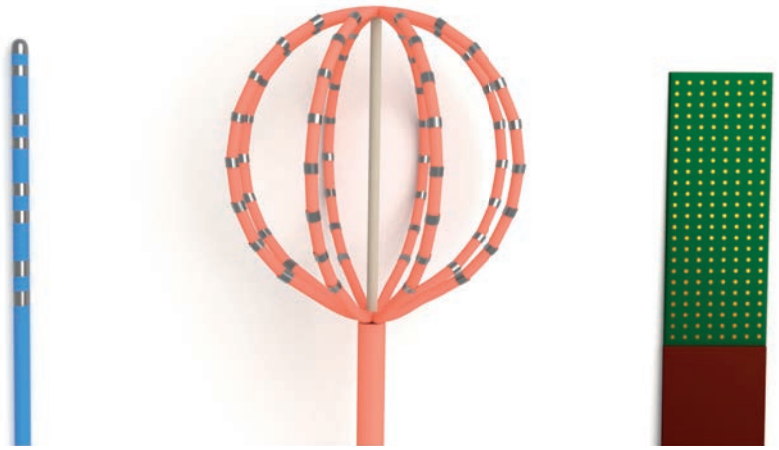

Figure 4. Examples of current mapping tools.
Left: standard electrophysiological catheter used for endocardial mapping containing 8 electrodes or 4 sets of bipolar electrodes. Middle: basket catheter containing 64 electrodes distributed over 8 spines, which are deployed within the atrium and adjusted to the atrial size for optimal endocardial contact. Right: electrode array of 192 electrodes closely spaced together used for epicardial mapping.

wave of depolarization passing by an electrode results in a positive peak followed by a negative peak on a unipolar recorded electrogram. A depolarization wave changing direction or discontinuous activation of the tissue in the electrode recording area can cause appearance of potentials with multiple positive and negative peaks (fractionation).[39, 40] In clinical practice and mapping studies the most used recording mode has long been the bipolar recording mode. Only recently new mapping systems have also reverted back to unipolar electrograms. A bipolar electrogram is the difference between two unipolar electrograms and eliminates most farfield electrical activity (unintended recorded electrical activity from sources at a distance). As farfield signals are very similar shaped and timed between two electrodes, they are nearly completely subtracted and the local signal remains (Figure 5). In atrial unipolar electrograms the farfield ventricular electrical activity is often prominently present and can interfere with marking atrial signals. Particularly during atrial arrhythmias, ventricular electrical activity can occur simultaneously with atrial electrical activity and atrial and ventricular signals are less well coordinated complicating atrial marking of unipolar electrograms. However, unlike the morphology of bipolar electrograms, morphology of unipolar electrograms is not influenced by the direction of the wave front and distance between electrodes.[41, 42] A bipolar electrogram requires a time shift of the potential between the poles. If a wave fronts travels perpendicular to the two poles passing by each electrode at the same time, subtracting the similar unipolar potentials will lead to a zero bipolar potential or a bipolar potential of very low amplitude.

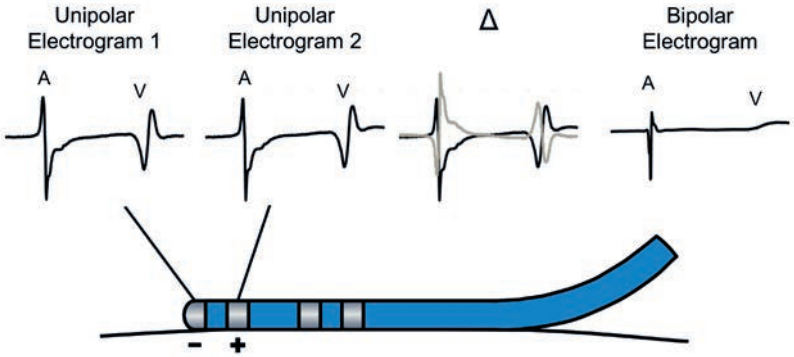

Figure 5. Unipolar and bipolar electrograms.
A catheter placed on the atrial wall records unipolar electrograms at each electrode, the electrogram at the negative pole (-) is subtracted from the electrogram at the positive pole (+) resulting in a bipolar electrogram. Unipolar electrograms have prominent ventricular farfield electrical activity (V) which (nearly) disappears in bipolar electrograms leaving only the atrial signal (A).

Ablation procedures for atrial fibrillation

The past years, several ablation procedures have been introduced in order to treat persistent AF based on the proposed mechanisms. First invasive procedure developed for AF was a surgical procedure that split the atria into an electrical maze by creating multiple lines of scar aiming to prevent circling of multiple wavelets or macro-re-entry circuits.[43] Since then the Cox Maze procedure has been further developed over the years. The original final procedure was the Cox Maze III with a cut-and-sew technique with success in 97% after 5 years.[44] However, the Cox Maze III procedure is very invasive and time-consuming due to its complexity. The introduction of ablation tools for creating scars instead of cutting and sewing made the procedure more efficient and lead to the Cox Maze IV procedure.[45] The Cox Maze IV remained very successful (90% after 2 years) with fewer complications than the Cox Maze III and is currently the standard surgical procedure for AF.[46] Less invasive procedures trying to simulate the Maze procedure were developed in the electrophysiology laboratory where catheters were used to create ablation lines on the inside of the atria. Unfortunately, the success of the surgical procedure was not achieved.[47] In 2004, ablation of complex fractionated atrial electrograms was performed in an attempt to target specific areas with conduction disorders or drivers sustaining AF, however no benefit was seen in later studies.[47,48] Eight years later, ablation of rotors and focal sources was introduced and became a popular new procedure for AF.[33] The promising initial successful results have not been repeated in following studies.[49,50] All AF catheter ablation procedures in addition to isolation of the pulmonary veins are therefore not established as beneficial procedures in current consensus and surgical ablation has more established success in treatment of persistent AF.[10] Because catheter ablation is less invasive, one or more additional catheter ablation procedures combined with inspection for re-connected pulmonary veins are

often still attempted before surgical ablation. The greatest difference between AF and other atrial arrhythmias that usually have very high success rates of ablative treatment, is that the electrophysiological pathophysiological mechanism is known for these arrhythmia contrary to AF. Diagnosing the electrophysiological mechanism in action during AF requires advancement of current mapping tools and procedures.

THESIS OUTLINE

The first chapters of this thesis will demonstrate new ways to map conduction disorders with high detail in patients with AF and to discriminate conduction disorders between patients with different heart diseases underlying AF. **Chapters 2 and 3** explain the current troubles with ablation of AF due to limited knowledge of its electrophysiological pathophysiology and propose a new study design to find the arrhythmogenic substrate underling AF in different patients. **Chapters 4 and 5** introduce a new high-resolution epicardial mapping approach for mapping of AF during standard and minimally invasive cardiac surgery. **Chapters 6 and 7** focus on occurrence of high-resolution conduction disorders during sinus rhythm in the entire atria and specifically Bachmann's bundle in patients with valvular heart disease and the differences between those with and without AF. **Chapter 8** presents the differences in occurrence of high-resolution conduction disorders during sinus rhythm at the pulmonary vein area, where ectopic discharges from the pulmonary veins first enter the atria, between patients with and without AF.

The second part of this thesis focusses on asynchronous activation of the epicardial and endocardial layers, its contribution to the pathophysiology of AF and the value of fractionation on unipolar electrograms to identify asynchrony between the atrial layers. **Chapter 9** presents proof for the previously described theory of endo-epicardial dissociation in conduction during AF by simultaneous mapping of the endo- and epicardium in 14 patients. **Chapter 10** demonstrates the endo-epicardial distribution of breakthrough waves during 10 seconds in a case of longstanding AF. **Chapter 11** reviews the pathophysiology and heterogeneity in definitions of electrogram fractionation. The differences in morphology between epicardial and endocardial unipolar electrograms and reflection of endo-epicardial asynchrony on unipolar electrograms are described in **Chapter 12**. In **Chapter 13**, the occurrence, consequences and challenges in current clinical practice of endo-epicardial asynchrony are briefly explained. **Chapter 14** clarifies if unipolar or bipolar electrograms are better suited to detect endo-epicardial asynchrony in clinical practice. The presence of endo-epicardial asynchrony during atrial extrasystoles is demonstrated in **Chapter 15**. The implications of the findings in this thesis and future perspectives are discussed in **Chapter 16**.

REFERENCES

1. Chugh SS, Havmoeller R, Narayanan K, Singh D, Rienstra M, Benjamin EJ, Gillum RF, Kim YH, McAnulty JH Jr, Zheng ZJ, Forouzanfar MH, Naghavi M, Mensah GA, Ezzati M, Murray CJ. Worldwide epidemiology of atrial fibrillation: a Global Burden of Disease 2010 Study. Circulation. 2014;129:837-847.
2. Lloyd-Jones DM, Wang TJ, Leip EP, Larson MG, Levy D, Vasan RS, D'Agostino RB, Massaro JM, Beiser A, Wolf PA, Benjamin EJ. Lifetime risk for development of atrial fibrillation: the Framingham Heart Study. Circulation. 2004;110:1042-1046.
3. Stewart S, Hart CL, Hole DJ, McMurray JJ. A population-based study of the long-term risks associated with atrial fibrillation: 20-year follow-up of the Renfrew/Paisley study. Am J Med. 2002;113:359-364.
4. Wolf PA, Abbott RD, Kannel WB. Atrial fibrillation as an independent risk factor for stroke: the Framingham Study. Stroke. 1991;22:983-988.
5. Friberg L, Rosenqvist M, Lip GY. Evaluation of risk stratification schemes for ischaemic stroke and bleeding in 182 678 patients with atrial fibrillation: the Swedish Atrial Fibrillation cohort study. Eur Heart J. 2012;33:1500-1510.
6. Lip GY, Nieuwlaat R, Pisters R, Lane DA, Crijns HJ. Refining clinical risk stratification for predicting stroke and thromboembolism in atrial fibrillation using a novel risk factor-based approach: the euro heart survey on atrial fibrillation. Chest. 2010;137:263-272.
7. Investigators AFADS. Maintenance of sinus rhythm in patients with atrial fibrillation: an AFFIRM substudy of the first antiarrhythmic drug. J Am Coll Cardiol. 2003;42:20-29.
8. De Vos CB, Limantoro I, Pisters R, Delhaas T, Schotten U, Cheriex EC, Tieleman RG, Crijns HJ. The mechanical fibrillation pattern of the atrial myocardium is associated with acute and long-term success of electrical cardioversion in patients with persistent atrial fibrillation. Heart Rhythm. 2014;11:1514-1521.
9. Ganesan AN, Shipp NJ, Brooks AG, Kuklik P, Lau DH, Lim HS, Sullivan T, Roberts-Thomson KC, Sanders P. Long-term outcomes of catheter ablation of atrial fibrillation: a systematic review and meta-analysis. J Am Heart Assoc. 2013;2:e004549.
10. Calkins H, Hindricks G, Cappato R, et al. 2017 HRS/EHRA/ECAS/APHRS/SOLAECE expert consensus statement on catheter and surgical ablation of atrial fibrillation: Executive summary. Europace. 2018;20:157-208.
11. Kerr CR, Humphries KH, Talajic M, Klein GJ, Connolly SJ, Green M, Boone J, Sheldon R, Dorian P, Newman D. Progression to chronic atrial fibrillation after the initial diagnosis of paroxysmal atrial fibrillation: results from the Canadian Registry of Atrial Fibrillation. Am Heart J. 2005;149:489-496.
12. Andrade J, Khairy P, Dobrev D, Nattel S. The clinical profile and pathophysiology of atrial fibrillation: relationships among clinical features, epidemiology, and mechanisms. Circ Res. 2014;114:1453-1468.
13. Staerk L, Sherer JA, Ko D, Benjamin EJ, Helm RH. Atrial Fibrillation: Epidemiology, Pathophysiology, and Clinical Outcomes. Circ Res. 2017;120:1501-1517.
14. Calvo N, Ramos P, Montserrat S, Guasch E, Coll-Vinent B, Domenech M, Bisbal F, Hevia S, Vidorreta S, Borras R, Falces C, Embid C, Montserrat JM, Berruezo A, Coca A, Sitges M, Brugada J, Mont L. Emerging risk factors and the dose-response relationship between physical activity and lone atrial fibrillation: a prospective case-control study. Europace. 2016;18:57-63.
15. Elosua R, Arquer A, Mont L, Sambola A, Molina L, Garcia-Moran E, Brugada J, Marrugat J. Sport practice and the risk of lone atrial fibrillation: a case-control study. Int J Cardiol. 2006;108:332-337.

16. Thelle DS, Selmer R, Gjesdal K, Sakshaug S, Jugessur A, Graff-Iversen S, Tverdal A, Nystad W. Resting heart rate and physical activity as risk factors for lone atrial fibrillation: a prospective study of 309,540 men and women. Heart. 2013;99:1755-1760.
17. Rodriguez CJ, Soliman EZ, Alonso A, Swett K, Okin PM, Goff DC, Jr., Heckbert SR. Atrial fibrillation incidence and risk factors in relation to race-ethnicity and the population attributable fraction of atrial fibrillation risk factors: the Multi-Ethnic Study of Atherosclerosis. Ann Epidemiol. 2015;25:71-76,76.e1.
18. Darby AE, Dimarco JP. Management of atrial fibrillation in patients with structural heart disease. Circulation. 2012;125:945-957.
19. Manuguerra R, Callegari S, Corradi D. Inherited Structural Heart Diseases With Potential Atrial Fibrillation Occurrence. J Cardiovasc Electrophysiol. 2016;27:242-252.
20. Allessie M, Ausma J, Schotten U. Electrical, contractile and structural remodeling during atrial fibrillation. Cardiovasc Res. 2002;54:230-246.
21. Nattel S, Harada M. Atrial remodeling and atrial fibrillation: recent advances and translational perspectives. J Am Coll Cardiol. 2014;63:2335-2345.
22. Wiersma M, Meijering RAM, Qi XY, Zhang D, Liu T, Hoogstra-Berends F, Sibon OCM, Henning RH, Nattel S, Brundel B. Endoplasmic Reticulum Stress Is Associated With Autophagy and Cardiomyocyte Remodeling in Experimental and Human Atrial Fibrillation. J Am Heart Assoc. 2017;6:e006458.
23. Ausma J, Litjens N, Lenders MH, Duimel H, Mast F, Wouters L, Ramaekers F, Allessie M, Borgers M. Time course of atrial fibrillation-induced cellular structural remodeling in atria of the goat. J Mol Cell Cardiol. 2001;33:2083-2094.
24. Schotten U, Duytschaever M, Ausma J, Eijsbouts S, Neuberger HR, Allessie M. Electrical and contractile remodeling during the first days of atrial fibrillation go hand in hand. Circulation. 2003;107:1433-1439.
25. Yu WC, Lee SH, Tai CT, Tsai CF, Hsieh MH, Chen CC, Ding YA, Chang MS, Chen SA. Reversal of atrial electrical remodeling following cardioversion of long-standing atrial fibrillation in man. Cardiovasc Res. 1999;42:470-476.
26. Ausma J, van der Velden HM, Lenders MH, van Ankeren EP, Jongsma HJ, Ramaekers FC, Borgers M, Allessie MA. Reverse structural and gap-junctional remodeling after prolonged atrial fibrillation in the goat. Circulation. 2003;107:2051-2058.
27. Sato T, Mitamura H, Kurita Y, Takeshita A, Shinagawa K, Miyoshi S, Kanki H, Hara M, Takatsuki S, Soejima K, Ogawa S. Recovery of electrophysiological parameters after conversion of atrial fibrillation. Int J Cardiol. 2001;79:183-189.
28. Haïssaguerre M, Jaïs P, Shah DC, Takahashi A, Hocini M, Quiniou G, Garrigue S, Le Mouroux A, Le Metayer P, Clementy J. Spontaneous initiation of atrial fibrillation by ectopic beats originating in the pulmonary veins. N Engl J Med. 1998;339:659-666.
29. de Groot NMS, Houben RPM, Smeets JL, Boersma E, Schotten U, Schalij MJ, Crijns H, Allessie MA. Electropathological Substrate of Longstanding Persistent Atrial Fibrillation in Patients With Structural Heart Disease Epicardial Breakthrough. Circulation. 2010;122:1674-1682.
30. Sanders P, Nalliah CJ, Dubois R, Takahashi Y, Hocini M, Rotter M, Rostock T, Sacher F, Hsu LF, Jönsson A, O'Neill MD, Jaïs P, Haïssaguerre M. Frequency mapping of the pulmonary veins in paroxysmal versus permanent atrial fibrillation. J Cardiovasc Electrophysiol. 2006;17:965-972.
31. Moe GK. A conceptual model of atrial fibrillation. J Electrocardiol 1968;1:145-146.
32. Moe GK, Abildskov JA. Atrial fibrillation as a self-sustaining arrhythmia independent of focal discharge. Am Heart J. 1959;58:59-70.

33. Narayan SM, Krummen DE, Rappel WJ. Clinical mapping approach to diagnose electrical rotors and focal impulse sources for human atrial fibrillation. J Cardiovasc Electrophysiol. 2012;23:447-454.
34. Allessie MA, de Groot NM, Houben RP, Schotten U, Boersma E, Smeets JL, Crijns HJ. Electropathological substrate of long-standing persistent atrial fibrillation in patients with structural heart disease: longitudinal dissociation. Circ Arrhythm Electrophysiol. 2010;3:606-615.
35. Hansen BJ, Zhao J, Csepe TA, Moore BT, Li N, Jayne LA, Kalyanasundaram A, Lim P, Bratasz A, Powell KA, Simonetti OP, Higgins RS, Kilic A, Mohler PJ, Janssen PM, Weiss R, Hummel JD, Fedorov VV. Atrial fibrillation driven by micro-anatomic intramural re-entry revealed by simultaneous sub-epicardial and sub-endocardial optical mapping in explanted human hearts. Eur Heart J. 2015;36:2390-2401.
36. Lee S, Sahadevan J, Khrestian CM, Cakulev I, Markowitz A, Waldo AL. Simultaneous Biatrial High-Density (510-512 Electrodes) Epicardial Mapping of Persistent and Long-Standing Persistent Atrial Fibrillation in Patients: New Insights Into the Mechanism of Its Maintenance. Circulation. 2015;132:2108-2117.
37. Child N, Clayton RH, Roney CH, Laughner JI, Shuros A, Neuzil P, Petru J, Jackson T, Porter B, Bostock J, Niederer SA, Razavi RS, Rinaldi CA, Taggart P, Wright MJ, Gill J. Unraveling the Underlying Arrhythmia Mechanism in Persistent Atrial Fibrillation: Results From the STARLIGHT Study. Circ Arrhythm Electrophysiol. 2018;11:e005897.
38. Lee S, Sahadevan J, Khrestian CM, Markowitz A, Waldo AL. Characterization of Foci and Breakthrough Sites During Persistent and Long-Standing Persistent Atrial Fibrillation in Patients: Studies Using High-Density (510-512 Electrodes) Biatrial Epicardial Mapping. J Am Heart Assoc. 2017;6:e005274.
39. Gardner PI, Ursell PC, Fenoglio JJ, Jr., Wit AL. Electrophysiologic and anatomic basis for fractionated electrograms recorded from healed myocardial infarcts. Circulation. 1985;72:596-611.
40. Spach MS, Dolber PC. Relating extracellular potentials and their derivatives to anisotropic propagation at a microscopic level in human cardiac muscle. Evidence for electrical uncoupling of side-to-side fiber connections with increasing age. Circ Res. 1986;58:356-371.
41. Correa de Sa DD, Thompson N, Stinnett-Donnelly J, Znojkiewicz P, Habel N, Muller JG, Bates JH, Buzas JS, Spector PS. Electrogram fractionation: the relationship between spatiotemporal variation of tissue excitation and electrode spatial resolution. Circ Arrhythm Electrophysiol. 2011;4:909-916.
42. Stevenson WG, Soejima K. Recording techniques for clinical electrophysiology. J Cardiovasc Electrophysiol. 2005;16:1017-1022.
43. Cox JL, Schuessler RB, D'Agostino HJ, Jr., Stone CM, Chang BC, Cain ME, Corr PB, Boineau JP. The surgical treatment of atrial fibrillation. III. Development of a definitive surgical procedure. J Thorac Cardiovasc Surg. 1991;101:569-583.
44. Prasad SM, Maniar HS, Camillo CJ, Schuessler RB, Boineau JP, Sundt TM, 3rd, Cox JL, Damiano RJ, Jr. The Cox maze III procedure for atrial fibrillation: long-term efficacy in patients undergoing lone versus concomitant procedures. J Thorac Cardiovasc Surg. 2003;126:1822-1828.
45. Voeller RK, Bailey MS, Zierer A, Lall SC, Sakamoto S, Aubuchon K, Lawton JS, Moazami N, Huddleston CB, Munfakh NA, Moon MR, Schuessler RB, Damiano RJ Jr. Isolating the entire posterior left atrium improves surgical outcomes after the Cox maze procedure. J Thorac Cardiovasc Surg Apr 2008;135:870-877.
46. Weimar T, Schena S, Bailey MS, Maniar HS, Schuessler RB, Cox JL, Damiano RJ, Jr. The cox-maze procedure for lone atrial fibrillation: a single-center experience over 2 decades. Circ Arrhythm Electrophysiol. 2012;5:8-14.
47. Verma A, Jiang CY, Betts TR, Chen J, Deisenhofer I, Mantovan R, Macle L, Morillo CA, Haverkamp W, Weerasooriya R, Albenque JP, Nardi S, Menardi E, Novak P, Sanders P; STAR AF II Investigators. Approaches to catheter ablation for persistent atrial fibrillation. N Engl J Med. 2015;372:1812-1822.

48. Nademanee K, McKenzie J, Kosar E, Schwab M, Sunsaneewitayakul B, Vasavakul T, Khunnawat C, Ngarmukos T. A new approach for catheter ablation of atrial fibrillation: mapping of the electrophysiologic substrate. J Am Coll Cardiol. 2004;43:2044-2053.
49. Buch E, Share M, Tung R, Benharash P, Sharma P, Koneru J, Mandapati R, Ellenbogen KA, Shivkumar K. Long-term clinical outcomes of focal impulse and rotor modulation for treatment of atrial fibrillation: A multicenter experience. Heart Rhythm. 2016;13:636-641.
50. Gianni C, Mohanty S, Di Biase L, Metz T, Trivedi C, Gökoğlan Y, Güneş MF, Bai R, Al-Ahmad A, Burkhardt JD, Gallinghouse GJ, Horton RP, Hranitzky PM, Sanchez JE, Halbfaß P, Müller P, Schade A, Deneke T, Tomassoni GF, Natale A. Acute and early outcomes of focal impulse and rotor modulation (FIRM)-guided rotors-only ablation in patients with nonparoxysmal atrial fibrillation. Heart Rhythm. 2016;13:830-835.

2

What's to come after isolation of the pulmonary veins?

Lisette van der Does
Natasja de Groot

Treatment of atrial fibrillation (AF), the most prevalent tachyarrhythmia worldwide, remains a great challenge. About 15 years ago, when Haïssaguerre et al.[1] first described episodes of AF triggered by focal activity originating from the pulmonary veins, the way was paved for ablative therapy of AF by pulmonary vein isolation (PVI). Despite a successful PVI, electric pulmonary vein reconnections still occur frequently requiring additional procedures. To this end new mapping, navigation, imaging and ablation techniques continue to be developed thereby facilitating and increasing success rates of PVI.

The results of the endoscopic laser balloon ablation system (EAS) for PVI have been presented by Gal et al.[2] in 50 patients with mostly paroxysmal AF (82%). The EAS provides an elegant manner for optimal circumferential contact and ablation lesions with one device applicable in pulmonary veins of various sizes. Furthermore, an endoscope within the device provides real-time visualisation of the ablation area. This resulted in isolation of 99.5% of the pulmonary veins during the ablation procedure. However, the long-term results were similar to other techniques and were somewhat lower compared with other studies using the EAS. The authors believe this may be due to inexperience with this novel technology, although other influential factors could be that this study, in contrast to others, also included some patients with persistent AF and had a longer follow-up period. Unfortunately, the study did not report how many pulmonary veins were in fact electrically reconnected with re-ablation procedures. This could provide more information on the long-term success of isolation with the EAS. In addition, it would give insight into the incidence of AF recurrence despite successful isolation of the pulmonary veins. For example, one study[3] using this technique reported AF recurrence in 28% of patients with persistent pulmonary vein isolation after a median of 12-month follow-up. Moreover, three months after PVI, 14% of ablated pulmonary veins were reconnected in 38% of the patients, which entails that a large proportion of patients had at least one pulmonary vein electrically reconnected. We commend the authors for their contribution to optimising PVI outcomes and encourage them in their ongoing efforts to improve the PVI procedure with this refined technique. However, AF recurrences may also have aetiologies outside of our current understanding and perhaps these unknown pathological or physiological processes prevent further improvements in successful long-term outcomes. For this, it is of utmost importance to learn more about the pathophysiology of AF.

The revolutionary findings of Haïssaguerre et al. made it possible for a majority of patients with AF to be successfully treated with PVI. Unfortunately, another large proportion of patients continue to have AF, and PVI seems to be insufficient. For this reason different ablation strategies were implemented, such as boxlines, roof, floor and isthmus lines, complex fractionated atrial electrogram ablation and ablation of ganglionated plexi. Nonetheless, AF still recurs and the pathophysiological background to support these additional strategies is controversial.

To take new steps toward successful treatments for AF, we must further understand the underlying mechanism of AF, just as Haïssaguerre et al. did almost two decades ago. In previous mapping studies, we demonstrated that longitudinal dissociation in conduction and focal fibrillation waves are the key elements in persistence of AF.[4,5] Figure 1 shows an example of an epicardial high-resolution wavemap (244 electrode, interelectrode distance 2.5 mm) of the right atrial free wall obtained from a patient with longstanding persistent AF demonstrating a complex pattern of activation. The wavemap shows individual fibrillation waves represented by colors according to their sequence of appearance. A previously described mapping algorithm was used to classify them into peripheral waves (entering the mapping area from outside the electrode array), breakthrough waves (appearing at the epicardial surface inside the mapping area) or discontinuous conduction waves (fibrillation waves starting with a delay of 13 to 40 ms from boundaries of other waves). During this AF episode of *only* 140 ms, the mapping area (diameter: 4 cm) is activated by as many as 15 fibrillation waves including 5 peripheral, 4 epicardial breakthrough and 6 discontinuous waves. Hence, when patterns of activation during AF become too complex, the end stage of AF might have been reached and it is likely that PVI in these patients will be unsuccessful. We believe that by understanding the pathophysiology of AF we can come to new successful treatment strategies, which can be used when PVI just is not enough. Presumably, this will entail a tailor-made treatment determined by different mechanisms underlying AF.

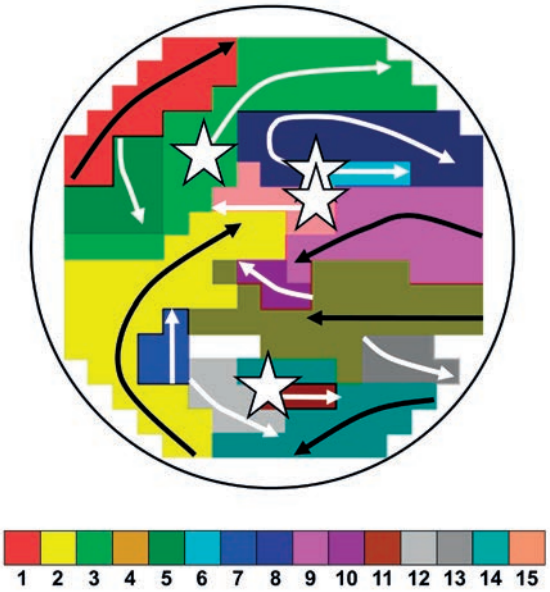

Figure 1. Wavemap constructed during longstanding persistent atrial fibrillation.
Sites of epicardial breakthroughs are indicated by white stars; white arrows indicate direction(s) of expansion of epicardial breakthrough or discontinuous fibrillation waves; black arrows indicate waves coming from outside the mapping area.

REFERENCES

1. Haïssaguerre M, Jaïs P, Shah DC, Takahashi A, Hocini M, Quiniou G, Garrigue S, Le Mouroux A, Le Metayer P, Clementy J. Spontaneous initiation of atrial fibrillation by ectopic beats originating in the pulmonary veins. N Engl J Med. 1998;339:659-66.
2. Gal P, Smit JJ, Adiyaman A, Ramdat Misier AR, Delnoy PP, Elvan A. First Dutch experience with the endoscopic laser balloon ablation system for the treatment of atrial fibrillation. Neth Heart J. 2015;23:96-9.
3. Dukkipati SR, Neuzil P, Kautzner J, Petru J, Wichterle D, Skoda J, Cihak R, Peichl P, Dello Russo A, Pelargonio G, Tondo C, Natale A, Reddy VY. The durability of pulmonary vein isolation using the visually guided laser balloon catheter: multicenter results of pulmonary vein remapping studies. Heart Rhythm. 2012;9:919-25.
4. Allessie MA, de Groot NM, Houben RP, Schotten U, Boersma E, Smeets JL, Crijns HJ. Electropathological substrate of long-standing persistent atrial fibrillation in patients with structural heart disease: longitudinal dissociation. Circ Arrhythm Electrophysiol. 2010;3:606-15.
5. de Groot NMS, Houben RPM, Smeets JL, Boersma E, Schotten U, Schalij MJ, Crijns H, Allessie MA. Electropathological substrate of longstanding persistent atrial fibrillation in patients with structural heart disease: epicardial breakthrough. Circulation. 2010;122:1674-82.

3

QUest for the Arrhythmogenic Substrate of Atrial fibRillation in patients undergoing cardiac surgery (QUASAR study): rationale and design

Lisette van der Does
Ameeta Yaksh
Charles Kik
Paul Knops
Eva Lanters
Christophe Teuwen
Frans Oei
Pieter van de Woestijne
Jos Bekkers
Ad Bogers
Maurits Allessie
Natasja de Groot

ABSTRACT

The heterogeneous presentation and progression of atrial fibrillation (AF) implicate the existence of different pathophysiological processes. Individualized diagnosis and therapy of the arrhythmogenic substrate underlying AF may be required to improve treatment outcomes. Therefore, this single-center study aims to identify the arrhythmogenic areas underlying AF by intraoperative, high-resolution, multi-site epicardial mapping in 600 patients with different heart diseases. Participants are divided into 12 groups according to the underlying heart diseases and presence of prior AF episodes. Mapping is performed with a 192-electrode array for 5-10 seconds during sinus rhythm and (induced) AF of the entire atrial surface. Local activation times are converted into activation and wave maps from which various electrophysiological parameters are derived. Postoperative cardiac rhythm registrations and a five year follow-up will show the incidence of postoperative and persistent AF. This project provides the first step in the development of a tool for individual AF diagnosis and treatment.

INTRODUCTION

Atrial fibrillation (AF) is characterized by beat-to-beat changes in the pattern of activation within the atria, unlike organized arrhythmias such as atrial flutter and atrial tachycardia. This chaotic nature poses a challenge with regard to understanding the pathophysiology and effective treatment of AF as shown by the frequent recurrences after AF therapy.[1-4] Due to the limited knowledge about the mechanisms involved, each AF patient is currently approached in the same manner. Based on the symptomatology and a clinical assessment the arrhythmia is either accepted or attempts are made to retain sinus rhythm with non-selective treatment modalities. However, this approach does not take account of the diversity among AF patients. AF occurs, for example, in association with mitral valve disease, hypertension, congenital heart disease or cardiac surgery, or in young or older patients without any comorbidity ("lone AF").[5,6] Furthermore, AF can have different clinical manifestations including paroxysmal, persistent or longstanding persistent. On the structural level, the degree of fibrotic tissue in AF patients demonstrated heterogeneity as well and does not always predict the severity of the AF burden.[7] Therefore, it is likely that the pathophysiological mechanisms may differ between patients with AF. If these can be unraveled the possibility for targeted treatments may arise.

So far, several ablation procedures have been developed aiming to ablate a trigger site for initiation of AF or an arrhythmogenic substrate perpetuating AF. The isolation of triggers residing in the pulmonary veins demonstrated to be most successful in patients with paroxysmal AF. Nonetheless, recurrences occur frequently especially in patients with persistent AF, suggesting an incomplete eradication, reformation or progression of the arrhythmogenic substrate. Other strategies include the ablation of rotors, ganglionated plexi and complex fractionated electrograms.[8-10] However, these therapies have similar, limited success rates and there are no guidelines as to which strategy to choose for an individual patient.

The present study has been designed to identify the arrhythmogenic substrate in individual AF patients with the use of a high-resolution epicardial mapping approach. In previous studies, high-resolution epicardial mapping of patients with Wolf-Parkinson-White syndrome or longstanding persistent AF demonstrated to be a valuable tool in discriminating between patients.[11,12] However, mapping was performed at only 3 locations and in a limited number of patients with a variety of heart disorders. In this study, subjects are categorized according to the underlying heart disorder(s) and predisposition for developing spontaneous episodes of AF before or after cardiac surgery and epicardial mapping will be performed of the entire epicardial surface.[13,14] The electrophysiological properties of the atria will be analyzed aiming to find the arrhythmogenic substrate and to contribute to the current knowledge of the pathophysiology of AF.

METHODS

Study population

All patients of 18 years and older with structural or coronary heart disease scheduled for elective cardiac surgery will be asked to participate. Patients who have a high risk of complications during surgery or hemodynamic instability by inducing AF such as Wolff-Parkinson-White syndrome, poor left ventricular function (<40%), presence of assist devices, hemodynamic instability, usage of inotropic agents and kidney or liver failure are excluded from this study. Furthermore, patients with medical histories predisposing them for adhesions making epicardial mapping unfeasible or presence of an iatrogenically altered atrial electrophysiology such as prior radiation of the chest for malignancies, redo-cardiac surgery, paced atrial rhythms and prior ablative therapy in the atria are excluded as well. Each patient, prior to enrolling in the study, will be provided with a written explanation of the study procedure together with an assessment of risks in participating in the study. Patients will be enrolled after the written informed consent form is signed. After enrollment patients are assigned to a group according to the underlying heart disease and whether their medical history includes AF. These groups consist of the following surgical procedures: coronary artery bypass grafting (CABG), mitral valve surgery, aortic valve surgery, mitral valve surgery with CABG, aortic valve surgery with CABG, and congenital heart surgery. Each of these groups are divided into separate groups for patients with and without prior AF episodes. Figure 1 demonstrates the inclusion and following procedures for patients participating in the study.

Study procedure

Epicardial mapping is performed during open heart surgery.[13] Patients will be under general anesthesia and vital signs will be monitored continuously throughout the procedure. Mapping will be performed before going on extracorporeal circulation, during sinus rhythm and (induced) AF. AF is induced by fixed rate pacing at the right atrial appendage with a pulse width of 2 ms delivered by temporary pacemaker wires. Pacing bursts will start at a rate of 250 bpm and will be increased with steps of 50 bpm each time AF is not induced after 3 attempts. If AF is not induced at a pacing rate of 400 bpm or loss of capture occurs, attempts will be terminated. As AF is induced it may terminate spontaneously, otherwise, if an induced arrhythmia sustains after the mapping procedure, electrical cardioversion will be performed immediately afterwards. If a patient is in AF at the onset of the mapping procedure, mapping will be performed during AF and during sinus rhythm after electrical cardioversion if there is no atrial thrombus present on transesophageal echocardiogram.

Epicardial mapping of the right and left atria will be performed using a custom-made electrode array (192 electrodes, diameter 0.45 mm, 2 mm interelectrode distance; GS

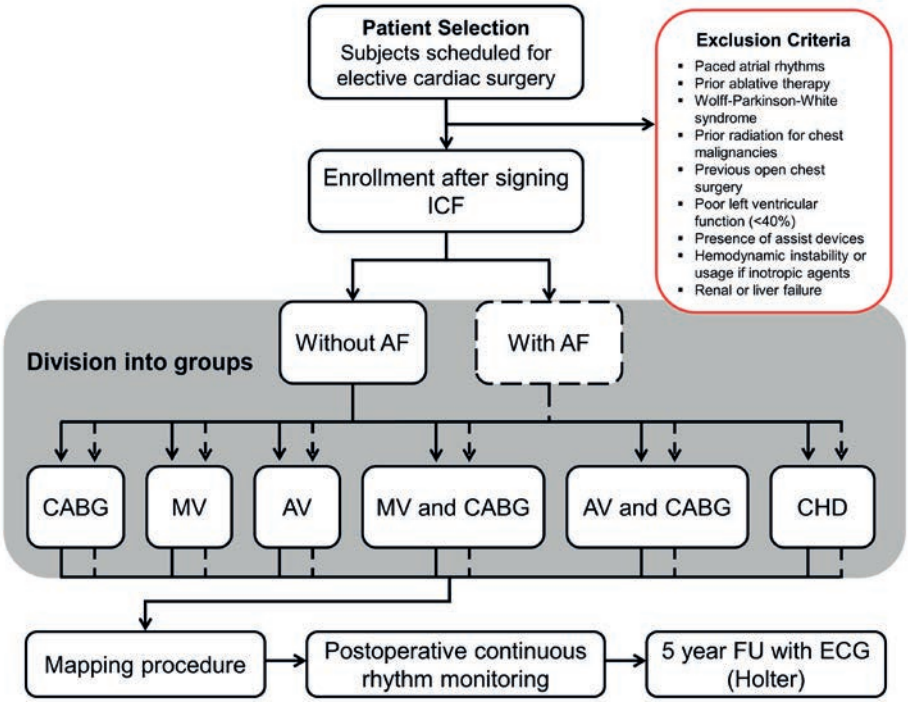

Figure 1. Flow-chart of patient inclusion and following study procedures.
After enrollment patients are assigned to 1 of 12 groups for data analysis according to the presence of previous atrial fibrillation (AF) occurrence and the type of surgery that will be performed (i.e. underlying heart disease). Subsequently, all patients are mapped during surgery and continuously monitored after surgery to detect postoperative AF. During the 5-year of follow-up (FU) the additional tests consist of an electrocardiogram (ECG) and Holter monitoring when patients indicate symptoms suspected of AF. ICF, informed consent form; CABG, coronary artery bypass grafting; MV, mitral valve surgery; AV, aortic valve surgery; CHD, congenital heart disease.

Swiss, Küssnacht, Swiss). All electrograms recorded by the electrode are stored on hard disk after amplification (gain 1000), filtering (bandwidth 0.5-400 Hz), sampling (1 KHz) and analogue to digital conversion (16 bits). An indifferent electrode is attached to a steel wire fixed in subcutaneous tissue and a reference signal is attached to the right atrium. In addition, a ventricular surface electrocardiogram (ECG) is recorded simultaneously. Signals will be recorded at 9 right and left atrial sites during sinus rhythm for 5 seconds per site and during (induced) AF for 10 seconds per site. Mapping is initiated at the lower right atrium and is proceeded upwards over the right atrial appendage. Thereafter, the left atrium will be mapped starting between the pulmonary veins and will continue along the atrioventricular groove from the lower pulmonary veins to the left atrial appendage and finally at the roof of the left atrium for Bachmann's bundle. The entire mapping procedure will not prolong the surgical procedure by more than 10-15 minutes.[13]

Follow-up and study endpoint

The postoperative heart rhythm is continuously monitored until hospital discharge and rhythm registrations will be stored in order to determine the incidence of early postoperative AF. After discharge, all patients will be scheduled to visit an out-patient clinic, 2 times during the first year and thereafter once a year during the following 4 years. Clinical history focused on tachyarrhythmias will be taken and a surface ECG will be made. If indicated, a 24-hour Holter recording will be performed. If patients, for any reason, are unable to visit the out-patient clinic, follow-up is done by telephone. In the event that documented rhythm disorders have occurred, records will be requested from the visited hospital. The main endpoint of the study is reached when persistent AF develops.

Data and statistical analysis

Local activation times of the recorded atrial signals will be marked, from which color-coded activation and wave maps will be reconstructed by custom-made software which has previously been described in more detail.[11] Data exclusion criteria include progressive in- or decrease in AF cycle length (AFCL) between sequential recordings (recorded via the reference signal) indicated by an approximately two times in- or decrease in AFCL, recordings of other rhythms than sinus rhythm or AF, or ≥50% of missing recording data. Data analysis and the criteria for data inclusion are demonstrated in Figure 2.

Electrophysiological parameters that will be derived include conduction velocity, incidence of conduction block, number of fibrillation waves, incidence of epicardial breakthroughs, AFCL, dominant frequency, electrogram voltage (the amplitude of the highest deflection in case of fractionation) and fractionation.[11,12] For analysis, the electrodes of the mapping array are assigned to quadrants of 1 cm^2. The variables will consist of averaged values or the percentage of occurrence/ incidence for each quadrant. Figure 3 illustrates the construction of an activation map during sinus rhythm, quadrant partition and its conversion into various parameters of all atrial sites. Figure 4 shows a wave map during AF and the variables that will be analyzed. Furthermore, rotor occurrence and the relation between patterns of activation, fractionation, fibrillation intervals, conduction abnormalities and voltage will be studied and compared between the different atrial sites, atrial rhythms and patient groups. Rotors will be defined as a wave of excitation rotating around a phase singularity for one or more cycles[15] and analyzed by determining the dominant frequencies at each recording site in order to identify high-to-low frequency gradients and determination of the degree of linking of fibrillation waves, indicative of repetitive patterns of activation. Linear regression analysis and paired Student's t-test will be used to compare various electrophysiological parameters between different sites and different atrial rhythms. Unpaired Student's t-test will be used to compare various electrophysiological parameters between patient groups.

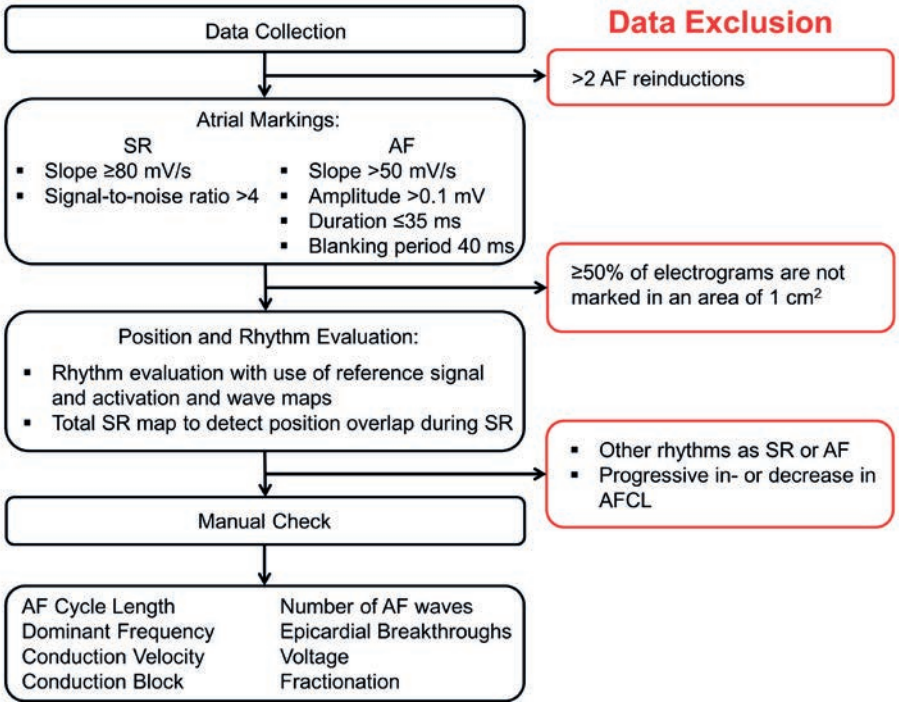

Figure 2. Flow-chart of data evaluation.
Atrial fibrillation (AF) data from patients who were reinduced >2 times is excluded. Custom-made software detects atrial markings with the presented properties for sinus rhythm (SR) and AF. If ≥50% of a 1 cm^2 quadrant is not marked, this quadrant will be excluded from further analysis. Rhythm evaluation is performed with use of the activation and wave maps and the position in SR is evaluated for overlap with a total SR map constructed with use of the reference signal. All data is manually checked, from which the parameters are derived afterwards.

The present study is the first that will explore the value of various parameters in discriminating the arrhythmogenic substrate of different patients with AF. We aim for a sample of (at least) 50 subjects in each group for the following reasons. First, our initiative should be considered as an exploratory study. We want to obtain early results in a relative limited number of patients, which will provide a basis for future (in depth) investigations. Therefore, we accept that our study will be underpowered to draw definite conclusions with good precision. Additionally, it is relevant to obtain estimates with sufficient precision, also in early, hypothesis generating studies such as ours. In the binomial distribution, a probability of an observation of 50% is achieved with the greatest measurement error. Taking that probability as the 'worst case', in a dataset of 50 patients, the 95% confidence intervals (CIs) around an observation would be ±14%. In the 6*50 = 300 AF patients together, the 95% CIs would be ±6%. We consider these precisions acceptable for this exploratory study that will, hopefully, discover parameters that may be used in future studies to discriminate between AF patients with different underlying heart diseases.

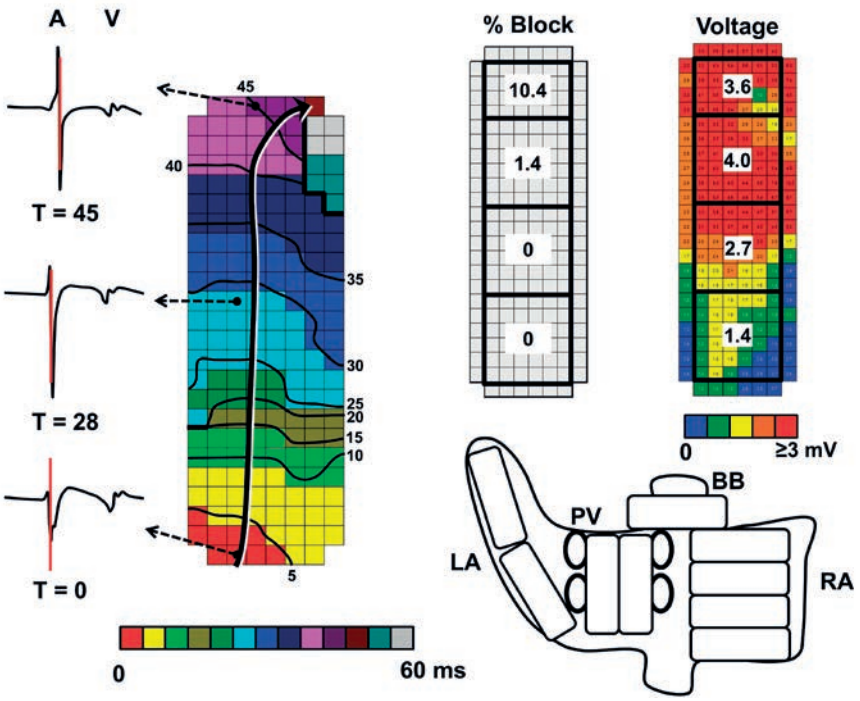

Figure 3. Activation mapping and quadrant data analysis.
Left: Activation map constructed during sinus rhythm. The atrial complexes (A) of all 192 recordings are automatically detected and marked at the steepest deflection. The electrode with the earliest atrial marking is set at time (T) 0. Activation times of the other electrodes are in reference to T_0. Isochrones are set at 5 ms intervals after T_0. The black/white arrow illustrates the direction of conduction. Conduction block (<17 cm/s) is represented by thick black lines. V, ventricular complex. Right: The mapping surface is divided into quadrants and parameters such as block % and mean voltage are determined for each quadrant of each mapping location (total: 36 quadrants). LA, left atrium; PV, pulmonary veins; BB, Bachmann's bundle; RA, right atrium.

Ethics

The study protocol was approved in February 2010 by the Medical Ethics Committee (2010-054) in the Erasmus Medical Center, Rotterdam, The Netherlands.

DISCUSSION

Study population and mapping sites

Previous epicardial mapping studies for AF were performed in small numbers of patients and at only a few atrial sites or with a low resolution.[11,12,16-19] The present study is the first to perform intraoperative high-resolution *epicardial mapping* in a large number of patients and enables analyses between patients with different heart diseases. In addition, all

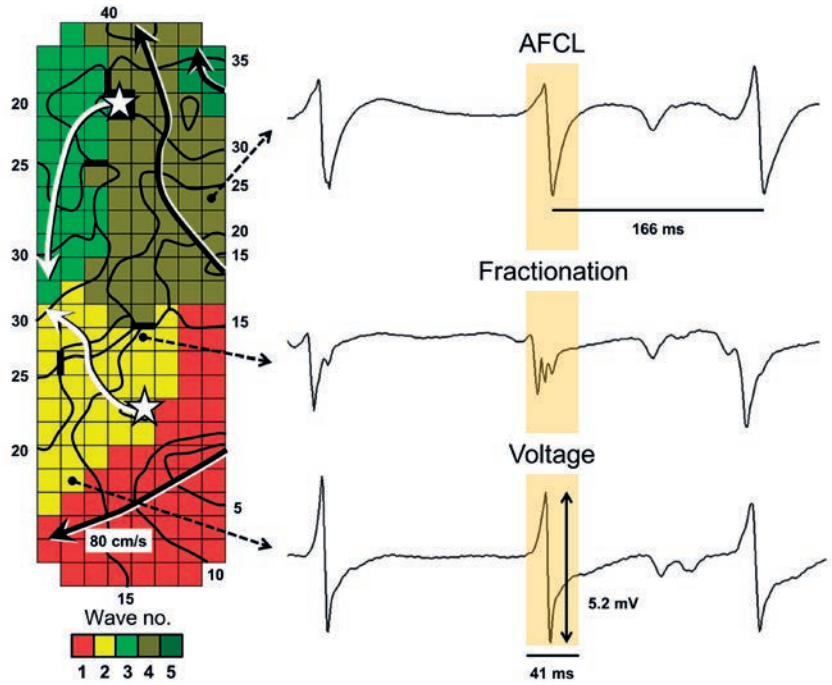

Figure 4. Wave mapping and electrophysiological parameters
Left: Wave map during atrial fibrillation at the right atrial free wall. A total of 5 waves activate the recording area in 41 ms; 3 peripheral waves (black arrows) and 2 initiate at epicardial breakthroughs (white star and white arrows). Black lines between electrodes indicate conduction block (<17 cm/s). Isochrones of waves are set at steps of 5 ms after T_0. Parameters derived from the wavemap include number of epicardial breakthroughs, waves and conduction velocity. Right: Examples of corresponding electrograms are shown. The parameters that will be derived from electrograms include atrial fibrillation cycle length (AFCL), fractionation and voltage.

sites of both the right and the left atrium accessible from the epicardial side are mapped including Bachmann's bundle. Bachmann's bundle might have an important role in the pathophysiology of AF.[20] By mapping the entire surface of both atria there is an increased chance of finding the arrhythmogenic substrate, which might be located in different atrial regions among AF patients.

The arrhythmogenic substrate in atrial fibrillation

The heterogeneous nature in which AF presents and the frequently failing AF treatments so far, demonstrate the importance for an individualized strategy in the treatment of AF. The first step is a better understanding of the pathophysiology underlying initiation and perpetuation of AF. The focus for initiation of AF often originates in the pulmonary veins and Moe et al. described the concept of self-sustaining fibrillatory waves responsible for

perpetuation of AF.[21,22] However, recurrences of persistent AF after successful isolation of the pulmonary veins cannot be explained by these concepts alone. The occurrence of longitudinal dissociation during AF was demonstrated later on and showed to be most prominent in persistent AF.[11] Furthermore, focal fibrillation waves emerging within the recording area, referred to as epicardial breakthroughs, occur much more frequently during persistent AF than during acute AF,[12] as well as drivers such as rotors and focal sources.[23] These findings suggest that progressive electro-pathological changes within the atria are associated with persistent AF. Nonetheless, the exact pathophysiological changes and locations at which they occur are not yet known. The underlying diseases most likely initiate different pathophysiological mechanisms that lead to AF. For example, valvular disorders give rise to atrial pressure or volume overload, coronary artery disease can cause atrial ischemia and infarction, and congenital heart diseases may also include congenital atrial abnormalities. For this reason, the patients in this study are divided in separate groups according to the underlying heart disorders and AF occurrence prior to surgery.

Previous studies have investigated the underlying cause responsible for perpetuation of AF. Atrial fibrosis has been suggested to be an important element in the pathophysiology of AF. There is a significant larger amount of atrial fibrosis seen in patients with AF.[7,24] An excessive extracellular matrix leads to uncoupling of cells and may facilitate inhomogeneous conduction, re-entry and multiple wavelets. MRI or electro-anatomical voltage mapping can be helpful diagnostic tools for the determination of degree of fibrosis in AF patients and identification of areas of fibrosis. However, no association has been found between the amount of fibrosis and clinical AF characteristics.[7,24] Electrical signal conduction involves processes on a structural, cellular and molecular level and these together determine if conduction is altered and AF occurs. Therefore, the arrhythmogenic substrate can probably be more accurately localized by measuring electrical potentials and conduction. In the present study, both the recorded extracellular potentials and the spatial domain of the electrograms enables conversion into specific electrophysiological parameters that could identify areas with conduction abnormalities. If proven successful, this strategy can be developed into a diagnostic tool for each individual AF patient. In addition, current ablation strategies aimed at identifying and targeting arrhythmogenic areas are not effective in a large proportion of patients and might even lead to new arrhythmias.[25] If patients that can benefit could be selected beforehand, effectiveness of these treatments might improve.

Study limitations

Currently, epicardial mapping can only be performed during open-chest cardiac surgery. Therefore, it is not possible to perform epicardial mapping in patients with non-diseased hearts. However, with constantly advancing techniques it may become possible in the future to perform epicardial mappings during video-assisted thoracoscopic surgery in

patients without any heart disease. Secondly, although epicardial mapping can reach sites endocardial mapping cannot, some sites are not accessible, for example, the atrial septum. Therefore, epicardial mapping is not able to analyze conduction in the entire area of the atria. In addition, recordings are performed sequentially, as simultaneous high-resolution mapping of the entire surface is not possible yet with currently available technical equipment. As time during surgery is limited, mapping is performed immediately after AF induction or electrical conversion. Consequently, if a progressive in- or decrease in AFCL occurs during the recordings, this data will have to be excluded.[26-28] General anesthesia may also increase AFCL.[29] However, the same anesthetic protocol is applied in all patients and previous studies have shown that there remain differences in AF between patients despite anesthesia.[11,12] Furthermore, recent studies have shown that endo-epicardial dissociation can occur during AF and might be associated with persistent AF.[30] This suggests that it is important to investigate endocardial and epicardial conduction simultaneously as conduction can be disturbed in all 3 dimensions. Finally, there is a small chance asymptomatic persistent AF episodes may be undetected during follow-up. The measured incidence of persistent late postoperative AF may therefore underestimate the true incidence of persistent late postoperative AF.

Clinical relevance

This project can provide the tools to discriminate the arrhythmogenic substrate of AF in patients with different heart diseases and is potentially the first step towards a patient-tailored strategy for the treatment of AF.

REFERENCES

1. Gaita F, Caponi D, Scaglione M, Montefusco A, Corleto A, Di Monte F, Coin D, Di Donna P, Giustetto C. Long-term clinical results of 2 different ablation strategies in patients with paroxysmal and persistent atrial fibrillation. Circ Arrhythm Electrophysiol. 2008;1:269-275.
2. Ganesan AN, Shipp NJ, Brooks AG, Kuklik P, Lau DH, Lim HS, Sullivan T, Roberts-Thomson KC, Sanders P. Long-term outcomes of catheter ablation of atrial fibrillation: a systematic review and meta-analysis. J Am Heart Assoc. 2013;2:e004549.
3. Mulder AA, Wijffels MC, Wever EF, Boersma LV. Freedom from paroxysmal atrial fibrillation after successful pulmonary vein isolation with pulmonary vein ablation catheter-phased radiofrequency energy: 2-year follow-up and predictors of failure. Europace. 2012;14:818-825.
4. Lafuente-Lafuente C, Valembois L, Bergmann JF, Belmin J. Antiarrhythmics for maintaining sinus rhythm after cardioversion of atrial fibrillation. Cochrane Database Syst Rev. 2015;3:CD005049..
5. Kannel WB, Wolf PA, Benjamin EJ, Levy D. Prevalence, incidence, prognosis, and predisposing conditions for atrial fibrillation: population-based estimates. Am J Cardiol. 1998;82:2N-9N.
6. Psaty BM, Manolio TA, Kuller LH, Kronmal RA, Cushman M, Fried LP, White R, Furberg CD, Rautaharju PM. Incidence of and risk factors for atrial fibrillation in older adults. Circulation. 1997;96:2455-61.
7. Kottkamp H. Human atrial fibrillation substrate: towards a specific fibrotic atrial cardiomyopathy. Eur Heart J. 2013;34:2731-8.
8. Nademanee K, McKenzie J, Kosar E, Schwab M, Sunsaneewitayakul B, Vasavakul T, Khunnawat C, Ngarmukos T. A new approach for catheter ablation of atrial fibrillation: mapping of the electrophysiologic substrate. J Am Coll Cardiol. 2004;43:2044-53.
9. Narayan SM, Krummen DE, Shivkumar K, Clopton P, Rappel WJ, Miller JM. Treatment of atrial fibrillation by the ablation of localized sources: CONFIRM (Conventional Ablation for Atrial Fibrillation With or Without Focal Impulse and Rotor Modulation) trial. J Am Coll Cardiol. 2012;60:628-36.
10. Scherlag BJ, Nakagawa H, Jackman WM, Yamanashi WS, Patterson E, Po S, Lazzara R. Electrical stimulation to identify neural elements on the heart: their role in atrial fibrillation. J Interv Card Electrophysiol. 2005;13 Suppl 1:37-42.
11. Allessie MA, de Groot NM, Houben RP, Schotten U, Boersma E, Smeets JL, Crijns HJ. Electropathological substrate of long-standing persistent atrial fibrillation in patients with structural heart disease: longitudinal dissociation. Circ Arrhythm Electrophysiol. 2010;3:606-15.
12. de Groot NMS, Houben RPM, Smeets JL, Boersma E, Schotten U, Schalij MJ, Crijns H, Allessie MA. Electropathological substrate of longstanding persistent atrial fibrillation in patients with structural heart disease: epicardial breakthrough. Circulation. 2010;122:1674-82.
13. Yaksh A, van der Does LJ, Kik C, Knops P, Oei FB, van de Woestijne PC, Bekkers JA, Bogers AJ, Allessie MA, de Groot NM. A novel intra-operative, high-resolution atrial mapping approach. J Interv Card Electrophysiol. 2015;44:221-5.
14. Yaksh A, Kik C, Knops P, Roos-Hesselink JW, Bogers AJ, Zijlstra F, Allessie M, de Groot NM. Atrial fibrillation: to map or not to map? Neth Heart J. 2014;22:259-66.
15. Chen J, Mandapati R, Berenfeld O, Skanes AC, Gray RA, Jalife J. Dynamics of wavelets and their role in atrial fibrillation in the isolated sheep heart. Cardiovasc Res. 2000;48:220-32.
16. Kanagaratnam P, Kojodjojo P, Peters NS. Electrophysiological abnormalities occur prior to the development of clinical episodes of atrial fibrillation: observations from human epicardial mapping. Pacing Clin Electrophysiol. 2008;31:443-53.
17. Lee G, Kumar S, Teh A, Madry A, Spence S, Larobina M, Goldblatt J, Brown R, Atkinson V, Moten S, Morton JB, Sanders P, Kistler PM, Kalman JM. Epicardial wave mapping in human long-lasting

persistent atrial fibrillation: transient rotational circuits, complex wavefronts, and disorganized activity. Eur Heart J. 2014;35:86-97.
18. Nitta T, Ishii Y, Miyagi Y, Ohmori H, Sakamoto S, Tanaka S. Concurrent multiple left atrial focal activations with fibrillatory conduction and right atrial focal or reentrant activation as the mechanism in atrial fibrillation. J Thorac Cardiovasc Surg. 2004;127:770-8.
19. Sueda T, Nagata H, Shikata H, Orihashi K, Morita S, Sueshiro M, Okada K, Matsuura Y. Simple left atrial procedure for chronic atrial fibrillation associated with mitral valve disease. Ann Thorac Surg. 1996;62:1796-800.
20. van Campenhout MJ, Yaksh A, Kik C, de Jaegere PP, Ho SY, Allessie MA, de Groot NM. Bachmann's bundle: a key player in the development of atrial fibrillation? Circ Arrhythm Electrophysiol. 2013;6:1041-6.
21. Haïssaguerre M, Jaïs P, Shah DC, Takahashi A, Hocini M, Quiniou G, Garrigue S, Le Mouroux A, Le Metayer P, Clementy J. Spontaneous initiation of atrial fibrillation by ectopic beats originating in the pulmonary veins. N Engl J Med. 1998;339:659-66.
22. Moe GK, Abildskov JA. Atrial fibrillation as a self-sustaining arrhythmia independent of focal discharge. Am Heart J. 1959;58:59-70.
23. Baykaner T, Lalani GG, Schricker A, Krummen DE, Narayan SM. Mapping and ablating stable sources for atrial fibrillation: summary of the literature on Focal Impulse and Rotor Modulation (FIRM). J Interv Card Electrophysiol. 2014;40:237-44.
24. Boldt A, Wetzel U, Lauschke J, Weigl J, Gummert J, Hindricks G, Kottkamp H, Dhein S. Fibrosis in left atrial tissue of patients with atrial fibrillation with and without underlying mitral valve disease. Heart. 2004;90:400-5.
25. Wu SH, Jiang WF, Gu J, Zhao L, Wang YL, Liu YG, Zhou L, Gu JN, Xu K, Liu X. Benefits and risks of additional ablation of complex fractionated atrial electrograms for patients with atrial fibrillation: a systematic review and meta-analysis. Int J Cardiol. 2013 25;169:35-43.
26. Ravelli F, Masè M, Del Greco M, Faes L, Disertori M. Deterioration of organization in the first minutes of atrial fibrillation: a beat-to-beat analysis of cycle length and wave similarity. J Cardiovasc Electrophysiol. 2007;18:60-5.
27. Haïssaguerre M, Sanders P, Hocini M, Hsu LF, Shah DC, Scavée C, Takahashi Y, Rotter M, Pasquié JL, Garrigue S, Clémenty J, Jaïs P. Changes in atrial fibrillation cycle length and inducibility during catheter ablation and their relation to outcome. Circulation. 2004;109:3007-13.
28. Roithinger FX, Karch MR, Steiner PR, SippensGroenewegen A, Lesh MD. Relationship between atrial fibrillation and typical atrial flutter in humans: activation sequence changes during spontaneous conversion. Circulation. 1997;96:3484-91.
29. Holm M, Johansson R, Smideberg B, Lührs C, Olsson SB. Effect of cardiac exposure by median sternotomy on atrial fibrillation cycle length. Europace. 1999;1:248-57.
30. Eckstein J, Zeemering S, Linz D, Maesen B, Verheule S, van Hunnik A, Crijns H, Allessie MA, Schotten U. Transmural conduction is the predominant mechanism of breakthrough during atrial fibrillation: evidence from simultaneous endo-epicardial high-density activation mapping. Circ Arrhythm Electrophysiol. 2013;6:334-41.

4

A Novel Intra-Operative, High-Resolution Atrial Mapping Approach

Ameeta Yaksh
Lisette van der Does
Charles Kik
Paul Knops
Frans Oei
Pieter van de Woestijne
Jos Bekkers
Ad Bogers
Maurits Allessie
Natasja de Groot

ABSTRACT

Background: A new technique is demonstrated for extensive high-resolution intra-operative atrial mapping that will facilitate the localization of atrial fibrillation (AF) sources and identification of the substrate perpetuating AF.

Methods: Prior to the start of extra-corporal circulation, a 8x24-electrode array (2 mm interelectrode distance) is placed subsequently on all right and left epicardial atrial sites, including Bachmann's Bundle, for recording of unipolar electrograms during sinus rhythm and (induced) AF. AF is induced by high frequency pacing at the right atrial free wall. A pacemaker wire stitched to the right atrium serves as a reference signal. The indifferent pole is connected to a steel wire fixed to subcutaneous tissue. Electrograms are recorded by a computerized mapping system and after amplification (gain 1000), filtering (bandwidth 0.5-400 Hz), sampling (1 Khz) and analogue to digital conversion (16 bits) automatically stored on hard disk. During the mapping procedure, real-time visualization secures electrogram quality. Analysis will be performed offline.

Conclusions: We introduce the first epicardial atrial mapping approach with a high resolution of ≥1728 recording sites which can be performed in a procedure time of only ±9 minutes. This mapping technique can potentially identify areas responsible for initiation and persistence of AF and hopefully can individualize both diagnosis and therapy of AF.

INTRODUCTION

Atrial fibrillation (AF) can be eliminated by ablation of either the trigger or the substrate perpetuating AF. A multi-site, high-resolution mapping approach of the entire atria which can, beside localizing sources generating AF in patients with trigger-driven AF, identify the substrate responsible for perpetuation of AF would be desirable. Such a mapping approach would allow individualization of the diagnosis of AF and subsequently also of AF therapy which is at present not available. In this report, we introduce a novel high-resolution, multi-site epicardial mapping technique of the entire atria as a routine procedure during open chest surgery aiming for identification of the arrhythmogenic substrate underlying AF.

MATERIAL AND METHODS

Surgical technique

Prior to commencement to extra-corporal circulation, after heparinization and arterial cannulation, a temporary bipolar epicardial pacemaker wire is stitched to the right atrial free wall serving as a temporal reference electrode. The indifferent electrode consists of a steel wire fixed to subcutaneous tissue of the thoracic cavity (Figure 1). Epicardial mapping during sinus rhythm and (induced) AF is performed with a custom-made flexible 192 unipolar electrode mapping array, mounted on a custom-made spatula if preferred by the surgeon. The spatula can be bended to match the atrial curvature (Figure 2). If AF is not the presenting rhythm, AF is induced by fixed rate pacing at the right atrial free wall using a different temporary bipolar pacing wire. Recordings of real-time epicardial electrograms from Bachmann's bundle are used to confirm atrial capture. Fixed rate pacing is started at a rate of 200 beats per minute (bpm). If an AF induction attempt is not successful after 3 burst attempts, the rate is increased by 50 bpm, up to maximal 400 bpm until AF occurs or atrial refractoriness is reached. After completion of the mapping procedure, AF is terminated by electrical cardioversion or sustained until cardioplegia is conducted, depending on the operator's preference. In case of AF as the initial heart rhythm, electrical cardioversion is performed in order to map sinus rhythm after completing mapping of AF.

Mapping is sequentially conducted along several imaginary lines between anatomical borders in order to cover the entire right and left atrium (Figure 3). The mapping array is shifted along these imaginary lines with a fixed orientation at each position visually trying to avoid omission of areas at the expense of possible overlap between successive mapping sites. Mapping of the right atrium starts at the cavotricuspid isthmus continuing up to the right atrial appendage, perpendicular to the caval veins. Bachmann's bundle is mapped from the roof of the left atrium towards the superior cavo-atrial junction. For the left

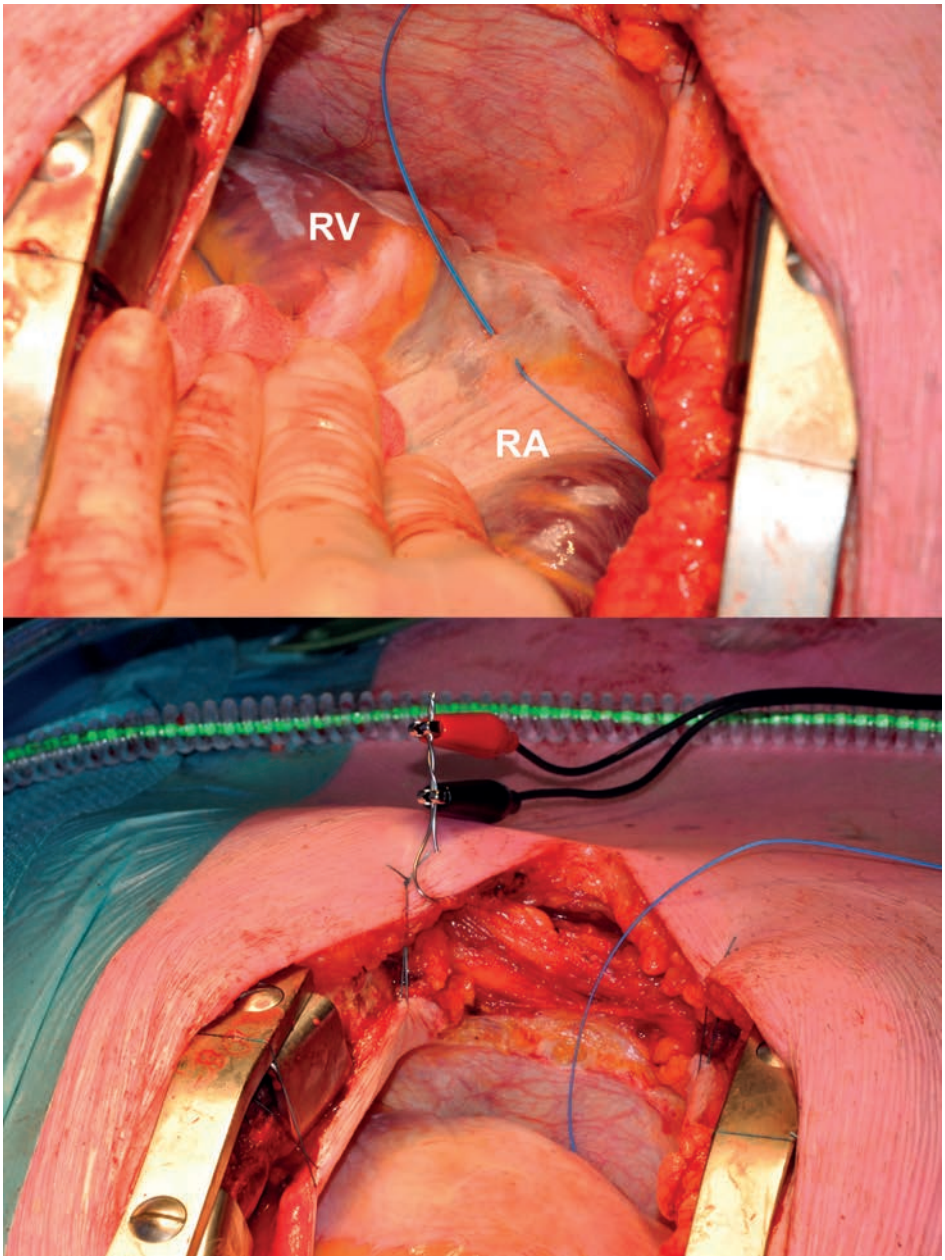

Figure 1. Epicardial mapping preparations.
Top: A pacemaker wire stitched to the right atrial free wall serving as a temporal reference electrode. Bottom: A steel wire fixed to (sub)cutaneous tissue serving as the indifferent electrode. RA, right atrium; RV, right ventricle.

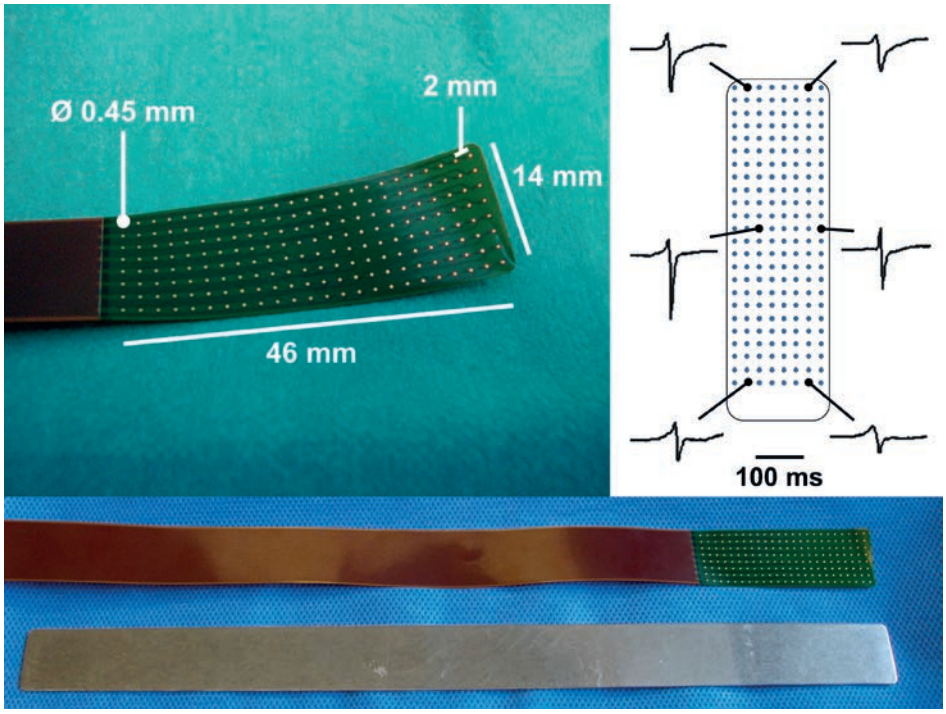

Figure 2. Electrode array for epicardial mapping.
Top left: Mapping array containing 192 unipolar electrodes. Top right: Examples of recorded electrograms at proximal, middle and distal electrodes of the array. Bottom: Mapping array and the identically-shaped steel spatula.

atrium, mapping is performed along the left atrioventricular groove from the lower border of the left inferior pulmonary vein towards the left atrial appendage and from the sinus oblique fold along the border of respectively the right and left pulmonary veins down to the atrioventricular groove. Figure 4 shows the positions of the 192-electrode array along these mapping lines. The mapping array is held in place through either light manual pressure or by means of the spatula. In case of the posterior area between the pulmonary veins, pressure from the weight of the heart and underlying structures provides stability for the mapping array. This technique was performed in 168 patients of 18 years and older, with coronary and/or structural heart disease, with or without AF, electively scheduled for cardiac surgery and a ventricular ejection fraction above 40%. The mean duration of the entire mapping procedure including preparation time was 9±2 minutes. Complications related to the mapping procedure during or after cardiac surgery were not observed.

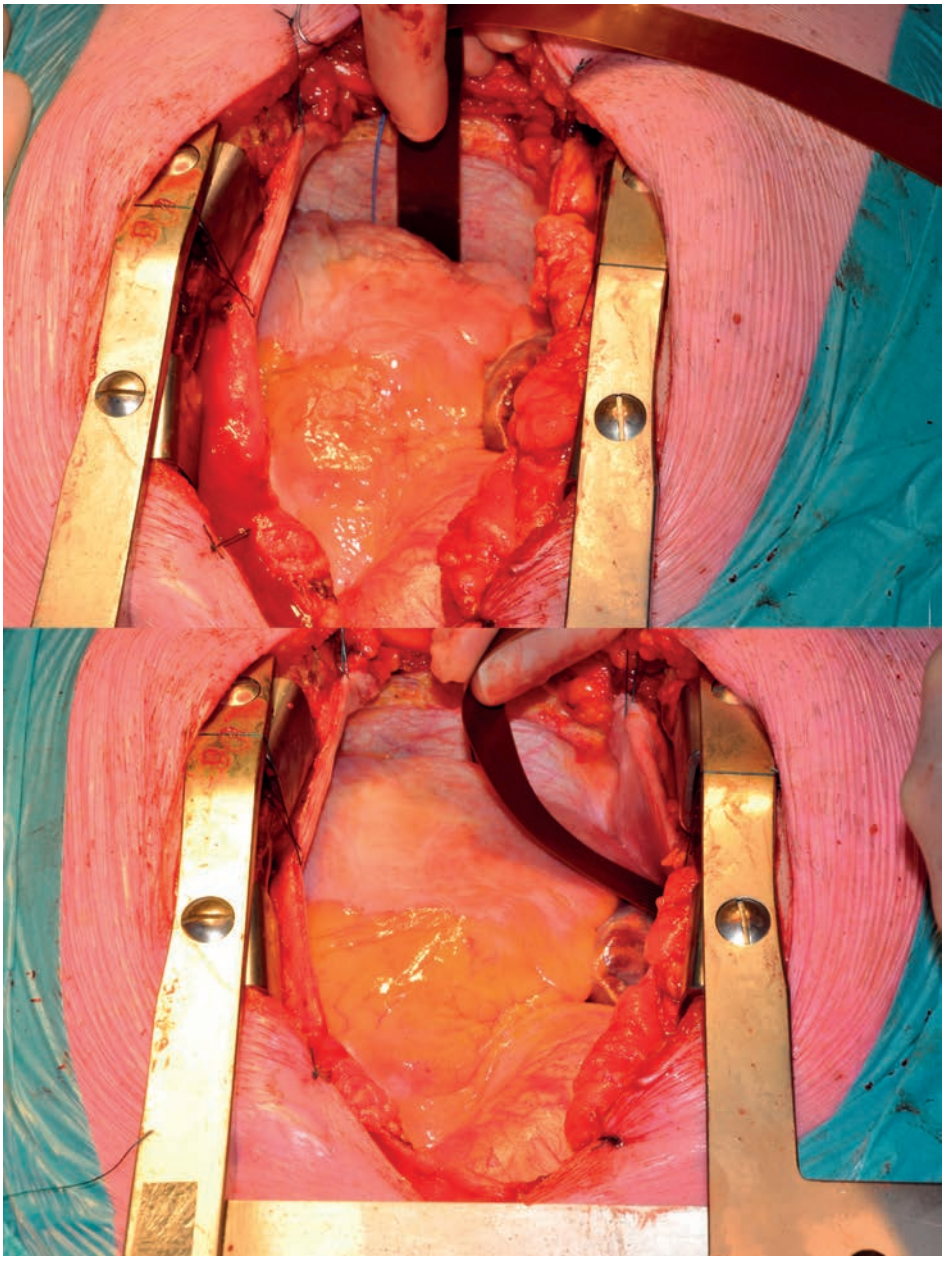

Figure 3. Demonstration of intraoperative epicardial mapping.
The electrode array placed between the pulmonary veins in the oblique sinus (top) and on the right atrial wall (bottom) during recording of epicardial electrograms.

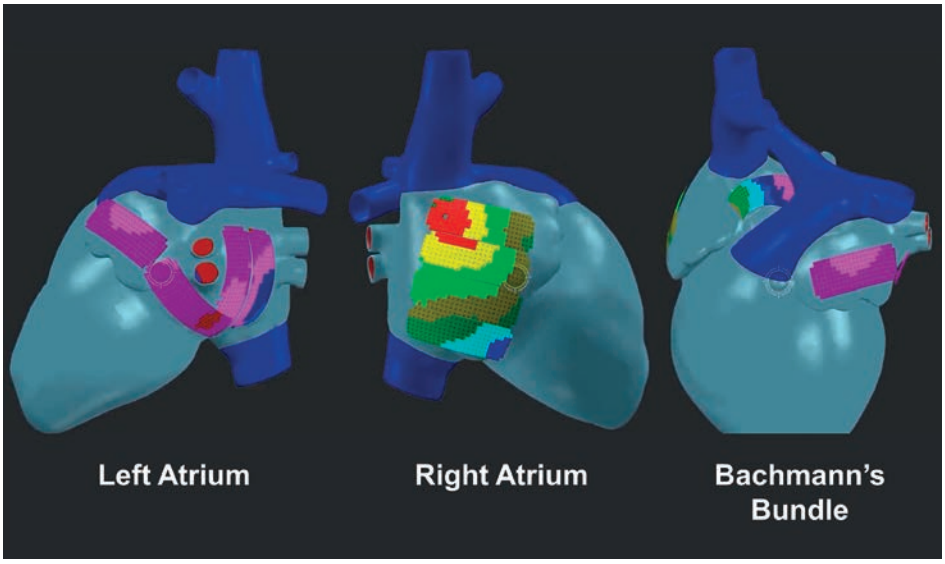

Figure 4. Mapping scheme demonstrating positions of the 192-electrode array on a 3D model. The left and right atrium are covered by 4 positions each, to reach Bachmann's bundle the array is placed within the transverse sinus between the aorta and pulmonary artery.

Mapping technique

The mapping array consists of an electroless nickel immersion gold (ENIG) plated electrode array, mounted on a thin, flexible DuPont™ Pyralux® copper-clad (25 µm thickness) polyimide laminate, and coverlay composite (25 µm) film (0.18 mm), manufactured by GS Swiss PCB AG, Küssnacht, Switzerland. Sterilization is performed by the local sterilization unit before use in the operation room. The sterilized array is connected to 3 meters long, shielded flat cables delivered to the surgeon in a sterile sack. The flat cables are connected to a battery-driven, custom computerized mapping system which is connected to a laptop computer. Custom-made software visualizes real-time atrial electrograms recorded at all 192 electrodes to secure atrial recordings with good electrogram quality. Three channels are designated to display the surface ECG, reference signal and a calibration signal of 1 mV amplitude and 1000 ms pulse width. Five seconds of sinus rhythm and 10 seconds of AF are recorded at every mapping site. All recordings are amplified (gain 1000), filtered (bandwidth 0.5-400 Hz), sampled (1 KHz) and analogue to digital converted (16 bits) and automatically stored on hard disk as E01-files labelled with the atrial rhythm, mapping site and patient identification code. Analysis will be performed offline as previously described.[1]

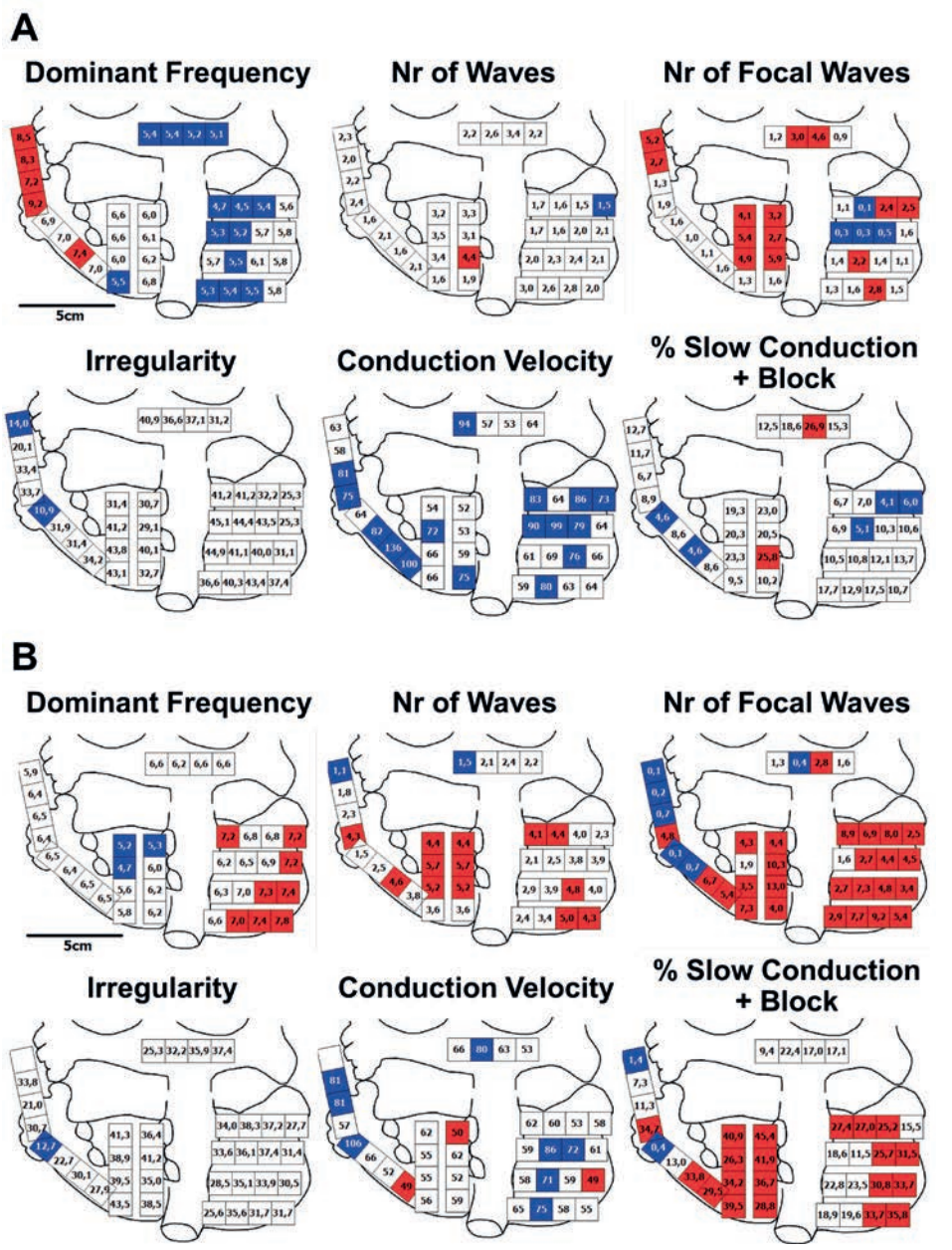

Figure 5. Mapping of induced (A) vs longstanding persistent atrial fibrillation (B).
Intra-atrial variation in various electrophysiological parameters measured during 10 s of AF, including dominant frequency (blue: <6 Hz, white: 6-7 Hz, red: >7 Hz), number of fibrillation waves (blue: <2 cm^2/s, white: 3-4 cm^2/s, red: >3 cm^2/s), number of focal waves (blue: <1 cm^2/s, white: 1-4 cm^2/s, red: >4 cm^2/s), irregularity (blue: <20 ms, white: 20-50 ms, red: >50 ms), conduction velocity (blue: ≥70 cm/s, white: 51-69 cm/s, red: ≤50 cm/s), incidence of slow conduction and block (red: >25%, white: 6-25%, blue: ≤6%). See text for further description.

DISCUSSION

Previous AF mapping studies during surgery did not cover the entire surface of both atria, used low-resolution arrays or recordings of short durations.[2,3] Our mapping approach is the first high-resolution, multi-site mapping approach. It consists of a fixed mapping scheme with a 192-electrode mapping array, which results in a minimum of 1728 recording sites. The mapping array covers large areas of atrial tissue at each position resulting in a short all-over procedure time of 9 minutes without increasing cardiopulmonary bypass time. Unfortunately, high-resolution multi-site mapping is not performed simultaneously as this is technically not yet possible. However, with the reference signal from the right atrial free wall we are able to construct a timeline between the different recordings and create an overall conduction map during sinus rhythm. This map can also demonstrate the possible overlap between recording sites. During AF, the reference signal obtains information about the changes in AF cycle length in order to assess the consistency of the arrhythmia. Previously, the indifferent electrode was fixed to the sternum, however, electrogram quality improved when the indifferent electrode was fixed to subcutaneous tissue. Mapping studies were only performed in patients undergoing elective cardiac surgery for the first time as mapping is technically unfeasible with prior cardiac surgery or pericardiocentesis due to pericardial scarring limiting access to atrial sites.

An advantage of epicardial mapping is that some potential arrhythmogenic structures such as Bachmann's bundle can only be reached from the epicardial site and not from the endocardium. However, the interatrial septum cannot be mapped using a closed beating heart approach and the electrode array does not cover the myocardial sleeves within the pulmonary veins. In recent mapping studies of AF we introduced a so-called 'wavemapping' technique to classify and quantify electrophysiological properties of fibrillation waves.[1,4] This unique mapping approach makes it possible to study features of AF both in the spatial domain, like focal fibrillation waves or areas of conduction block, and the temporal domain, like irregularity of fibrillation intervals.

As an example, intra-atrial variation of various electrophysiological parameters, assessed during 10 s of induced AF in a patient with coronary artery disease is summarized in Figure 5A. Using specific cut-off values, every quadrant was depicted as blue (low), white (intermediate) or red (high). The dominant frequency was 6.1 Hz and ranged from 4.5 to 9.2 Hz. The number of fibrillation and epicardial focal waves was on average respectively 2.3/cm^2/s and 2.1/cm^2/s, varying between 1.5 to 4.4/cm^2/s and 0.1 to 5.9/cm^2/s. The averaged beat-to-beat irregularity was 35.0 ms and the averaged conduction velocity 72.2 cm/s; the degree of conduction delay and block during AF varied from 4.1 to 26.9% (on average 12.6%).

In comparison, electrophysiological parameters quantified during long-standing persistent AF in a patient with mitral valve disease are demonstrated in Figure 5B. The dominant frequency was 6.7 (range: 4.7 to 7.8) Hz. Compared to all quadrants in the patient with coronary artery disease, the number of fibrillation and epicardial focal waves was considerably higher (number of fibrillation waves: 3.5±1.3 (1.1-5.7)/cm^2/s, P<0.001, number of focal waves: 4.3±3.2 (0.1-13.0)/cm^2/s, P<0.001). The averaged beat-to-beat irregularity was comparable (32.9 ms). Conduction velocity was on average 63 cm/s (P<0.01) and the degree of conduction delay and block varied from 0.4 to 45.4% (on average 24.8%, P<0.001). Hence, during longstanding persistent AF, the number of fibrillation waves and incidence of focal waves was higher and conduction abnormalities occurred more frequently; the areas involved are shown in the quadrant maps.

Therefore, this mapping technique can potentially identify vulnerable areas responsible for initiation and persistence of AF by localizing and quantifying the degree of electropathology in the individual patient. Furthermore, by understanding the electropathological substrate in AF patients and providing individualized diagnoses, high-resolution mapping might be able to direct current AF therapies more efficiently or may lead to new insights for treatment strategies which could in turn improve current treatment outcomes.

REFERENCES

1. Allessie MA, de Groot NM, Houben RP, Schotten U, Boersma E, Smeets JL, Crijns HJ. Electropathological substrate of long-standing persistent atrial fibrillation in patients with structural heart disease: longitudinal dissociation. Circ Arrhythm Electrophysiol. 2010;3:606-15.
2. Sueda T, Nagata H, Shikata H, Orihashi K, Morita S, Sueshiro M, Okada K, Matsuura Y. Simple left atrial procedure for chronic atrial fibrillation associated with mitral valve disease. Ann Thorac Surg. 1996;62:1796-800.
3. Nitta T, Ishii Y, Miyagi Y, Ohmori H, Sakamoto S, Tanaka S. Concurrent multiple left atrial focal activations with fibrillatory conduction and right atrial focal or reentrant activation as the mechanism in atrial fibrillation. J Thorac Cardiovasc Surg. 2004;127:770-8.
4. de Groot NMS, Houben RPM, Smeets JL, Boersma E, Schotten U, Schalij MJ, Crijns H, Allessie MA. Electropathological substrate of longstanding persistent atrial fibrillation in patients with structural heart disease: epicardial breakthrough. Circulation. 2010;122:1674-82.

5

Epicardial Atrial Mapping during Minimally Invasive Cardiothoracic Surgery

Lisette van der Does
Frans Oei
Paul Knops
Ad Bogers
Natasja de Groot

ABSTRACT

Mapping of the unorganized activation patterns of atrial fibrillation requires a high-resolution mapping approach in order to diagnose substrate-mediated pathophysiological mechanisms. Epicardial mapping is for now the only approach able to acquire electrograms of >200 high-density sites simultaneously. This study introduces a technique to perform high-resolution mapping in minimally invasive surgery. In three patients with mitral valve disease epicardial mapping of the right atrium, Bachmann's bundle and parts of the left atrium was safely performed via minimal right thoracotomy.

INTRODUCTION

Atrial fibrillation is often triggered by impulses from the pulmonary veins, and isolation of the pulmonary veins is the standard ablative approach. However, recurrences occur frequently and can be due to recovery of pulmonary-atrial conduction or due to remodeling of atrial tissue serving as a substrate for persistence of atrial fibrillation.[1] To improve the success of ablative therapy, patients would benefit from an individualized approach. Analyzing the electrical activation patterns of atrial fibrillation, or so-called mapping, could not only guide treatment strategies but also determine the effect of the applied scars and evaluate the need for additional treatment. Minimally invasive surgical approaches are gaining ground and are currently widely employed in patients with mitral valve disease, in whom a high incidence of atrial fibrillation is observed.[2] Therefore, we developed a technique to map atrial activation patterns at high resolution during minimally invasive surgical procedures. Here, we present our first evaluation in three patients without a history of arrhythmia to assess the usability of the mapping approach.

Three patients, aged 67, 59 and 62 years, scheduled for mitral valve repair using a minimally invasive approach were informed and gave consent to participate in the study protocol approved by the local ethics committee (Halt & Reverse, MEC2014-393). All patients had severe mitral valve insufficiency and normal left ventricular function and underwent mitral valve surgery alone.

SURGICAL TECHNIQUE

Preparation

General anesthesia was applied, and patients were intubated with a double-lumen respiration tube and received a transoesophageal echo probe and a central and arterial line, with electrocardiogram (ECG) monitoring. The patients were positioned supine and turned 30˚ to their left side on the operation table with an inflatable cushion supporting the right scapula. Minimal right thoracotomy of 4-5 cm was performed at the 4th intercostal space, and the videoscope was introduced via a port in the 3rd intercostal space. The pericardium was opened with a reversed L-incision exposing the heart. Cannulas for cardiopulmonary bypass were placed in the femoral vein and femoral artery and advanced towards the superior vena cava and aortic arch, respectively. The critical position of the tip of the venous cannula in the superior vena cava was confirmed by transoesophageal echocardiography.

Mapping procedure

A reference signal during mapping was obtained by a bipolar pacemaker wire stitched on the terminal crest of the right atrium. A steel wire was fixed to subcutaneous tissue at the femoral access site of the cannulas and served as an indifferent electrode. A rectangular flexible 192-electrode array (1.4x4.6 cm), fixed on a similar shaped spatula made from bendable steel for stability (Figure 1), was connected via 3 meter shielded cables wrapped in a sterile sack to a custom computerized mapping system.

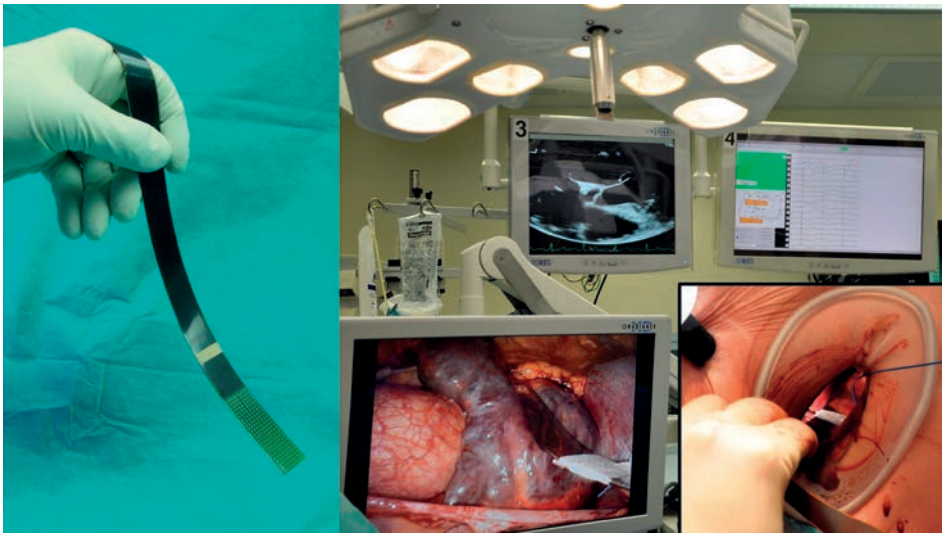

Figure 1. Epicardial mapping during minimally invasive surgery.
Left: The flexible 192-electrode mapping array fixed on a bendable steel spatula. Right: Epicardial mapping during a minimally invasive surgical procedure.

For mapping, the electrode array is moved along imaginary lines to directly record electric potentials on the atrial surface. At the right atrium, the array is positioned perpendicular to the caval veins and recording starts at the top of the right atrial appendage, near the superior caval vein (Figure 2). After each 5 to 10-second recording, the array is moved further downwards over the right atrial appendage until the cavotricuspid isthmus is reached. The intercaval area including the terminal crest is mapped from Waterston's groove, with the array positioned in the longitudinal direction of the caval veins. The posterior left atrium is mapped below the inferior pulmonary veins along the atrioventricular groove from the left inferior pulmonary vein towards the right inferior pulmonary vein. Mapping of Bachmann's bundle was performed from the roof of the left atrium towards the superior cava-atrial junction. Then, by advancing the array past Bachmann's bundle, the left atrial appendage was reached and mapped from the tip to its base.

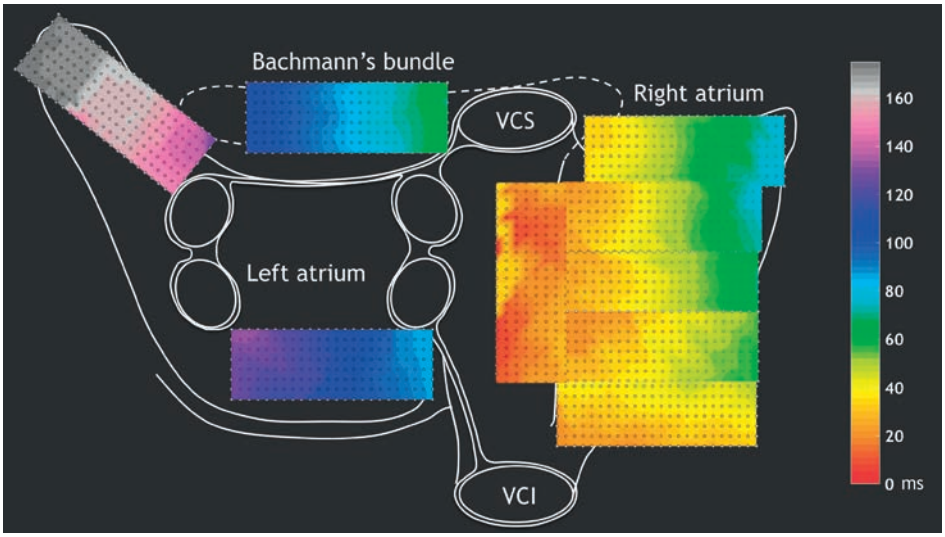

Figure 2. An overview of the high-resolution atrial activation pattern.
The color-coded activation map demonstrates the overall atrial activation pattern during sinus rhythm in high resolution.

Fixed high-rate pacing was performed at the right atrial appendage with the aim to induce atrial fibrillation and map atrial fibrillation patterns using the same protocol. If there was no spontaneous return of sinus rhythm after mapping of induced atrial fibrillation, sinus rhythm was restored with electrical cardioversion or atrial fibrillation stopped when cardioplegia was applied. The pacemaker wire and steel wire were removed and the operation proceeded as scheduled.

Postoperative course

Two patients did not have any arrhythmias or complications in the postoperative period, and the other patient had multiple episodes of postoperative atrial fibrillation, which converted spontaneously with amiodarone. Two weeks after surgery, this patient also developed Dressler syndrome which was successfully treated with medications. His atrial fibrillation episodes progressed to persistent atrial fibrillation 4 months after surgery and sinus rhythm was restored with electrical cardioversion .

DISCUSSION

Clinical results

The reported cases are the first experience with this technique performed using a minimally invasive surgical approach. However, our experience in a large study cohort of, now,

>500 patients with an open-heart surgical approach has demonstrated this mapping procedure to be safe, and it can be performed within 10 minutes with experienced personnel.[3]

Epicardial mapping

Epicardial mapping and ablation are being utilized nowadays for ventricular tachyarrhythmias to treat origin sites that cannot be reached endocardially. Recently, we demonstrated that asynchrony of the epicardial and endocardial atrial wall occurs during atrial fibrillation, and epicardial activation can remain undetected recording from the endocardial side alone.[4,5] Therefore, epicardial atrial mapping may be getting a more important role in the treatment of atrial fibrillation as well. Previous studies mapping atrial fibrillation epicardially were all performed during open-heart surgery and those arrays seem unsuitable for minimal invasive procedures.[6,7] The large and specifically shaped arrays of Lee et al. for simultaneous biatrial mapping seem difficult and time consuming to position with retractors.[6] The triangular shaped electrode with sides of approximately 4 cm in the study of Walters et al. will not be able to reach areas behind tight spaces such as the pulmonary vein area and Bachmann's bundle.[7] However, for clinical purposes, a minimally invasive approach would be preferred.

Advantages

One of the most important advantages of epicardial atrial mapping is that it has a higher resolution than endocardial atrial mapping. This feature is of great significance in the mapping of the complex patterns of electric activity during atrial fibrillation. The unorganized activation patterns of atrial fibrillation differ beat-to-beat, and waves decrease in size with persistence of atrial fibrillation.[8] Therefore, a high number of simultaneously acquired electrograms with small interelectrode spacing are required to map atrial fibrillation waves. Another advantage is that mapping can precisely evaluate the continuity of ablative lesions to pinpoint the exact location in case of a gap. If this technique is combined with an electroanatomical mapping system that can store the location of the site and guide the ablation tool[9], a gap can be located and treated accordingly. The minimally invasive approach makes high-resolution mapping potentially suitable for a much wider public of patients experiencing atrial fibrillation and not only patients needing cardiac surgery. A individually tailored approach could improve the success of atrial fibrillation therapy, which mapping of atrial fibrillation could provide by identifying for each patient, the remodeled atrial sites critical in supporting the persistence of atrial fibrillation and deliver targeted ablation therapy to those sites.[10] In this study, we demonstrated that qualitative high-resolution epicardial mapping during sinus rhythm and (induced) atrial fibrillation is feasible during minimally invasive cardiothoracic surgery.

Limitations

The standard incisions for minimally invasive mitral valve surgery do not provide access for epicardial mapping of the entire left atrium. The posterior left atrium below the pulmonary veins could only be reached in one of the three patients. The left atrium could possibly be reached (better) with an additional incision site at the left side. The atrial septum cannot be mapped with an epicardial approach.

Future directions

To implement high-resolution mapping guided ablation during surgery, electroanatomical mapping systems that can guide ablation tools as set-up in electrophysiology laboratories should be made available for high-resolution mapping arrays.[9] In addition, more research on atrial fibrillation mapping is required to find mechanisms sustaining atrial fibrillation and possible target sites to stop it. This may also result in the decision to not ablate a patient if mapping demonstrates the atria are too electrically diseased for intervention to be successful.

REFERENCES

1. Iwasaki YK, Nishida K, Kato T, Nattel S. Atrial fibrillation pathophysiology: implications for management. Circulation. 2011;124:2264-74.
2. Grigioni F, Avierinos JF, Ling LH, Scott CG, Bailey KR, Tajik AJ, Frye RL, Enriquez-Sarano M. Atrial fibrillation complicating the course of degenerative mitral regurgitation: determinants and long-term outcome. J Am Coll Cardiol. 2002;40:84-92.
3. Yaksh A, van der Does LJ, Kik C, Knops P, Oei FB, van de Woestijne PC, Bekkers JA, Bogers AJ, Allessie MA, de Groot NM. A novel intra-operative, high-resolution atrial mapping approach. J Interv Card Electrophysiol. 2015;44:221-5.
4. de Groot N, van der Does L, Yaksh A, Lanters E, Teuwen C, Knops P, van de Woestijne P, Bekkers J, Kik C, Bogers A, Allessie M. Direct Proof of Endo-Epicardial Asynchrony of the Atrial Wall During Atrial Fibrillation in Humans. Circ Arrhythmia Electrophysiol. 2016;9:e003648.
5. van der Does LJ, Knops P, Teuwen CP, Serban C, Starreveld R, Lanters EA, Mouws EM, Kik C, Bogers AJ, de Groot NM. Unipolar atrial electrogram morphology from an epicardial and endocardial perspective. Heart Rhythm. 2018;15:879-887.
6. Lee S, Sahadevan J, Khrestian CM, Markowitz A, Waldo AL. Characterization of Foci and Breakthrough Sites During Persistent and Long-Standing Persistent Atrial Fibrillation in Patients: Studies Using High-Density (510-512 Electrodes) Biatrial Epicardial Mapping. J Am Heart Assoc. 2017;6:e005274.
7. Walters TE, Lee G, Spence S, Kalman JM. The effect of electrode density on the interpretation of atrial activation patterns in epicardial mapping of human persistent atrial fibrillation. Heart Rhythm. 2016;13:1215-20.
8. Allessie MA, de Groot NM, Houben RP, Schotten U, Boersma E, Smeets JL, Crijns HJ. Electropathological substrate of long-standing persistent atrial fibrillation in patients with structural heart disease: longitudinal dissociation. Circ Arrhythm Electrophysiol. 2010;3:606-15.
9. Knackstedt C, Schauerte P, Kirchhof P. Electro-anatomic mapping systems in arrhythmias. Europace. 2008;10:iii28-34.
10. van der Does LJ, Yaksh A, Kik C, Knops P, Lanters EA, Teuwen CP, Oei FB, van de Woestijne PC, Bekkers JA, Bogers AJ, Allessie MA, de Groot NM. QUest for the Arrhythmogenic Substrate of Atrial fibRillation in Patients Undergoing Cardiac Surgery (QUASAR Study): Rationale and Design. J Cardiovasc Transl Res. 2016;9:194-201.

6

The Effects of Valvular Heart Disease on Atrial Conduction during Sinus Rhythm

Lisette van der Does
Eva Lanters
Christophe Teuwen
Elisabeth Mouws
Ameeta Yaksh
Paul Knops
Charles Kik
Ad Bogers
Natasja de Groot

ABSTRACT

Background: Chronic atrial stretch due to valvular heart disease initiates structural remodeling which in turn can disturb electrical conduction and lead to atrial fibrillation (AF). Different mechanisms of remodeling may underlie aortic valve (AV) and mitral valve (MV) disease. This study aimed to identify the differences in conduction disorders during sinus rhythm between patients with AV and MV disease and to find predilection sites of conduction disorders in AF patients.

Methods: High-density epicardial mapping was performed after sternotomy in patients undergoing AV or MV surgery. Unipolar electrograms were recorded from the entire left and right atrial surface during sinus rhythm with a 128 or 192-electrode-array (circa 1880 electrograms per patient) and activation maps were analyzed for presence of conduction delay/block between electrodes (CD Δ7-11 ms; CB Δ≥12 ms).

Results: A history of AF was present in 17 of 85 AV patients and 21 of 54 MV patients. CD and CB was most pronounced at the superior intercaval area (2.5% of surface, maximal degree 6.6%/cm^2). MV patients had a higher maximal degree of CD at the lateral left atrium than AV patients (4.2 vs 2.3%/cm^2, P=0.001). A history of AF was most strongly correlated to CD/CB at Bachmann's bundle (P<0.001, r=0.40) and age (P=0.006, r=0.31).

Conclusions: Although MV patients have more conduction disorders at the lateral left atrium, disturbed conduction at Bachmann's bundle during sinus rhythm indicates the presence of atrial remodeling which is related to AF episodes.

INTRODUCTION

Valvular heart disease predisposes to the occurrence of atrial tachyarrhythmias. Significant stenosis or regurgitation of heart valves has important hemodynamic effects on the atria that lead to structural atrial remodeling. In situations of pressure or volume overload the increased pressure on the atrial wall causes atrial dilation.[1] Chronic mechanical stretch initiates pathways that produce fibrosis and alter myocyte coupling and function.[2,3] Consequently, electrical conduction in the atria becomes disrupted and can result in areas with slow and discontinuous conduction which may act as a substrate for tachyarrhythmias. The incidence of atrial fibrillation (AF) is higher in patients with mitral valve (MV) disease (26-54%) then in patients with aortic valve (AV) disease (10-13%), most likely due to higher left atrial loads in MV disease.[4,5] Therefore, different types of atrial remodeling may take place in AV and MV disease.

It has been previously demonstrated that structural remodeling and not electrical remodeling is the major contributor to development of AF in models of chronic atrial stretch.[3] The electrophysiological disturbances due to structural alterations in patients with valvular heart disease may also be identifiable during sinus rhythm. The purpose of this study is first to identify differences in the amount and distribution of high-resolution conduction disorders during sinus rhythm between patients with AV and MV disease. Secondly, we aim to determine if predilection sites of conduction disorders during sinus rhythm exist in patients with valvular heart disease who have developed clinical AF. A high-resolution epicardial mapping approach was performed to locate atrial areas with conduction abnormalities and identify the differences in conduction disorders between patients with AV and MV disease requiring surgical treatment.

METHODS

Study population

Patients of 18 years and older undergoing AV (mainly for aortic stenosis) or MV (for mitral regurgitation) surgery with or without coronary artery bypass grafting participated in this study. The study is part of the QUASAR study that was approved by the local ethics committee and all patients gave informed consent prior to surgery.[6]

Study procedure

During surgery and prior to cardiopulmonary bypass, epicardial mapping was performed of the entire atrial surface with an electrode array containing 128 or 192 unipolar electrodes with an electrode diameter of 0.65 or 0.45 mm and interelectrode spacing of 2 mm

(GS Swiss PCB AG, Küssnacht, Switzerland). Five-second recordings of sinus rhythm were sequentially acquired from all epicardial accessible sites at the right atrium, left atrium and Bachmann's bundle. Patients that were in AF at the start of the procedure were electrically converted to sinus rhythm. A temporary pacemaker wire stitched to the terminal crest served as a reference signal during the recordings. The mapping procedure and mapping sites were previously described in detail.[7] Mapping locations are also illustrated in the upper right panel of Figure 1. In case of the 128-electrode mapping array, each 192-array location consisted of two 128-array recordings. Unipolar electrograms were stored on hard disk after amplification, filtering (bandwidth 0.5-400 Hz), sampling (1 KHz) and analogue to digital conversion (16 bits).

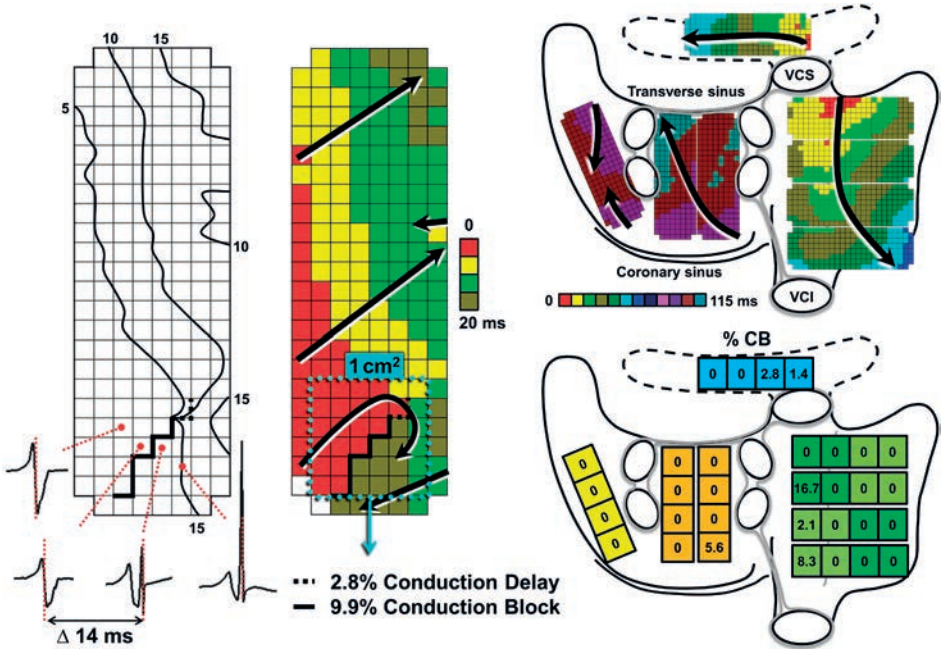

Figure 1. Intraoperative epicardial mapping scheme and data analysis.
Left: Example of an isochronal and activation map demonstrating the analysis of conduction delay (CD) and conduction block (CB) on a high-resolution scale. An isochronal map with electrograms at the site of CB and the activation map demonstrate differences ≥12 ms in activation times between adjacent electrodes (interelectrode distance 2 mm). Thick (dashed) black lines indicate sites with CD (dashed line, Δ7-11 ms) and CB (solid line, Δ≥12 ms). In an area of 1 cm^2 the number of lines with CD and CB are 2.8% and 9.9% of the total number of lines within the 1 cm^2 quadrant. Right: High-resolution activation maps are recorded at all epicardial accessible sites: the right atrium, Bachmann's bundle, posterior left atrial wall between the pulmonary veins and lateral left atrium including the appendage. The entire atrial surface in this patient is activated in 115 ms. The total recording area divided into 1 cm^2 quadrants represents the amount of CD and CB at specific sites; the amount of CB is depicted in this example. The quadrants are assigned to 7 atrial areas: superior and inferior intercaval right atrium, the superior and inferior lateral right atrium (shades of green), Bachmann's bundle (blue), posterior left atrium (orange) and lateral left atrium (yellow). For Bachmann's bundle, the average degree of CB in this example is 1.0%, and the maximal degree of CB is 2.8%. VCS, vena cava superior; VCI, vena cava inferior.

Mapping data analysis

Atrial deflections were detected automatically by marking of the steepest negative deflection with a minimal slope of 80 mV/s and signal to noise ratio >4 for each recorded electrogram in order to construct activation maps.[6] The marked electrograms and activation maps were thereafter checked and manually corrected if necessary. Aberrant and premature atrial beats were excluded from analysis. Sinus rhythm activation maps were used to determine the incidence of conduction delay (CD) and conduction block (CB) on a high-resolution scale (left panel, Figure 1). CD and CB were defined as a difference in activation time between adjacent electrodes of, respectively, 7-11 ms and ≥12 ms (translating to an effective conduction velocity of 17–28 cm/sec and <17 cm/sec).[8] The amount of CD and CB was calculated as a percentage per 1 cm^2 quadrants. Figure 1 illustrates the subdivision of the entire mapping surface of each patient in 1 cm^2 quadrants in which the percentages of CD and CB were determined.

Atrial distribution

The prevalence and degree of CD and CB in the patient groups were assessed separately for 7 atrial areas: 4 areas at the right atrium (the superior (1) and inferior (2) intercaval/terminal crest area and the superior (3) and inferior (4) lateral right atrium), Bachmann's bundle (5), posterior left atrium between the pulmonary veins (6) and the lateral left atrium/ left atrial appendage (LAA) (7) (Figure 1, right lower panel). The prevalence of CD/CB per area is defined as the percentage of patients with presence of CD or CB in that area. For each area in every patient, the average degree of CD and CB was determined (average percentage CD/CB of the 1 cm^2 quadrants in that area) and also the maximal degree of CD and CB in 1 cm^2 (CD/CB of the 1 cm^2 quadrant with the highest amount of CD/CB).

Statistical analysis

Categorical clinical characteristics between the AV and MV group were compared with Chi-square or Fisher's exact tests. Continuous clinical data and electrophysiological data were not normally distributed and differences between the AV and MV group were evaluated with Mann-Whitney U tests. Electrophysiological mapping data are presented as median (minimum-maximum) values. To evaluate differences between areas, the area with the highest average and maximal degree of CD/CB was identified for each patient and the total incidences of highest amount of CD/CB were determined for each area. Differences in the incidence distributions between areas were first evaluated with the overall Cochran's Q test. Subsequently, McNemar tests were applied for a pair-wise comparison of each of the areas. We applied Bonferroni correction to adjust for inflation of type I error with repeated tests. A *P*-value ≤0.05/7 was considered statistically significant for the comparison of patient groups (AV vs MV) within the 7 areas, whereas for the inter-areal comparisons a *P*-value threshold of ≤0.05/21 was used. The rank-biserial correlation coefficient (skewed

continuous/ordinal data) and Phi coefficient (binary data) were determined to quantify the correlation between electrophysiological/clinical variables and a history of AF. Binary logistic regression analysis was performed to relate electrophysiological and clinical variables with incidence of postoperative AF. All analyses were performed with IBM SPSS Statistics version 21 (IBM corp.,Armonk, NY).

RESULTS

Clinical characteristics

Epicardial high-resolution mapping during sinus rhythm was performed in 139 patients who underwent cardiac surgery for valvular heart disease. There were 89 (64%) male and 50 (36%) female patients with a median age of 70 (IQR=62-75) years. MV surgery was performed in 54 (39%) patients and 85 (61%) patients had valvular cardiac surgery for only AV disease. A total of 66 (47%) patients had significant coronary artery disease and 38 (27%) had a history of AF. All clinical characteristics are demonstrated in Table 1. Patients with MV disease presented more often with left atrial enlargement, left ventricular dysfunction and AF prior to surgery, hypertension was more often observed in AV disease.

Mapping data

The median number of electrogram recordings of the entire atrial surface acquired by high-resolution mapping was 1880 (945-2356) per patient. Quadrants containing <50% electrogram recordings were excluded from analysis, which resulted in exclusion of 2.6% of the 4644 quadrants in total, and 32 (18-42) quadrants per patient were analyzed for presence of CD and CB. Median cycle length during mapping of sinus rhythm was not different between AV and MV patients (786 ms (473-1735) and 784 ms (533-1178), *P*=0.28). Cardioversion was performed before mapping of sinus rhythm in 16 patients (42%) with a history of AF. However, there were no differences in the amount of conduction disorders between patients with AF who received a cardioversion and those who were spontaneously in sinus rhythm.

Overall conduction delay and block in valvular heart disease

A certain amount of both CD and CB was present in (nearly) all of the patients during sinus rhythm and the prevalence ranged respectively between 0.17-3.4% (median 1.26%) and 0-3.58% (median 1.15%) of the atrial surface. Figure 2 demonstrates the degree of CD and CB of the entire atria in patients with AV and MV disease. There was no difference in the atrial amount of CD/CB between patients with AV or MV disease. Both maximal peak gradient of patients with only aortic valve stenosis (n=64, 78±23 mmHg) and cycle length were not correlated to the total amount of CD and CB (*P*=0.30 and *P*=0.93).

Table 1. Clinical characteristics

	Total N(%)	AV patients N(%)	MV patients N(%)	*P*-value
No. of patients	139	85	54	
Age, years [IQR]	70 [12]	69 [13]	70 [14]	0.641
Male gender	89 (64)	59 (69)	30 (56)	0.097
Hypertension	67 (48)	48 (57)	19 (35)	0.014
Hypercholesterolemia	29 (21)	18 (21)	11 (20)	0.909
Diabetes mellitus	22 (16)	15 (18)	7 (13)	0.461
Coronary artery disease	66 (48)	43 (51)	23 (43)	0.358
Peripheral vascular disease	7 (5)	4 (5)	3 (6)	1.000
Atrial fibrillation	38 (27)	17 (20)	21 (39)	0.015
Valvular disease*				
Aortic stenosis	81 (58)	74 (87)	7 (13)	
Aortic regurgitation	26 (19)	18 (21)	8 (15)	
Mitral stenosis	5 (4)	0	5 (9)	
Mitral regurgitation	54 (39)	0	54 (100)	
Tricuspid regurgitation	13 (9)	0	13 (24)	
Left ventricular function				0.019
normal	103 (74)	70 (82)	33 (61)	
mild dysfunction	25 (18)	11 (13)	14 (26)	
moderate dysfunction	11 (8)	4 (5)	7 (13)	
severe dysfunction	0	0	0	
Left atrial enlargement (>45 mm)	40 (29)	11 (13)	29 (54)	<0.001

* Valvular heart disease for which corrective surgery was performed. AV = aortic valve; MV = mitral valve; IQR = interquartile range.

Atrial distribution of conduction delay and block

Figure 3 demonstrates the average degree of CD and CB in each area for both groups. In Table 2 the maximal degrees of CD and CB for each area are shown. The largest difference in CD/CB between patients with AV and MV disease was seen at the lateral left atrial/LAA area. The maximal degree of CD at the lateral left atrium was higher in patients with MV disease and there was an overall trend towards more CD/CB at this site in the MV disease group. The average and maximal degree of CB was highest at the superior intercaval/terminal crest area of the right atrium (respectively 2.5% and 6.6%/cm^2, all $P \leq 0.001$). Long lines of CB are often seen towards the posterior area of the right atrium, also in two out of three of the youngest patients in our study group (21-24 years).

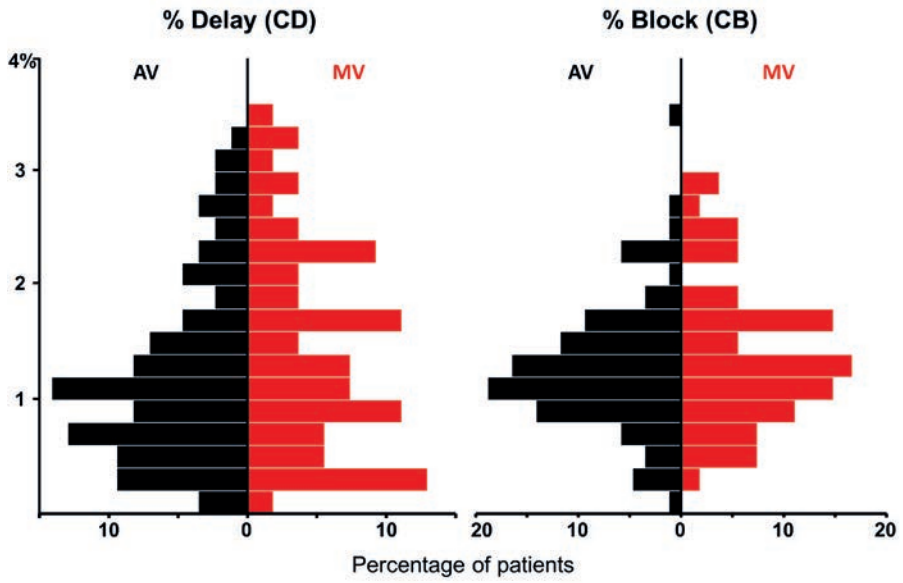

Figure 2. Overall conduction delay and block in valvular heart disease.
Histograms of the amount of conduction delay and block (CD/CB) of the entire atrial surface in patients with aortic valve (AV) and mitral valve (MV) disease.

Table 2. Prevalence and maximal degree of CD and CB per area

		All		AV		MV		*P*-value*
		Prevalence (% patients)	Max degree (%/cm^2)	Prevalence (% patients)	Max degree (%/cm^2)	Prevalence (% patients)	Max degree (%/cm^2)	
RA-ICS	CD	78	4.1 (0-20.8)	79	4.2 (0-17.4)	77	4.0 (0-20.8)	0.391
	CB	73	6.6 (0-34.7)	74	6.3 (0-30.6)	72	6.9 (0-34.7)	0.635
RA-ICI	CD	70	2.8 (0-13.9)	72	2.8 (0-13.9)	66	2.9 (0-11.1)	0.578
	CB	55	2.1 (0-22.5)	53	2.1 (0-22.5)	59	2.8 (0-22.5)	0.696
RA-RAS	CD	63	1.4 (0-13.0)	65	1.4 (0-13.0)	59	1.4 (0-9.7)	0.489
	CB	32	0 (0-22.2)	38	0 (0-22.2)	24	0 (0-14.7)	0.138
RA-RAI	CD	53	1.4 (0-15.3)	47	0 (0-13.9)	62	1.5 (0-15.3)	0.118
	CB	20	0 (0-12.5)	15	0 (0-10.3)	26	0 (0-12.5)	0.086
BB	CD	84	4.2 (0-18.1)	82	4.2 (0-18.1)	87	4.2 (0-13.9)	0.847
	CB	70	3.5 (0-22.2)	71	2.8 (0-20.8)	67	4.2 (0-22.2)	0.630
PLA	CD	81	4.2 (0-18.8)	79	4.2 (0-18.8)	85	4.7 (0-18.1)	0.380
	CB	58	2.0 (0-23.6)	58	2.1 (0-23.6)	59	1.8 (0-19.6)	0.975
LLA	CD	75	2.8 (0-23.6)	69	2.8 (0-12.5)	85	4.2 (0-23.6)	0.001†
	CB	50	0 (0-20.8)	45	0 (0-20.8)	58	1.8 (0-17.4)	0.037

**P*-value of maximal degree of CB/CD between AV and MV patients. †Significant after Bonferroni correction; CD = conduction delay; CB = conduction block; RA = right atrium; ICS/I = intercaval superior/ inferior; RAS/I = right appendage superior/ inferior; BB = Bachmann's bundle; PLA = posterior left atrium; LLA = lateral left atrium.

Relation of conduction disorders with pre- and postoperative AF

Table 3 illustrates the relation and differences in clinical and electrophysiological parameters between patients with and without preoperative AF. AF patients were older, had more left atrial enlargement (>45 mm), total CD/CB and more CD/CB at Bachmann's bundle and the lateral left atrium. The strongest parameter correlated with preoperative AF was CD/CB at Bachmann's bundle (r_{rb}=0.40, *P*<0.001) followed by age (r_{rb}=0.31, *P*=0.006).

Postoperative continuous rhythm registrations of 121 (87%) patients were available and analyzed for occurrence of early postoperative AF. Postoperative AF occurred in 52%. Presence of total amount of atrial CD and CB in the upper quartile, preoperative AF, left atrial enlargement, left ventricular dysfunction, hypertension, diabetes did not predict postoperative AF, only age was a limited risk factor for developing postoperative AF (OR 1.071, CI 1.023-1.122, *P*=0.004). Neither univariate or multivariate logistic regression including CD and CB in the upper quartile per area separately showed associations between electrophysiological parameters and postoperative AF.

Table 3. Correlation between a history of AF and clinical and electrophysiological characteristics

	No AF N=101	AF N=38	*P*-value	Correlation coefficient
Age, yr [IQR]	68 [12]	73 [11]	0.006	0.31
Hypertension (%)	58	45	0.161	
Diabetes mellitus (%)	14	21	0.301	
LA >45 mm (%)	22	47	0.003	0.25†
LV function (N-R-M %)	72 - 19 - 9	79 - 16 - 5	0.401	
CD/CB (average % [IQR])				
Total	2.3 [2.0]	2.7 [2.3]	0.044	0.22
RA-ICS	4.7 [6.6]	4.5 [5.0]	0.277	
RA-ICI	2.5 [5.1]	1.1 [5.7]	0.183	
RA-RAS	0.5 [1.8]	0.8 [1.8]	0.718	
RA-RAI	0.4 [1.4]	0.4 [1.3]	0.456	
BB	2.3 [4.4]	5.9 [6.4]	0.000*	0.40
PLA	1.6 [2.3]	1.8 [3.2]	0.125	
LLA	1.0 [1.9]	1.8 [2.5]	0.009	0.29

* significant after Bonferroni correction; † Phi coefficient; AF = atrial fibrillation; IQR = interquartile range; LA = left atrium; LV = left ventricular; N-R-M = normal-reduced-moderate; CD = conduction delay; CB = conduction block; RA = right atrium; ICS/I = intercaval superior/ inferior; RAS/I = right appendage superior/ inferior; BB = Bachmann's bundle; PLA = posterior left atrium; LLA = lateral left atrium.

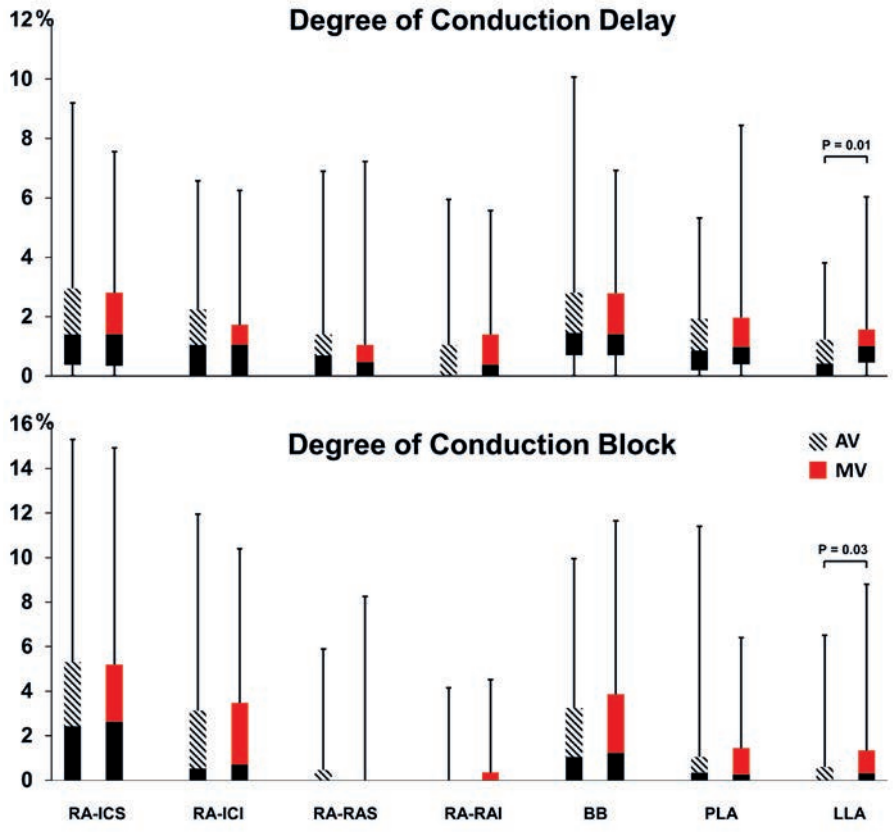

Figure 3. Conduction delay and block per atrial area.
Boxplots of the average percentage of conduction delay and block (CD/CB) in each area in patients with AV and MV disease (error bars indicate minimum and maximum, box indicates Q1-median-Q3). The right atrial intercaval superior area (RA-ICS) has the highest amount of CB (P<0.001, significant after Bonferroni correction). Patients with MV disease tend to have more CD/CB at the lateral left atrium (LLA). RA, right atrium; ICS/I, intercaval superior/ inferior; RAS/I, right appendage superior/ inferior; BB, Bachmann's bundle; PLA, posterior left atrium; LLA, lateral left atrium.

DISCUSSION

High-resolution mapping of the atria in patients with valvular heart disease demonstrated a high and heterogeneous occurrence of disturbances in electrical conduction during sinus rhythm. The highest prevalence was seen at the high right atrium. The overall degree of CD and CB did not differ between patients with AV and MV disease. However, the lateral left atrium demonstrated a higher maximal degree of CD per 1 cm^2 in patients with MV disease. Preoperative AF was most strongly correlated with conduction disorders at Bachmann's bundle and age.

Conduction block at the high right atrium

Both groups demonstrated a high prevalence and degree of CB at the high right atrium which is not specific for patients with left-sided valvular heart disease and is also observed in patients with coronary artery disease.[8] The high right atrium is characterized by the sinoatrial node area and fractionated atrial electrograms are common at this site in patients with sinus node dysfunction.[9] However, likely CB seen at this site is not caused by sinus node disease with advancing age, but anatomically determined. Even young patients in this study had long lines of CB lateral to the site of first activation. Previous studies have demonstrated that the sinus node is surrounded by arteries and connective tissue protecting the node from external electrical influences and that action potentials of the sinus node are conducted to atrial myocardium via specific exit pathways located superiorly and inferiorly. Lateral conduction towards the atrial septum, however, is blocked by the insulating tissue.[10,11] Furthermore, the neighboring terminal crest is known for anisotropic conduction properties and slow conduction parallel to the crest which may also contribute to the observed CB at the high right atrium.[12]

Conduction disorders in aortic versus mitral valve disease

Both AV and MV disease have been associated with changes in the myocardial structure of the atria due to the altered hemodynamic effects.[13,14] Structural remodeling can alter atrial electrophysiology and predispose to development of atrial tachyarrhythmias. The higher incidence of AF in MV disease suggests the presence of a higher degree of atrial remodeling in these patients. Roberts-Thomson et al. indeed demonstrated a larger amount of functional delay in conduction during pacing at the posterior left atrial wall in patients with MV disease compared to AV disease.[15] However, these differences were not present during sinus rhythm. We have investigated the entire atrial surface and identified the lateral left atrium as a location with increased conduction delay in patients with MV disease.

Atrial fibrillation and conduction disorders during sinus rhythm

In sinus rhythm, more CD was observed at the left posterior wall in MV patients with persistent AF than without AF.[16] In our study, patients with MV disease had more conduction disorders at the lateral left atrium and a higher prevalence of AF. However, preoperative AF was most strongly correlated with conduction disturbances at Bachmann's bundle. Teuwen et al. has recently found that a high amount and long lines of CB at Bachmann's bundle during sinus rhythm predisposes for early postoperative AF in patients with coronary artery disease.[17] The highly organized structure and anisotropic features could leave Bachmann's bundle more vulnerable to structural remodeling and disturbances in conduction that can even be identified during sinus rhythm. The myocardial strands crossing the right and left atrial roof are not enclosed by fibrous tissue and may perhaps be easily disrupted by stretch due to overload of either atrium.[18] The histological study

of Becker et al. demonstrated in fact that structural continuity of Bachmann's bundle is often compromised, especially in patients with AF.[19] Conduction disorders at Bachmann's bundle have been proposed to be a measure of more general atrial electrical pathology.[20] However, we found that conduction disturbances in other areas during sinus rhythm are not related to AF.

Study limitations

The routine preoperative echocardiograms did not allow for a retrospective sampling of exact dimensions. This parameter was therefore limited to the used cut-off dimension. The atrial septum cannot be reached by epicardial mapping and is therefore not included in this study. The atrial areas are recorded in a sequential manner due to technical restrictions which may cause some overlap between recordings.

Clinical relevance

This study is the first to describe conduction disorders in high-resolution of the entire atrial surface during sinus rhythm in patients with valvular heart disease. It demonstrated that left atrial overload in MV disease also translates to more conduction disorders at the lateral left atrium during sinus rhythm and that Bachmann's bundle is most affected in MV and AV patients with AF. These findings help to further understand the structural damage caused by valvular heart disease that alters electrical conduction and most likely creates susceptibility for AF.

CONCLUSIONS

Excitation of the atria during sinus rhythm is heterogeneously disrupted in patients with AV and MV disease, however, in MV disease more conduction disorders present at the lateral left atrium. The occurrence of AF in presence of valvular heart disease is associated with increased conduction disturbances in sinus rhythm at Bachmann's bundle. Further research is necessary to determine the role of Bachmann's bundle and lateral left atrium in the occurrence of AF in patients with valvular heart disease.

REFERENCES

1. Darby AE, Dimarco JP. Management of atrial fibrillation in patients with structural heart disease. Circulation. 2012;125:945-57.
2. Verheule S, Wilson E, Everett T 4th, Shanbhag S, Golden C, Olgin J. Alterations in atrial electrophysiology and tissue structure in a canine model of chronic atrial dilatation due to mitral regurgitation. Circulation. 2003;107:2615-22.
3. Kumar S, Teh AW, Medi C, Kistler PM, Morton JB, Kalman JM. Atrial remodeling in varying clinical substrates within beating human hearts: relevance to atrial fibrillation. Prog Biophys Mol Biol. 2012;110:278-94.
4. Iung B, Baron G, Tornos P, Gohlke-Bärwolf C, Butchart EG, Vahanian A. Valvular heart disease in the community: a European experience. Curr Probl Cardiol. 2007;32:609-61.
5. Sauter HJ, Dodge HT, Johnston RR, Graham TP. The Relationship of Left Atrial Pressure and Volume in Patients with Heart Disease. Am Heart J. 1964;67:635-642.
6. van der Does LJME, Yaksh A, Kik C, Knops P, Lanters EAH, Teuwen CP, Oei FBS, van de Woestijne PC, Bekkers JA, Bogers AJJC, Allessie MA, de Groot NMS. QUest for the Arrhythmogenic Substrate of Atrial fibRillation in Patients Undergoing Cardiac Surgery (QUASAR Study): Rationale and Design. J Cardiovasc Transl Res. 2016;9:194-201.
7. Yaksh A, van der Does LJ, Kik C, Knops P, Oei FB, van de Woestijne PC, Bekkers JA, Bogers AJ, Allessie MA, de Groot NM. A novel intra-operative, high-resolution atrial mapping approach. J Interv Card Electrophysiol. 2015;44:221-5.
8. Lanters EAH, Yaksh A, Teuwen CP, van der Does LJME, Kik C, Knops P, van Marion DMS, Brundel BJJM, Bogers AJJC, Allessie MA, de Groot NMS. Spatial distribution of conduction disorders during sinus rhythm. Int J Cardiol. 2017;249:220-225.
9. Centurion OA, Fukatani M, Konoe A, Tanigawa M, Shimizu A, Isomoto S, Kaibara M, Hashiba K. Different distribution of abnormal endocardial electrograms within the right atrium in patients with sick sinus syndrome. Br Heart J. 1992;68:596-600.
10. Fedorov VV, Schuessler RB, Hemphill M, Ambrosi CM, Chang R, Voloshina AS, Brown K, Hucker WJ, Efimov IR. Structural and functional evidence for discrete exit pathways that connect the canine sinoatrial node and atria. Circ Res. 2009;104:915-23.
11. Fedorov VV, Glukhov AV, Chang R, Kostecki G, Aferol H, Hucker WJ, Wuskell JP, Loew LM, Schuessler RB, Moazami N, Efimov IR. Optical mapping of the isolated coronary-perfused human sinus node. J Am Coll Cardiol. 2010;56:1386-94.
12. Becker R, Bauer A, Metz S, Kinscherf R, Senges JC, Schreiner KD, Voss F, Kuebler W, Schoels W. Intercaval block in normal canine hearts : role of the terminal crest. Circulation. 2001;103:2521-6.
13. Anné W, Willems R, Roskams T, Sergeant P, Herijgers P, Holemans P, Ector H, Heidbüchel H. Matrix metalloproteinases and atrial remodeling in patients with mitral valve disease and atrial fibrillation. Cardiovasc Res. 2005;67:655-66.
14. Kim SJ, Choisy SC, Barman P, Zhang H, Hancox JC, Jones SA, James AF. Atrial remodeling and the substrate for atrial fibrillation in rat hearts with elevated afterload. Circ Arrhythm Electrophysiol. 2011;4:761-9.
15. Roberts-Thomson KC, Stevenson IH, Kistler PM, Haqqani HM, Goldblatt JC, Sanders P, Kalman JM. Anatomically determined functional conduction delay in the posterior left atrium relationship to structural heart disease. J Am Coll Cardiol. 2008;51:856-62.

16. Roberts-Thomson KC, Stevenson I, Kistler PM, Haqqani HM, Spence SJ, Goldblatt JC, Sanders P, Kalman JM. The role of chronic atrial stretch and atrial fibrillation on posterior left atrial wall conduction. Heart Rhythm. 2009;6:1109-17.
17. Teuwen CP, Yaksh A, Lanters EA, Kik C, van der Does LJ, Knops P, Taverne YJ, van de Woestijne PC, Oei FB, Bekkers JA, Bogers AJ, Allessie MA, de Groot NM. Relevance of Conduction Disorders in Bachmann's Bundle During Sinus Rhythm in Humans. Circ Arrhythm Electrophysiol. 2016;9:e003972.
18. Ho SY, Anderson RH, Sánchez-Quintana D. Gross structure of the atriums: more than an anatomic curiosity? Pacing Clin Electrophysiol. 2002;25:342-50.
19. Becker AE. How structurally normal are human atria in patients with atrial fibrillation? Heart Rhythm. 2004;1:627-31.
20. van Campenhout MJ, Yaksh A, Kik C, de Jaegere PP, Ho SY, Allessie MA, de Groot NM. Bachmann's bundle: a key player in the development of atrial fibrillation? Circ Arrhythm Electrophysiol. 2013;6:1041-6.

7

Sinus Rhythm Conduction Properties across Bachmann's Bundle: Impact of Underlying Heart Disease and Atrial Fibrillation

Christophe Teuwen
Lisette van der Does,
Charles Kik
Elisabeth Mouws
Eva Lanters
Paul Knops
Yannick Taverne
Ad Bogers
Natasja de Groot

ABSTRACT

Background: Valvular heart disease (VHD) is a common risk factor for atrial fibrillation (AF). Conduction abnormalities (CA) during sinus rhythm (SR) across Bachmann's bundle (BB) are associated with AF development. The study goal is to compare electrophysiological characteristics across BB during SR between patients with ischemic (IHD) and/or VHD either with or without ischemic heart disease ((I)VHD), with/without AF history using high-resolution intraoperative epicardial mapping.

Methods: High-resolution intraoperative epicardial mapping of BB with 128 or 192-unipolar electrode arrays was performed. Entry sites of SR wavefronts into BB were classified as right, middle and/or left. Length and amount of CA lines were calculated.

Results: In total, 304 patients (IHD: N=193, (I)VHD: N=111) were mapped; 40 patients (13%) had a history of AF. In 116 patients (38%) there was a mid-entry site with a trend towards more mid-entry sites in patients with (I)VHD vs IHD (P=0.061), whereas patients with AF had significant more mid-entry sites than without AF (P=0.007). CA were present in 251 (95%) patients without AF compared to 39 (98%) with AF. The amount of CA was comparable in patients with IHD and (I)VHD (P>0.05); AF history was positively associated with the amount of CA (P<0.05). ROC-curve showed 85.0% sensitivity and 86.4% specificity for cut-off values of CA lines of respectively ≤6 mm and ≥26 mm. Patients without a mid-entry site or long CA lines (≥12 mm) were unlikely to have AF (sensitivity 90%, P=0.002).

Conclusions: There are no significant differences in entry-sites of wavefronts and long lines of CA between patients with IHD compared to (I)VHD. Yet, patients with AF have more wavefronts entering in the middle of BB and a higher incidence of long CA lines compared to patients without a history of AF. Moreover, in case of absence of a mid-entry site or long line of CA, patients most likely have no history of AF.

INTRODUCTION

Propagation of electrical wavefronts during sinus rhythm (SR) occurs from the right atrium towards the left atrium through different connections such as the coronary sinus, fossa ovalis and Bachmann's bundle (BB).[1] Because of limited access to the epicardially located BB, electrical activation across BB has rarely been studied. In patients with ischemic heart disease (IHD), it was recently shown that although BB was thought to be of paramount importance for interatrial conduction from the right to left atrium during SR, it was also activated by SR wavefronts emerging in the middle and left site of the bundle.[2] In addition, patients with atrial fibrillation (AF) had a higher degree of conduction disorders across BB. This observation suggests a possible role of BB in development of AF which has also been proposed by other investigators.[3, 4]

The suggested role of BB in AF development was mainly based on subtle ECG changes.[5] These ECG findings were associated with clinical outcomes such as stroke and AF (Bayés syndrome).[5] Furthermore, pacing at BB instead of the usual right atrial appendage might be effective for prevention of AF paroxysms and progression to persistent AF, although studies showed conflicting results.[6, 7]

Valvular heart disease (VHD) is one of the major risk factors predisposing to development of AF.[8] Conduction across BB might be affected by VHD, as VHD and conduction disorders across BB are both correlated to development of AF. Yet, the effect of underlying heart disease such as VHD on conduction across BB is so far unknown in humans, as detailed activation mapping of BB has only been described in patients with IHD. The aim of the present study was 1) to examine electrophysiological properties during SR including entry sites and conduction disorders across BB during SR, 2) to compare these properties between patients with ischemic and/or valvular heart disease and 3) to correlate these electrophysiological properties with the occurrence of previous AF episodes.

METHODS

Study population

A total of 304 patients of at least 18 years of age who underwent open chest cardiac surgery for coronary artery bypass graft and/or VHD (aortic or mitral valve) were included. Patients were classified into 2 groups; IHD and VHD. The group of IHD mainly consists of patients analyzed in our previous report (N=185).[2] The latter containing patients with solely VHD and VHD in combination with IHD. As VHD is considered a leading risk factor for development of AF and to maintain sufficient statistical power by comparing similar

group sizes, these patients are initially categorized as one: (I)VHD. Yet, complete sub-analyses for entry-sites and conduction disorders for patients with IHD only, IVHD and VHD only are shown in Supplemental Table 1. Echocardiographic examination was part of standard protocol prior to the surgical procedure, whereas other imaging techniques (e.g. MRI) were not. Patients were excluded in case of paced atrial rhythm, Wolff-Parkinson-White syndrome, severe renal failure, previous open chest cardiac surgery, prior ablative therapy, hemodynamic instability (presence of assist devices, usage of inotropic) and prior radiation for chest malignancies.

This study is part of the prospective observational projects QUASAR and HALT & REVERSE which were both approved by the Medical Ethical Committee in the Erasmus Medical Center (MEC 2010-054 and MEC 2014-393).[9] Written informed consent was provided by all patients prior to the surgical procedure.

Mapping procedure

High-resolution epicardial mapping was performed as previously described.[2, 9] A bipolar pacemaker-wire was stitched to the right atrial free wall (terminal crest), serving as temporal reference electrode. A steel wire was fixed in the thoracic subcutaneous tissue serving as indifferent electrode. The initial 161 patients were mapped with a 128-unipolar electrode (8x16) mapping array, whereas the remaining patients were mapped with a mapping array containing 192-unipolar electrodes (8x24) (interelectrode distance 2.0 mm).[2] The mapping array was positioned on BB by placing it over the interatrial roof behind the aorta with the tip against the left atrial appendage (upper panel Figure 1). Mapping of BB with the 128-electrode array was performed by shifting the array backwards towards the superior cavo-atrial junction resulting in 2 consecutive positions. Solely patients with electrical activation present at >75% of the mapping area were included. Although this may be the result of low voltage areas, limited contact of the mapping array on the myocardium cannot be excluded and therefore this cut-off value was chosen. SR was recorded during 5 seconds, including a surface ECG lead, a calibration signal of 2 mV and 1000 ms, unipolar epicardial electrograms and a bipolar reference electrogram.[2, 9]

Mapping data analysis

Mapping data were analyzed using our custom-made software.[2, 9] The steepest negative deflection of the unipolar atrial potentials was annotated as local activation time. Based on the activation times, color-coded activation maps were automatically constructed as demonstrated in the middle panel of Figure 1. An averaged beat was subsequently created after excluding premature and aberrant beats. The averaged maps were used for analysis of patterns of activation and quantification of conduction disorders. Patterns of activation were classified according to entry-sites; right, middle and left (lower panel Figure 1). A

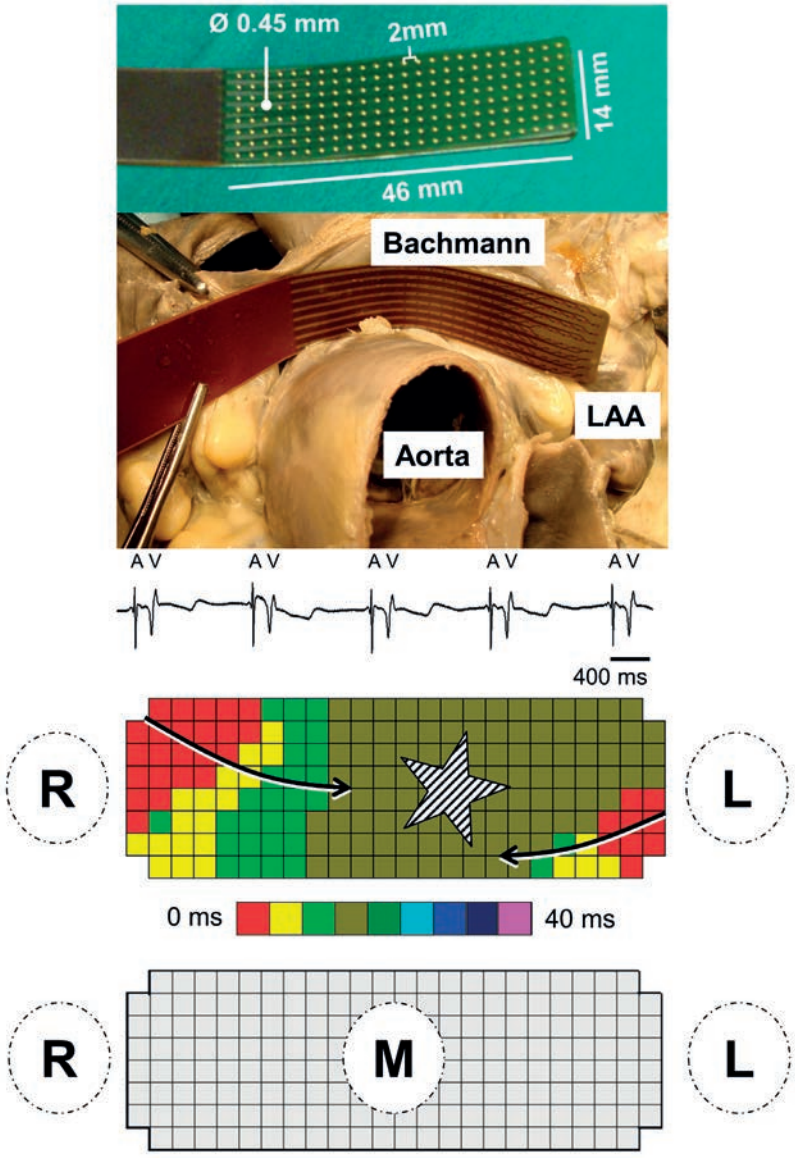

Figure 1. Mapping procedure of Bachmann's bundle.
Top: 192-unipolar electrode mapping array including measurements of length, interelectrode distance and electrode diameter. The mapping array is subsequently positioned at Bachmann's bundle, by placing the array behind the aorta with the tip against the left atrial appendage. Middle: unipolar electrogram with steep atrial deflection(A) and far-field ventricular signal(V). After marking all atrial deflections, a color-coded activation map is constructed. The arrows depict direction of wavefront propagation. The striped star illustrates an area of simultaneous excitation/focal wave. In the current example, the mid-entry corresponds to location of the interatrial septum and transition of BB to left atrial roof (posterior). Bottom: schematic overview of 192-unipolar electrode mapping array. Entry sites are denoted with R (right), M (middle) and L (left). LAA, left atrial appendage.

wavefront entering the area under the mapping array from the right atrial side from where it propagates towards the left side was defined as right entry site, whereas in case this was observed vice versa it was defined as left entry site. An area of simultaneous excitation or a wavefront emerging in the center of the mapping array as focal wave was defined as mid-entry site.[2] Also wavefronts entering from the anterior or posterior borders in the middle part of the mapping array, were also defined as mid-entry. In a previous study from our group, we described the origin of these mid-entry wavefronts based on anatomy of dissected hearts. Either these wavefronts propagate from the interatrial septum upwards to BB, which are connected in some patients, or these wavefronts enter BB through parallel bundles that merge either on the anterior or posterior site of BB.[10] For quantification of conduction disorders, difference in local activation times between 2 adjacent electrodes were determined. Conform previous studies, conduction delay (CD) was determined as time differences of 7–11 ms (conduction velocity: <29 cm/s) between 2 adjacent electrodes. In case time difference was ≥12 ms between 2 adjacent electrodes (conduction velocity: <17 cm/s), this area was marked as conduction block (CB).[2, 9] The amount of conduction delay and/or block was measured as a percentage of all interelectrode conduction times. The number of lines of CD/CB and their length were measured separately. When lines of CD and CB were connected to each other, they were denoted as CDCB.

Statistical analysis

Normally distributed data are described by mean±SD, whereas skewed data are described by median (interquartile range) and categorical data as numbers and percentages. Normally distributed data are analyzed with Student's T-test or one way ANOVA, skewed data with Kruskall-Wallis test or Mann-Whitney U-test and categorical data with $\chi 2$ or Fisher exact test when appropriate. The correlation between patient characteristics in the entire study population or IHD/(I)VHD separately and conduction disorders was performed using Spearman rank correlation. A correlation of 0.1 – 0.3 was considered weak, 0.3 – 0.5 moderate and >0.5 strong. For further clinical interpretation of observed conduction disorders, ROC-curves from previous AF episodes were extracted to calculate CB/CDCB cut-off values for sensitivity and specificity. Subsequently, based on previous data showing an association between lines of CB ≥12 mm with development of postoperative AF, we also studied the relation of previous AF episodes and lines of CB/CDCB ≥12 mm. With current findings, we added a mid-entry site to these analysis and determined sensitivity and specificity with $\chi 2$. In addition, we investigated the relation between late postoperative AF (LPAF) using previous long-term follow-up data and presence of lines of CB/CDCB ≥12 mm and/or mid-entry site. LPAF was detected on ECG or 24-hour Holter recordings, performed either on regular base or on indication during outpatient clinic control. Finally, the association of potential determinants (e.g. age, left ventricular function, left atrial dilatation) with CB/CDCB ≥12 mm or mid-entry site was tested using univariate binary logistic

regression models. Due to skewness, age was transformed to a binary value with top 25% (≥72.5 years) set as 'high'. Aging, gender and underlying heart disease were subsequently selected for multivariate binary logistic regression, next to determinants with a *P*-value ≤0.20. A *P*-value <0.05 was considered statistically significant. Statistical Package of Social Sciences version 21.0 for Windows(SPSS Inc. Chicago, IL, USA) was used.

RESULTS

Study population

Study population characteristics (N=304, 237 male (78%), age 66±10 years) are shown in Table 1. Mean age in the entire study population was 66±10 years. Patients had either IHD (N=193, 63.5%), VHD (N=62, 20.4%) or a combination of ischemic and valvular heart disease (N=49, 16.1%). Patients underwent cardiac surgery different valvular pathology including aortic valve stenosis (N=70, 23.0%), aortic valve insufficiency (N=20, 6.6%), mitral valve stenosis (N=3, 1.0%) and mitral valve insufficiency (N=41, 13.5%). Two-hundred thirty patients (75.7) used antiarrhythmic drugs prior to surgical procedure; class II (N=211, 69.4%), class III (N=9, 3.0%) and class IV (N=10, 3.3%). The majority of patients had a normal left ventricular function (N=234, 77%) and only 10 patients (3%) had a moderate/severe left ventricular dysfunction. Left atrial dilatation was present in 54 patients (18%); half of them had isolated IHD.

A total of 40 patients (13%) had a history of AF; 32 paroxysmal, 7 persistent and 1 longstanding persistent. Of the latter two groups, all patients underwent electrical cardioversion prior to epicardial mapping. Comparing the presence of AF for different underlying heart disease, relatively most patients had AF in combination with mitral valve disease (N=14, 34%), aortic valve disease (N=12, 17%) and finally IHD solely (N=14, 7%). Due to a limited number of patients with (longstanding) persistent AF, further comparison is not performed between different types of AF. Mapping was performed with mean rate of 72±14 beats/min.

For further comparison of groups, patients were divided in having IHD or VHD. The right side in Table 1 demonstrates differences between these groups. Although age was comparable (65.5±9.2 vs 66.8±11.4), other characteristics which may potentially affect atrial conduction were different; either with a higher incidence in patients with IHD including hypertension, hypercholesterolemia, diabetes mellitus, antiarrhythmic drug usage and history of myocardial infarction (*P*<0.004), or a higher incidence in patients with VHD such as left atrial dilatation and a history of AF (*P*<0.001).

Table 1. Patient characteristics

	Total	IHD	(I)VHD	*P*-value
Number of patients, N	304	193	111	
Age, years (mean ± SD)	66.0 ± 10.1	65.5 ± 9.2	66.8 ± 11.4	0.415
Male gender, N (%)	237 (78.0)	163 (84.5)	74 (66.7)	<0.001
BSA, m^2 (mean ± SD)	2.02 ± 0.21	2.05 ± 0.20	1.96 ± 0.21	0.564
Hypertension, N (%)	170 (55.9)	120 (62.2)	50 (45.0)	0.004
Hypercholesterolemia, N (%)	111 (36.5)	84 (43.5)	27 (24.3)	0.001
Diabetes mellitus, N (%)	85 (28.0)	68 (35.2)	17 (15.3)	<0.001
AAD, N (%)	230 (75.7)	166 (86.0)	64 (57.7)	<0.001
PCI, N (%)	70 (23.0)	58 (30.1)	12 (10.8)	<0.001
Myocardial infarction, N (%)	94 (30.9)	85 (44.0)	9 (8.1)	<0.001
Indication VHD, N (%)				
VHD	62 (20.4)		62 (55.9)	
IVHD	49 (16.1)		49 (44.1)	
Aortic valve stenosis	70 (23.0)		70 (63.1)	
Aortic valve insufficiency	20 (6.6)		20 (18.0)	
Mitral valve disease	3 (1.0)		3 (2.7)	
Mitral valve insufficiency	41 (13.5)		41 (36.9)	
Left ventricular function, N (%)				0.618
Normal	234 (77.0)	146 (75.6)	88 (79.3)	
Mild dysfunction	60 (19.7)	39 (20.2)	21 (18.9)	
Moderate dysfunction	8 (2.6)	6 (3.1)	2 (1.8)	
Severe dysfunction	2 (0.7)	2 (1.0)	0	
Left atrial dilatation >45mm, N (%)	54 (17.8)	27 (14.0)	27 (24.3)	0.001
History of AF, N (%)	40 (13.2)	14 (7.3)	26 (23.4)	<0.001
Paroxysmal	32 (10.5)	14 (7.3)	18 (16.2)	
Persistent	7 (2.3)	0	7 (6.3)	
Longstanding persistent	1 (0.3)	0	1 (0.9)	

AAD = antiarrhythmic drugs; AF = atrial fibrillation; BSA = body surface area; IHD = ischemic heart disease; (I)VHD = (ischemic) valvular heart disease; PCI = percutaneous coronary intervention; SD = standard deviation.

Impact of heart disease and atrial fibrillation on entry sites

We investigated whether the underlying heart disease and/or a history of AF has a relation with the number of wavefront entry sites into BB during SR and the location of these entry sites (right, middle, left or combinations). In total, the number of entry sites was either 1 site solely in 211 patients (69%) or multiple sites (2 sites: N=73, 24%, 3 sites: N=20, 7%). As BB is a major route of interatrial conduction, the vast majority of patients (N=23, 92%) had at least 1 wavefront entering BB from only the right (N=186, 61%) or a right entry site combined with other entry sites (N=95, 31%) (upper panel Figure 2). Furthermore, 116

patients (38%) had a wavefront entering BB in the middle including an entry site in the middle only (N=22, 7.2%), right and middle (N=72, 23.7%), middle and left (N=1, 0.3%) and right, middle and left (N=21, 6.9%).

Whereas the number of entry sites was comparable between patients with IHD (N=59, 31%) and (I)VHD (N=37, 33%) (*P*=0.48), patients with AF had more often >1 entry-site than patients without a history of AF (N=19, 48% vs N=77, 29%; *P*=0.02). Additionally, the middle panel of Figure 2 demonstrates that patients with a history of AF had more frequently a wavefront entering in the middle of BB compared to patients without AF (N=23, 58% vs N=93, 35%; *P*=0.007). In comparison, there was only a trend towards a higher incidence of mid entry sites in patients with (I)VHD compared to IHD (*P*=0.061). For all 3 groups separately, solely patients with IVHD combined with AF had more mid-entry sites, although this group only consisted of 6 patients (see Supplemental Table 1).

Correlation between heart disease or atrial fibrillation with conduction disorders

A total of 283 (93%) patients had at least 1 area of CD, 236 (78%) patients CB and 212 (70%) patients a continuous line of CDCB. In these patients, the longest lines of CD, CB and CDCB consisted of respectively 6 mm (4–8), 6 mm (2–16) and 12 mm (0–22) (upper panels Figure 3). In the entire study population, a median of 1.8% (0.9–2.9) CD, 1.2% (0.3–3.2) CB and 3.2% (1.6–6.0) continuous lines of CDCB was measured, as demonstrated in the lower panels of Figure 3. Although there was a significant positive correlation between the amount of CDCB and aging in the entire study population, the correlation was solely moderate (rho 0.326, *P*<0.001). Furthermore, in patients with (I)VHD, diabetes mellitus and left atrial dilatation was weakly correlated with the amount of CDCB, respectively rho 0.257 (*P*=0.007) and rho 0.282 (*P*=0.008), whereas the remaining patient characteristics demonstrated no correlation. Furthermore, the amount of conduction disorders is comparable between patients with IHD only, IVHD and VHD only (see Supplemental Table 1).

Figure 4 demonstrates conduction disorders in patients with IHD (upper panels), (I)VHD (lower panels), without a history of AF (left panels) and with a history of AF (right panels). As shown in Figure 4, the amount of conduction disorders is nearly comparable between patients with IHD and (I)VHD; CB 0.9% vs 1.4% (*P*=0.155) and CDCB 3.0 vs 3.2% (*P*=0.488) in patients without a history of AF. Also in patients with a history of AF there were no significant differences between IHD and (I)VHD; CB 2.9% vs 3.0% (*P*=0.90) and CDCB 6.5% vs 5.7% (*P*=0.79) (see also Supplemental Table 1 for separate analyses).

In total, 39 (98%) patients with AF and 251 (95%) without AF had at least some areas of CDCB. Yet, patients with AF, both with IHD and (I)VHD, have a higher amount of CB and

CDCB compared to patients without a history of AF, respectively IHD 0.9% vs 2.9% CB (*P*=0.019), 3.0% vs 6.5% CDCB (*P*=0.006) and (I)VHD 1.4% vs 3.0% CB (*P*=0.018) and 3.2 vs 5.7% CDCB (*P*=0.015).

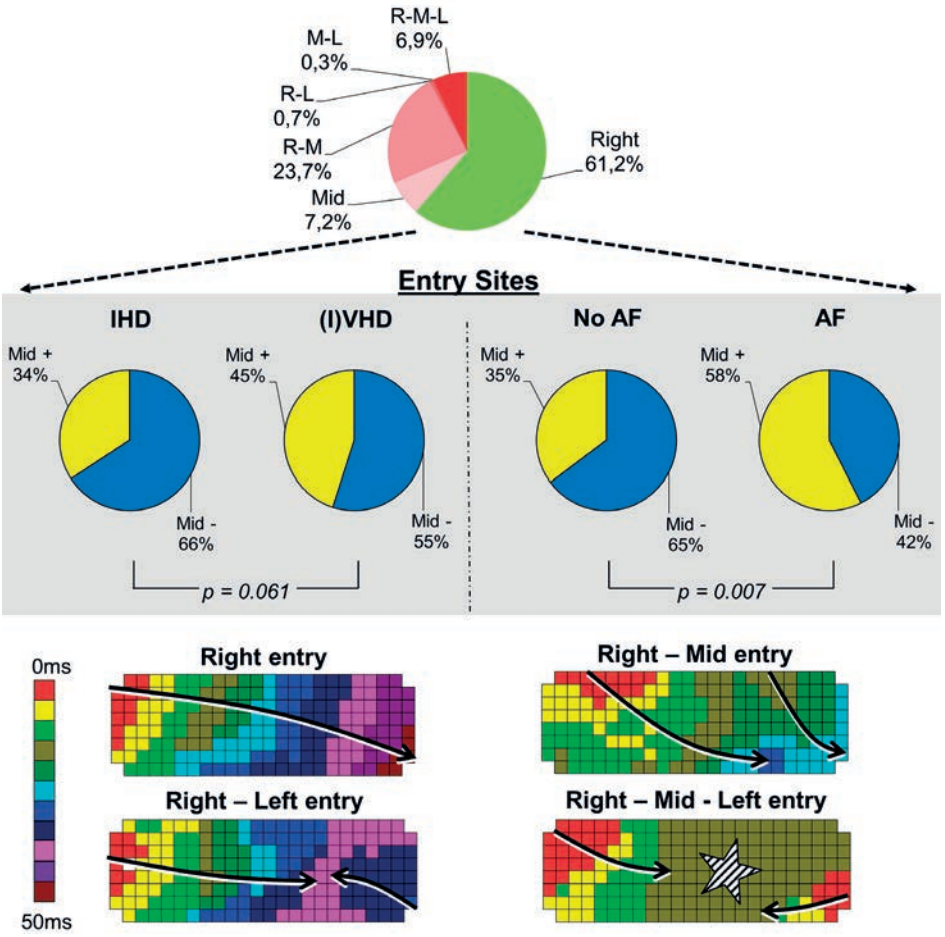

Figure 2. Entry sites and patterns of activation at Bachmann's bundle.
Top: frequency pie illustrating all different entry sites in the entire study population including right entry site only (green) and other entry sites (red). Middle: frequency pies demonstrating the number of patients without a mid-entry site (blue) and with a mid-entry site (yellow) of wavefronts. The left panels illustrate the difference for underlying heart disease, the right panels for patients with/without a history of AF. Bottom: examples of color-coded activation maps of BB during SR demonstrating different activation patterns; entry site only from the right (left upper map), right and middle (right upper map), right and left (left lower map) and right, middle and left (right lower map). Arrows indicate the main propagation direction of wavefronts, stars an area of simultaneous excitation/focal wave. AF, atrial fibrillation; IHD, ischemic heart disease; (I)VHD, (ischemic) valvular heart disease; L, left entry; M, mid entry; R, right entry.

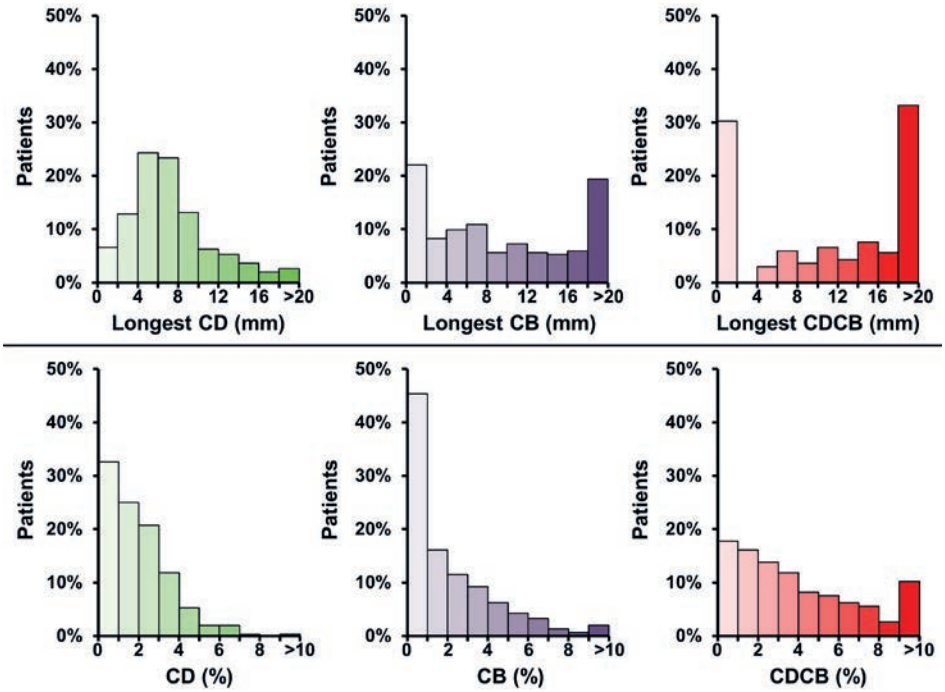

Figure 3. Incidence and extensiveness of conduction disorders.
Top: Frequency histograms depicting the longest measured line of conduction delay (green), block (purple) and connected conduction delay and block (red) per patient. Bottom: Frequency histogram illustrating the percentage of conduction delay (green), block (purple) and combined (red) per patient. CB, conduction block; CD, conduction delay; CDCB (mm), length of connected conduction delay and block; CDCB (%), sum of conduction delay and block.

In line with these results, patients with early postoperative AF also had a higher amount of conduction disorder, respectively IHD 0.9% vs 1.7% CB (*P*=0.022), 2.7% vs 4.2% CDCB (*P*=0.026) and (I)VHD 1.5% vs 1.7% CB (*P*=0.119) and 3.4 vs 3.8% CDCB (*P*=0.030). Furthermore, long-term follow-up was present in 266 patients (88%) with a median follow-up period of 24 months (range 3–36). In these patients, solely 10 patients (4%) developed LPAF of whom 8 patients had preoperative AF. Comparison between patients with/without LPAF and the amount of conduction disorders was not performed due to the limited number of patients with LPAF.

Diagnostic value for atrial fibrillation

Figure 5 illustrates the diagnostic value of longest CB/CDCB for AF. The diagnostic value of the longest lines of CB/CDCB is shown in the ROC-curve in Figure 5 with an area under the curve of 0.697. In addition, cut-off values for high sensitivity and specificity (≥85%) are respectively 6 mm and 26 mm (right upper panel Figure 5).

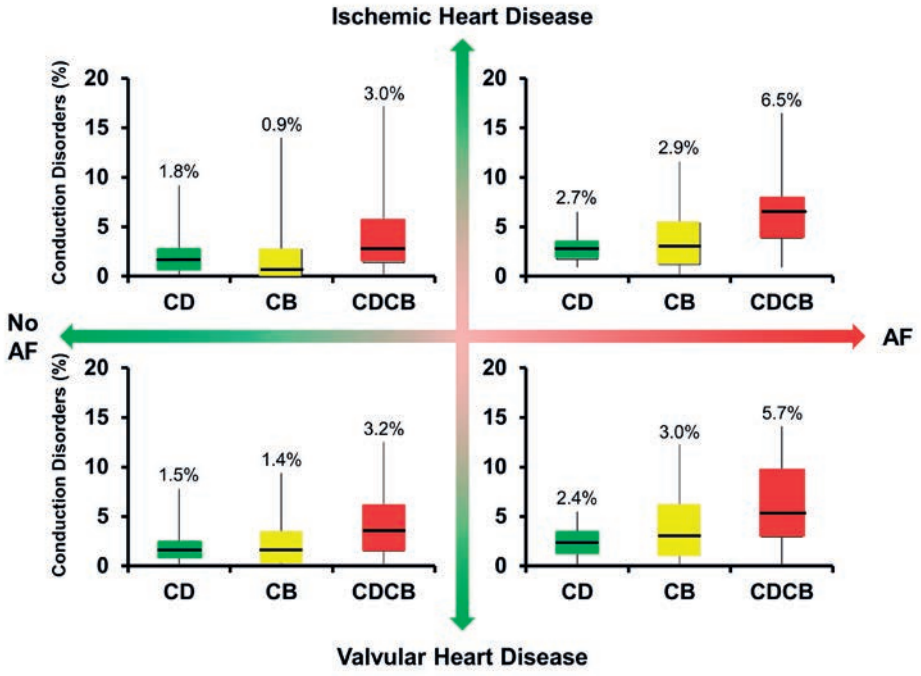

Figure 4. Relation between underlying heart disease, atrial fibrillation and conduction disorders. Differences in the amount of conduction delay (green), block (yellow) and combined (red) between patients with ischemic heart disease (top panels) and valvular heart disease (bottom panels). In addition, difference in conduction disorders are shown between patients without atrial fibrillation (left panels) and with a history of atrial fibrillation (right panels). AF, atrial fibrillation; CB, conduction block; CD, conduction delay; CDCB, sum of conduction delay and block.

The diagnostic value of a mid-entry and previous AF episodes was studied. As mentioned, patients with AF had relatively more frequently a wavefront entering in the middle of BB (see Supplemental Table 1). A total of 116 patients (38%) had a mid-entry of whom 23 patients (58%) had AF, leading to a sensitivity and specificity of respectively 58% and 65%. Also, patients with AF, as previously described, had more conduction disorders. Thirty patients (75%) with AF and 124 patients (47%) without AF had a line of CB or CDCB ≥12 mm, resulting in a sensitivity of 75% and specificity of 53% for previous episodes of AF (both not shown in Figure 5).

When combining these results, a mid-entry or a line of CB/CDCB ≥12 mm, nearly all patients with AF (N=36, 90%) met these criteria compared to 159 patients (60%) of patients without AF (lower panel Figure 5). Therefore, although there is a significant group of patients without AF with a mid-entry or CB/CDCB ≥12 mm, a patient was highly unlikely to have AF in the absence of these criteria (sensitivity 90%). Absence of one of these electrophysiologi-

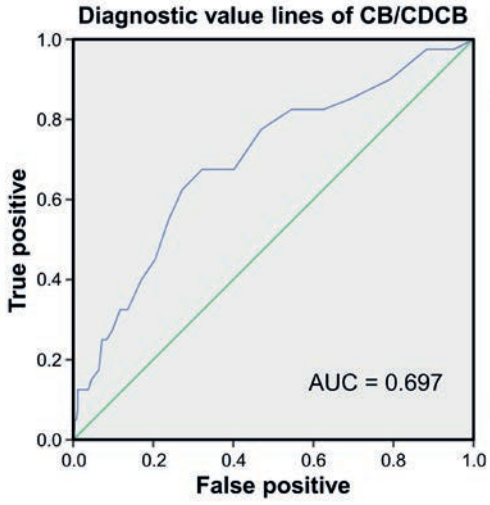

Cut-off longest CB/CDCB (mm)	Sensitivity (%)	Specificity (%)
0	97.5	4.9
2	97.5	11.7
4	90.0	20.8
6	85.0	31.1
8	82.5	37.5
10	82.5	45.5
12	77.5	53.0
14	67.5	59.8
16	67.5	67.8
18	62.5	72.7
20	55.0	76.1
22	45.0	79.5
24	40.0	83.0
26	32.5	86.4
28	32.5	88.3
30	27.5	90.2
32	25.0	91.7
34	25.0	92.8
36	17.5	93.6

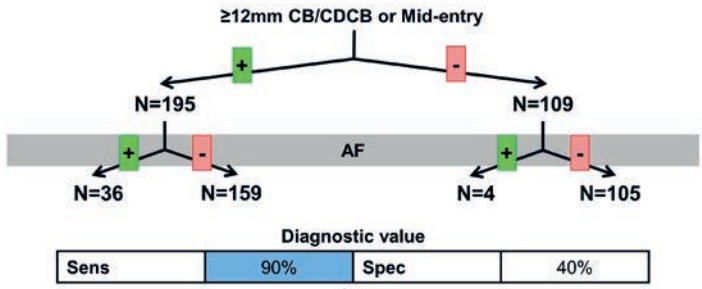

Figure 5. Predictive value of entry-site and conduction disorders.
Top: Predictive value of the length of conduction disorders for previous AF episodes. The left panel depicts a ROC curve for length of lines of conduction disorders, The right panel cut-off values of the length of conduction disorders and previous AF episodes. Bottom: Flowchart demonstrating the predictive value of mid-entry site and a line of conduction block or CDCB of 12 mm or more. Table shows sensitivity and specificity. AF, atrial fibrillation; CB, conduction block; CDCB, connected conduction delay and block; Sens, sensitivity; Spec, specificity.

cal criteria is strongly associated with patients without AF (P=0.002). If both a mid-entry and a line of CB/CDCB ≥ 12 mm are present, sensitivity is reduced to 50% (not shown in Figure). Furthermore, selection of patient characteristics (P≤0.20 univariate analysis) for multivariate analysis including age, gender, history of AF, IHD/VHD and diabetes mellitus demonstrated a history of AF (P=0.007) and aging (P=0.009) were both significantly associated with a mid-entry or CB/CDCB ≥12 mm, whereas gender (P=0.72), VHD (P=0.32) and diabetes mellitus (P=0.16) were not.

DISCUSSION

The current study demonstrates that both patients with IHD and VHD mainly have propagation of SR wavefronts across BB from the right towards the left atrial appendage. Yet, in over one third of patients, a wavefront emerges in the middle of BB towards surrounding sites. Furthermore, nearly all patients have conduction disorders across BB. There are no significant differences in wavefronts emerging in the middle of BB or the amount of conduction disorders between patients with IHD and VHD. In contrast, patients with previous episodes of AF have more conduction disorders and more frequently a wavefront entering BB in the middle compared to patients without a history of AF. Taking both electrophysiological properties into account, patients without a mid-entry site or long lines of conduction disorders seldom have AF.

Atrial remodeling in atrial fibrillation

Both cardiovascular and non-cardiovascular diseases contribute to development of AF. However, how these different diseases exactly contribute to AF development is still not completely unraveled. In general, several mechanisms have been proposed to underlie AF, including an ectopic rapid firing focus or re-entry from which waves originate with fibrillatory conduction or conduction of multiple wavelets.[11] Moreover, electrical asynchrony between the epi- and endocardial layer was recently found as potential cause for maintenance of AF.[12] Irrespective of the underlying mechanism, conduction abnormalities (e.g. due to atrial fibrosis) have always been found to increase AF vulnerability. Müller-Edenborn et al. performed endocardial high-density voltage mapping in patients with persistent AF undergoing pulmonary vein isolation.[13] They investigated the location of areas or bipolar low voltages in the left atrium (peak-to-peak <0.5 and <1.0 mV) during SR. Subsequently, they related these areas of low voltages with alterations of P-wave morphology and risk of AF recurrence. The investigators concluded that low voltage areas are most often observed at the anteroseptal left atrial area which consists of myocardial fibers originating from BB. Furthermore, depending on location of low voltages in the left atrium, P-wave morphology may be altered and increased. Moreover, P-wave alterations and areas of low voltage enable risk stratification of AF recurrence after pulmonary vein isolation. They suggested, also based on previous anatomical studies[14], that conduction disorders might be correlated to local fibrosis. In our previous study focusing on conduction across BB in patients with IHD, we observed that patients with AF have a higher amount and longer lines of conduction disorders across BB compared to patients without AF.[2] As expected, the current study illustrates again that patients with AF have more and longer lines of conduction disorders. In line with findings by Müller-Edenborn et al., conduction disorders observed in the current study may be the result of local fibrosis. Although conduction disorders at BB may reflect pathology through the entire atrial myocardium such as the

anteroseptal insertion, in our preliminary data with epicardial mapping of the entire atrial surface, conduction disorders seem mainly limited to BB in patients with AF which was not shown in the current study due to the extensiveness of data.[15] Yet, it remains unknown whether conduction disorders at BB facilitated development of AF or whether AF episodes further increased the amount of conduction disorders.

It is commonly known that atrial remodeling during AF enhances AF maintenance ("AF begets AF").[16] AF initiates electrical remodeling and is considered a cause of progression to persistent AF. In brief, electrical remodeling consists of e.g. shortening of atrial refractoriness due to ion-channels adaptations.[17-20] The remodeling is reversible; time until normal state depends on the duration of AF. Next to electrical remodeling during AF, structural remodeling has been characterized as well, such as myocyte hypertrophy, myolysis and accumulation of glycogen (dedifferentiation).[17-20] It is still a matter of debate whether AF itself also causes degeneration of myocytes with fibrotic deposition. In the goat model of persistent AF, structural remodeling was observed without production of fibrosis after >20 weeks of persistent AF induced by rapid atrial pacing.[18] In contrast, others suggest that atrial fibrosis might be enhanced during AF which in turn makes AF more persistent and therapeutic resistant.[19, 20]

The current study showed that conduction disorders are more present in patients with previous AF episodes, but the cause of the higher amount of conduction disorders is unknown. This is a non-longitudinal observational study and therefore the previous effects of conditions such as hypertension (blood pressure alterations) and atrial pressure that change over time and which may contribute to conduction disorders remain poorly understood. In addition, we did not observe clear differences in conduction disorders between patients with IHD and VHD after correction for AF history, although the incidence of AF was higher in patients with VHD conform previous many clinical studies. The similar amount of conduction disorders between IHD and VHD may be caused by the complex pathophysiology in patients with IHD (e.g. atrial ischemia, elevated left ventricular pressure, diastolic dysfunction) and VHD (e.g. myocyte loss, increased effective refractory period due to reversible interstitial fibrosis, diastolic atrial dilatation).[21, 22] Moreover, there were differences in patient characteristics such as gender, hypertension and diabetes mellitus that may have a confounding effect on conduction disorders. Yet, further analyses demonstrated either no significant effect or a weak significant correlation ($r < 0.30$) in each group.

Altogether, this leads to a chicken-and-egg situation; does VHD contribute to conduction disorders across BB predisposing to AF development? Or does AF enhance production of

fibrosis resulting in a higher amount of conduction disorders across BB? Future longitudinal and experimental studies could provide more insights in these unanswered questions.

Relation between mid-entry and patients with atrial fibrillation

BB is described as an important inter-atrial connection for conduction of electrical wavefronts.[5] As expected, BB was in the majority of our patients activated from the right to left. Yet, in line with a previous study,[2] we also observed SR wavefronts entering in the middle of BB. This pattern of activation was more frequently observed in patients with AF.

There are 2 possible explanations why patients with AF have a higher incidence of wavefronts activating BB from the middle area. First, patients with AF have significantly more conduction disorders across BB which are also frequently longer than in patients without AF. Due to these long lines of conduction disorders, wavefronts are forced to propagate outside BB and around these lines, subsequently entering BB in the middle ('quasi mid-entry') behind these lines of conduction disorders. Second, previously it was demonstrated that the interatrial septum has connections with BB that provides the possibility for wavefronts to propagate to the middle of BB.[23] Propagation of SR wavefronts across BB from either right to left or from the middle (septum) to surrounding areas could depend on 2 factors: distance (S) or conduction velocity (CV) from sinus node to BB. Dobrzynski et al. and Ho et al. previously described that the sinoatrial node is more a sleeve rather than a node like structure at the intercaval region.[24, 25] In patients with AF, the sinus node origin may vary, resulting in a longer distance between the initial excitation site and the right side of BB (↑ S), although Li et al. did not always find a relation between origin of the sinus node (intranodal) 'pacing' area and earliest atrial activation sites.[26] Furthermore, patients with AF have more conduction disorders across BB. These conduction disorders might also be more present between the sinus node and BB such as the preferential upper sinoatrial conduction pathway.[26] As a result, wavefronts propagate slower towards the right side of BB (↓ CV) and, therefore, propagation occurs through a different faster route such as towards the septum and subsequently upwards to BB.

Study limitations

High-resolution epicardial mapping was performed of BB, but conduction properties of the remainder of the atria were not described. Therefore, it is unknown what the effect of conduction disorders in the remaining of the atria is on for example wavefront entry sites. Simultaneous endo- and epicardial of the entire atria could provide more insight in e.g. wavefront propagation, but this is so far technically impossible. Furthermore, patients were using antiarrhythmic drugs including mainly class II. Although some patients were using class III antiarrhythmic drugs which may affect conduction properties, these effects were not analyzed due to the limited number of patients. Patients with AF episodes were

included. Yet, asymptomatic AF episodes in patients might have been missed which could result in an underestimation of the number of patients with a history of AF. In line with that, both sensitivity and specificity of a mid-entry site and long lines of conduction disorders for the presence of AF episodes could be positively/negatively affected in case none of the AF episodes were missed. Moreover, this also accounts for LPAF as episodes of LPAF may have been missed during follow-up which made further analyses impossible for e.g. conduction disorders and development of LPAF.

CONCLUSION

Conduction disorders are equally present between patients with IHD and VHD, but patients with AF have more and longer lines of conduction disorders. Propagation of wavefronts across BB during SR occurs mainly from the right atrial site towards left atrial site, but wavefronts also emerge in the middle of BB. Wavefronts entering BB in the middle were seen in patients with all different types of underlying heart diseases, but these were especially observed in patients with a history of AF. Altogether, a wavefront entering BB in the middle and/or long lines of conduction disorders are associated with absence of previous AF episodes.

REFERENCES

1. Markides V, Schilling RJ, Ho SY, Chow AW, Davies DW, Peters NS. Characterization of left atrial activation in the intact human heart. Circulation 2003;107:733-9.
2. Teuwen CP, Yaksh A, Lanters EA, Kik C, van der Does LJ, Knops P, Taverne YJ, van de Woestijne PC, Oei FB, Bekkers JA, Bogers AJ, Allessie MA, de Groot NM. Relevance of Conduction Disorders in Bachmann's Bundle During Sinus Rhythm in Humans. Circ Arrhythm Electrophysiol 2016;9:e003972.
3. Khaja A, Flaker G. Bachmann's bundle: does it play a role in atrial fibrillation? Pacing Clin Electrophysiol 2005;28:855-63.
4. van Campenhout MJ, Yaksh A, Kik C, de Jaegere PP, Ho SY, Allessie MA, de Groot NM. Bachmann's bundle: a key player in the development of atrial fibrillation? Circ Arrhythm Electrophysiol 2013;6:1041-6.
5. Baranchuk A. Interatrial Block and Supraventricular Arrhythmias: Clinical Implications of Bayés' Syndrome: Cardiotext Publishing; 2017.
6. Bailin SJ, Adler S, Giudici M. Prevention of chronic atrial fibrillation by pacing in the region of Bachmann's bundle: results of a multicenter randomized trial. J Cardiovasc Electrophysiol 2001;12:912-7.
7. Nigro G, Russo V, Politano L, Della Cioppa N, Rago A, Arena G, Papa AA, Paoli LD, de Chiara A, Russo MG, Golino P, Calabro R. Does Bachmann's bundle pacing prevent atrial fibrillation in myotonic dystrophy type 1 patients? A 12 months follow-up study. Europace 2010;12:1219-23.
8. Benjamin EJ, Levy D, Vaziri SM, D'Agostino RB, Belanger AJ, Wolf PA. Independent risk factors for atrial fibrillation in a population-based cohort. The Framingham Heart Study. JAMA 1994;271:840-4.
9. Lanters EAH, Yaksh A, Teuwen CP, van der Does L, Kik C, Knops P, van Marion DMS, Brundel B, Bogers A, Allessie MA, de Groot NMS. Spatial distribution of conduction disorders during sinus rhythm. Int J Cardiol 2017;249:220-225.
10. Knol WG, Teuwen CP, Kleinrensink GJ, Bogers A, de Groot NMS, Taverne Y. The Bachmann bundle and interatrial conduction: comparing atrial morphology to electrical activity. Heart Rhythm. 2019;16:606-14.
11. Moe GK, Abildskov JA. Atrial fibrillation as a self-sustaining arrhythmia independent of focal discharge. Am Heart J. 1959;58:59-70.
12. de Groot N, van der Does L, Yaksh A, Lanters E, Teuwen C, Knops P, van de Woestijne P, Bekkers J, Kik C, Bogers A, Allessie M. Direct Proof of Endo-Epicardial Asynchrony of the Atrial Wall During Atrial Fibrillation in Humans. Circ Arrhythm Electrophysiol. 2016;9:e003648.
13. Müller-Edenborn B, Chen J, Allgeier J, Didenko M, Moreno-Weidmann Z, Neumann FJ, Lehrmann H, Weber R, Arentz T, Jadidi A. Amplified sinus-P-wave reveals localization and extent of left atrial low-voltage substrate: implications for arrhythmia freedom following pulmonary vein isolation. Europace. 2020;22:240-249.
14. Legato MJ, Bull MB, Ferrer MI. Atrial ultrastructure in patients with fixed intra-atrial block. Chest. 1974;65(3):252-61.
15. van der Does LJME, Lanters EAH, Teuwen CP, Mouws EMJP, Yaksh A, Knops P, Kik C, Bogers AJJC, de Groot NMS. The Effects of Valvular Heart Disease on Atrial Conduction During Sinus Rhythm. J Cardiovasc Transl Res. 2020;13:632-639.
16. Wijffels MC, Kirchhof CJ, Dorland R, Allessie MA. Atrial fibrillation begets atrial fibrillation. A study in awake chronically instrumented goats. Circulation. 1995;92:1954-68.
17. Ausma J, Wijffels M, Thone F, Wouters L, Allessie M, Borgers M. Structural changes of atrial myocardium due to sustained atrial fibrillation in the goat. Circulation. 1997;96:3157-63.

18. Dispersyn GD, Ausma J, Thoné F, Flameng W, Vanoverschelde JL, Allessie MA, Ramaekers FC, Borgers M. Cardiomyocyte remodelling during myocardial hibernation and atrial fibrillation: prelude to apoptosis. Cardiovasc Res. 1999;43:947-57.
19. Lin CS, Pan CH. Regulatory mechanisms of atrial fibrotic remodeling in atrial fibrillation. Cell Mol Life Sci. 2008;65:1489-508.
20. Frustaci A, Chimenti C, Bellocci F, Morgante E, Russo MA, Maseri A. Histological substrate of atrial biopsies in patients with lone atrial fibrillation. Circulation. 1997;96:1180-4.
21. Aguero J, Galan-Arriola C, Fernandez-Jimenez R, Sanchez-Gonzalez J, Ajmone N, Delgado V, Solis J, Lopez GJ, de Molina-Iracheta A, Hajjar RJ, Bax JJ, Fuster V, Ibáñez B. Atrial Infarction and Ischemic Mitral Regurgitation Contribute to Post-MI Remodeling of the Left Atrium. J Am Coll Cardiol. 2017;70:2878-89.
22. Goette A, Kalman JM, Aguinaga L, Akar J, Cabrera JA, Chen SA, Chugh SS, Corradi D, D'Avila A, Dobrev D, Fenelon G, Gonzalez M, Hatem SN, Helm R, Hindricks G, Ho SY, Hoit B, Jalife J, Kim YH, Lip GY, Ma CS, Marcus GM, Murray K, Nogami A, Sanders P, Uribe W, Van Wagoner DR, Nattel S. EHRA/HRS/APHRS/SOLAECE expert consensus on atrial cardiomyopathies: definition, characterization, and clinical implication. Europace. 2016;18:1455-90.
23. Platonov PG, Mitrofanova L, Ivanov V, Ho SY. Substrates for intra-atrial and interatrial conduction in the atrial septum: anatomical study on 84 human hearts. Heart Rhythm. 2008;5:1189-95.
24. Dobrzynski H, Li J, Tellez J, Greener ID, Nikolski VP, Wright SE, Parson SH, Jones SA, Lancaster MK, Yamamoto M, Honjo H, Takagishi Y, Kodama I, Efimov IR, Billeter R, Boyett MR. Computer three-dimensional reconstruction of the sinoatrial node. Circulation. 2005;111:846-54.
25. Ho SY, Sanchez-Quintana D. Anatomy and pathology of the sinus node. J Interv Card Electrophysiol. 2016;46:3-8.
26. Li N, Hansen BJ, Csepe TA, Zhao J, Ignozzi AJ, Sul LV, Zakharkin SO, Kalyanasundaram A, Davis JP, Biesiadecki BJ, Kilic A, Janssen PML, Mohler PJ, Weiss R, Hummel JD, Fedorov VV. Redundant and diverse intranodal pacemakers and conduction pathways protect the human sinoatrial node from failure. Sci Transl Med. 2017;9:eaam5607.

SUPPLEMENTAL MATERIAL CHAPTER 7

Supplemental Table 1. Sub-analyses electrophysiological characteristics in patients with ischemic heart disease only, valvular heart disease only and ischemic and valvular heart disease combined.

	IHD	VHD	IVHD	
CD (%), med (Q)	1.8 (0.9–2.9)	1.6 (0.9–2.7)	1.8 (0.9–3.0)	ns
CB (%), med (Q)	1.1 (0–2.9)	1.3 (0.2–2.9)	2.1 (0.7–4.5)	ns
CDCB (%), med (Q)	3.0 (1.5–5.6)	3.2 (1.5–5.5)	3.8 (2.3–7.3)	ns
Total, N	193	62	49	
Mid-entry (%)	66 (34%)	28 (45%)	22 (45%)	ns
CDCB ≥12mm (%)	90 (46%)	35 (56%)	29 (59%)	ns
Mid-entry or CDCB ≥12mm (%)	116 (60%)	44 (71%)	35 (71%)	ns
No AF, N	179	42	43	
Mid-entry (%)	60 (34%)	17 (40%)	16 (37%)	ns
CDCB ≥12mm (%)	81 (45%)	19 (45%)	24 (56%)	ns
Mid-entry or CDCB ≥12mm (%)	104 (58%)	26 (61%)	29 (67%)	ns
AF, N	14	20	6	
Mid-entry (%)	6 (43%)	11 (55%)	6 (100%)	
CDCB ≥12mm (%)	9 (64%)	16 (80%)	5 (83%)	ns
Mid-entry or CDCB ≥12mm (%)	12 (86%)	18 (90%)	6 (100%)	ns

AF = atrial fibrillation; CD = conduction delay; CB = conduction block; CDCB = connected conduction delay and block; IHD = ischemic heart disease; IVHD = ischemic and valvular heart disease; med = median; N = number; ns = not significant (P>0.05); Q = quartiles; VHD = valvular heart disease.

8

Impact of the Arrhythmogenic Potential of Long Lines of Conduction Slowing at the Pulmonary Vein Area

Elisabeth Mouws
Lisette van der Does
Charles Kik
Eva Lanters
Christophe Teuwen
Paul Knops
Ad Bogers
Natasja de Groot

ABSTRACT

Background: Areas of conduction delay (CD) or block (CB) are associated with higher recurrence rates after ablative therapy for atrial fibrillation (AF). Thus far, there are no reports on quantification of the extensiveness of CD and CB at the pulmonary vein area (PVA) and their clinical relevance.

Methods: Intraoperative high-density epicardial mapping of the PVA (interelectrode distance: 2 mm) was performed during sinus rhythm (SR) in 268 patients (67±11 (21-84) years) with and without preoperative AF. For each patient, extensiveness of CD (17-29 cm/s) and CB (<17 cm/s) was assessed and related to the presence and type of AF.

Results: CD and CB occurred in respectively 242 (90%) and 183 (68%) patients. AF patients showed a higher incidence of continuous CDCB lines (AF: N=37 (76%); No AF: N=132 (60%); *P*=0.046), a two-fold number of lines per patient (CD: 7 (0-30) vs 4 (0-22), *P*<0.001; CB: 3 (0-11) vs 1 (0-12), *P*=0.003; CDCB: 2 (0-6) vs 1 (0-8), *P*=0.004) and a higher incidence of CD or CB lines ≥6 mm and CDCB lines ≥16 mm (*P*=0.011, *P*=0.025, *P*=0.027). Extensiveness of CD, CB, CDCB could not distinguish between the different AF types.

Conclusions: AF patients more often present with continuous lines of adjacent areas of CD and CB, whereas in patients without AF, lines of CD and CB are shorter and more often separated by areas with normal intra-atrial conduction. Between patients with a history of paroxysmal and persistent AF, however, a considerable overlap in the amount of conduction abnormalities at the PVA was observed.

INTRODUCTION

The pulmonary vein area (PVA) has been of particular interest in the pathophysiology of atrial fibrillation (AF) ever since Haïssaguere et al. demonstrated bursts of rapid ectopic beats as triggers for spontaneous AF.[1] Since then, treatment strategies for AF mainly focus on isolation of the pulmonary vein area by endocardial and/or epicardial ablation. Yet, recurrence rates are considerable for both patients with paroxysmal and persistent AF and are likely the result of either reconduction or transition of AF from a trigger driven to a more substrate driven disease.[2] To date, AF recurrences after ablation procedures remain difficult to predict. Yet, fibrosis at the left atrial posterior wall, resulting in conduction delay or block, appears to be associated with higher recurrence rates.[3, 4] It has been suggested that assessment of electropathology - including low voltages, fractionation and conduction abnormalities - during SR at the PVA may facilitate identification of target sites for ablation or can be used to predict AF recurrences after ablative therapy.[5–9]

In several mapping studies, a line of conduction block (CB) running vertically between the right and left pulmonary veins during SR was identified.[10–12] This CB line varied between patients in its continuity and could in some patients be altered by pacing, indicating that it was partly functional in nature.[10–12] Furthermore, this line was more frequently observed in patients with AF or mitral valve regurgitation.[11, 12] Based on histological findings in post-mortem hearts, the authors suggested that abnormal conduction was the result of a change in myocardial fiber direction.[10] Aside from this line of CB, other areas of conduction disorders were observed in only a minority of patients.[10–12] However, the degree and extent of conduction abnormalities during SR at the PVA have never been quantified and correlated with the different types of AF as defined by the ESC guidelines.[13] The goal of the present intraoperative high-resolution epicardial mapping study was therefore to detect and quantify conduction abnormalities at the PVA in a large cohort of patients during sinus rhythm (SR) and to investigate the association with AF persistence.

METHODS

Study population

The study population consisted of 268 successive adult patients undergoing elective coronary artery bypass grafting, aortic or mitral valve surgery, or a combination of valvular and bypass grafting surgery. This study was approved by the institutional medical ethical committee (MEC2010-054/MEC2014-393). Written informed consent was obtained from all patients and clinical data was extracted from electronic patient files.

Mapping procedure

Epicardial high-resolution mapping of the PVA was performed during SR from the sinus transversus along the borders of the right and left pulmonary veins (PVR and PVL) down towards the atrioventricular groove (Figure 1), as previously described in detail.[14] Local activation maps of PVR and PVL during SR were constructed by annotating the steepest negative slope of atrial potentials recorded at every electrode (see also Supplemental Figure 1). Heterogeneity in conduction was determined by quantifying the amount, number and length of lines of CD, CB and CDCB and its differences between patient groups on a 2 mm resolution scale. Lines of CD and CB were defined as time differences (Δt) of respectively 7-11 ms and ≥12 ms between adjacent electrodes.[15, 16]

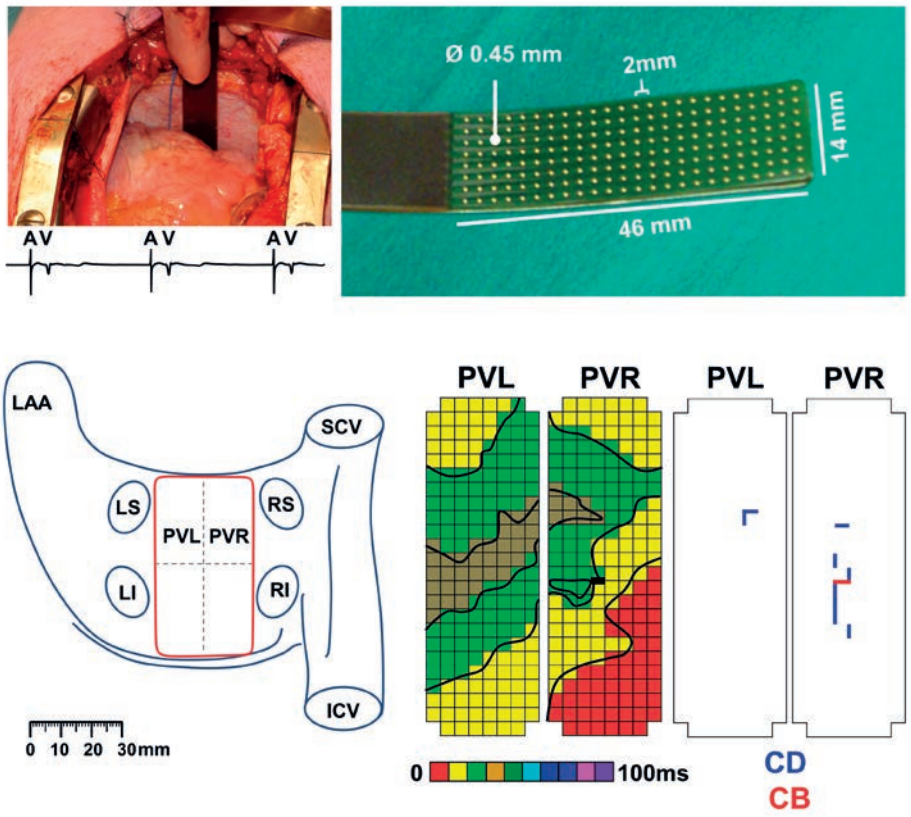

Figure 1. Mapping of the pulmonary vein area.
Top: Mapping of the pulmonary vein area with a 192-electrode array and corresponding electrograms recorded during 5 seconds of SR. Bottom: Schematic view of the pulmonary vein area (PVA) (left) and activation maps and conduction delay/block map (right, CD: blue lines, CB: red lines). A, atrial; V, ventricular; LAA, left atrial appendage; SCV, superior caval vein; ICV, inferior caval vein; PVL, pulmonary veins left; PVR, pulmonary veins right; LS, left superior; LI, left inferior; RS, right superior; RI, right inferior; CD, conduction delay; CB, conduction block.

Statistical analysis

Normally distributed data are described by mean±SD (minimum-maximum). Skewed data are described by median (minimum; interquartile range; maximum) and analyzed by Mann-Whitney U tests. Categorical data are expressed as numbers and percentages and analyzed with χ^2 or Fisher exact test when appropriate. ROC-curves for the difference in CD and CB lengths were constructed and cut-off values were based on sensitivity >50% and 1-specificity <50%. Multivariate regression analysis was performed to identify independent predictors for CD and CB. A *P*-value <0.05 was considered statistically significant.

RESULTS

Study population

Characteristics of the study population (N=268, 196 male (73%), 67±11 (21-84) years, BMI 28±5 (18-55) kg/m^2) are summarized in Table 1. Patients had either IHD (N=157, 59%) or (i) VHD (N=111, 41%; only valvular disease: N=63 (24%)). LA dilation was present in 58 patients (22%) and 49 patients (18%) had a history of AF. Most patients had a normal left ventricular function (N=203, 76%) and used class II antiarrhythmic drugs (AAD) (N=183, 68%).

Incidence of conduction delay and conduction block

Most patients showed lines of CD (N=242, 90%) and CB (N=183, 68%) at the PVA during SR. The number of lines of CD (4 (0-30)) was significantly higher than of CB lines (1 (1-12); *P*<0.001), though the maximum length of CB lines was longer (CD: 6 (2;4-10;20) mm; CB: 8 (2;4-12;44) mm; *P*<0.001, Figure 2). A clear turning point was observed at a length of ≥8 mm, from which point on, the incidence of CB lines exceeded the incidence of CD lines. Most patients also had continuous lines of CDCB (N=169 (63%), median no. 1 (0-6)); maximum length: 14 (4-72) mm.

A longitudinal line of CD or CB running vertically between the left and right pulmonary veins from superior to inferior was observed in 14 patients (5%), though varying in its continuity and length. Typical examples of activation maps and corresponding isochrones and CD/CB maps of these patients are shown in Figure 3. The incidence of this line was similar between patients without and with AF (*P*=0.295), as well as between IHD and (i) VHD patients (*P*=0.503). However, this line was more often observed in patients with LA dilation (N=6 (10%) than patients without LA dilation N=8 (4%), *P*=0.048). As displayed in Table 2, multivariate regression analysis revealed only the presence of AF episodes as an independent predictor for long lines of CD and CB at the PVA; clinical characteristics, including IHD, (i)VHD, LA dilation, gender, BMI, older age and LV dysfunction were not.

Table 1. Patient characteristics

Number of patients	268
Age (years)	67±11 (21–84)
Male	196 (73)
BMI (kg/m^2)	28±5 (18-55)
Underlying heart disease	N (%)
IHD	157 (59)
(i)VHD	111 (41)
Aortic valve stenosis	69 (26)
Aortic valve insufficiency	6 (2)
Mitral valve insufficiency	36 (13)
Left Atrial Dilation >45mm	58 (22)
History of AF	49 (18)
Paroxysmal	38 (14)
Persistent	11 (4)
Left ventricular function	
Normal	203 (76)
Mild dysfunction	52 (19)
Moderate dysfunction	11 (4)
Severe dysfunction	2 (1)
Antiarrhythmic drugs	197 (74)
Class I	2 (1)
Class II	183 (68)
Class III	12 (5)
Class IV	3 (1)

AF = atrial fibrillation; BMI = body mass index; IHD = ischemic heart disease; VHD = valvular heart disease; (i) VHD = ischemic and valvular heart disease.

Association between atrial fibrillation and heterogeneity in conduction

The upper panel of Figure 4 displays typical examples of activation maps and corresponding CD/CB maps obtained from a patient without AF and a patient with AF. Patients with AF more often have continuous lines of CDCB compared to patients without AF, as demonstrated in the middle left panel (AF: N=37, 76%; No AF: N=132, 60%; *P*=0.046). The number of lines of CD, CB and CDCB in patients with AF was approximately two-fold the number observed in patients without AF (CD: 7 (0-30) vs 4 (0-22), *P*<0.001; CB: 3 (0-11) vs 1 (0-12), *P*=0.003; CDCB: 2 (0-6) vs 1 (0-8), *P*=0.004 respectively). As demonstrated in Figure 4, the incidence of both CD and CB lines ≥6 mm was higher in patients with AF compared to patients without AF (CD: 69% (N=34) vs. 49% (N=108), *P*=0.011; CB: 59% (N=29) vs. 42% (N=91), *P*=0.025 respectively). Maximum lengths of continuous CDCB lines in patients with AF ranged from 8 to 72 mm, whereas in patients without AF these lengths ranged from 4 to 42 mm; CDCB lines ≥16 mm occurred more often in patients with AF (N=20 (41%) versus N=50 (25%), *P*=0.027).

Table 2. Analysis of risk factors for CD and CB maximum length in the upper 50th percentile

		CD			CB	
Univariate Analysis	OR	95%CI	*P*	OR	95%CI	*P*
Age (per year)	1.026	0.999-1.053	0.060	1.005	0.982-1.028	0.700
Male gender	0.602	0.339-1.067	0.082	0.961	0.547-1.688	0.891
(i)VHD	1.183	0.696-2.011	0.535	0.797	0.478-1.330	0.386
IHD	0.846	0.497-1.437	0.535	1.254	0.752-2.093	0.386
LA dilation	1.347	0.725-2.503	0.346	0.702	0.373-1.319	0.271
LVF (compared to normal function)						
mild dysfunction	1.390	0.726-2.659	0.320	1.162	0.620-2.179	0.640
moderate dysfunction	1.500	0.423-5.322	0.530	0.697	0.179-2.711	0.603
severe dysfunction	2.625	0.161-42.69	0.498	1.859	0.115-30.17	0.663
AF history	2.082	1.097-3.950	0.025	1.630	0.869-3.057	0.128
Multivariate Analysis						
Age (per year)	1.020	0.993-1.048	0.139			
Male gender						
(i)VHD						
IHD				1.370	0.792-2.370	0.260
LA dilation				0.670	0.347-1.292	0.232
LVF (compared to normal function)						
mild dysfunction						
moderate dysfunction						
severe dysfunction						
AF history	1.872	0.971-3.609	0.061	1.967	1.005-3.851	0.048
Hosmer and Lemeshow	0.808			0.778		

AF = atrial fibrillation; CB = conduction block; CD = conduction delay; CI = confidence interval; IHD = ischemic heart disease; LA = left atrial; LVF = left ventricular function; OR = odds ratio; VHD = valvular heart disease; (i)VHD = ischemic and valvular heart disease.

Hence, the presence of AF episodes was strongly associated with increased heterogeneity in conduction, marked not only by a higher incidence of CB and CDCB, but also by a higher number of lines of CD, CB and CDCB and more importantly longer lines of CD, CB and CDCB. Thus, AF patients more often present with continuous lines of adjacent areas of CD and CB, whereas in patients without AF, lines of CD and CB are more often separated by areas with normal intra-atrial conduction. These findings were validated in an age (5 year range), BMI (2 kg/m^2 range), gender and type of surgery matched case–control analysis (AF-No AF, 35-35). In addition, patients who developed de novo AF in the early postoperative phase (N=70, 32% of patients without preoperative AF) showed a trend towards more CB lines (*P*=0.055), a higher number of continuous CDCB lines (*P*=0.030) at the PVA and a trend towards a higher incidence of long CB lines >6 mm (*P*=0.073).

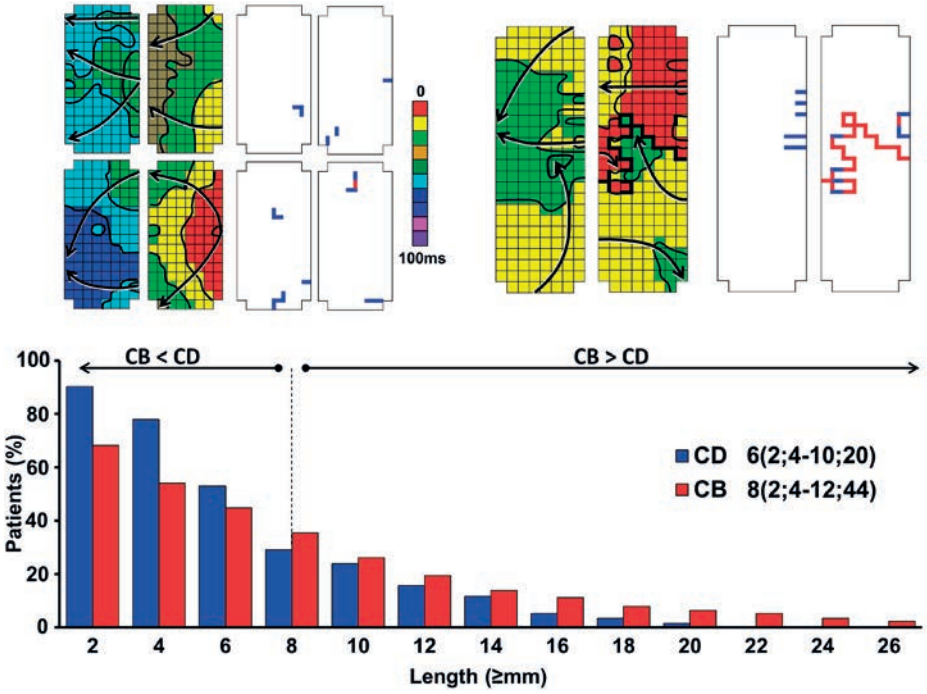

Figure 2. Characteristics of conduction delay and block.
Activation maps showing the typical difference between lines of conduction delay (blue lines) and lines of conduction block (red lines): lines of conduction block occur less frequently, yet extent over longer lengths. A turning point was observed at a length of 8 mm, as displayed in the lower panel. CD, conduction delay; CB, conduction block. Color-classes per 10 ms.

Severity of conduction abnormalities versus clinical atrial fibrillation classification

Figure 5 provides typical examples of PVA activation combined with corresponding CD and CB maps obtained from 2 patients with paroxysmal AF and 2 patients with persistent AF; the amount of conduction abnormalities in the one patient with paroxysmal AF is even higher than in the patient with persistent AF. Figure 5 shows that there is a large inter-individual variation in the amount of conduction abnormalities in both the paroxysmal and persistent AF group. There is also no difference between patients with paroxysmal AF and persistent AF in the number of CD, CB, CDCB lines (P=0.442, P=0.535 and P=0.951). Also, incidences of CD, CB and CDCB were similar (P=0.204, P=0.835 and P=0.708); nor could ROC-curve analyses identify a cut-off value for the length of lines distinguishing patients with persistent AF from paroxysmal AF. Duration of AF history was similar for patients with paroxysmal and persistent AF (P=0.429). Hence, although this is only a small group of patients, the overlap in severity of conduction abnormalities suggests that severity of conduction abnormalities at the PVA does not seem to clearly discriminate patients with paroxysmal AF from patients with persistent AF.

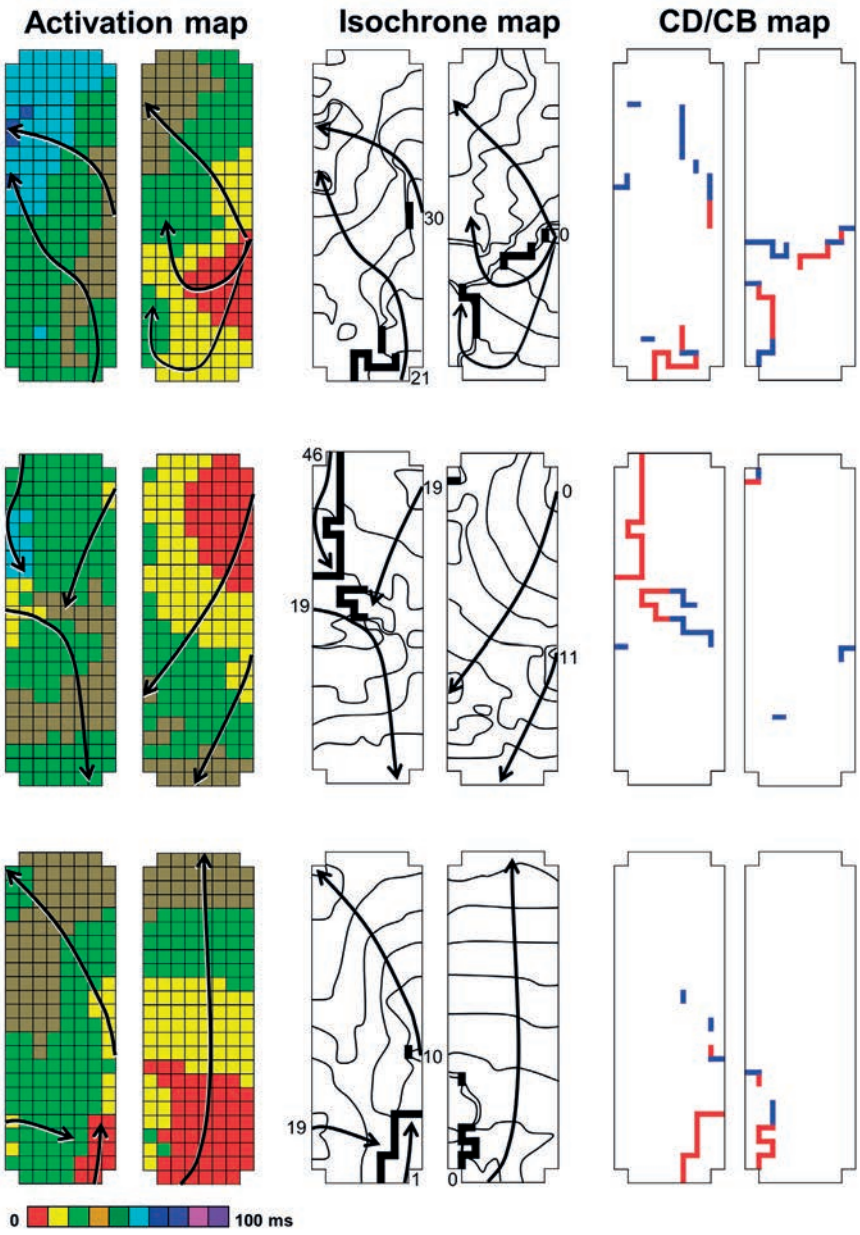

Figure 3. Longitudinal line of conduction delay/ block between the right and left pulmonary veins. Typical examples of activation maps with a line of CD (blue lines), CB (red lines) or CDCB running downwards between the right and left pulmonary veins, varying in its continuity. Corresponding isochrone maps (per 5 ms) and CD/CB maps are shown next to the activation maps. Arrows indicate the main wave trajectory; local activation times are provided next to the arrows. Lightning bolts indicate areas of simultaneous activation. Color-classes per 10 ms.

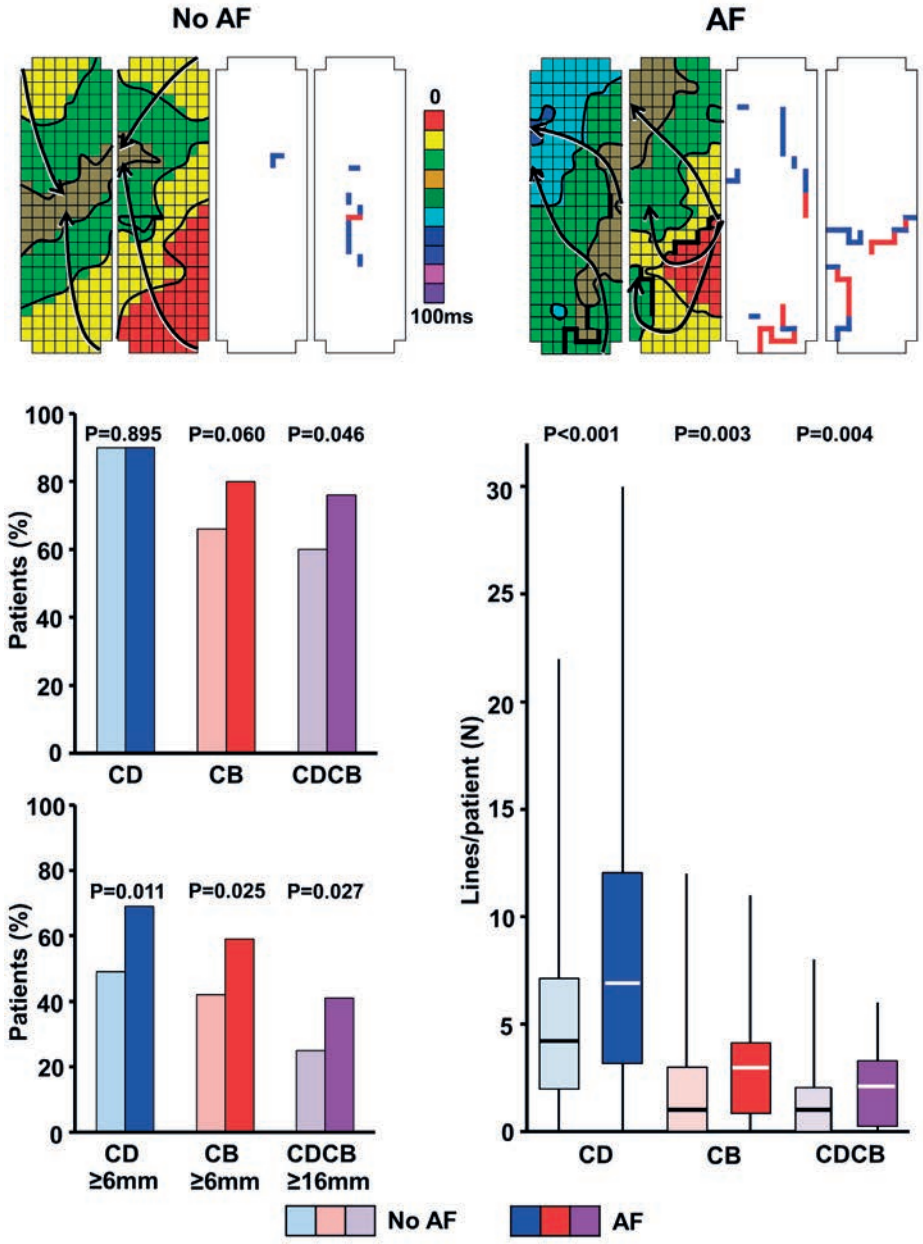

Figure 4. Differences in electropathology between patients without and with atrial fibrillation.
Top: Typical examples of activation maps of a patient without AF and a patient with AF. Patients with AF show more electropathology at the PVA, as displayed in the middle and bottom panels. AF patients particularly show a higher incidence of CB and continuous CDCB, a higher number of CD, CB and CDCB lines per patients and also longer lengths of CD (blue lines), CB (red lines) and CDCB lines. AF, atrial fibrillation; CD, conduction delay; CB, conduction block; CDCB, continuous conduction delay and block. Color-classes per 10 ms.

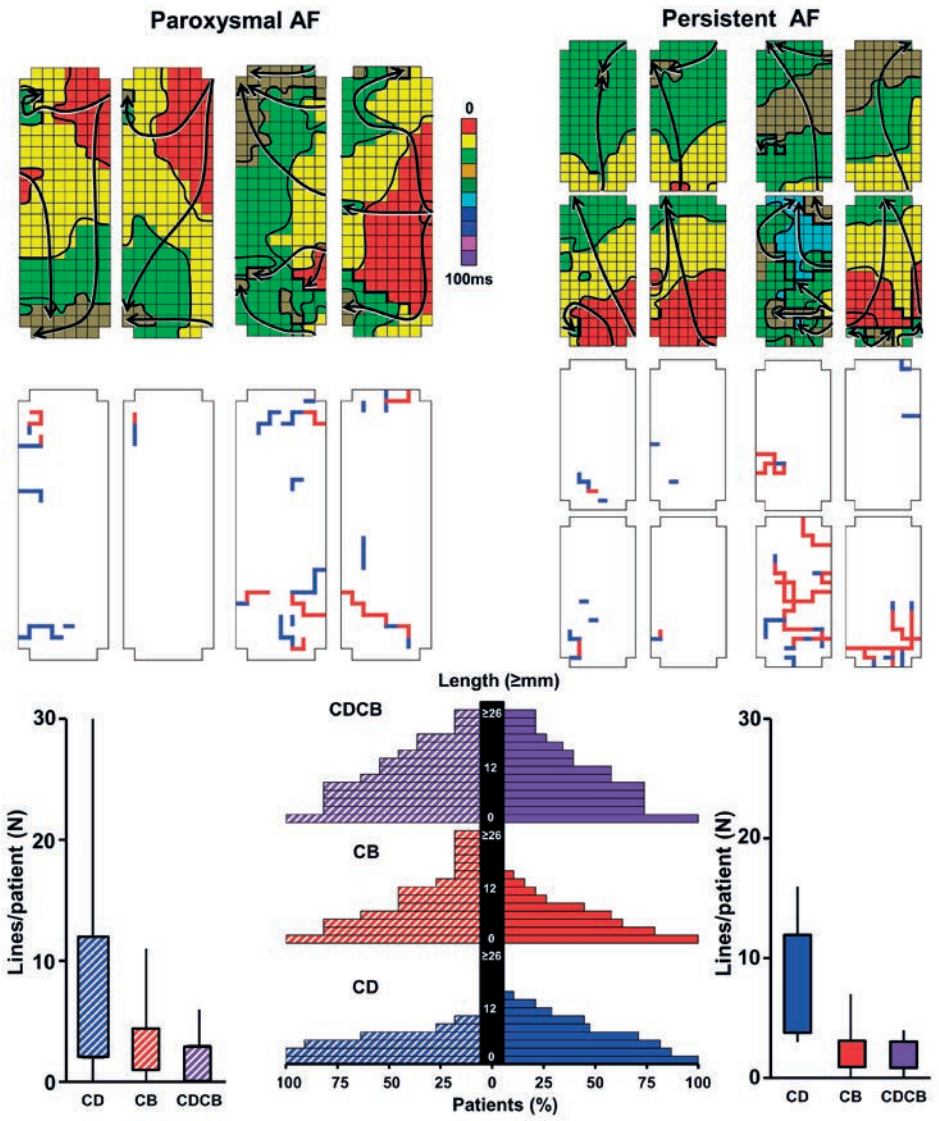

Figure 5. Overlap in electropathology between paroxysmal and persistent atrial fibrillation.
The top left panel shows activation maps of an IHD and VHD patient with paroxysmal AF both diagnosed 3 months prior to surgery. Corresponding CD/CB maps (CD: blue lines, CB: red lines) show a relatively small amount of CD/CB in the first patient, whereas the second patient has a large amount of CD/CB. The top right panel shows activation maps of patients with persistent AF. Both patients underwent mitral valve surgery and were diagnosed with persistent AF respectively 3 and 6 months prior to surgery; both patients underwent electrocardioversion to SR prior to mapping. In this case also the one patient has a relatively small amount of electropathology, whereas the other patient has a large amount of CD/CB. Hence, a considerable overlap in the amount of conduction disorders is observed between paroxysmal and persistent AF, which is also quantified in the bottom panel showing the number of lines per patient and the distribution of lengths of these lines. Color-classes per 10 ms.

DISCUSSION

Key findings

Intraoperative high-resolution epicardial mapping of the PVA during SR for the first time quantified and characterized different types of conduction abnormalities and related it to the presence of AF episodes. Current data demonstrated that patients with AF have more and longer lines of CD, CB and continuous CDCB whereas in patients without AF, short lines (<6 mm) of CD and CB separately are more diffusely present. Furthermore, the severity of conduction abnormalities at the PVA during SR does not discriminate between patients with paroxysmal and persistent AF.

Conduction abnormalities at the pulmonary vein area

To our best knowledge, only 3 previous studies have investigated conduction abnormalities at the posterior wall of the LA in humans during SR. In an endocardial noncontact mapping study by Markides et al., conduction at the LA was analyzed during SR in 19 patients with a history of paroxysmal AF.[10] They observed a vertical line of conduction block (interelectrode time interval 30 ms) extending from the LA roof across the posterior LA wall turning septally below the ostium of the right inferior pulmonary vein proceeding anteriorly towards the septal mitral annulus.[10] This CB line was present in all patients, though varied in its continuity, particularly during pacing from different sites.[10] In a minority of patients, the CB line disappeared completely during pacing.[10] Based on histological findings in postmortem hearts they suggested that the line of CB was caused by an abrupt change in myocardial fiber orientation at the subendocardium.[10]

Roberts-Thomson et al. performed epicardial mapping during SR in 34 patients without AF.[11] They observed a similar line of functional CD, defined as a conduction velocity between 10-20 cm/s, running vertically across the PVA, though only occurring in a minority of 5 patients.[11] In contrast to the findings of Markides et al., during pacing from superior and inferior positions at the PVA the line of CD now appeared in all patients.[11] In a subsequent study, epicardial SR mapping after electrocardioversion in 16 patients without AF and 5 patients with persistent AF showed a similar vertical CD line in 2 patients without AF, whereas this was observed in 4 of the AF patients.[12] However, when pacing from different sites, the CD line again appeared in all patients without AF and the number of CD lines increased in patients with AF to a maximum of 3 vertical lines running parallel to each other across the PVA.[12] Though the findings of Markides et al. and Roberts-Thomson et al. appear to contradict each other, it may be concluded that this line of CD was more evident in AF patients and was, at least in part, functional, as it varied during different pacing conditions. Moreover, besides the vertical line of abnormal conduction, no other CD/CB lines were observed in these studies.

In contrast to these previous studies, we observed conduction abnormalities scattered across the PVA with no clear predilection site. Lines of CD occurred in almost all patients and CB in approximately seventy percent of the population. The fact that the aforementioned studies did not observe any other lines of CD or CB at the PVA is remarkable, especially since study populations consisted of IHD patients, AF patients and patients with LA dilation due to mitral regurgitation. In all these patients, areas of fibrosis would be expected, particularly at the LA posterior wall. Our CB criteria correspond with a conduction velocity <17 cm/s, which is in the range of the CD criteria of Roberts-Thomson et al. Therefore, although our cut-off criteria are slightly more sensitive, the higher incidence of CD/CB cannot be totally explained by differences in cut-off values. Yet, the higher resolution of the mapping system used in current study may be the explanation for this discrepancy, as it contains the unique ability to identify lines of CD and CB with a minimum length of 2 mm. Furthermore, we did not set a minimum length or wavefront propagation criterion for lines of CD and CB, as opposed to previous studies. In our cohort, only a minority of patients showed a longitudinal line running downwards between the left and right pulmonary veins, which might be similar to the line observed in previous studies. However, this line varied in length and continuity and practically never consisted of a line of CB running continuously from the superior to the inferior of the posterior wall. The precise nature of this line, so far, remains unclear. If, as suggested by previous studies, a histological change in fiber direction would be the underlying cause, we would expect it to occur in the majority of patients during SR.

Conduction abnormalities and atrial fibrillation

In correspondence to previous studies, increased amounts of CD, CB and CDCB at the PVA were observed in AF patients. In AF patients, a higher incidence of CB, continuous CDCB and an almost two-fold number of separate CD, CB and CDCB lines per patient was observed. Also, CD, CB and CDCB lines extended over larger areas. These observations suggest a critical role for the spatial distribution of conduction abnormalities in AF development. A certain length of an area of abnormal conduction is required for re-entry to occur; this phenomenon was first demonstrated by Ortiz et al. in 7 canine hearts with sterile pericarditis.[17] In this study, the critical role of the length of an area of functional block in the right atrial free wall was observed. In case of stable atrial flutter, a functional CB line of 24 mm was observed, enabling re-entry to occur.[17] When the cycle length decreased, areas of slow conduction disappeared, resulting in a shorter line of functional CB with a mean length of 16 mm.[17] This resulted in unstable re-entrant circuits migrating across the atrial wall, giving rise to AF.[17] When the atrial wall already contains continuous long lines of structural CD and CB, it is likely more vulnerable to re-entry circuits to occur or for areas of functional block to connect, thereby reaching the critical length for AF initiation.

The future of atrial fibrillation therapy

Despite the fact that conduction abnormalities are more profound in patients with AF, the clinical categories of AF do not correspond with the amount of conduction disorders at the PVA during SR. In a previous study, we demonstrated a considerable intra-atrial variation in the distribution of conduction disorders across the right and left atrium, indicating that a low amount of CB at the PVA does not necessarily implicate a low amount of CB at other atrial regions.[18] Hence, either the arrhythmogenic substrate underlying AF is not located at the PVA in these patients or, although CD and CB measured during SR are indicators of structural conduction abnormalities, functional conduction disorders may only be revealed during triggers or AF. To date, ablative treatment strategies for AF focus primarily on isolation of the pulmonary veins. However, recurrence rates remain unsatisfactory. Recent studies have shown the complex and heterogeneous etiology of fractionated potentials, providing a possible explanation of the low success rate of ablative therapy targeting these complex fractionated potentials.[19]

Furthermore, recent studies have revealed that, aside from well-known effects of increased renin-angiotensin-system activation, cardiac endothelin-1 levels may also play an in important role in AF pathogenesis.[20] Endothelin-1 expression, promoting myocyte hypertrophy and interstitial fibrosis, was increased during AF compared to SR.[20] Particularly, endothelin-1 levels were higher at the LA and in patients with VHD, leading to the presumption this may play a substantial role in the vulnerability of these patients for AF development.[20] Also, increased endothelin-1 levels are regarded as an important factor in AF persistence. As endothelin-1 production is stretch mediated, atrial regions subjected to greater wall stress may also produce higher levels of endothelin-1, thereby leading to a regional differences in conduction abnormalities.[20]

Limitations

Whether general anesthesia influences conduction is yet to be investigated; however, as a standard anesthetic protocol was used for all patients, equal dispersion of possible effects can be assumed. The number of AF patients was relatively small; thereby, when comparing patients with persistent and paroxysmal AF, conclusions should be drawn cautiously. In addition, although LGE-MRI is a feasible technique to detect cardiac fibrosis, it was logistically and financially not possible to perform LGE-MRI prior to surgery in these patients.

CONCLUSION

Intraoperative high-resolution epicardial mapping of the PVA during SR for the first time quantified and characterized different types of conduction abnormalities and dem-

onstrated that presence of AF episodes is associated with continuous lines of adjacent areas of CD and CB, whereas in patients without AF, lines of CD and CB are shorter and more often separated by areas with normal intra-atrial conduction. AF patients showed a two-fold number of CD, CB and CDCB lines per patient, which also extended over longer lengths. This study demonstrated a considerable overlap in the amount of conduction abnormalities at the PVA between patients with a history of paroxysmal and persistent AF. Studies quantifying of the extensiveness of electropathology by various parameters, including conduction abnormalities, may contribute to the future development of a more accurate risk estimation of recurrent AF after ablative therapy and will thereby enable more patient tailored care in the future.

REFERENCES

1. Haïssaguerre M, Jaïs P, Shah DC, Takahashi A, Hocini M, Quiniou G, Garrigue S, Le Mouroux A, Le Metayer P, Clementy J. Spontaneous initiation of atrial fibrillation by ectopic beats originating in the pulmonary veins. N Engl J Med. 1998;339:659-66.
2. Yaksh a, Kik C, Knops P, Roos-Hesselink JW, Bogers a JJC, Zijlstra F, Allessie M, de Groot NMS. Atrial fibrillation: to map or not to map? Neth Heart J. 2014;22:259–66.
3. Ferrari R, Bertini M, Blomstrom-Lundqvist C, Dobrev D, Kirchhof P, Pappone C, Ravens U, Tamargo J, Tavazzi L, Vicedomini GG. An update on atrial fibrillation in 2014: From pathophysiology to treatment. Int J Cardiol. 2016;203:22–29.
4. Oakes RS, Badger TJ, Kholmovski EG, Akoum N, Burgon NS, Fish EN, Blauer JJ, Rao SN, DiBella EV, Segerson NM, Daccarett M, Windfelder J, McGann CJ, Parker D, MacLeod RS, Marrouche NF. Detection and quantification of left atrial structural remodeling with delayed-enhancement magnetic resonance imaging in patients with atrial fibrillation. Circulation. 2009;119:1758–1767.
5. Rolf S, Kircher S, Arya A, Eitel C, Sommer P, Sergio R, Gaspar T, Bollmann A, Altmann D, Piedra C, Hindricks G, Piorkowski C. Tailored atrial substrate modification based on low-voltage areas in catheter ablation of atrial fibrillation. Circ Arrhythmia Electrophysiol. 2014;7:825–833.
6. Vlachos K, Efremidis M, Letsas KP, Bazoukis G, Martin R, Kalafateli M, Lioni L, Georgopoulos S, Saplaouras A, Efremidis T, Liu T, Valkanas K, Karamichalakis N, Asvestas D, Sideris A. Low-voltage areas detected by high-density electroanatomical mapping predict recurrence after ablation for paroxysmal atrial fibrillation. J Cardiovasc Electrophysiol. 2017;28:1393–1402.
7. Masuda M, Fujita M, Iida O, Okamoto S, Ishihara T, Nanto K, Kanda T, Tsujimura T, Matsuda Y, Okuno S, Ohashi T, Tsuji A, Mano T. Left atrial low-voltage areas predict atrial fibrillation recurrence after catheter ablation in patients with paroxysmal atrial fibrillation. Int J Cardiol. 2018;257:97–101.
8. Pachon MJC, Pachon MEI, Pachon MJC, Lobo TJ, Pachon MZ, Vargas RNA, Pachon DQ V, Lopez M FJ, Jatene AD. A new treatment for atrial fibrillation based on spectral analysis to guide the catheter RF-ablation. Europace. 2004;6:590–601.
9. Roberts-Thomson KC, Kistler PM, Sanders P, Morton JB, Haqqani HM, Stevenson I, Vohra JK, Sparks PB, Kalman JM. Fractionated atrial electrograms during sinus rhythm: Relationship to age, voltage, and conduction velocity. Heart Rhythm. 2009;6:587–591.
10. Markides V, Schilling R, Ho S, Chow A, Wyn Davies D, Peters N. Characterization of Left Atrial Activation in the Intact Human Heart. Circulation. 2003;107:733–739.
11. Roberts-Thomson KC, Stevenson IH, Kistler PM, Haqqani HM, Goldblatt JC, Sanders P, Kalman JM. Anatomically Determined Functional Conduction Delay in the Posterior Left Atrium. Relationship to Structural Heart Disease. J Am Coll Cardiol. 2008;51:856–862.
12. Roberts-Thomson KC, Stevenson I, Kistler PM, Haqqani HM, Spence SJ, Goldblatt JC, Sanders P, Kalman JM. The role of chronic atrial stretch and atrial fibrillation on posterior left atrial wall conduction. Heart Rhythm. 2009;6:1109–1117.
13. Kirchhof P, Benussi S, Kotecha D et al. 2016 ESC Guidelines for the management of atrial fibrillation developed in collaboration with EACTS. Eur Heart J. 2016;37:2893–2962.
14. Mouws EMJP, Lanters EAH, Teuwen CP, van der Does LJME, Kik C, Knops P, Yaksh A, Bekkers JA, Bogers AJJC, de Groot NMS. Impact of Ischemic and Valvular Heart Disease on Atrial Excitation:A High-Resolution Epicardial Mapping Study. J Am Heart Assoc. 2018;7:e008331.
15. de Groot N, Houben R, Smeets J, Boersma E, Schotten U, Schalij M, Crijns H, Allessie M. Electropathological Substrate of Longstanding Persistent Atrial Fibrillation in Patients With Structural Heart Disease: Epicardial Breakthrough. Circulation. 2010;122:1674–1683.

16. Spach MS, Dolber PC, Heidlage JF. Influence of the passive anisotropic properties on directional differences in propagation following modification of the sodium conductance in human atrial muscle. A model of reentry based on anisotropic discontinuous propagation. Circ Res. 1988;62:811–832.
17. Ortiz J, Niwano S, Abe H, Rudy Y, Johnson NJ, Waldo AL. Mapping the conversion of atrial flutter to atrial fibrillation and atrial fibrillation to atrial flutter. Insights into mechanisms. Circ Res. 1994;74:882–894.
18. Lanters EAH, Yaksh A, Teuwen CP, van der Does LJME, Kik C, Knops P, van Marion DMS, Brundel BJJM, Bogers AJJC, Allessie MA, de Groot NMS. Spatial distribution of conduction disorders during sinus rhythm. Int J Cardiol. 2017;249:220–225.
19. van der Does LJME, Knops P, Teuwen CP, Serban C, Starreveld R, Lanters EAH, Mouws EMJP, Kik C, Bogers AJJC, de Groot NMS. Unipolar atrial electrogram morphology from an epicardial and endocardial perspective. Heart Rhythm. 2018;15:879–887.
20. Mayyas F, Niebauer M, Zurick A, Barnard J, Gillinov AM, Chung MK, Van Wagoner DR. Association of left atrial endothelin-1 with atrial rhythm, size, and fibrosis in patients with structural heart disease. Circ Arrhythm Electrophysiol. 2010;3:369–79.

SUPPLEMENTAL MATERIAL CHAPTER 8

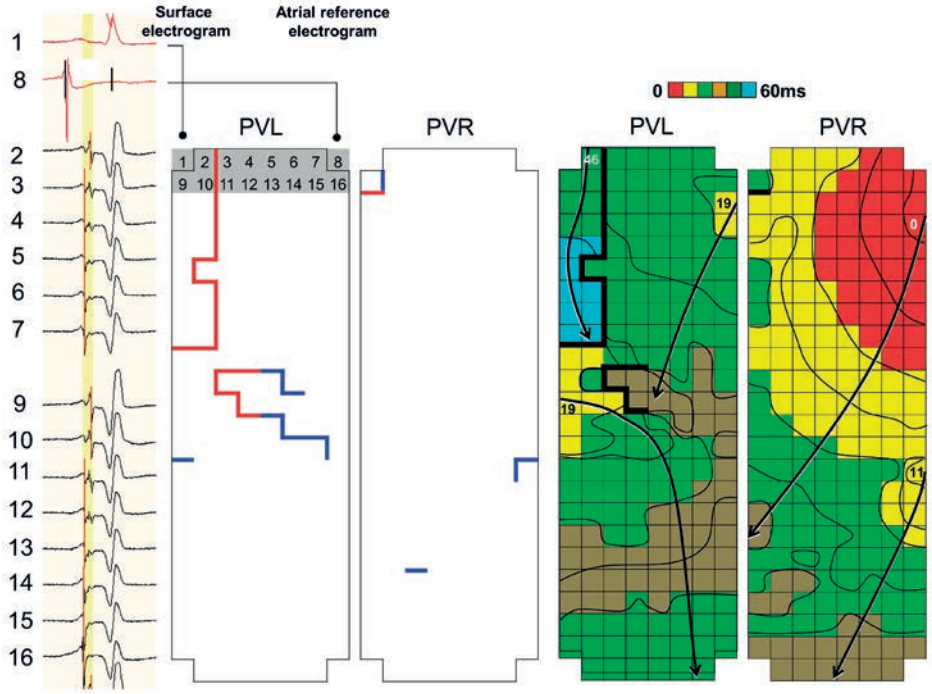

Supplemental Figure 1. Identification of conduction abnormalities.
From left to right, first a sample of potentials recorded simultaneously from the first 2 rows of electrodes on the electrode array at the left PVA is shown. The surface electrogram and the atrial reference electrogram are recorded on electrode 1 and 8 respectively. The steepest negative slope is annotated by a red marking and indicates the local activation time. Note the clear difference in the position of the red marking between electrode 2 and 3 and between electrode 10 and 11. Following, the conduction delay and block map is shown, in which the line of conduction block between electrodes 2 and 3 and between electrodes 10 and 11 is visualized by a red line, which is also identifiable by the shift in color-class (per 10 ms) in the activation map and by the crowding of isochrones (per 5 ms) at these areas.

9

Direct Proof of Endo-Epicardial Asynchrony of the Atrial Wall During Atrial Fibrillation in Humans

Natasja de Groot
Lisette van der Does
Ameeta Yaksh
Eva Lanters
Christophe Teuwen
Paul Knops
Pieter van de Woestijne
Jos Bekkers
Charles Kik
Ad Bogers
Maurits Allessie

ABSTRACT

Background: The presence of focal fibrillation waves during atrial fibrillation (AF) can, beside ectopic activity, also be explained by asynchronous activation of the atrial endo- and epicardial layer and transmurally propagating fibrillation waves. In order to provide direct proof of endo-epicardial asynchrony, we performed simultaneous high-resolution mapping of the right atrial endo- and epicardial wall during AF in humans.

Methods: Intraoperative mapping of the endo- and epicardial right atrial wall was performed during (induced) AF in 10 patients with AF (paroxysmal: N=3, persistent: N=4, longstanding persistent: N=3) and 4 patients without a history of AF. A clamp made of two rectangular 8x16 electrode arrays (interelectrode distance 2 mm) was inserted into the incision in the right atrial appendage. Recordings of 10 seconds of AF were analyzed to determine the incidence of asynchronous endo-epicardial activation times (≥15 ms) of opposite electrodes.

Results: Asynchronous endo-epicardial activation ranged between 0.9-55.9% without preference for either side. Focal waves appeared equally frequent at endocardium and epicardium (11% vs 13%, *P*=0.18). Using strict criteria for breakthrough (presence of an opposite wave within 4 mm and ≤14 ms before the origin of the focal wave), the majority (65%) of all focal fibrillation waves could be attributed to endo-epicardial excitation.

Conclusions: We provided the first evidence for asynchronous activation of the endo-epicardial wall during AF in humans. Endo-epicardial asynchrony may play a major role in the pathophysiology of AF and may offer an explanation why in some patients therapy fails.

INTRODUCTION

Epicardial high density mapping in patients with AF and valvular heart disease has demonstrated that a considerable portion of fibrillation waves showed a focal spread of activation.[1] These focal waves were rarely repetitive and mainly appeared as solitary events. They could occur virtually everywhere in the atria and their coupling interval was often longer than the dominant AF cycle length. In addition, unipolar electrograms recorded at the origin of focal waves, exhibited small R-waves. Based on this indirect evidence, it was postulated that fibrillation waves with a focal pattern of activation could result from endo-epicardial breakthrough (EEB).[1] Since EEBs can only occur in the presence of electrical asynchrony between the endo- and epicardial layer, we hypothesized that the substrate of AF consists of layers of dissociated fibrillation waves that constantly 'feed' each other.[1] In order to demonstrate that endo-epicardial asynchrony (EEA) exists during AF, we performed simultaneous high-resolution, mapping of the endo- and epicardial wall of the right atrium in patients with or without a history of AF undergoing cardiac surgery for coronary artery disease and/or valvular heart disease.

METHODS

Study population

The study sample consisted of 14 patients (10 male, 67±8.3 years) without a history of AF (N=4) and with a history of AF (N=10). Surgical procedures that were performed included cardiac coronary bypass surgery (N=9), mitral valve surgery (N=7), aortic valve replacement (N=2) and tricuspid valve surgery (N=4). Three patients had paroxysmal AF, 4 persistent AF and 3 had persistent AF lasting longer than a year (LSPAF). Atrial enlargement was present in 5 patients. Clinical characteristics of the study population are provided in Table 1.

The mapping protocol was approved by the institutional ethical committee (MEC2010-054) and written informed consent was obtained from all patients prior to the surgical procedure. This study adhered to the declaration of Helsinki principles.

Intraoperative mapping procedure

The mapping study was performed immediately after sternotomy. Following heparinization and arterial cannulation, a temporary bipolar epicardial pacemaker wire was stitched to the right atrial free wall and served as a temporal reference electrode. The indifferent electrode consisted of a steel wire fixed to subcutaneous tissue of the thoracic cavity. If patients were in sinus rhythm at the onset of the mapping procedure, AF was induced by fixed rate pacing at the right atrial free wall using an additional temporary bipolar pacing

wire. The induction protocol started at a rate of 200 beats per minute (bpm). If induction was not successful after 3 burst attempts, the rate was increased by 50 bpm, up to maximal 400 bpm until AF occurred or atrial refractoriness was reached.

Table 1. Clinical characteristics

ID no.	Age (y)	Gender	History of AF	Cardiac surgery	LVF	Atrial dimension
1	65	M	No AF	CABG	good	normal
2	56	M	Persistent	MVP+TVP	good	normal
3	82	M	No AF	CABG	good	normal
4	53	M	Persistent	CABG	poor	RA enlargement
5	66	M	Persistent	MVP+AVR	moderate	LA+RA enlargement
6	80	M	Paroxysmal	CABG+MVP	good	normal
7	63	F	No AF	CABG	good	normal
8	67	M	No AF	CABG	good	normal
9	75	F	LSPAF	MVP+TVP	good	LA+RA enlargement
10	59	M	Persistent	CABG	moderate	normal
11	64	F	LSPAF	MVP+TVP	good	LA enlargement
12	64	M	Paroxysmal	CABG+AVR	good	normal
13	70	F	LSPAF	MVP+TVP	good	LA+RA enlargement
14	71	M	Paroxysmal	CABG+MVP	moderate	normal

M = male; F = female; AF = atrial fibrillation; LSPAF = longstanding persistent atrial fibrillation; CABG = coronary artery bypass grafting; MVP/R = mitral valve plasty/ replacement; TVP = tricuspid valve plasty; AVR = aortic valve replacement; LVF = left ventricular function; RA = right atrium; LA = left atrium.

Prior to commencement to extra-corporal circulation, a high-resolution endo-epicardial mapping clamp was introduced through the right atrial incision for the venous cannula and closed with a purse-string suture. The mapping device was positioned towards the crista terminalis and consisted of two identical rectangular electrode arrays of 8x16 electrodes (interelectrode distance 2 mm) positioned opposite to each other (Figure 1). The electrode arrays (GS Swiss PCB AG, Küssnacht, Switzerland) consist of an electroless nickel immersion gold (ENIG) plated electrode array, mounted on a thin, flexible DuPont™ Pyralux® copper-clad (25 µm thickness) polyimide laminate, and coverlay composite (25 µm) film (0.18 mm). As the space constant of the atrial myocardium is ≈2 mm, the effective spatial resolution of 2.0 mm makes it unlikely that narrow fibrillation wavefronts will not be detected.[2]

All recordings were amplified (gain 1000), filtered (bandwidth 0.5-400 Hz), sampled (1 KHz) and analogue to digital converted (16 bits). A calibration signal of 2 mV amplitude and 1000 ms pulse width was stored simultaneously with atrial electrograms on hard disk using a computerized mapping system. After completion of the mapping procedure, AF was terminated by electrical cardioversion or sustained until cardioplegia was conducted, depending on the operators' preference. Ten seconds of AF were recorded from every patient.

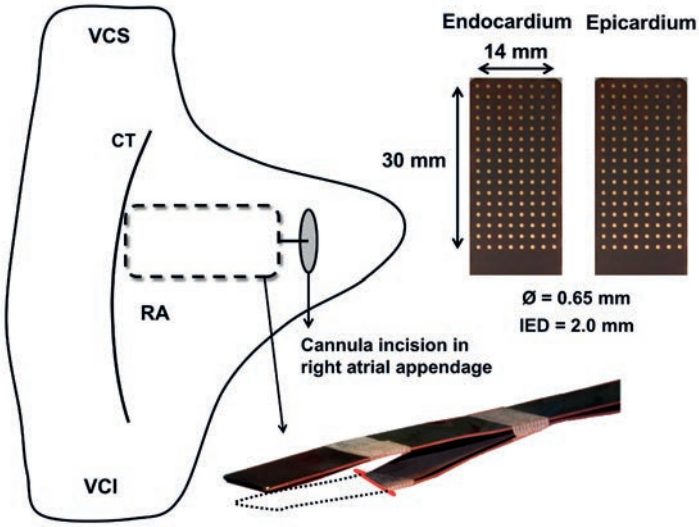

Figure 1. Endo-epicardial mapping device and technique.
The mapping device consists of two rectangular 8x16 electrode arrays with an interelectrode distance (IED) of 2 mm fixed to spatulas and positioned precisely opposite to each other. During endo-epicardial mapping, the endocardial leg is inserted in the right atrium (RA) through the incision of the venous cannula and closed with a purse-string suture. The array is positioned towards the crista terminalis (CT). VCS/VCI, vena cava superior/ inferior.

Mapping data

Series of endo- and epicardial wavemaps of 10 seconds AF were reconstructed from the two sets of 128 unipolar fibrillation electrograms, using custom-made software which has been previously described in detail.[1,3] For every electrode, local activation times were determined by marking the steepest negative deflection of the unipolar fibrillation electrograms. In case of a fractionated potential, the steepest negative deflection was chosen. At every electrode at either the endo- or epicardial layer, differences in endo-epicardial activation times were determined by measuring the smallest time delay within the opposite square base of 3x3 electrodes (Figure 2). The total amount of EEA during the entire recording period was expressed as the percentage of transmural differences of ≥15 ms for all endo- and epicardial recording sites. The combined asynchrony map (lower right panel of Figure 2) shows the longest time delay for every endo-epicardial electrode couple.

Wavemapping was used to identify the individual fibrillation waves. The starting point of the first fibrillation waves was the earliest activated site within the mapping area. Next, the entire mapping area was scanned in steps of 1 ms. For all electrodes activated during every step, the shortest time difference with the 8 neighboring electrodes was calculated. When the time difference was ≤12 ms (17 ms for oblique distances), the electrode site was added

to the territory of the surrounding wave. In case of a time difference >12 ms, the electrode was annotated as the starting point of a new wave. In the wavemap, fibrillation waves are color-coded according to their moment of entrance in the mapping area and the colors demarcate the area activated by that specific fibrillation wave.[4] Wavemaps also identify focal waves at either the endo- or epicardial surface. Focal fibrillation waves had to meet previously defined criteria. The breakthrough site of the focal fibrillation wave had to be located at least 2 electrodes away from the border of the mapping array and at least 1 reliable activation time should be available between the breakthrough site and the border of the mapping area. The morphology of the electrograms in the breakthrough region should not be distorted by large QRS complexes or artifacts. If this is the case, the wave is excluded from analysis. The focal wave should at least cover 4 electrodes. The origin of a focal wave

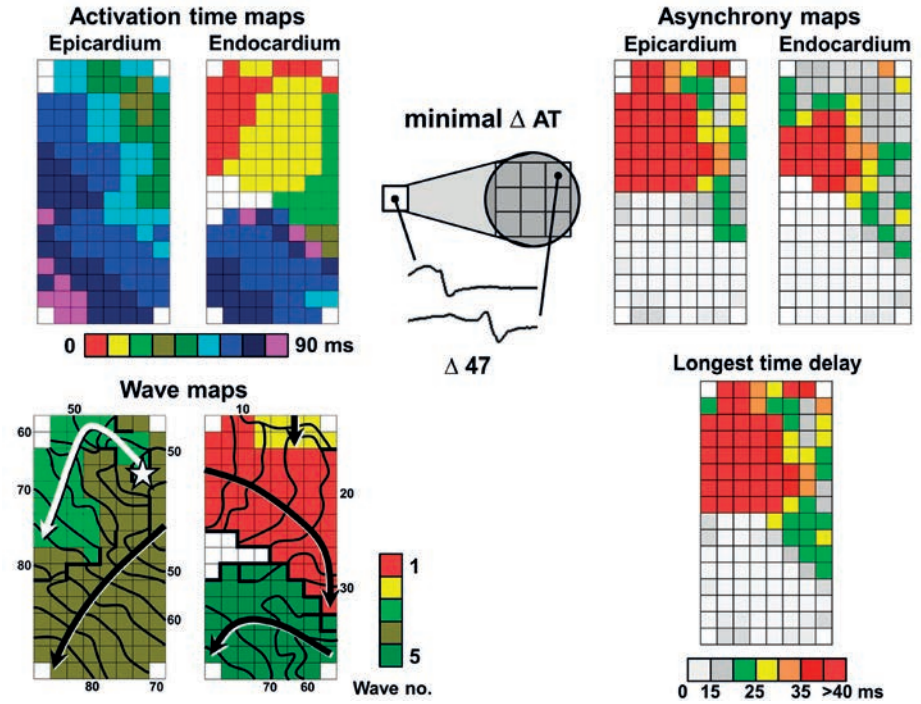

Figure 2. Construction of activation, wave and asynchrony maps.
Activation times determined at each individual electrode of endocardial and epicardial arrays are depicted in color-coded activation maps starting at the time of first activation. Wavemaps are automatically constructed which demonstrate the number and sequence of appearance of different waves activating the mapping area and also illustrate the origin of focal waves beginning within the mapping area (white star). Isochrones are set with intervals of 5 ms and indicate the main trajectory of each wave (black/white arrows). Thick black lines indicate conduction block (Δ≥12 ms). The asynchrony map of either the endocardial or epicardial layer consists of the endo-epicardial activation times defined by the smallest interval of the opposite nine activation times; the total asynchrony map shows the longest time delay assessed at every coupled recording site.

had to be activated earlier than all surrounding electrodes. If electrodes adjacent to the origin were activated simultaneously, all electrodes surrounding this area should also be activated later. Shift of the local activation time to a maximum of 3 ms earlier or later at the earliest activated electrode(s) should not result in disappearance of the focal wave. If a breakthrough site emerged along the border of another fibrillation wave, the time delay between that wave and the origin of the breakthrough had to be at least 40 ms.[1] All these criteria were checked manually by 2 independent investigators. A more detailed description of the mapping criteria with examples is provided in the supplemental material.

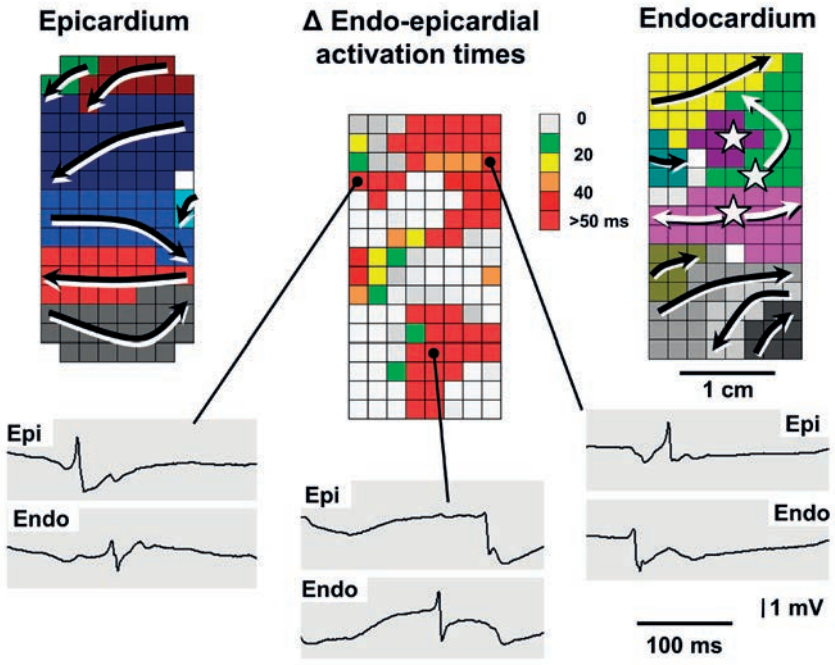

Figure 3. Endo-epicardial asynchrony in a patient with longstanding persistent atrial fibrillation.
The maps represent a single AF-cycle of 190 ms. The left and right panels show simultaneous wavemaps of the sub-epicardium and sub-endocardium of a part of the free wall of the right atrium (3.0 x 1.4 cm). The colors indicate the sequence of appearance of the different fibrillation waves (rainbow scheme followed by a grayscale). The arrows indicate the main trajectories of the waves. The sub-epicardium of the right atrium was activated by 7 narrow fibrillation waves, entering the mapping area from various directions. The endocardium was activated by 9 waves, 3 of them arising as focal waves in the middle of the mapping area (white stars). The local endo-epicardial time-differences are plotted in the central map. As a result of the different activation patterns at the endocardial and epicardial surface, major differences in endo-epicardial activation times existed (up to >50 ms). There was considerable spatial dispersion in EEA, with differences in endo- and epicardial activation times ranging from 0 to >50 ms. The 3 electrogram-pairs at the bottom, clearly show the marked differences in endocardial and epicardial activation times. Sometimes the epicardium was activated earlier (left panel), sometimes the endocardium (middle and right panels).

To assess whether focal fibrillation waves could originate from endo-epicardial breakthrough, in each case the opposite layer was examined for the presence of a fibrillation wave that could have served as a source for the focal wave. The presence of an opposite wavefront, within 4 mm distance and less than 15 ms before the origin of the focal wave, was considered to reflect transmural conduction based on normal atrial conduction properties. In this case, the focal wave could from a theoretically point of view be attributed to endo-epicardial breakthrough.

Statistical analysis

The Wilcoxon signed rank test was performed to assess the occurrence of EEA and focal waves between the epi- and endocardium.

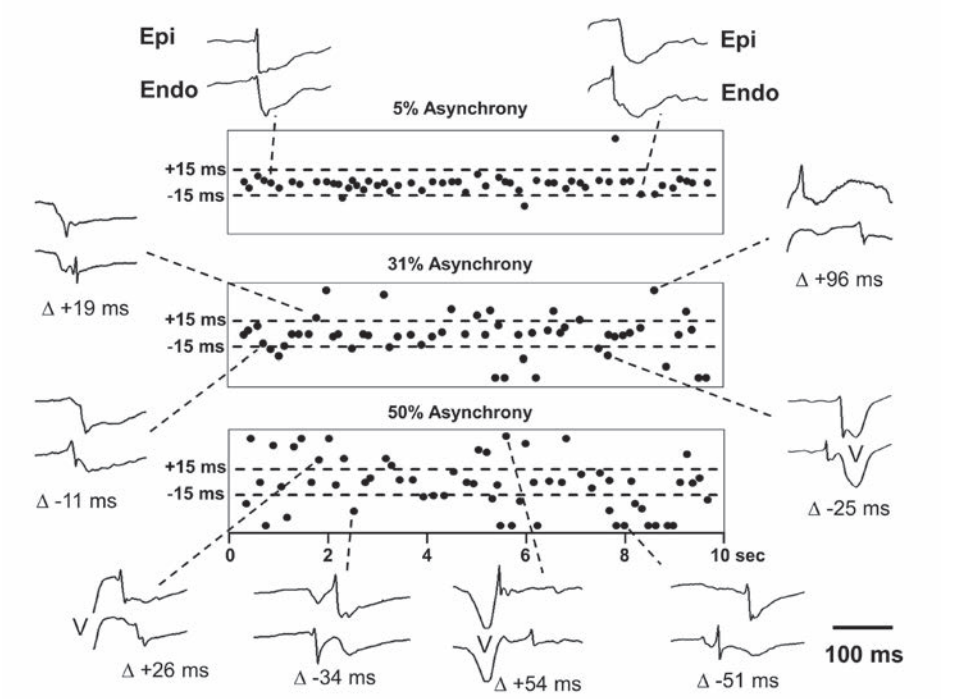

Figure 4. Spatial and temporal variation in endo-epicardial asynchrony during longstanding persistent AF. Endo-epicardial asynchrony plots of 10 seconds of AF, recorded at 3 different locations of the right atrial free wall in a patient with AF. The dashed horizontal lines demarcate the band of endo-epicardial synchrony; data points > ±50 ms are clipped. At different sites, the degree of EEA (delay ≥15 ms) varied from 5% (top panel), 31% (middle) and 50% (bottom). In addition to spatial dispersion, EEA also showed a strong temporal variation. As can be seen from the middle and lower plots, differences in endo-epicardial activation time seemed to occur randomly, without a clear predominance of either the sub-endocardial or sub-epicardial layer. Examples of pairs of unipolar endocardial and epicardial electrograms demonstrating the spatial temporal variation are given around the plots.

RESULTS

Endo-epicardial asynchrony

In the entire study population, the average percentage of missing data due to poor contact of the mapping array was 7.8±4.9%. The amount of conduction block was similar in the epicardial and endocardial plane with incidences of respectively 10.8±5.1% and 10.8±4.6%. Simultaneous epi- and endocardial wavemaps of a single AF-cycle recorded in a patient with longstanding persistent AF demonstrating EEA are shown in Figure 3. In this example, marked differences in activation patterns of the endo- and epicardial wall existed; almost all fibrillation waves at the endo- and epicardial surface appeared at different times and/or propagated in different directions.

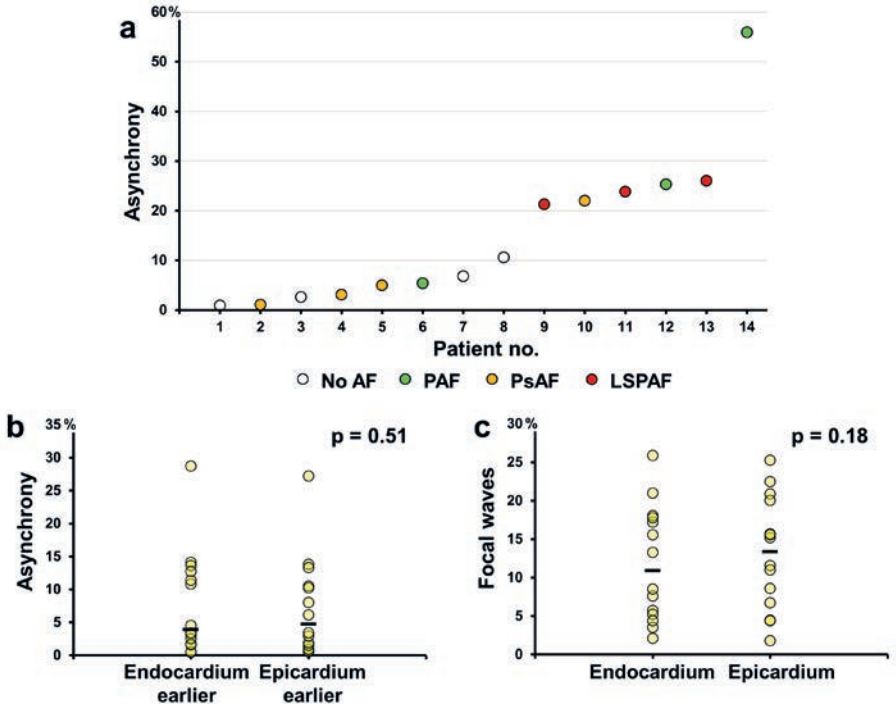

Figure 5. Endo-epicardial asynchrony levels and focal waves.
A: Graph demonstrating the total amount of EEA plotted for every patient separately; patients are ranked according to the degree of EEA. Type of AF (none, paroxysmal, persistent, longstanding persistent) is illustrated by the different grayscale tones. B and C: Dot plots and medians of (b) the incidence of asynchrony where endocardium versus epicardium is activated earlier in respect to the other and (c) the percentage of focal waves (of total number of waves) recorded at the endocardium and epicardium. For both parameters, there was no difference between the endocardial and epicardial layer (*P*=0.51 and *P*=0.18).

Table 2. Endo-epicardial asynchrony and focal waves

ID no.	AFCL (ms)	Endo-epicardial asynchrony (%)	Endocardium earlier (%)	Epicardium earlier (%)	Endo-epicardial activation SD (ms)	Endocardial fibrillation waves			Epicardial fibrillation waves		
						Number waves	Focal	Breakthroughs (% of focal)	Number waves	Focal	Breakthroughs (% of focal)
1	206±28	0.9	0.4	0.5	4.2	115	4	75	112	2	100
2	181±28	1.1	0.5	0.6	4.4	140	8	87	140	12	92
3	175±32	2.6	1.7	0.9	7.7	192	10	60	224	10	80
4	246±28	3.1	1.6	1.5	5.5	186	32	56	187	42	81
5	150±28	5.0	3.1	1.9	8.5	277	21	90	294	34	94
6	182±40	5.4	2.5	2.9	9.4	347	54	81	257	39	92
7	141±24	6.8	3.4	3.4	12.7	239	5	40	251	11	73
8	140±27	10.6	4.5	6.1	12.3	445	59	83	337	37	73
9	147±40	21.3	10.8	10.5	18.2	553	116	66	657	137	55
10	189±40	22.0	14.1	8.0	19.6	494	89	54	470	94	55
11	224±46	23.8	13.6	10.2	23.7	343	61	69	345	54	57
12	189±40	25.3	11.4	13.8	25.4	321	83	55	329	83	59
13	151±35	26.0	12.7	13.3	20.4	480	21	86	372	25	80
14	183±37	55.9	28.7	27.2	37.2	188	16	25	257	40	30
Total/ mean	-	15.0	7.8	7.2	-	4320	579	66	4232	620	65

AFCL = atrial fibrillation cycle length; SD = standard deviation.

In this same patient, the spatio-temporal variation in EEA during 10 seconds of AF is demonstrated in Figure 4. The degree of EEA varied considerably at different locations and at different times. No clear predominance of either the endocardial or the epicardial layer was observed. Examples of unipolar electrogram-pairs around the plots illustrate the high spatio-temporal variation in EEA.

As demonstrated in Figure 5, the total degree of EEA in our study population varied widely between 0.9 and 55.9% and there was no clear difference between endo-epicardial and epi-endocardial asynchrony (respectively 7.8±7.7% and 7.2±7.2%).

Focal fibrillation waves

In total 1199 focal fibrillation waves were observed, 579 arising at the sub-endocardium and 620 at the sub-epicardium. The equal distribution of focal fibrillation waves between both sides is shown in panel C of Figure 5. Applying the previously stated strict criteria for endo-epicardial breakthrough, 784 of all 1199 focal waves (65%) could be attributed to result from endo-epicardial excitation presuming that normal conduction occurs between

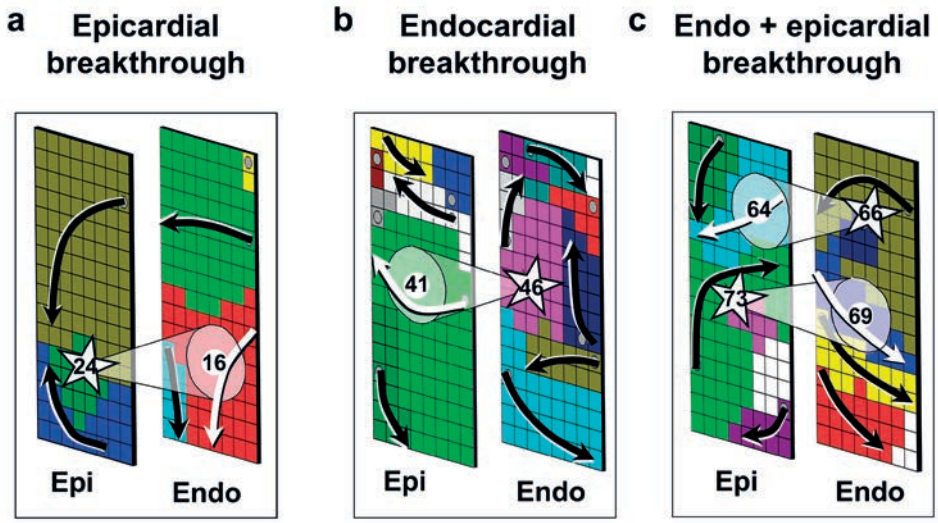

Figure 6. Three examples of endo-epicardial breakthroughs in a patient with longstanding persistent AF. A: A focal wave appeared at the epicardial surface at t=24 (white star). As can be seen from the associated endocardial wavemap, just a couple of milliseconds before an endocardial fibrillation wave (red) had passed that site at t=16 ms. A transmural conduction time of only 8 ms was taken as supportive evidence that the focal wave could be due to endo-epicardial breakthrough. B: An example of a focal wave arising at the endocardium at t=46. Again a fibrillation wave in the opposed layer (green) had passed that site just 5 ms before (at t=41). C: Two breakthroughs occurred at about the same time, one at the endocardium at t=66 and one at the epicardium at t=73 ms. In both cases, in the opposite layer a fibrillation wave passing the site of origin of the focal waves a few ms earlier at respectively t=64 and t=69, indicating that the focal waves could result from endo-epicardial breakthrough.

endo-epicardium (66% of the endocardial and 65% of the epicardial focal waves) (Table 2). Examples of pairs of endo-epicardial wavemaps showing focal fibrillation waves originating from EEB of fibrillation waves from the opposite layer are given in Figure 6.

DISCUSSION

Despite the relatively small number of patients, our data clearly show that a significant degree of EEA is present in the right atrium in patients with AF. Simultaneous endo-epicardial mapping of isolated canine atria, both during sinus rhythm and atrial pacing, only showed small differences in activation times (<1 ms). However, during atrial tachyarrhythmias, activation of the endo- and epicardial layers has been shown to become more asynchronous (up to 25 ms), particularly in the thicker parts of the atria.[5,6] In isolated fibrillating sheep atria, breakthrough sites appeared to be related to sub-endocardial muscle structures, the three-dimensional structure of the atria determining the appearance of focal waves during AF.[7] The concept that endo-epicardial dissociation might play an important role in the maintenance of AF, stems from experimental studies in the goat model of persistent AF.[8-10] These studies showed that the endo- and epicardial layers of the atrial wall became progressively dissociated during the first 6 months of AF. After that time, fibrillation waves in the endo- and epicardial layers often propagated at different speed and in different directions, and endo-epicardial breakthroughs became more abundant.[8,9]

In this study, the incidence of endo-epicardial asynchrony tended to be higher in patients with AF, though we did not observe a clear relation between duration of AF and degree of EEA. This can be explained by the fact that we did not map the left atrium and that if EEA of the left atrial wall also exists, it may play a more important role in the pathophysiology of AF. Also, our study population contained a small number of patients with a variety of cardiac diseases.

We provided additional data that most focal fibrillation waves could be explained by endo-epicardial excitation. Lee et al. also frequently observed focal fibrillation waves without any sustained focal activity in 18 patients with persistent AF.[11] In contrast, low-density mapping studies using a 64-pole basket catheter, have suggested that AF is maintained by a limited number of rapid stable sources (rotors and/or ectopic foci).[12,13] Body surface mapping during AF elucidated the presence of non-sustained re-entries and focal breakthroughs in certain domains of the atria.[14] Recently, we have discussed the discrepancies in the interpretation of high- and low-resolution mapping of AF in detail in a crosstalk paper.[15,16] The present study supports the concept that during AF, the endo- and epicardial layers of the atrial wall can be asynchronously activated.[1,16] The presence of dissociated

layers of fibrillation waves, will highly stabilize the fibrillatory process because, as soon as fibrillation waves die out, they can be replaced by breakthroughs from the opposite side.

In such a substrate, each layer will serve as a multi-site generator for the other layer. During 10 seconds of AF, more than 20-30 focal waves appeared at each side of the atrial wall, in an area of only 2.6 cm.[1] Extrapolating this number to the entire atrial surface, the total number of focal breakthrough waves can be estimated to exceed 10.000 per minute. However, we like to emphasize that the presence of EEA, off course does not disprove that also re-entry and focal activity may contribute to the maintenance of AF. In different stages of the development of a substrate of AF, the contribution of different mechanisms for perpetuation of AF may vary. We fully acknowledge the large body of evidence that re-entrant and focal mechanisms are operative during atrial fibrillation.[17-20] In fact, not all focal fibrillation waves in our patients could be attributed to endo-epicardial breakthrough, and sometimes two focal waves appeared simultaneously at the endo- and epicardial surface. Equally, our data do not rule out the possibility that some of the endo-epicardial breakthroughs formed part of a transmural re-entrant circuit. However, we venture to suggest that progressive, AF induced, structural atrial remodeling gradually transforms the atrial wall into multiple layers of narrow dissociated wavelets. With time, more and more focal breakthroughs will be generated, which progressively stabilizes the fibrillatory process. At the end, the main source of fibrillation waves is formed by an abundant number of focal breakthroughs, occurring virtually everywhere in the atria. This is in agreement with the recent finding of Haïssaguerre et al., that the number of driver regions increased with the duration of AF, until after 6 months almost the entire atrial wall acted as a driver (6 of all 7 regions).[14] It also explains why the termination rate of AF by driver ablation sharply declined after 6 months of AF.[14]

Study limitations

Our study population is presently limited to 14 patients and a larger number of patients is obviously required for a meaningful statistical analysis and to study the relation between persistence of AF and the degree of electrical asynchrony. Expanding the study population will also allow for statements about a possible correlation between EEA and breakthroughs. Moreover, the effective spatial resolution of the recordings is dependent on the number of electrodes with good tissue contact. Another limitation is, that so far, only a limited part of the atria has been accessible for endo-epicardial mapping (4.2 cm^2 of the right atrium). In order to get a full understanding of the role of EEA in the development of the substrate of AF, endo-epicardial mapping of the left atrium is needed as well. However, the left atrium is not standardly opened during cardiac surgery, only during selected procedures. In addition, opening the left atrium before cardiopulmonary bypass is associated with a considerable increase in the risk for air embolism which may cause brain injury. Therefore,

we decided it was not ethically responsible to perform endo-epicardial mapping of the left atrium for this pilot study.

Clinical implications

Knowledge of the substrate and various mechanisms of perpetuation of human AF is of great importance to understand the natural history of AF. At different stages, the substrate of AF may require different treatment modalities. At an early stage pulmonary vein isolation alone might be sufficient, whereas in a later stage also compartmentalization of the atria will be necessary to restore sinus rhythm. Furthermore, when the endo- and epicardial layers of the atria have become electrically dissociated, even extensive ablative therapies may be ineffective and palliative therapy would be a better option. Knowledge of the vulnerable parameter(s) for perpetuation of AF, and the ability to diagnose the stage of development of the substrate of AF, are essential for an individualized and staged therapy of atrial fibrillation.

REFERENCES

1. de Groot NMS, Houben RP, Smeets JL, Boersma E, Schotten U, Schalij MJ, Crijns H, Allessie MA. The electropathological substrate of longstanding persistent atrial fibrillation in patients with structural heart disease: epicardial breakthrough. Circulation. 2010;122:1674-1682.
2. Sakamoto Y, Goto M. A study of the membrane constant in the dog myocardium. Jap J Physiol. 1970;20:30-41.
3. Allessie MA, de Groot NM, Houben RP, Schotten U, Boersma E, Smeets JL, Crijns HJ. The electropathological substrate of longstanding persistent atrial fibrillation in patients with structural heart disease: longitudinal dissociation. Circ Arrhythm Electrophysiol. 2010;3:606-615.
4. Rogers JM, Usui M, KenKnight BH, Ideker RE, Smith WM. Recurrent wavefront morphologies: a method for quantifying the complexity of epicardial activation patterns. Ann Biomed Eng. 1997;25:761-768.
5. Schuessler RB, Kawamoto T, Hand DE, Mitsuno M, Bromberg BI, Cox JL, Boineau JP. Simultaneous epicardial and endocardial activation sequence mapping in the isolated canine right atrium. Circulation. 1993;88:250-263.
6. Derakhchan K, Li D, Courtemanche M, Smith B, Brouillette J, Pagé PL, Nattel S. Method for simultaneous epicardial and endocardial mapping of in vivo canine heart: application to atrial conduction properties and arrhythmia mechanisms. J Cardiovasc Electrophysiol. 2001;12:548-555.
7. Gray RA, Pertsov AM, Jalife J. Incomplete reentry and epicardial breakthrough patterns during atrial fibrillation in the sheep heart. Circulation. 1996;94:2649-2661.
8. Eckstein J, Maesen B, Linz D, Zeemering S, van Hunnik A, Verheule S, Allessie M, Schotten U. Time course and mechanisms of endo-epicardial electrical dissociation during atrial fibrillation in the goat. Cardiovasc Res. 2011;4:816-824.
9. Eckstein J, Zeemering S, Linz D, Maesen B, Verheule S, van Hunnik A, Crijns H, Allessie MA, Schotten U. Transmural conduction is the predominant mechanism of breakthrough during atrial fibrillation: evidence from simultaneous endo-epicardial high-density activation mapping. Circ Arrhythm Electrophysiol. 2012;6:334-341.
10. Verheule S, Eckstein J, Linz D, Maesen B, Bidar E, Gharaviri A, Schotten U. Role of endo-epicardial dissociation of electrical activity and transmural conduction in the development of persistent atrial fibrillation. Progress in Biophysics and Molecular Biology. 2014;115:173-185.
11. Lee G, Kumar S, Teh A, Madry A, Spence S, Larobina M, Goldblatt J, Brown R, Atkinson V, Moten S, Morton JB, Sanders P, Kistler PM, Kalman JM. Epicardial wave mapping in human long-lasting persistent AF: transient rotational circuits, complex wave fronts and disorganized activity. Eur Heart J. 2014;35:86-97.
12. Narayan SM, Krummen DE, Shivkumar K, Clopton P, Rappel WJ, Miller JM. Treatment of atrial fibrillation by the ablation of localized sources: CONFIRM (CONventional ablation for atrial fibrillation with or without Focal Impulse and Rotor Modulation) trial. J Am Coll Cardiol. 2012;60:628-636.
13. Narayan SM, Shivkumar K, Krummen DE, Miller JM, Rappel WJ. Panoramic electrophysiological mapping but not electrogram morphology identifies stable sources for human atrial fibrillation: stable atrial fibrillation rotors and focal sources relate poorly to fractionated electrograms. Circ Arrhythm Electrophysiol. 2013;6:58-67.
14. Haïssaguerre M, Hocini M, Denis A, Shah AJ, Komatsu Y, Yamashita S, Daly M, Amraoui S, Zellerhoff S, Picat MQ, Quotb A, Jesel L, Lim H, Ploux S, Bordachar P, Attuel G, Meillet V, Ritter P, Derval N, Sacher F, Bernus O, Cochet H, Jaïs P, Dubois R. Driver domains in persistent atrial fibrillation. Circulation. 2014;130:530-538.

15. Narayan SM, Jalife J. CrossTalk proposal: Rotors have been demonstrated to drive human atrial fibrillation. J Physiol. 2014;592:3163-3166.
16. Allessie MA and de Groot NM. CrossTalk opposing view: Rotors have not been demonstrated to be the drivers of atrial fibrillation. J Physiol. 2014;592:3167-3170.
17. Andrade J, Khairy P, Dobrev D, Nattel S. The clinical profile and pathophysiology of atrial fibrillation: relationships among clinical features, epidemiology, and mechanisms. Circ Res. 2014;114:1453-1468.
18. Nattel S, Shiroshita-Takeshita A, Brundel BJ, Rivard L. Mechanisms of atrial fibrillation: lessons from animal models. Prog Cardiovasc. Dis. 2005;48:9-28.
19. Schotten U, Verheule S, Kirchhof P, Goette A. Pathophysiological mechanisms of atrial fibrillation: a translational appraisal. Physiol Rev. 2011;91:265–325.
20. Heijman J, Voigt N, Nattel S, Dobrev D. Cellular and molecular electrophysiology of atrial fibrillation initiation, maintenance, and progression. Circ Res. 2014;114:1483-1499.

SUPPLEMENTAL MATERIAL CHAPTER 9: MAPPING CRITERIA

Step I. Subtraction of ventricular complexes

Before determination of the local activation time, ventricular complexes were eliminated from the unipolar electrograms using a subtracting technique as previously described in detail by Hoekstra et al.[1] In short, for each fibrillation electrogram an individual template of the ventricular far field was obtained by averaging all time windows of ±70 ms around the R-waves detected from surface ECG lead I. Subtraction of these individual QRS templates from the fibrillation electrograms reduces the ventricular far field potentials and results in a more or less 'clean' unipolar atrial fibrillation electrograms.

Step II. Determination of the local activation time

Examples of electrograms recorded from both the endo- and epicardium showing endo-epicardial (a)synchrony are demonstrated in Supplemental Figure 1.

Local activation times were determined by detecting the maximum downslope of the unipolar fibrillation potential, as this coincides with the moment of maximum rate of rise of the transmembrane potential (time differences less than 50 μs).[2] In turn, the maximum rate of rise of the transmembrane potential corresponds with the maximum increase in sodium current and its conductance.[3] The height of the negative slope is measured during a 2 ms period. From the moment of the maximum downslope, time windows both backward and forward in time are scanned to detect the moment of respectively the positive and negative peak of the fibrillation potential. The duration of a non-fractionated potential is then defined as the time difference between the moment of its negative and positive peak. In case of a fractionated potential, the deflection with the steepest down slope was chosen; its duration is defined as the time between the preceding positive and following negative deflection.[4] The duration of a fibrillation potential had to be ≤35 ms. The negative slope and amplitude of the unipolar fibrillation potentials depend on numerous variables.[5,6] Hence, cut-off values applied also vary, depending on the signal-to-noise ratios of the recordings and lower limits were set at 0.05 V/sec and 0.2 mV.[5,6,7,8] All fibrillation potentials with slopes <0.05 V/sec, amplitudes < 0.2 mV and durations >35 ms are thus regarded as either far field or poor contact potentials.

After detection of the local activation time, a blanking period of 40 ms was applied in both directions. Though we do not know exactly what the refractory period during AF is, it is estimated to be approximately 50±13 ms.[9] Hence, comparable to previous studies, by choosing a blanking period of 40 ms we avoid overestimation of the number of fibrillation waves by marking fibrillation potentials, which are most likely double potentials with interspike intervals between >0 and ≤40 ms caused by areas of conduction block. [10,11]

Step III. WaveMapping

A wavemapping approach was used to identify individual fibrillation waves. This wavemapping technique has also been described in prior studies.[2,3,12,13] The starting point of the first fibrillation waves was the earliest activated site within the mapping area. Next, the entire mapping area was scanned in steps of 1 ms. For all electrodes activated during every step, the shortest time difference with the 8 neighboring electrodes was calculated. When the time difference was ≤12 ms (17 ms for oblique distances), the electrode site was added to the territory of the surrounding wave. In case of a time difference >12 ms, the electrode was annotated as the starting point of a new wave. In the wavemap, fibrillation waves are color-coded according to their moment of entrance in the mapping area and the colors demarcate the area activated by that specific fibrillation wave. The cut-off value of >12ms used for separating individual fibrillation waves corresponds for 2 mm interelectrode distances with an effective conduction velocity of 17 cm/s, which is equivalent to the continuous conduction velocities reported for atrial myocardium of intact hearts.[14] For separation of the fibrillation waves the requirement of a lower limit CV must be fulfilled along the whole boundary of the wave which off course does not exclude the possibility of slow conduction within parts of the fibrillation waves. Choosing a different cut-off value will lead to a lower or higher number of fibrillation waves. However, this change is very gradual and has no major effects on the measured differences in the number of focal waves. Only at extreme cut-off values our analysis will become useless because it either no longer separates the different fibrillation waves, or results in a very high degree of spatial fractionation, resembling a mosaic-like pattern of numerous small waves that only propagate over very short distances.

Based on the origin of the fibrillation wave, three different types of fibrillation waves were distinguished 1) peripheral waves, entering the mapping area from outside the electrode array, 2) epicardial breakthrough, appearing at the epicardial surface inside the mapping area, and 3) discontinuous conduction waves; defined as fibrillation waves starting with a delay of 13 to 40 ms from the boundary of another wave.[12-13] If a fibrillation wave originates along the border of another fibrillation wave it could theoretically be the result of very slow conduction. In order to avoid overestimation of the number of focal waves, we classified these waves as discontinuous fibrillation waves. Applications of this wavemapping technology have been described previously.[12-13]

Focal fibrillation waves had to meet several criteria. The breakthrough site of the focal fibrillation wave had to be located at least 2 electrodes away from the border of the mapping array and at least 1 reliable activation time should be available between the breakthrough site and the border of the mapping area in order to exclude propagation from the border of the mapping array. An example is given in Supplemental Figure 2. The relation between

the percentage of endocardial or epicardial focal fibrillation waves and the distance from the origin of the focal wave to the border of the mapping array is shown in Supplemental Table 1. Next, it is manually checked whether the morphology of fibrillation potentials in the breakthrough region is distorted by large QRS complexes or artifacts due to e.g. movements of the electrodes in order to avoid false positive focal waves; examples are shown in Supplemental Figure 3.

In case of a fractionated electrogram, marking of one of the other deflections should not result in disappearance of the focal fibrillation wave (Supplemental Figure 4). In order to include only focal waves which have a more or less considerable impact on endo-epicardial asynchrony, we choose cut-off value of 4 electrodes. Supplemental Table 2 shows how many focal waves will disappear when a cut-off value of 5 or 6 electrodes would have been chosen. The origin of a focal wave had to be activated earlier than all surrounding electrodes. If electrodes adjacent to the origin were activated simultaneously, all electrodes surrounding this area should also be activated later. Shift of the local activation time to a maximum of 3 ms earlier or later at the earliest activated electrode(s) should not result in disappearance of the focal wave. Typical examples of focal waves resulting from these criteria are provided in Supplemental Figure 5.

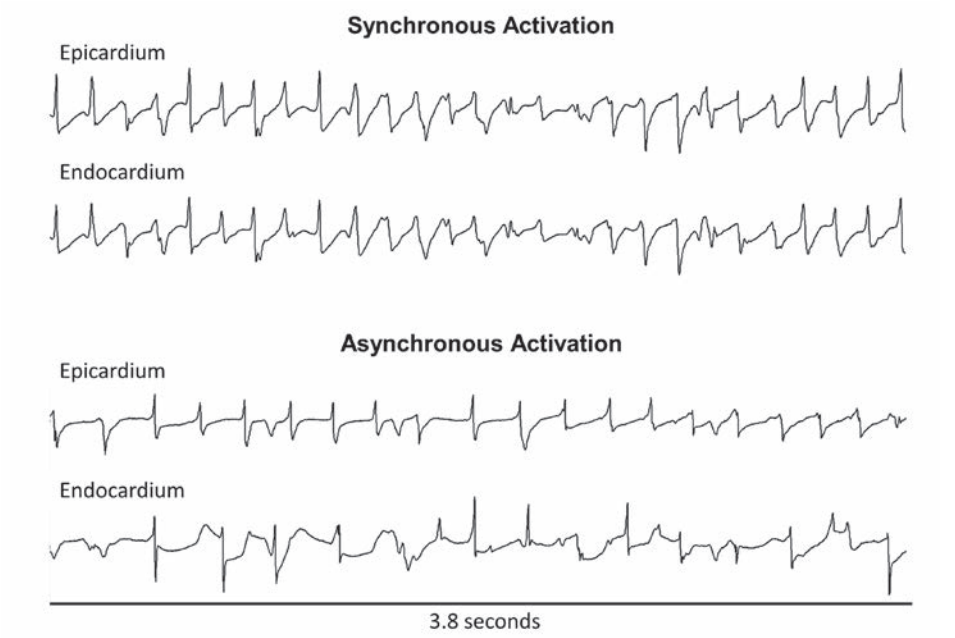

Supplemental Figure 1. Examples of two opposite electrogram recordings showing synchronous and asynchronous activation.

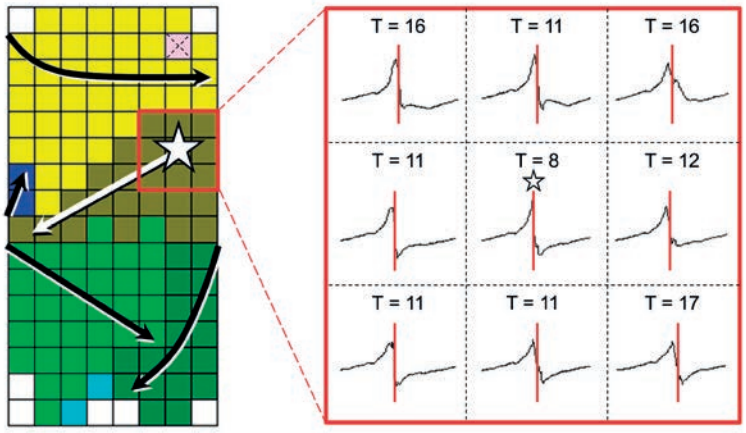

Supplemental Figure 2. Focal wave originating near the border of the mapping array.

Supplemental Figure 3. Distortion of the morphology of an atrial fibrillation potential by a far field ventricular complex.

Supplemental Figure 4. Fractionated potential next to the origin of a 'focal' wave.

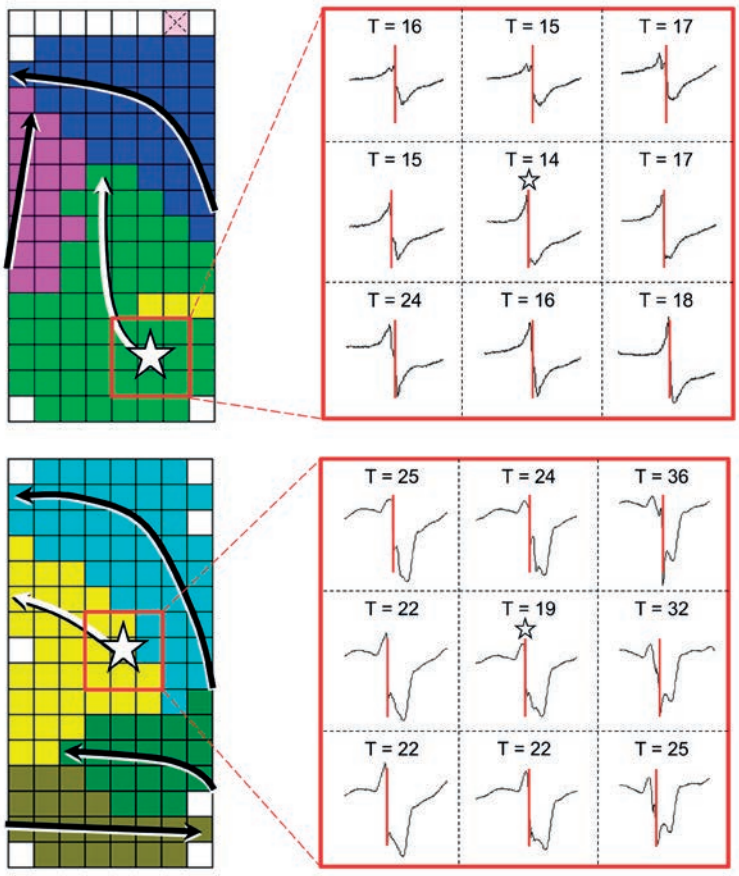

Supplemental Figure 5. Wavemaps demonstrating typical examples of focal fibrillation waves.

Supplemental Table 1. Location of the origin of focal fibrillation waves

Row distance to border	Endocardial focal waves	Epicardial focal waves
2	25%	25%
3	37%	36%
4	38%	39%

Supplemental Table 2. Size of the focal waves

	Endocardial focal waves	Epicardial focal waves
4 electrodes	5.0%	5.6%
5 electrodes	4.5%	5.2%
6 electrodes	3.8%	4.6%

REFERENCES

1. Hoekstra BP, Diks CG, Allessie MA, DeGoede J. Spatial correlation analysis of atrial activation patterns during sustained atrial fibrillation in conscious goats. Arch Physiol Biochem. 2000;108;313-331.
2. Spach MS, Dolber PC. Relating extracellular potentials and their derivatives to anisotropic propagation at a microscopic level in human cardiac muscle. Evidence for electrical uncoupling of side-to-side fiber connections with increasing age. Circ Res. 1986;58:356-371.
3. Spach MS, Kootsey JM. Relating the sodium current and conductance to the shape of transmembrane and extracellular potentials by simulation: effects of propagation boundaries. IEEE Trans Biomed Eng. 1985;32:743-755.
4. Rogers JM, Usui M, KenKnight BH, Ideker RE, Smith WM. Recurrent wavefront morphologies: a method for quantifying the complexity of epicardial activation patterns. Ann Biomed Eng. 1997;25:761-768.
5. Kleber AEG, Rudy Y. Basic Mechanisms of Cardiac Impulse Propagation and Associated Arrhythmias. Physiol Rev. 2004;84:431-488.
6. de Groot NMS, Schalij MJ, Zeppenfeld K, Blom NA, van der Velde ET, van der Wall EE, Schalij MJ. Voltage and activation mapping: how the recording technique affects the outcome of catheter ablation procedures in patients with congenital heart disease. Circulation. 2003;108:2099-2106.
7. Biermann M, Shenasa M, Borggrefe M, Hindricks G, Haverkamp W, Breithard G. Chapter 2. The interpretation of cardiac electrograms, 15-39. From Cardiac Mapping, 2nd edition. From Cardiac Mapping. Shenasa M, Borggrefe M, Breithard G.
8. Biermann M, Borggrefe M, Johna R, Haverkamp W, Shenasa M, Breithardt G. Precision and reproducibility of cardiac mapping. Chapter 8. Precision and reproducibility of cardiac mapping. Chapter 8. 157-186. From Cardiac Mapping, 2nd edition. From Cardiac Mapping. Shenasa M, Borggrefe M, Breithard G.
9. Hertevig EJ, Yuan S, Carlson J, Kongstad-Rasmussen O, Olsson SB. Evidence for electrical remodelling of the atrial myocardium in patients with atrial fibrillation. A study using the monophasic action potential recording technique. Clin Physiol Funct Imaging. 2002;22:8-12
10. Konings KT, Kirchhof CJ, Smeets JR, Wellens HJ, Penn OC, Allessie MA. High-density mapping of electrically induced atrial fibrillation in humans. Circulation. 1994;89:1665-1680.
11. Konings KT, Smeets JL, Penn OC, Wellens HJ, Allessie MA. Configuration of unipolar atrial electrograms during electrically induced atrial fibrillation in humans. Circulation. 1997;95:1231-1241.
12. Allessie MA, de Groot NM, Houben RP, Schotten U, Boersma E, Smeets JL, Crijns HJ. The electropathological substrate of longstanding persistent atrial fibrillation in patients with structural heart disease: longitudinal dissociation. Circ Arrhythm Electrophysiol. 2010;3:606-615.
13. de Groot NMS, Houben RP, Smeets JL, Boersma E, Schotten U, Schalij MJ, Crijns H, Allessie MA. The electropathological substrate of longstanding persistent atrial fibrillation in patients with structural heart disease: epicardial breakthrough. Circulation. 2010;122:1674-1682.
14. Spach MS, Dolber PC, Heidlage JF. Influence of the passive anisotropic properties on directional differences in propagation following modification of the sodium conductance in human atrial muscle. A model of reentry based on anisotropic discontinuous propagation. Circ Res. 1988;62:811-832.

10

Dynamics of Endo- and Epicardial Focal Fibrillation Waves at the Right Atrium in a Patient with Advanced Atrial Remodelling

Lisette van der Does
Charles Kik
Ad Bogers
Maurits Allessie
Natasja de Groot

ABSTRACT

Focal waves appear frequently at the epicardium during persistent atrial fibrillation (AF), however, the origin of these waves is under debate. We performed simultaneous endo-epicardial mapping of the right atrial wall during longstanding persistent AF in a patient undergoing cardiac surgery. During 10 seconds 53 and 59 focal waves appeared at random at respectively the endocardium and epicardium. Repetitive focal activity did not last longer than 3 cycles. Transmural asynchrony and conduction might be the origin of focal waves. Asynchronous propagation of fibrillation waves in three dimensions would stabilize the arrhythmia and could explain the limited success of persistent AF ablation.

Persistent atrial fibrillation (AF) is associated with the frequent occurrence of epicardial fibrillation waves presenting focally which may represent important drivers for the perpetuation of AF. These focal waves appear mainly as single events widely spread over the epicardial surface without any clear preferential site.[1] However, not much is known about the occurrence of focal waves at the endocardial side and the interplay between both sides. This could provide more insights into the origin of focal fibrillation waves. In this report we demonstrate the dynamics of focal fibrillation waves at the epicardium and endocardium simultaneously in a patient with longstanding persistent AF.

A 63-year-old female patient underwent mitral and tricuspid valve surgery due to rheumatic mitral valve disease with severe insufficiency. A preoperative echocardiogram showed a mildly reduced left ventricular function and an enlarged left atrium. AF had been persistent for 1.5 years and was medically treated with digoxin and verapamil. Before surgery, the patient gave informed consent for a mapping study approved by the local ethics committee. Before the start of cardiopulmonary bypass, the endo- and epicardial side of the right atrial free wall were simultaneously mapped during longstanding persistent AF. Mapping was performed with two 8x16 electrode arrays (2 mm interelectrode distance) positioned precisely opposite to each other in a clamp, and inserted in the right atrium through the incision for the venous cannula. Ten-second recordings of the endo- and epicardium were analyzed with custom-made software for focal fibrillation waves that appear within the mapping area as previously described in detail.[1,2] Figure 1 shows the appearance of focal fibrillation waves at the endocardium and epicardium during 10 seconds of longstanding persistent AF. Each star represents an emerging focal wave and the star size increases each time another focal wave presents at the same location. Focal waves appear equally frequent at the endocardium and the epicardium (53 vs 59). Mostly, they appear at random either on one side, or at different locations on both sides. A few appear at the same time and location on the epicardial and endocardial side. Repetitive focal

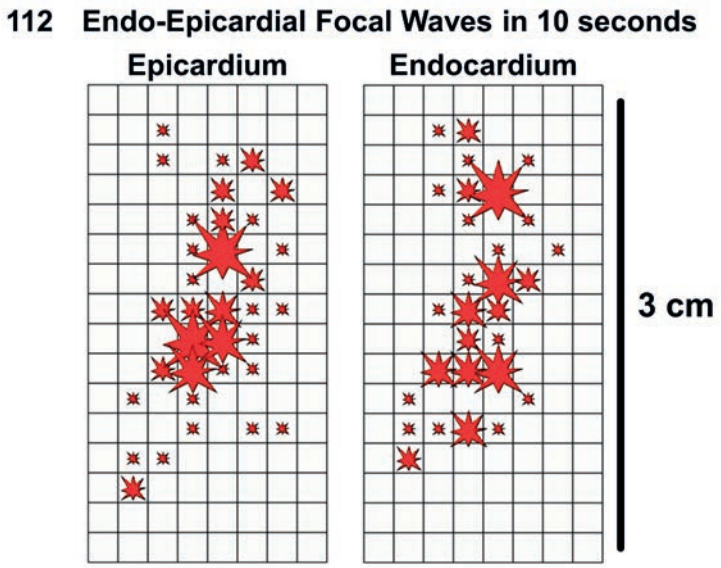

Figure 1. Focal fibrillation waves during 10 seconds of atrial fibrillation.
Summary of the 112 focal fibrillation waves (red stars) that occurred during 10 seconds of longstanding persistent atrial fibrillation at the endocardium and epicardium. The size of the star is proportional to the number of focal waves that appeared (size increases with each focal wave).

activation at a single location is seen at most for only 3 cycles with a variable cycle length. Rotor activity was not responsible for these repetitive focal waves as shown in Figure 2.

Several mechanisms for focal waves have been proposed such as re-entry, rotors, ectopic foci and endo-epicardial breakthrough.[1,3] The random appearance of focal waves pleads against stable ectopic foci or fixed rotors being the source for focal fibrillation waves in this example. Furthermore, most focal waves appear as single events on only one side instead of both sides, which translates either to an ectopic focus/ re-entry or rotor with transmural conduction block or transmural conduction of an opposite traveling wave. Both explanations suggest the occurrence of dissociative endo-epicardial conduction. Previously, a correlation was demonstrated between the anatomy of the right atrial appendage with the pectinate muscles and endo-epicardial conduction delay and epicardial focal waves.[4,5] The distinctive architecture of the right atrial appendage may be an important contributor to the occurrence of endo-epicardial breakthroughs, though, perhaps not always in the way of stable intramural re-entry circuits acting as drivers.[5] Theoretically, if random endo-epicardial breakthroughs indeed occur this frequently in longstanding persistent AF, it might offer an explanation why therapies for persistent AF are not always effective even after the elimination of AF drivers. After all, a 3-dimensional source for new fibrillation waves would highly stabilize the process of AF.

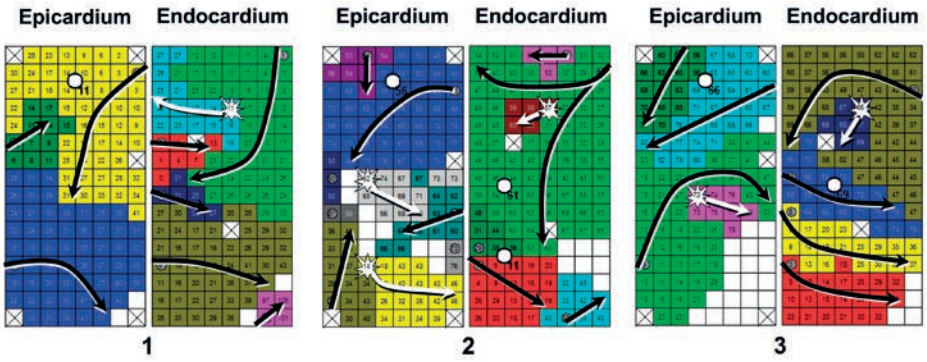

Figure 2. Three repetitive focal waves.
Three repetitive focal waves (white star) on the endocardial side demonstrated in 3 consecutive wave maps. Different colors illustrate the different fibrillation waves. Activation times are depicted in each electrode and are in respect to the first activated electrode (T=0). White circles refer to the site from where transmural conduction could theoretically be responsible for the opposite focal wave. Rotor activity was not the cause of the only repetitive focal activity that was observed in this patient. This is mostly clearly demonstrated in the second and third set of maps where the focal wave appears much later than the surrounding tissue with only limited conduction.

A mitral valve and tricuspid valve repair was performed in combination with cryoablation of the right and left atrium following a Cox-Maze III pattern. The patient developed episodes of postoperative AF with spontaneous conversions to sinus rhythm. During the last days before discharge there were no more AF episodes.

REFERENCES

1. de Groot NMS, Houben RPM, Smeets JL, Boersma E, Schotten U, Schalij MJ, Crijns H, Allessie MA. Electropathological substrate of longstanding persistent atrial fibrillation in patients with structural heart disease: epicardial breakthrough. Circulation. 2010;122:1674-82.
2. Allessie MA, de Groot NM, Houben RP, Schotten U, Boersma E, Smeets JL, Crijns HJ. Electropathological substrate of long-standing persistent atrial fibrillation in patients with structural heart disease: longitudinal dissociation. Circ Arrhythm Electrophysiol. 2010;3:606-15.
3. Baykaner T, Lalani GG, Schricker A, Krummen DE, Narayan SM. Mapping and ablating stable sources for atrial fibrillation: summary of the literature on Focal Impulse and Rotor Modulation (FIRM). J Interv Card Electrophysiol. 2014;40:237-44.
4. Gray RA, Pertsov AM, Jalife J. Incomplete reentry and epicardial breakthrough patterns during atrial fibrillation in the sheep heart. Circulation. 1996;94:2649-61
5. Hansen BJ, Zhao J, Csepe TA, Moore BT, Li N, Jayne LA, Kalyanasundaram A, Lim P, Bratasz A, Powell KA, Simonetti OP, Higgins RS, Kilic A, Mohler PJ, Janssen PM, Weiss R, Hummel JD, Fedorov VV. Atrial fibrillation driven by micro-anatomic intramural re-entry revealed by simultaneous sub-epicardial and sub-endocardial optical mapping in explanted human hearts. European Heart J. 2015;36:2390-2401.

11

The Inhomogeneity and Complexity in defining Fractionated Electrograms

Lisette van der Does
Natasja de Groot

ABSTRACT

Background: Ablation strategies targeting areas of complex fractionated atrial electrograms (CFAE) are not successful in the treatment of atrial fibrillation. Fractionation of atrial electrograms may have multiple causes of both pathological and non-pathological origin. In order to get insight in the definitions used for determining areas of fractionation a literature search was performed using a systematic approach.

Methods and Results: A Pubmed search for studies describing fractionation during human atrial electrophysiological measurements resulted in 348 articles that were screened for new definitions of fractionation. The 24 studies remaining after screening described 11 different visual definitions for fractionation, 3 automated CFAE detection programs and 7 new parameters for measuring fractionation. Five different definitions for continuous electrical activity were presented. Electrode properties were often not described and endocardial bipolar recordings in recent studies used electrode diameters ranging from 1-8 mm with a 2-5 mm interelectrode distance.

Conclusions: No uniform definition or recording method is used for measuring fractionation of cardiac atrial electrograms. The different electrophysiological causes for fractionation and the influence of recording device properties on fractionation complicate identification of true pathological inhomogeneous conduction. The first step in discrimination between origins for fractionation may be accomplished by relating electrogram morphology to the spatial patterns of activation. Before revisiting ablation of areas with fractionated electrograms, we need to determine the correct method for identifying pathological fractionation.

INTRODUCTION

To this day, atrial fibrillation (AF) is a major concern complicating worldwide healthcare and novel strategies are continuously being developed in an attempt to effectively treat this arrhythmia. One invasive modality developed in the previous decade is ablation of complex fractionated atrial electrograms (CFAE). It was first performed by Nademanee et al[1] and many studies have investigated the value of CFAE ablation.[2-6] In recent perspective, there seems no clinical beneficial effect of CFAE ablation in addition to pulmonary vein isolation for both paroxysmal and persistent AF.[4-6] There might even be an increased risk of organized atrial tachycardias after CFAE ablation.[3] Notably, the electrophysiological origin for CFAEs that are targeted during these ablation procedures is actually not exactly known, and different methods are used for identifying fractionated electrograms (EGMs). Therefore, we reviewed the electrophysiological basis of fractionation and investigated the measurement methods and definitions of atrial EGM fractionation using a systematic approach.

Pathophysiology

A unipolar recording of extracellular cardiac EGMs in homogenous tissue consists of a positive spike followed by a negative deflection, representing a depolarizing wave front approaching and moving away from the electrode, respectively. If the wave front originates or ends at the electrode site, the unipolar EGM morphology can also consist of only a negative or positive deflection.[7] The steepest point of deflection coincides with the rapid depolarization phase (phase 0) of the membrane potential and therefore local depolarization. Bipolar recordings subtract the potential at one recording site from an adjacent recording site, resulting in clearance of most farfield signals. Here, the initial peak is the local depolarization time.[7] However, bipolar EGM morphology is also affected by other factors that do not affect unipolar EGMs. For instance, the amplitude of the signal depends on the direction of the wavefront. A small spacing between the electrodes is important to diminish the impact of wave orientation. Furthermore, a bipolar EGM is the sum of two unipolar EGMs with a time delay due to the interelectrode distance. A significant time delay between two simple unipolar EGMs will result in a fractionated EGM when converted to a bipolar EGM as illustrated by Figure 1.

Fractionated electrograms consist of multiple deflections and are often prolonged. Several sources have been demonstrated to result in EGM fractionation. The causes for fractionation can be divided into three categories[8]: 1) artifacts, 2) remote activation, 3) inhomogeneous conduction of the tissue beneath the electrode. First, artifacts due to movement, signals from other muscles or filter settings can mimic fragmentation of the EGM.[9] Second, activation of remote regions may be recorded due to their proximity to

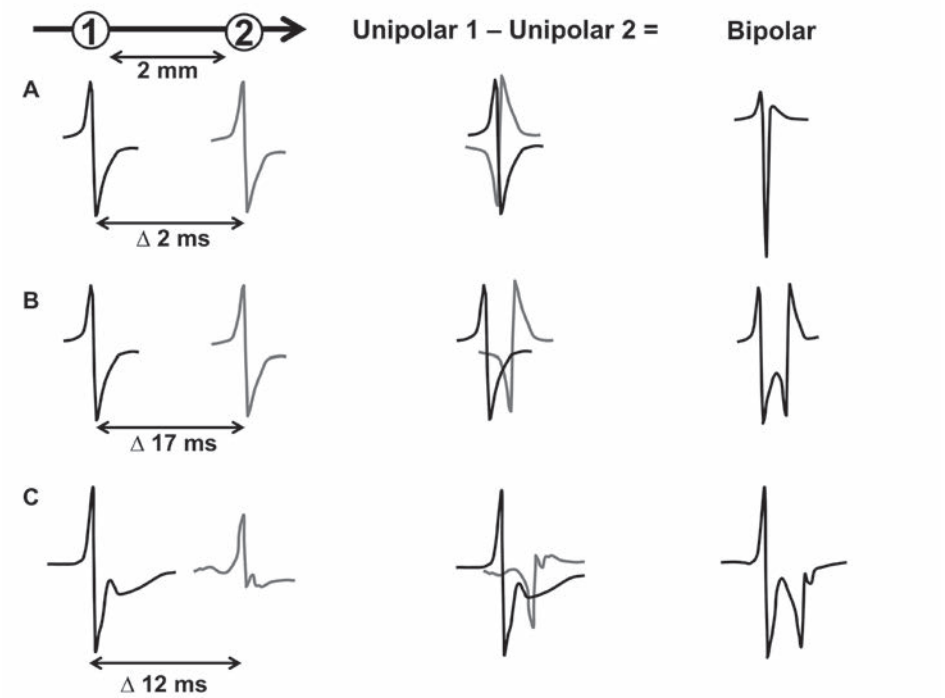

Figure 1. Fractionation in bipolar electrograms.
A depolarizing wavefront travels from electrode 1 to electrode 2 that are separated by an interelectrode distance of 2 mm. In situation A, the wavefront passes the electrodes with a time delay of 2 ms which results in a simple bipolar EGM. In situation B, the time delay is increased to 17 ms either due to increased electrode spacing or decreased velocity of the wavefront. This will result in an extra negative and increased positive bipolar deflections. C is an example of two real unipolar electrograms recorded during AF by electrodes with a diameter of 0.45 mm and 2 mm interelectrode spacing and filtered from 0.5-400 Hz. The time delay is 12 ms and conversion to a bipolar electrogram gives rise to a fractionated EGM.

the recording area. For example, excitation of adjacent macroscopic structures such as the coronary sinus or pulmonary veins, which may occur later in time than the recording site itself, can be recorded simultaneously. Besides recording artifacts or the activation of neighboring structures, fractionation can also originate from inhomogeneous conduction within the recording area. A single 1-mm electrode translates excitation of approximately 10,000 to 100,000 cardiac muscle cells into one signal. In case of a nonuniform pattern of myocyte excitation, EGM fractionation occurs (Figure 2).

Microscopic electrophysiological measurements have shown that even in normal cardiac tissue conduction velocity decreases and fractionation occurs with a transverse direction of propagation (anisotropy). Propagation in the transverse direction occurs more inhomogeneously with age, probably due to electric uncoupling caused by an increased presence

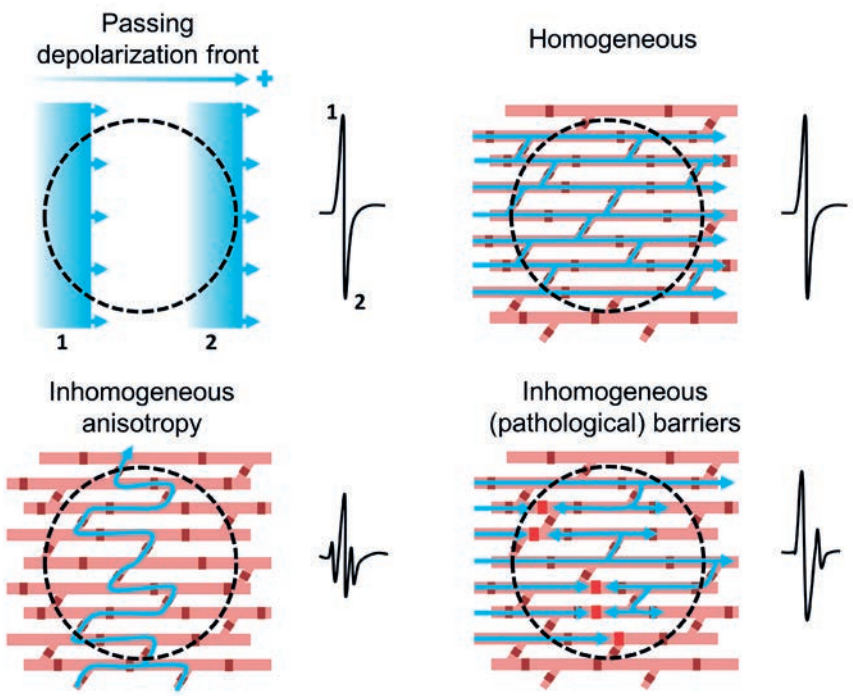

Figure 2. Myocardial activation patterns of simple and fractionated electrograms.
A homogeneous activation front across myocardial cells results in a simple electrogram (top panels). An inhomogeneous activation front, where the direction of the activation front changes, either due to the direction of propagation and coupling structure of myocardial fibers (anisotropy) or due to functional or pathological barriers between myocardial fibers, will result in a complex electrogram with multiple deflections (bottom panels).

of nonmuscular fibrous tissue.[10, 11] These structural barriers may lead to the circuitous path of conduction as proposed by Gardner et al.[11] Furthermore, high resistant gap junctions between myocytes or disrupted ion channel function due to antiarrhythmic drugs or genetic mutations can result in intracellular and/or intercellular barriers for conduction.[11] In normal functioning cardiomyocytes, premature or high-frequency stimulation within the refractory period creates an opportunity for dispersion of excitability and fractionation. In addition, it has recently been demonstrated that the right atrial endo- and epicardial myocardium is asynchronously activated during AF, which translates to a transmural inhomogeneity in conduction as well.[12, 13] Therefore, inhomogeneous conduction can occur in the presence of normal functionality and anatomy or occur due to pathological processes that cause structural or cellular barriers for homogeneous conduction. Figure 3 shows an overview of causes for fractionation. The methods and definitions used for identifying EGM fractionation need careful consideration because significant methodological differences can lead to a disparity in study results.

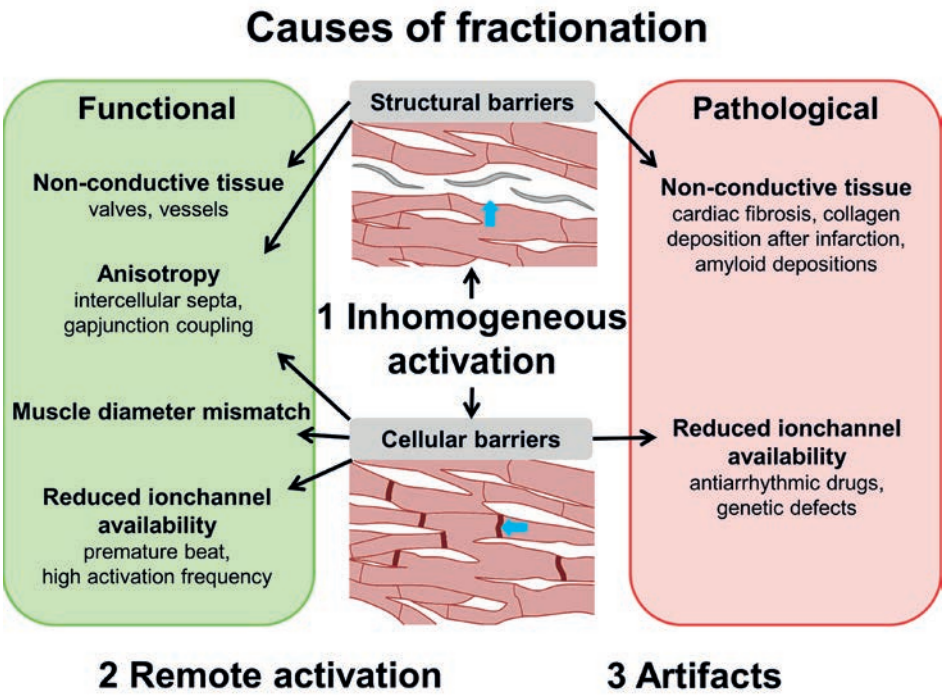

Figure 3. Schematic overview of the causes of fractionation.

METHODS

A PubMed database search was performed with the following MeSH terms: atrial fibrillation or heart atria, and humans, and cardiac electrophysiologic techniques or body surface potential mapping or electrocardiography or electrophysiology, and also containing in any of the fields: fractionated or fractionation or fragmented or AF nests. Editorials, comments, reviews and case reports were excluded from the search. The search resulted in 345 articles. To also include the most recent articles not yet indexed, an additional search without MeSH terms was performed within all fields containing the following words: atrial fibrillation or atria, and electrophysiology or epicardial mapping, and fractionated or fractionation or fragmented or AF nest. The results published in the past two years were screened for inclusion and three more articles were added. All 348 articles were screened for inclusion and exclusion criteria. A flowchart of inclusion and exclusion with criteria is shown in Figure 4. The definitions of these articles were compared and only the articles first describing a (different) definition were included. Dominant frequency was not considered a definition for fractionation, and these articles were excluded. A total of 24 articles remained after selection. Thereafter, definitions were checked for references to a previous article and, if so provided, the references were included instead.

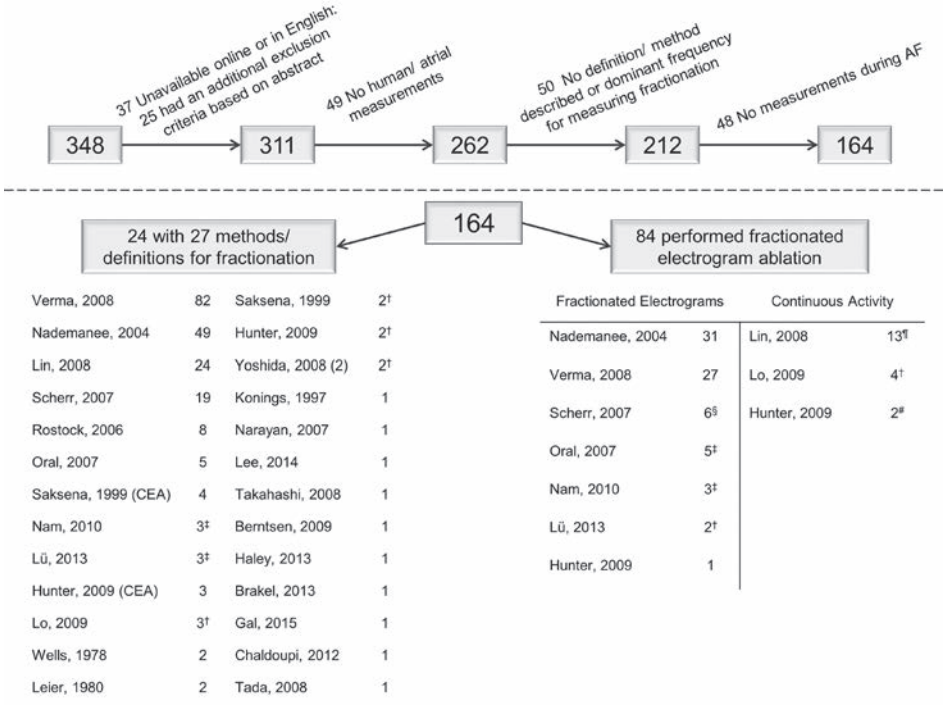

Figure 4. Flowchart of article in- and exclusion and definitions.
After the initial screening, 164 articles remained of which 24 described 27 methods/ definitions for fractionation. Of the 164 studies, 56 used multiple or a combination of these methods/ definitions. Fractionated electrogram ablation was performed by 84 studies, 10 used multiple or a combination of methods/ definitions. †/ ‡ all/ all but one article(s) of same research group, § ICL cut-offs described of >5 and >7 during 2.5 sec and ≥26 during 5 sec, ¶ Mean interval upper limit between 50-80 ms. # 70 or 75% of the recording time absence of isoelectric intervals of 70 or 50 ms. CEA, continuous electrical activity.

RESULTS

Definitions

The descriptions of fractionation that were found are given in Table 1. Eleven definitions were described in the articles found.[1, 14-24] Six studies that investigated characteristics of CFAE or aimed to find new manners to quantify CFAE introduced new parameters to describe CFAE.[25-30] In addition, 3 different automated software algorithms to detect CFAE were described: interval confidence level (ICL)[31, 32], CFE mean[32, 33] and an automated program calculating a CFAE percentage[34]. Figure 5 illustrates the manner in which these programs detected CFAE. Ablation of CFAE or continuous electrical activity was performed in 5 studies.[1, 18, 22, 33, 35] The definition of Nademanee et al.[1] is most often used, combined with the derived automated detection analysis algorithm CFE mean (Figure 4). Rostock et al.[36] made a minor change to the definition from ≥2 to ≥3 deflections. When continuous

Table 1. Definitions of fractionation

Study	Year	Electrogram Definition of Fractionation
Wells[14]	1978	Beat-to-beat complexes of variable morphology with an isoelectric baseline having perturbations of varying degrees.
Leier[15]	1980	Duration ≥80 ms
Konings[16]	1997	>2 deflections within 50 ms
Saksena[17]	1999	Prolongation of the duration of the local EGMs >50 ms with or without appearance of double or multiple potentials.
Nademanee[1]	2004	1) ≥2† deflections and/or perturbation of the baseline with continuous deflection of a prolonged activity complex over 10 sec recording, 2) very short cycle length ≤120 ms averaged over 10 sec.
Oral[18]	2007	Cycle length ≤120 ms or shorter than in the coronary sinus or that were fractionated or displayed continuous electric activity
Narayan[19]	2007	High-frequency with duration ≥60 ms
Hunter[20]	2009	Discrete, <70 ms and complex ≥5 direction changes
Nam[21]	2010	Highly fractionated, nearly continuous
Lü[22]/ Rostock[23]	2013/ 2008	Fractionated or continuous electrical activity, or locally short AF cycle length (<120 ms) or intermittent local burst activity
Lee[24]	2014	≥3 deflections over >50 ms duration separated by a discrete iso-electric baseline
Fractionation in parameters		
Yoshida[25]	2008	1. Complexity index: how often depolarizations changed polarity (+/-) per sec 2. Fractionation index: how often the direction (polarity) of the depolarization slope (dV/dt) changed per second
Takahashi[26]	2008	Number of deflections with an absolute value of >0.05 mV from the baseline
Berntsen[27]	2009	Number of deflections >50 μV/s
Haley[28]	2013	Percentage of time, deflections above baseline occurred, <120 ms apart
Brakel[29]	2013	Number of subsequent negative deflections within one EGM with a defined cycle length between two deflections of <120 ms expressed as median over a 10-s AF file
Gal[30]	2015	Number of deflections >0.015 mV/ms, >0.05 mV, per 1 sec, reduced by the number of main deflections
Automated fractionation detection		
Scherr[31]/ Nademanee[32]	2007/ 2006	During 2.5 sec recording, deflection peaks within 0.05-0.15 mV tagged, all interval measured between 2 peaks, number of intervals between 70-120 ms determined = ICL. CFAE site: >1 ICL.
Verma[33]/ Nademanee[32]	2008/ 2006	During 8 sec recording, CFE mean interval is determined of consecutive deflections exceeding a sensitivity threshold and down stroke morphology with maximum and minimum within a set time duration, and exceed a refractory period. CFAE site: CFE mean <120 ms
Chaldoupi[34]	2012	CFAEs: periods of successive atrial deflections with (a) dV/dt < –0.04 V/s, (b) amplitude >2% of the highest unipolar electrogram recorded in every tracing, (c) continuous atrial activation or deflections separated by an interval ≤104 ms
Electrogram definitions of continuous electrical activity		
Saksena[17]	1999	Variable morphology and cycle length, but indistinct/ absent isoelectric interval
Lin[37]	2008	Mean interval <50 ms
Tada[38]	2008	No isoelectric segments for ≥1 sec
Hunter[20]	2009	Continuous deflections without pause at the isoelectric line for ≥70 ms, occupying ≥70% of sample, with an uninterrupted segment of 1 sec
Lo[35]	2009	Fractionation or repetitive rapid activity lasting for >8 seconds

† Rostock et al. (2006)[36]: ≥3 deflections. AF = atrial fibrillation; CF(A)E = complex fractionated (atrial) electrograms; EGM = electrogram; ICL = interval confidence level.

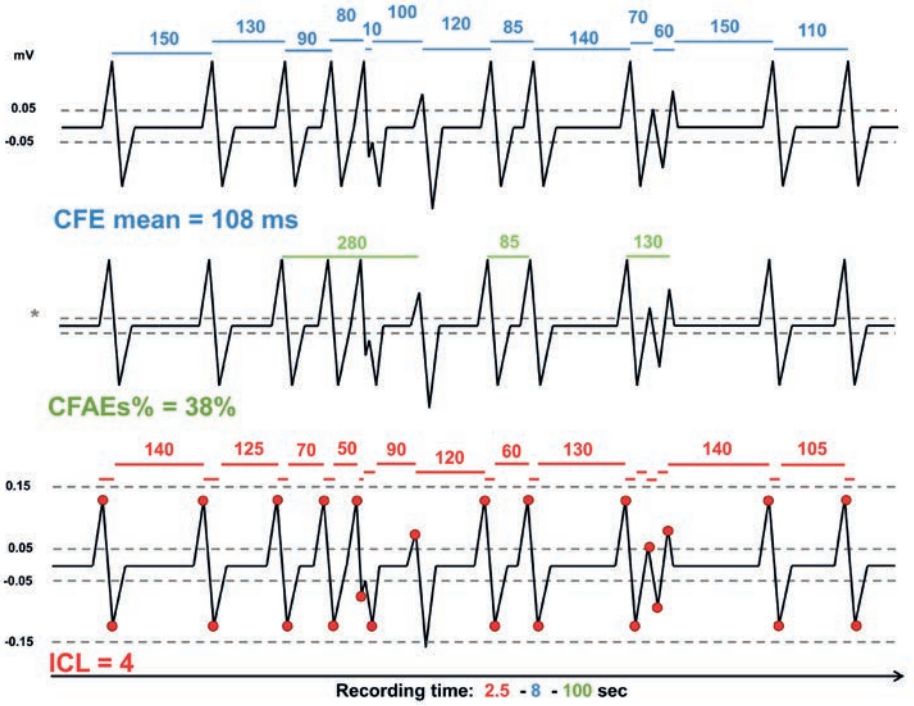

Figure 5. Algorithms for automated fractionation detection.
Schematic electrogram example illustrates the methods for determining CFE mean (blue), CFAE% (green), ICL (red). * >2% of highest amplitude. CF(A)E complex fractionated (atrial) electrograms; ICL interval confidence level.
Example calculations: CFE mean = (150+130+90+80+110+120+85+140+70+60+150+110)/12; CFAE% = % time periods intervals ≤104 ms = (280+85+130)/1295; ICL = number of intervals 70-120 ms = 4.

activity is defined apart from fractionation almost all studies define the absence of an isoelectric interval. However, different durations of continuous electrogram (EGM) deflections are described for the definition of continuous activity. The automated detection for continuous activity is set as a mean interval between deflections <50 ms.[17, 20, 35, 37, 38]

EGM parameters used to define fractionation are 1) number of deflections, 2) EGM duration, 3) interval duration between deflections, 4) number of short duration intervals between deflections, 5) amplitude of deflections, 6) slope of deflection, 7) number of polarity changes of deflections or slope of deflections (Figure 6), and 8) baseline. Three definitions use descriptive terms to define fractionation.[19, 21, 22] Nademanee et al.[1] use the most properties to define fractionation: number of deflections, EGM complex duration, baseline and interval duration between deflections. The automated CFE mean derived from this definition sets boundaries for the sensitivity of deflection detection with also a selectable amplitude level, refractory period and EGM width.

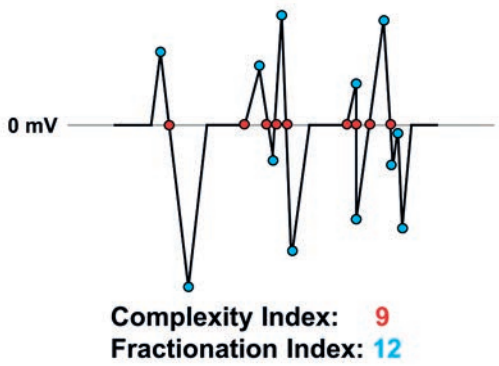

Figure 6. Fractionation parameters complexity index and fractionation index.
The complexity index (red) counts the number of polarity changes. The fractionation index (blue) counts the number of polarity changes of the derivative.

Table 2. Measuring method and device properties

Study	Endo-/ epicardial	Bi-/ unipolar	Electrode surface (mm)	Interelectrode spacing (mm)	Filter settings (Hz)
Wells, 1978	epi	bi	-	5-10	12-500
Leier, 1980	endo	bi	-	10	30-500
Konings, 1997	epi	uni	0.3	2.25	1-500
Saksena, 1999	endo	bi	-	2-5/8-2 + 5-10-5	-
Nademannee, 2004	endo	bi	-	-	30-500
Rostock, 2006	endo	bi	1	4-4-4	30-500
Oral, 2007	endo	bi	8	-	30-500
Narayan, 2007	endo	bi	-	-	30-500
Hunter, 2009	endo	bi	3.5	2-5-2	30-250
Nam, 2010	endo	bi	-	-	30-500
Lü, 2013	endo	bi	3.5	2-5-2	30-500
Lee, 2014	epi	bi	-	2.5	0.05-400
Yoshida, 2008	endo	bi	-	2.5	-
Takahashi, 2008	endo	bi	-	-	30-250
Berntsen, 2009	endo	bi	8 + 1	- + 2-5-2	30-400
Haley, 2013	endo	bi	3.5	2	0.5-250
Brakel, 2013	epi	bi	-	5	-
Gal, 2015	endo	bi	1	4-4-4	30-500
Scherr, 2007	endo	bi	3.5	-	30-400
Verma, 2008	endo	bi	3.5	2	30-500
Chaldoupi, 2012	endo	uni	-	5	0.05-500
Lin, 2008	endo	bi	4	-	-
Tada, 2008	endo	bi	3.5	2-5-2	30-500
Lo, 2009	endo	bi	4	-	-

Measuring methods

Table 2 lists the device properties and measuring methods that were used in these studies. Twenty studies used endocardial and 4 used epicardial mapping approaches. Two studies used unipolar recordings. In 11 studies electrode size was not described and in 8 the electrode spacing was not reported or could not be derived from the catheters that were used. Minimal electrode size for endocardial recordings was 1 mm, used in 3 studies, while the other 9 studies used electrode sizes of 3.5, 4 or 8 mm, substantially larger than the 0.3-mm electrode of the epicardial mapping study of Konings et al.[16] Interelectrode spacing mostly ranged between 2-5 mm and was only larger in the studies before the year 2000.

DISCUSSION

Clinical practice

Pathophysiological studies have shown that inhomogeneous conduction can give rise to both initiation and maintenance of AF.[39, 40] Therefore, Nademanee et al. proposed the ablation of areas with fractionated EGMs in order to terminate AF. At first, fractionated areas were identified visually; today automated detection software has been implemented in the CARTO (Biosense Webster, Diamond Bar, CA) and NavX (St. Jude Medical, Minneapolis, MN) 3-dimensional mapping systems and is most often used for the identification of CFAE areas. However, functional areas of fractionation could also be targeted during ablation. Limiting the number of unnecessary scars is important to decrease the risk of postablative iatrogenic atrial tachycardias. The first step towards delineating pathological from normal areas of fractionation or artefacts is to optimize the method in which fractionation is measured and to use a uniform definition for fractionation. This review has shown that definitions to date have widely varied, including definitions applied for ablation purposes.

Relation between definitions and the electrophysiological basis

Over 35 years, at least 11 definitions and 7 fractionation parameters have been used to define fractionation using 8 different EGM parameters. The studies that defined fractionation only by prolonged EGM duration, could have included areas where slow but homogeneous conduction occurs. Descriptive terms, mainly used in early studies, such as high-frequency, highly fractionated, or burst activity, provide insufficient information to distinguish the intended EGM morphology. Therefore, automated techniques for CFAE detection were developed including CFE mean, ICL and CFAE%, which utilize the AF cycle length to determine areas with highly frequent or short coupled activations. These methods are most often used in recent studies. However, the morphology of the EGM is not included with these methods. In addition, the refractory period that is set can overlook ‘true’ fractionated deflections caused by inhomogeneous conduction of myocytes

within the recording area. The close intervals that are detected are actually a measure of high-frequency activations, not inhomogeneous conduction per se. These CFAE could, for example, also represent a rotor or an ectopic focus (driver). In fact, these automated methods have shown to correlate poorly with each other and also corresponded poorly to inhomogeneous conduction patterns.[41]

Fractionated EGMs have been found both at the center and periphery of AF drivers.[42, 43] Narayan et al. found that electrograms with ≥7 short intervals in 4 sec mainly presented peripheral to driver sources.[42] Lin et al. reported fractionated electrograms defined as Nademanee et al.[1] at the center in 70% of rotors.[43] At high frequencies of activation, intermittent conduction block and interrupted patterns of activation occur, characterizing inhomogeneous or fibrillatory conduction. Anatomical transition sites demonstrated to be preferential sites for frequency-dependent conduction block[44] and could also exhibit significant conduction disturbances at an earlier stage in response to remodeling. The nature of conduction disorders during fibrillatory conduction can be physiological because of activation frequencies close to the refractory periods of surrounding myocytes or frequency-depended source to sink mismatch, or pathological because of structural/electrical remodeling of surrounding myocytes causing frequency-dependent conduction disorders. Fractionation at the center of rotors may be due to the sharp angle of the activation front representing as close-interval or continuous activity on the EGM, or the electrical remodeling is not homogeneously in the entire center causing conduction disturbances as well. In a recent report, rotors were accompanied by functional conduction disorders at the center that demonstrated “core” fractionation.[45]

EGMs in which atrial deflections comprise the entire recording time without an apparent baseline are referred to as continuous activity. Although definitions of continuous activity are more uniform, the length of the electrical activity before defining the EGM as continuous activity differed among studies. Continuous activity during AF is associated with multiple wavelets entering and exiting the recording area causing frequent wave collision and wave break.[46] Consequently, conduction is more inhomogeneous in areas with continuous activity and this explains the appearance of non-stop activity on the EGM. It features a high degree of inhomogeneous conduction of the multiple fibers representing the recording area. Therefore, continuous activity is likely the result from a low spatial resolution of the recording area and accordingly is related to the electrode diameter and recording modus.

Electrode size and spacing

The atrial EGM is the sum of the activation pattern of all muscle fibers underneath and closely surrounding the electrode. Therefore, a larger electrode size should increase the chance of the occurrence of fractionation. High-resolution epicardial mapping studies

recording with 0.3-mm electrodes have shown that delays in activation of >12 ms occur between sites at 2.25 mm distance.[47] Endocardial mapping studies often use electrode diameters of 3.5-4 mm covering an area of more than two high-density electrodes. Consequently, activation of an area with conduction block below the endocardial electrodes will exist of multiple activations leading to fractionation of the recorded signal. A computational model has shown that increasing the inhomogeneity of wavefronts increases the degree of fractionation more with a larger electrode size.[48] However, if a wavefront propagates homogeneous, the electrode size does not influence EGM morphology because there is no cause for fractionation to occur. The advantage of a smaller electrode size would thus be the ability to locate the inhomogeneous site more accurately. In addition, the required ratio of the area of inhomogeneity to the electrode size before the EGM becomes fractionated remains unclear and a smaller electrode also might be able to identify small areas of inhomogeneous conduction. On the other hand, a larger recording area may have the advantage of a zoomed-out perspective of the myocardial area creating a distant view for inhomogeneous conduction. However, a larger electrode will also increase the chance of recording remote activation. Nevertheless, this has not been validated in vivo yet, so the clinical relevance of electrode diameter can only be speculative. Increased electrode spacing in bipolar recordings has been shown to increase the degree of fractionation in vivo.[9, 41, 48] It is probably the consequence of the bipolar EGM being formed by the area of two, often, large electrodes of 3.5 or 4 mm. Increasing the interelectrode distance is followed by an increase of the recording area and of the differences between the EGMs recorded from the two poles. Because of the high level of inhomogeneity in AF, recordings of two poles can differ significantly during AF, making bipolar recordings less suitable, or should be recorded with an interelectrode distance <1 mm.[46] The multidirectional waves during AF can also cause a variation in bipolar EGM amplitudes. The study of Lau et al. demonstrated that unipolar fractionation is a better measure for inhomogeneity in conduction.[41] In the present study, electrode properties were often not described and the bipolar interelectrode distance was 2 mm or more.

Future directions

In future investigations, both the technical aspects and physiological causes of fractionation need to be determined in order to identify pathological areas of fractionation. We propose the following steps. First, device properties such as electrode diameter, interelectrode distance and filter settings will need to be investigated by using different device properties in areas with inhomogeneous conduction of different complexities. The next step is to relate spatial patterns of activation to EGM morphology. The complex patterns of high frequency, inhomogeneous activations during AF make it difficult to distinguish inhomogeneous conduction from “new” or remote activations. High-resolution electrophysiological mapping and optical mapping can provide more detailed answers in this

matter and could help discriminate between fractionation due to the presence of multiple wavefronts within the recording area and "true" fractionation due to discontinuity in propagation between cardiac myocytes. Finally, the functional and anatomical causes for fractionation should be identified. The significant role of the underlying atrial structure in physiological causes for fractionation means an approach will be required in which the anatomical structure of the recording site can be visualized. To this end, both in-vivo and ex-vivo human studies are necessary because the current, clinically applicable techniques have certain limitations that can be overcome by ex-vivo studies. In vivo local anisotropy in conduction determined by previously described methods[49] can be correlated to the degree of EGM fractionation and imaging techniques, such as magnetic resonance imaging, can be combined with EGM recordings to help identify fibrotic-related fractionation.[50] However, ex-vivo human studies that combine high-resolution endo-epicardial mapping with imaging or histology are essential to determine the specific anatomical structural causes of fractionation.[10, 51]

When these technical and pathophysiological issues in identifying pathological fractionation have been resolved, the clinical benefits of ablation of (pathological) fractionated EGMs can be reevaluated. Although research would benefit from a universal definition of fractionation, it does not seem possible at this time because of multiple factors complicating the interpretation of fractionation. In our opinion, fractionation during AF should be defined based on an EGM morphology with multiple deflections (>1 in unipolar and >2 in bipolar recordings) within the refractory period indicating "true" inhomogeneous conduction.

REFERENCES

1. Nademanee K, McKenzie J, Kosar E, Schwab M, Sunsaneewitayakul B, Vasavakul T, Khunnawat C, Ngarmukos T. A new approach for catheter ablation of atrial fibrillation: mapping of the electrophysiologic substrate. Journal of the American College of Cardiology 2004;43:2044-2053.
2. Hayward RM, Upadhyay GA, Mela T, Ellinor PT, Barrett CD, Heist EK, Verma A, Choudhry NK, Singh JP. Pulmonary vein isolation with complex fractionated atrial electrogram ablation for paroxysmal and nonparoxysmal atrial fibrillation: A meta-analysis. Heart Rhythm 2011;8:994-1000.
3. Wu SH, Jiang WF, Gu J, Zhao L, Wang YL, Liu YG, Zhou L, Gu JN, Xu K, Liu X. Benefits and risks of additional ablation of complex fractionated atrial electrograms for patients with atrial fibrillation: a systematic review and meta-analysis. Int J Cardiol 2013;169:35-43.
4. Verma A, Jiang CY, Betts TR, Chen J, Deisenhofer I, Mantovan R, Macle L, Morillo CA, Haverkamp W, Weerasooriya R, Albenque JP, Nardi S, Menardi E, Novak P, Sanders P; STAR AF II Investigators. Approaches to catheter ablation for persistent atrial fibrillation. N Engl J Med 2015;372:1812-1822.
5. Providencia R, Lambiase PD, Srinivasan N, Ganesh Babu G, Bronis K, Ahsan S, Khan FZ, Chow AW, Rowland E, Lowe M, Segal OR. Is There Still a Role for Complex Fractionated Atrial Electrogram Ablation in Addition to Pulmonary Vein Isolation in Patients With Paroxysmal and Persistent Atrial Fibrillation? Meta-Analysis of 1415 Patients. Circ Arrhythm Electrophysiol 2015;8:1017-1029.
6. Vogler J, Willems S, Sultan A, Schreiber D, Luker J, Servatius H, Schaffer B, Moser J, Hoffmann BA, Steven D. Pulmonary Vein Isolation Versus Defragmentation: The CHASE-AF Clinical Trial. Journal of the American College of Cardiology 2015;66:2743-2752.
7. Stevenson WG, Soejima K. Recording techniques for clinical electrophysiology. J Cardiovasc Electrophysiol 2005;16:1017-1022.
8. de Bakker JM, Wittkampf FH. The pathophysiologic basis of fractionated and complex electrograms and the impact of recording techniques on their detection and interpretation. Circ Arrhythm Electrophysiol 2010;3:204-213.
9. Waxman HL, Sung RJ. Significance of fragmented ventricular electrograms observed using intracardiac recording techniques in man. Circulation 1980;62:1349-1356.
10. Spach MS, Dolber PC. Relating extracellular potentials and their derivatives to anisotropic propagation at a microscopic level in human cardiac muscle. Evidence for electrical uncoupling of side-to-side fiber connections with increasing age. Circulation Research 1986;58:356-371.
11. Gardner PI, Ursell PC, Fenoglio JJ, Jr., Wit AL. Electrophysiologic and anatomic basis for fractionated electrograms recorded from healed myocardial infarcts. Circulation 1985;72:596-611.
12. de Groot NM, Houben RP, Smeets JL, Boersma E, Schotten U, Schalij MJ, Crijns H, Allessie MA. Electropathological substrate of longstanding persistent atrial fibrillation in patients with structural heart disease: epicardial breakthrough. Circulation 2010;122:1674-1682.
13. de Groot N, van der Does L, Yaksh A, Lanters E, Teuwen C, Knops P, van de Woestijne P, Bekkers J, Kik C, Bogers A, Allessie M. Direct Proof of Endo-Epicardial Asynchrony of the Atrial Wall During Atrial Fibrillation in Humans. Circ Arrhythm Electrophysiol 2016;9:e003648.
14. Wells JL, Jr., Karp RB, Kouchoukos NT, MacLean WA, James TN, Waldo AL. Characterization of atrial fibrillation in man: studies following open heart surgery. Pacing Clin Electrophysiol 1978;1:426-438.
15. Leier CV, Schaal SF. Biatrial electrograms during coarse atrial fibrillation and flutter-fibrillation. Am Heart J 1980;99:331-341.
16. Konings KT, Smeets JL, Penn OC, Wellens HJ, Allessie MA. Configuration of unipolar atrial electrograms during electrically induced atrial fibrillation in humans. Circulation 1997;95:1231-1241.

17. Saksena S, Giorgberidze I, Mehra R, Hill M, Prakash A, Krol RB, Mathew P. Electrophysiology and endocardial mapping of induced atrial fibrillation in patients with spontaneous atrial fibrillation. Am J Cardiol 1999;83:187-193.
18. Oral H, Chugh A, Good E, Wimmer A, Dey S, Gadeela N, Sankaran S, Crawford T, Sarrazin JF, Kuhne M, Chalfoun N, Wells D, Frederick M, Fortino J, Benloucif-Moore S, Jongnarangsin K, Pelosi F Jr, Bogun F, Morady F. Radiofrequency catheter ablation of chronic atrial fibrillation guided by complex electrograms. Circulation 2007;115:2606-2612.
19. Narayan SM, Franz MR. Quantifying fractionation and rate in human atrial fibrillation using monophasic action potentials: implications for substrate mapping. Europace 2007;9 Suppl 6:vi89-95.
20. Hunter RJ, Diab I, Thomas G, Duncan E, Abrams D, Dhinoja M, Sporton S, Earley MJ, Schilling RJ. Validation of a classification system to grade fractionation in atrial fibrillation and correlation with automated detection systems. Europace 2009;11:1587-1596.
21. Nam GB, Jin ES, Choi H, Song HG, Kim SH, Kim KH, Hwang ES, Park KM, Kim J, Rhee KS, Choi KJ, Kim YH. Mechanism of regular atrial tachyarrhythmias during combined pulomonary vein isolation and complex fractionated electrogram ablation in patients with atrial fibrillation. Circ J 2010;74:434-441.
22. Lu F, Adkisson WO, Chen T, Akdemir B, Benditt DG. Catheter ablation for long-standing persistent atrial fibrillation in patients who have failed electrical cardioversion. J Cardiovasc Transl Res 2013;6:278-286.
23. Rostock T, Steven D, Hoffmann B, Servatius H, Drewitz I, Sydow K, Mullerleile K, Ventura R, Wegscheider K, Meinertz T, Willems S. Chronic atrial fibrillation is a biatrial arrhythmia: data from catheter ablation of chronic atrial fibrillation aiming arrhythmia termination using a sequential ablation approach. Circ Arrhythm Electrophysiol 2008;1:344-353.
24. Lee G, Kumar S, Teh A, Madry A, Spence S, Larobina M, Goldblatt J, Brown R, Atkinson V, Moten S, Morton JB, Sanders P, Kistler PM, Kalman JM. Epicardial wave mapping in human long-lasting persistent atrial fibrillation: transient rotational circuits, complex wavefronts, and disorganized activity. Eur Heart J 2014;35:86-97.
25. Yoshida K, Ulfarsson M, Tada H, Chugh A, Good E, Kuhne M, Crawford T, Sarrazin JF, Chalfoun N, Wells D, Jongnarangsin K, Pelosi F Jr, Bogun F, Morady F, Oral H. Complex electrograms within the coronary sinus: time- and frequency-domain characteristics, effects of antral pulmonary vein isolation, and relationship to clinical outcome in patients with paroxysmal and persistent atrial fibrillation. J Cardiovasc Electrophysiol 2008;19:1017-1023.
26. Takahashi Y, O'Neill MD, Hocini M, Dubois R, Matsuo S, Knecht S, Mahapatra S, Lim KT, Jaïs P, Jonsson A, Sacher F, Sanders P, Rostock T, Bordachar P, Clémenty J, Klein GJ, Haïssaguerre M. Characterization of electrograms associated with termination of chronic atrial fibrillation by catheter ablation. Journal of the American College of Cardiology 2008;51:1003-1010.
27. Berntsen RF, Cheng A, Calkins H, Berger RD. Evaluation of spatiotemporal organization of persistent atrial fibrillation with time- and frequency-domain measures in humans. Europace 2009;11:316-323.
28. Haley CL, Gula LJ, Miranda R, Michael KA, Baranchuk AM, Simpson CS, Abdollah H, West AJ, Akl SG, Redfearn DP. Validation of a novel algorithm for quantification of the percentage of signal fractionation in atrial fibrillation. Europace 2013;15:447-452.
29. van Brakel TJ, van der Krieken T, Westra SW, van der Laak JA, Smeets JL, van Swieten HA. Fibrosis and electrophysiological characteristics of the atrial appendage in patients with atrial fibrillation and structural heart disease. J Interv Card Electrophysiol 2013;38:85-93.

30. Gal P, Linnenbank AC, Adiyaman A, Smit JJ, Ramdat Misier AR, Delnoy PP, de Bakker JM, Elvan A. Correlation of atrial fibrillation cycle length and fractionation is associated with atrial fibrillation free survival. Int J Cardiol 2015;187:208-215.
31. Scherr D, Dalal D, Cheema A, Cheng A, Henrikson CA, Spragg D, Marine JE, Berger RD, Calkins H, Dong J. Automated detection and characterization of complex fractionated atrial electrograms in human left atrium during atrial fibrillation. Heart Rhythm 2007;4:1013-1020.
32. Nademanee K, Schwab M, Porath J, Abbo A. How to perform electrogram-guided atrial fibrillation ablation. Heart Rhythm 2006;3:981-984.
33. Verma A, Novak P, Macle L, Whaley B, Beardsall M, Wulffhart Z, Khaykin Y. A prospective, multicenter evaluation of ablating complex fractionated electrograms (CFEs) during atrial fibrillation (AF) identified by an automated mapping algorithm: acute effects on AF and efficacy as an adjuvant strategy. Heart Rhythm 2008;5:198-205.
34. Chaldoupi SM, Linnenbank AC, Wittkampf FH, Boldt LH, van Wessel H, van Driel VJ, Doevendans PA, Hauer RN, de Bakker JM, Loh P. Complex fractionated electrograms in the right atrial free wall and the superior/posterior wall of the left atrium are affected by activity of the autonomic nervous system. J Cardiovasc Electrophysiol 2012;23:26-33.
35. Lo LW, Lin YJ, Tsao HM, Chang SL, Udyavar AR, Hu YF, Ueng KC, Tsai WC, Tuan TC, Chang CJ, Tang WH, Higa S, Tai CT, Chen SA. The impact of left atrial size on long-term outcome of catheter ablation of chronic atrial fibrillation. J Cardiovasc Electrophysiol 2009;20:1211-1216.
36. Rostock T, Rotter M, Sanders P, Takahashi Y, Jaïs P, Hocini M, Hsu LF, Sacher F, Clementy J, Haïssaguerre M. High-density activation mapping of fractionated electrograms in the atria of patients with paroxysmal atrial fibrillation. Heart Rhythm 2006;3:27-34.
37. Lin YJ, Tai CT, Kao T, Chang SL, Wongcharoen W, Lo LW, Tuan TC, Udyavar AR, Chen YJ, Higa S, Ueng KC, Chen SA. Consistency of complex fractionated atrial electrograms during atrial fibrillation. Heart Rhythm 2008;5:406-412.
38. Tada H, Yoshida K, Chugh A, Boonyapisit W, Crawford T, Sarrazin JF, Kuhne M, Chalfoun N, Wells D, Dey S, Veerareddy S, Billakanty S, Wong WS, Kalra D, Kfahagi A, Good E, Jongnarangsin K, Pelosi F Jr, Bogun F, Morady F, Oral H. Prevalence and characteristics of continuous electrical activity in patients with paroxysmal and persistent atrial fibrillation. J Cardiovasc Electrophysiol 2008;19:606-612.
39. Moe GK, Abildskov JA. Atrial fibrillation as a self-sustaining arrhythmia independent of focal discharge. Am Heart J 1959;58:59-70.
40. Kleber AG, Rudy Y. Basic mechanisms of cardiac impulse propagation and associated arrhythmias. Physiol Rev 2004;84:431-488.
41. Lau DH, Maesen B, Zeemering S, Kuklik P, van Hunnik A, Lankveld TA, Bidar E, Verheule S, Nijs J, Maessen J, Crijns H, Sanders P, Schotten U. Indices of bipolar complex fractionated atrial electrograms correlate poorly with each other and atrial fibrillation substrate complexity. Heart Rhythm 2015;12:1415-1423.
42. Narayan SM, Shivkumar K, Krummen DE, Miller JM, Rappel WJ. Panoramic electrophysiological mapping but not electrogram morphology identifies stable sources for human atrial fibrillation: stable atrial fibrillation rotors and focal sources relate poorly to fractionated electrograms. Circ Arrhythm Electrophysiol 2013;6:58-67.
43. Lin T, Rillig A, Bucur T, Metzner A, Mathew S, Wissner E, Wohlmuth P, Kuck KH, Ouyang F, Tilz RR. Focal impulse and rotor modulation using the novel 64-electrode basket catheter: electrogram characteristics of human rotors. Europace 2015;17:1791-1797.

44. Berenfeld O, Zaitsev AV, Mironov SF, Pertsov AM, Jalife J. Frequency-dependent breakdown of wave propagation into fibrillatory conduction across the pectinate muscle network in the isolated sheep right atrium. Circulation Research 2002;90:1173-1180.
45. Yamabe H, Kanazawa H, Ito M, Kaneko S, Ogawa H. Prevalence and mechanism of rotor activation identified during atrial fibrillation by noncontact mapping: Lack of evidence for a role in the maintenance of atrial fibrillation. Heart Rhythm 2016.
46. Konings KT, Kirchhof CJ, Smeets JR, Wellens HJ, Penn OC, Allessie MA. High-density mapping of electrically induced atrial fibrillation in humans. Circulation 1994;89:1665-1680.
47. Allessie MA, de Groot NM, Houben RP, Schotten U, Boersma E, Smeets JL, Crijns HJ. Electropathological substrate of long-standing persistent atrial fibrillation in patients with structural heart disease: longitudinal dissociation. Circ Arrhythm Electrophysiol 2010;3:606-615.
48. Correa de Sa DD, Thompson N, Stinnett-Donnelly J, Znojkiewicz P, Habel N, Muller JG, Bates JH, Buzas JS, Spector PS. Electrogram fractionation: the relationship between spatiotemporal variation of tissue excitation and electrode spatial resolution. Circ Arrhythm Electrophysiol 2011;4:909-916.
49. Houben RP, de Groot NM, Smeets JL, Becker AE, Lindemans FW, Allessie MA. S-wave predominance of epicardial electrograms during atrial fibrillation in humans: indirect evidence for a role of the thin subepicardial layer. Heart Rhythm 2004;1:639-647.
50. Hwang SH, Oh YW, Lee DI, Shim J, Park SW, Kim YH. Relation between left atrial wall composition by late gadolinium enhancement and complex fractionated atrial electrograms in patients with persistent atrial fibrillation: influence of non-fibrotic substrate in the left atrium. Int J Cardiovasc Imaging 2015;31:1191-1199.
51. Hansen BJ, Zhao J, Csepe TA, Moore BT, Li N, Jayne LA, Kalyanasundaram A, Lim P, Bratasz A, Powell KA, Simonetti OP, Higgins RS, Kilic A, Mohler PJ, Janssen PM, Weiss R, Hummel JD, Fedorov VV. Atrial fibrillation driven by micro-anatomic intramural re-entry revealed by simultaneous sub-epicardial and sub-endocardial optical mapping in explanted human hearts. Eur Heart J 2015;36:2390-2401.

12

Unipolar Atrial Electrogram Morphology from an Epicardial and Endocardial Perspective

Lisette van der Does
Paul Knops
Christophe Teuwen
Corina Serban
Roeliene Starreveld
Eva Lanters
Elisabeth Mouws
Charles Kik
Ad Bogers
Natasja de Groot

ABSTRACT

Background: Endo-epicardial asynchrony (EEA) and the interplay between the endocardial and epicardial layers could be important in the pathophysiology of atrial arrhythmias. The morphological differences between epicardial and endocardial atrial electrograms have not yet been described, and electrogram morphology may hold information about the presence of EEA. The purpose of this study was to directly compare epicardial to endocardial unipolar electrogram morphology during sinus rhythm (SR) and to evaluate whether EEA contributes to electrogram fractionation by correlating fractionation to spatial activation patterns.

Methods: In 26 patients undergoing cardiac surgery, unipolar electrograms were simultaneously recorded from the epicardium and endocardium at the inferior, middle and superior right atrial (RA) free wall during SR. Potentials were analyzed for epi-endocardial differences in local activation time, voltage, RS ratio and fractionation. The surrounding and opposite electrograms of fractionated deflections were evaluated for corresponding local activation times in order to determine whether fractionation originated from EEA.

Results: The superior RA was predisposed for delayed activation, EEA and fractionation. Both epicardial and endocardial electrograms demonstrated an S-predominance. Fractionation was mostly similar between the two sides; however, incidentally deflections up to 4 mV on one side could be absent on the other side. Remote activation was responsible for most fractionated deflections (95%) in SR, of which 4% could be attributed to EEA.

Conclusion: Local epi-endocardial differences in electrogram fractionation occur occasionally during SR but will likely increase during arrhythmias due to increasing EEA and (functional) conduction disorders. Electrogram fractionation can originate from EEA and this study demonstrated that unipolar electrogram fractionation can potentially identify EEA.

INTRODUCTION

Differences in electrophysiological properties of the ventricular epicardial and endocardial wall have been long recognized and linked to arrhythmogenesis.[1] Although wavefronts traveling out of sync at the epicardium and endocardium of the thin atrial wall were already demonstrated more than two decades ago,[2] unravelling of the link between endo-epicardial asynchrony (EEA) and atrial arrhythmias only started recently.[3] Asynchrony in epicardial versus endocardial propagating waves and the complex fiber arrangement of the atria may also give rise to epi-endocardial differences in the morphology of electrograms. Houben et al. have proposed that the ratio between the R-peak and S-peak of unipolar atrial electrograms may differ between the epicardium and endocardium and could identify the leading layer.[4] Other features of electrogram morphology such as amplitude and fractionation have been used to identify areas with scar tissue and arrhythmogenic areas.[5] Electrogram fractionation occurs when inhomogeneity in conduction occurs within or remotely from the recording site and can have structural or functional causes.[6] The intricate structure of the atria might be a substrate for epi-endocardial differences in fractionation and occurrence of EEA. Asynchronous activation within the wall could in turn be responsible for additional deflections in electrograms.

In a clinical setting, epicardial and endocardial mapping is never performed simultaneously; therefore, the differences and relationships between epi- and endocardial atrial electrogram morphology are so far unknown. This study is the first to directly compare unipolar epicardial electrograms to endocardial electrograms that were recorded simultaneously at the right atrial wall during sinus rhythm (SR) in order to evaluate whether 1) (local) morphological features differ between epicardial and endocardial electrograms and 2) a fractionated electrogram morphology can arise from local EEA in activation. To this end, we developed a method to classify fractionation to its electrophysiological origin by correlating fractionated potentials to spatial patterns of activation.

METHODS

Study population

Twenty-six adult patients undergoing first-time cardiac surgery with use of cardiopulmonary bypass were included (21 male; age 67±10 years). Nineteen patients (73%) were operated for coronary artery disease, 12 (46%) for (concomitant) valvular heart disease, 11 (42%) patients had a history of atrial fibrillation (AF), and 6 (23%) had impaired left ventricular function. Clinical characteristics are described in detail in Supplemental Table 1. The study protocol was approved by the local ethics committee (MEC2015-373) and all patients provided informed consent for inclusion before surgery.

Intraoperative endo-epicardial mapping

Two multi-electrode arrays, each containing 128 electrodes with 2 mm interelectrode spacing, were fixed on spatulas and positioned directly opposite to each other (Figure 1, left panel). After arterial cannulation for cardiopulmonary bypass, an incision was made in the RA appendage for venous cannulation. Before venous cannulation, one spatula was introduced in the right atrium through the incision and the opening around the spatula was closed with a purse-string suture.[7] Atrial epicardial and endocardial unipolar electrograms were simultaneously recorded for 5-10 seconds during SR at three different locations of the RA free wall: 1) inferior RA, 2) mid-RA, 3) superior RA. Unipolar electrograms were sampled at 1 kHz and stored on hard disk after amplification, filtering (0.5-500 Hz) and analogue-to-digital conversion. Detailed methods are provided in the Supplemental Material.

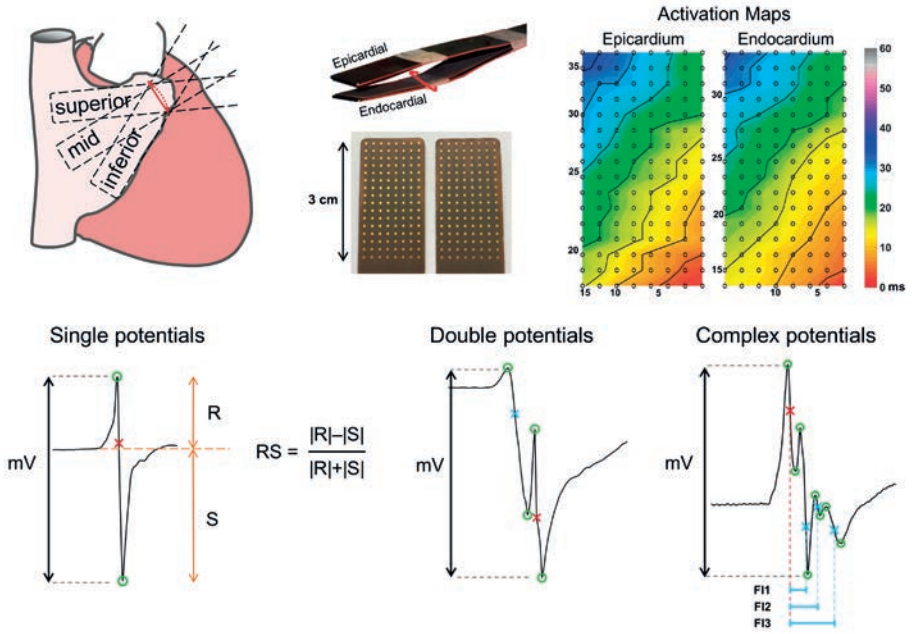

Figure 1. Endo-epicardial mapping and signal analyses.
Left: Two spatulas with 128-electrode arrays are fixed together and one spatula is introduced in the right atrium through the incision for venous cannulation. Unipolar electrogram recordings are made on 3 locations: towards the inferior vena cava (inferior RA), the superior vena cava (superior RA) and in between, towards the terminal crest (mid-RA). Middle: the steepest deflection is marked as local activation time (AT, red cross) and additional deflections (blue crosses) are marked as fractionated deflections if the criteria for fractionation are met (see text). Signal morphology is analyzed for number of deflections, the RS-ratio (only single potentials) and peak-to-peak amplitude (potentials with multiple deflections: amplitude between the maximal and minimal peak). Fractionation interval (FI) is the time between the fractionated deflection and local AT within the potential. Right: An example of epi-endocardial activation time maps with isochrones are shown on the top. For classification, two rings of electrograms around a fractionated deflection (blue dot) in the same and opposite plane are searched for coinciding (peak-to-peak time distance ±3 ms error margin) deflections of local ATs.

Data analysis

Electrogram morphology was analyzed semi-automatically in MATLAB R2016a (The MathWorks Inc., Natick, MA). Electrograms with injury potentials were excluded from analysis and recording sites with ≥25% excluded or missing electrograms were excluded in total (Supplemental Figure 1). SR potentials were analyzed for fractionation (number of deflections), peak-to-peak amplitude (voltage) and RS ratios; atrial extrasystoles were excluded. The potentials in each electrogram were averaged for voltage and RS ratio comparison. The steepest negative deflection of a potential was marked as local activation time (AT) if the slope was ≥0.05 mV/ms and the deflection had a signal-to-noise ratio >2. Additional deflections with a slope ≥10% of the local AT (and ≥0.05 mV/ms), peak-to-noise ratio >2, and either an amplitude >1/6 of the amplitude of the local activation deflection or a signal-to-noise ratio >5 were marked as fractionation (Supplemental Figure 2). Only nonfractionated potentials (single deflections) were analyzed for the ratio between the R-peak and S-peak (RS ratio).[4] All signal markings were manually checked and corrected in case of markings on electrical artifacts evaluated by a consensus of two investigators. Figure 1 shows the analysis of signal amplitudes and RS ratios. Delayed activation is defined as interelectrode differences in AT >11 ms (<17 cm/s) of electrodes in the *same* plane. The amount of delayed activation is expressed in millimeters: number of interelectrode differences >11 ms × interelectrode distance (2 mm).

Analysis of local epi-endocardial differences

Local differences in AT, RS ratio and fractionation between the epicardium and endocardium were determined by comparing each electrogram with the electrograms in the opposite square: the exact opposite electrogram and its 8 surrounding electrograms. The local difference was the minimal difference of the potentials in the opposite square, as previously described.[3] Border electrodes were excluded from analysis of local differences. For local differences in RS ratio, only recordings with <25% fractionated potentials were included. Fractionated potentials with ≥15 ms between the first and last deflections were analyzed for detection of all (separate) deflections on both sides at the same time (epi-endocardial comparison of coinciding deflections). Each deflection was tested whether its steepest point fell within peak-to-peak time limits (±3 ms error margin) of deflections at the opposite square. The deflections that were not detected on the other side, as no coinciding deflection meeting the annotation criteria was present, were also manually examined for visual absence.

Classification of fractionation

Each fractionated deflection was evaluated if it could be attributed to remote activation, that is, to delayed (discontinuous) activation in the surrounding tissue in the *same* layer or to EEA. The adjacent and opposite, first and second electrode rings around the fraction-

ated potential were searched for deflections of local ATs coinciding with the fractionated deflection. If the fractionated deflection fell within peak-to-peak time limits (±3 ms) of the deflections of local ATs, it was classified based on the plane(s) where the corresponding local AT(s) was located (Figure 1, right panel). Corresponding ATs were present in either 1) the same plane, 2) the opposite plane, 3) both planes or 4) none of the planes (absence of corresponding local AT). Border electrodes were excluded from analysis. Fractionation interval for fractionated deflections was defined as the time interval between the fractionated deflection and the deflection of the local AT (Figure 1, middle panel).

Statistical analysis

Normally distributed data are given as mean±SD and skewed data are given as median (p10-p90). Electrophysiological parameters were in square root or log-transformed in case of a non-normal distribution. Linear mixed models were used to investigate the associations between location (independent variable) and electrophysiological parameters (dependent variable). Random intercepts were used for location. When normal distributions could not be obtained using transformations, the Friedman test was used to investigate the associations. Comparison of epicardial and endocardial amounts of delayed activation was done with the Wilcoxon signed rank test. Spearman rho coefficient was used to determine the correlation between cycle length and amount of delayed activation.

The associations of location and side with morphological parameters of electrograms were evaluated using Generalized Estimated Equations. The skewed distribution of RS ratios could not be transformed to a normal distribution; therefore, RS ratios were converted to a binomial distribution by setting the lowest-quartile (<-0.51) of RS values as “highly” S-dominant. Correlation structure was chosen based on the goodness of fit in the guasi-likelihood function and the inferior RA served as the reference in the models evaluating locations. Statistical analyses were performed using IBM SPSS Statistics version 21 (IBM corp.,Armonk, NY).

RESULTS

Electrophysiological data and parameters

Recordings at the inferior, mid and superior RA of 26, 25 and 21 patients, respectively, were included. SR cycle lengths did not change between the RA locations; inferior 902±202, mid 908±193 (P=0.72) and superior 827±162 (P=0.17). The amount of delayed activation increased from the inferior to the superior RA: 12 (0-80) mm, 32 (0-99) mm (P=0.095), 74 (18-178) mm (P<0.001). At the superior RA, the endocardium demonstrated more delayed activation than the epicardium; 26 (0-61) mm vs. 44 (7-124) mm (P=0.010). No correlation

was present between SR cycle length and amount of delayed activation (r=0.05, *P*=0.81). A total of 102,129 potentials were analyzed in 16,954 electrograms, including 50,714 potentials of 8423 electrograms recorded at the epicardium and 51,415 potentials of 8531 electrograms recorded at the endocardium. An overview of the individual patient results is provided in Supplemental Table 2.

Unipolar voltages

From the inferior to the middle and superior RA, electrogram voltage decreased gradually from 8.0 (3.1-16.3) mV, to 6.4 (2.4-13.3) mV (*P*=0.001) and to 4.9 (1.7-11.7) mV (*P*<0.001). Opposite epicardial and endocardial electrogram amplitudes demonstrated a positive linear relationship (Figure 2, bottom left panel). Because it was expected that voltage is dependent on fractionation, potentials were categorized into singles, doubles and complex fractionated (>2 deflections) potentials. Figure 2 shows that unipolar voltage indeed decreased with more fractionated potentials at both the epicardium and endocardium. The largest epi-endocardial difference in amplitude was observed for unipolar potentials with single deflections that had an epicardial vs endocardial amplitude of respectively 8.3 (3.8-14.7) mV vs 6.7 (2.8-16.1) mV (*P*=0.08). Double potentials had epi-endocardial amplitudes of 4.1 (1.6-8.3) mV vs 3.8 (1.3-8.5) mV (*P*=0.45). Complex fractionated potentials had amplitudes of 2.5 (1.1-4.7) mV vs 2.7 (1.2-5.1) mV (*P*=0.08). The percentile ranges of endocardial potentials were wider than of epicardial potentials.

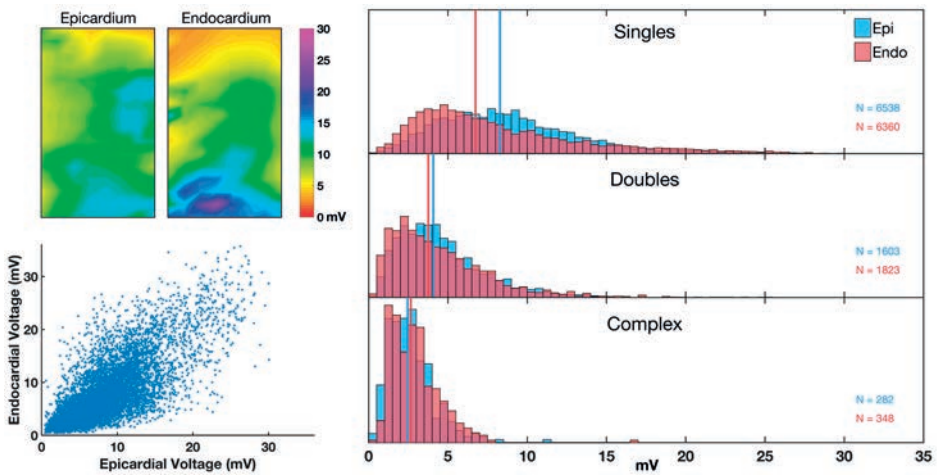

Figure 2. Epi-endocardial unipolar voltage.
Top left: Example of epicardial and endocardial voltage maps. Bottom left: Scatter plot of epi-endocardial unipolar voltages. Right: Relative frequency histograms of unipolar epicardial and endocardial electrogram voltage for singles, doubles and complex fractionated potentials. Vertical lines indicate the median.

RS ratio of epi-endocardial single deflections

The RS ratios of potentials with single deflections recorded at the epicardium and endocardium are shown in Figure 3 for each RA location. Both sides demonstrated a clear S-predominance, which increased at the mid-RA (*P*=0.001) and superior RA (*P*<0.001). Epicardial vs endocardial median RS ratios at the inferior RA were -0.23 (-0.53 to +0.26) vs. -0.25 (-0.53 to +0.26); at the mid-RA were -0.32 (-0.78 to +0.06) vs. -0.34 (-0.72 to +0.07); and at the superior RA were -0.43 (-0.96 to +0.09) vs. -0.46 (-0.97 to +0.11). Many potentials at the superior RA, the area of the sinus node, had an S-morphology (RS ratio of -1) at both sides (11% vs 13%). Local differences in RS ratios were between 0 and 0.22 for 95% of the data, without either side having more S-predominance than the other side (Figure 3).

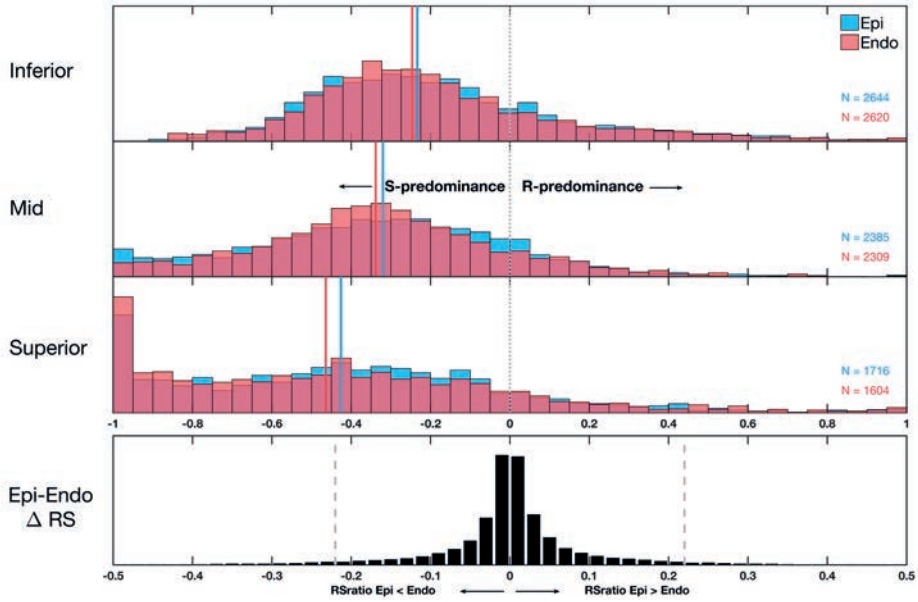

Figure 3. Relative frequency histograms of epicardial and endocardial RS-ratios and local epi-endocardial RS differences.

Top 3 panels: RS-ratios per location, negative values represent increasing S-predominance, positive values represent increasing R-predominance. Medians are indicated by vertical colored lines. Bottom panel: local differences in RS-ratio between epicardium and endocardium. Negative values represent smaller RS-ratio values at the epicardium, positive values represent smaller RS-ratio values at the endocardium. Between the dashed grey lines 95% of the data is represented.

Epi-endocardial differences in fractionation

Relative incidence of singles, doubles, triples and potentials with >3 deflections was 76%, 20%, 3% and <1%, respectively. The incidence of fractionated potentials (>1 deflection) showed an increasing trend from the inferior RA (16%) towards the mid-RA (22%, *P*=0.136) and was highest at the superior RA (36%, *P*<0.001). Epicardial vs endocardial incidence of

fractionation at the inferior RA was 15% vs 17% (*P*=0.29), at the mid-RA was 21% vs. 22% (*P*=0.45), and the superior-RA demonstrated a trend towards more fractionated potentials at the endocardium: 33% vs. 38% (*P*=0.09). Local epi-endocardial differences in the number of detected deflections occurred in 6.6% (Table 1).

Table 1. Epicardial vs. endocardial fractionation

	Total fractionation (%)								Local differences in fractionation Δ Epi-endo no. of deflections (%)			
	Singles		Doubles		Triples		Complex(>3)					
	Epi	Endo	Epi	Endo	Epi	Endo	Epi	Endo	0	1	2	3>
Inferior	84.7	82.9	12.8	14.5	2.3	2.4	0.2	0.2	95.7	4.1	0.2	<0.1
Mid	79.4	77.7	17.5	19.2	2.6	2.8	0.4	0.3	93.2	6.5	0.2	<0.1
Superior	67.3	62.0	27.1	30.6	4.4	6.4	1.2	1.1	90.8	8.7	0.5	<0.1
Total	77.8	75.0	18.6	20.8	3.0	3.7	0.6	0.5	93.4	6.3	0.3	<0.1

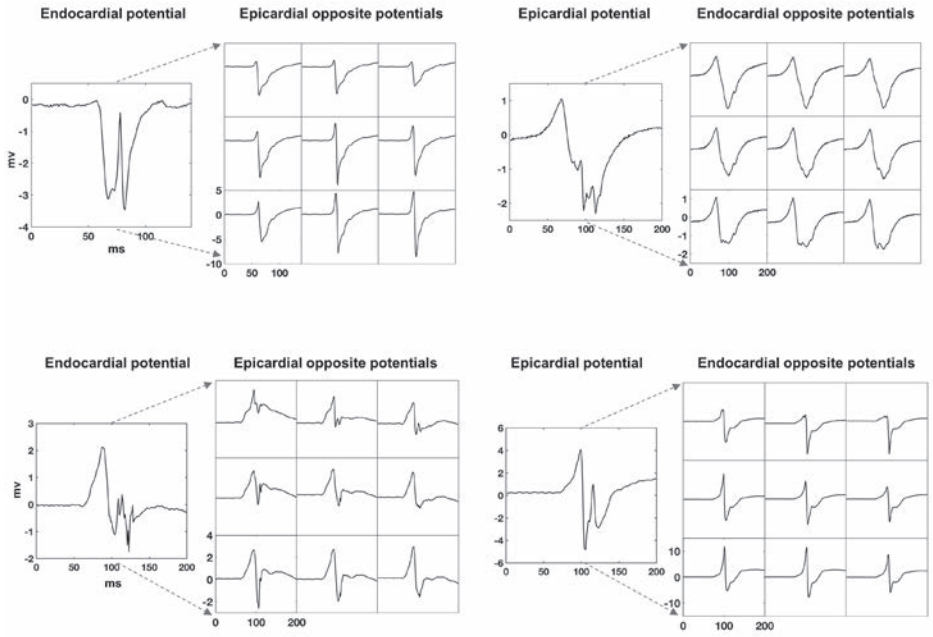

Figure 4. Examples of local differences in fractionation between epicardium and endocardium.
Four fractionated potentials are shown recorded at the epicardium or endocardium with the nine electrograms on the direct opposite side (direct opposite and its 8 surrounding electrograms). In the lower right example the second deflection of 4mV at the epicardium is totally absent at the endocardium.

A total of 1580 electrograms contained potentials with fractionated deflections having a fractionation interval ≥15 ms. In 271 of those 1580 cases, deflections remained undetected on the other side, based on the annotation criteria, and 53 of those 271 deflections were also visually completely absent. In 41 of 271 cases, the same number of deflections were present on both sides but with epi-endocardial time-differences between the corresponding deflections of 4-85 ms (median 13 ms). In the remaining 177 of 271 cases, a (small) deflection was visually observed that did not meet the criteria for a deflection. Examples of epi-endocardial differences in fractionation (Figure 4) demonstrate that deflections up to a maximum of 4 mV on one side could be absent at that location on the other side.

Endo-epicardial asynchrony during sinus rhythm

Right atrial EEA >14 ms, as previously defined for AF[3], occurred at the inferior RA in 12% of the patients, at the mid-RA in 19% and at the superior RA in 57%. EEA increased from the inferior to the superior RA (*P*=0.001). One patient had by far the most EEA of the study group (44.4% at the mid-RA) with an endocardial delay of >50 ms. EEA during SR is mainly determined by one side being delayed. The degree and incidence of EEA are provided in Supplemental Figure 3.

Fractionation attributable to delayed activation or endo-epicardial asynchrony

For the far majority (95%) of fractionated deflections, a corresponding local AT was present in the surrounding tissue of the same or opposite layer (Table 2). In 4%, a local AT was only observed in the *opposite* plane, which corresponds to sites with EEA (Figure 5A). In 9%, a corresponding local AT was only observed in the *same* plane, which corresponded to a site with delayed activation that was asymmetrical between the epicardium and endocardium (local delayed activation in one plane) (blue outlined potential, Figure 5B). In 83% of fractionated deflections, a matching local AT was present in both planes. This group contains 3 underlying causes: 1) symmetrical epi-endocardial delayed activation (Figure 5C), 2) asymmetrical epi-endocardial delayed activation; after the site with a delay in activation (Figure 5B), 3) short fractionation intervals (Figure 5C). Most can be attributed

Table 2. Classification of fractionated deflections corresponding with local activation times

	Doubles				Triples				Complex (>3)				Total
	N	%	FI (ms)		N	%	FI (ms)		N	%	FI (ms)		N (%)
Same plane	144	7	28	(14-58)	73	11	22	(10-27)	24	15	13	(11-47)	241 (9)
Opposite plane	69	3	27	(11-60)	26	4	26	(16-37)	8	5	38	(22-38)	103 (4)
Both planes	1682	85	12	(8-24)	553	82	12	(8-23)	99	63	14	(9-39)	2334 (83)
None	91	5	32	(17-60)	22	3	30	(18-56)	27	17	35	(21-35)	140 (5)

FI = fractionation interval.

to short fractionation intervals as the median fractionated interval for these deflections was only 12 ms (Table 2). For the remaining 5% of fractionated deflections, no matching local AT was found. Some of those had corresponding local ATs distanced >4 mm of the fractionated site (Figure 5B), and more than half (61%) were deflections on electrodes that did not have a complete second ring to search for corresponding ATs (relative border electrodes). Figure 5D shows an example of a fractionated deflection likely reflecting intramural inhomogeneity in conduction; it only appears in center electrodes without any corresponding local AT. Potentials with >3 deflections most often had deflections without any corresponding local AT compared to doubles and singles (17% vs 3% and 5%).

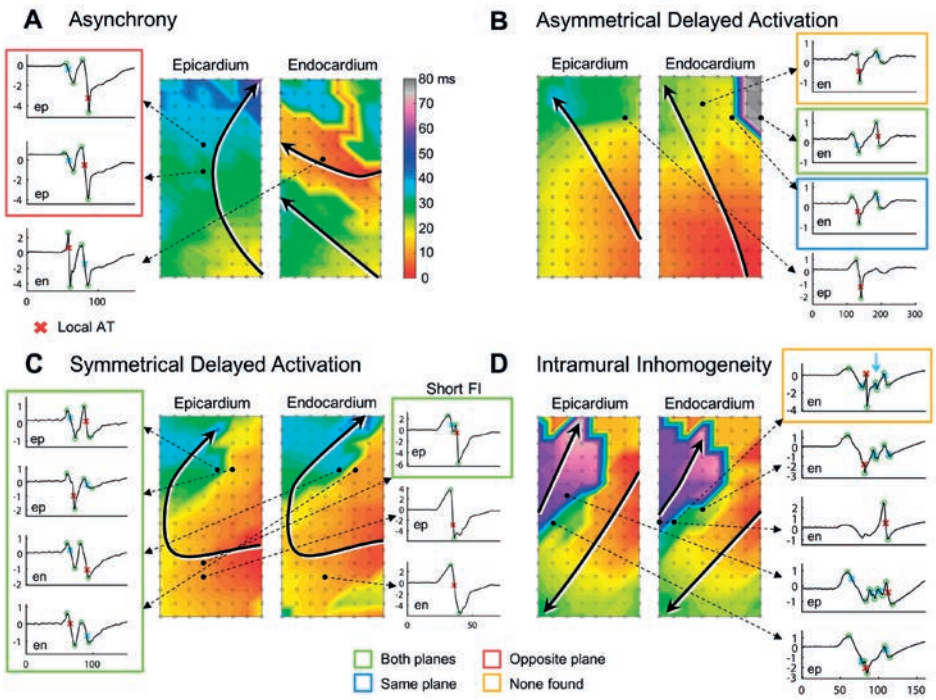

Figure 5. Fractionated potentials attributable to various patterns of conduction disorders.
Panels A-D demonstrate examples where fractionated potentials correspond to remote myocardial activation in the same plane (outlined in blue), in the opposite plane (outlined in red) or in both planes (outlined in green) or do not correspond with any remote activation (outlined in orange). A: Endo-epicardial asynchrony causes fractionated deflections (blue marked deflections) at the epicardium, matching local activation times (AT, red marked deflections) are only present in the opposite plane. B: At sites with asymmetrical delayed activation (DA), fractionated deflections in front of an area of DA correspond to local ATs in the same plane, however at the delayed site, fractionated deflections correspond to ATs in both planes. In some cases, even sites >4 mm of the DA site show corresponding fractionated potentials. C: Fractionated deflections at sites with symmetrical DA at both sides, local ATs are present in both planes. Deflections with short fractionation intervals (FI) similar to normal conduction velocity will also mostly have matching local ATs at both sides. D: The third deflection of the upper complex fractionated potential does not correspond to any local AT in the same or opposite plane, demonstrating intramural inhomogeneity in conduction.

DISCUSSION

Electrogram morphology is often used for the identification of structural or electrical remodeled areas with arrhythmogenic properties. In most settings, electroanatomical mapping is performed via endovascular catheters at the endocardial side. In recent perspective, it has become clear that asynchrony within the atrial wall can have an important role in the mechanism of atrial arrhythmias.[3,8] Our study has shown that EEA >50 ms can already be present during SR and that unipolar electrogram fractionation can represent the presence of EEA. However, electrical activity within or on the opposite side of the atrial wall can also occasionally be missed when electrograms are recorded only from one side of the wall. At the superior RA, the highest amount of delayed activation and EEA was observed and resulted, because of their interdependence, in the highest amount of fractionated electrograms and the lowest voltages.

Right atrial anatomy

Variations between epi- and endocardial unipolar voltage can be explained from the anatomical structure of the RA wall. The surface of the endocardial RA appendage, unlike the smooth epicardial side, is very irregular due to the pectinate muscles of varying diameters and the thick terminal crest. The mass of cardiac bundles is positively correlated to unipolar electrogram voltage and anatomical studies have shown that pectinate muscles can vary from <1 to 7 mm.[9,10] The different sizes and arrangement of the bundles also cause a variation in the level of contact with the electrodes on the flat array. Our high-resolution epicardial mapping study demonstrated recently that epicardial breakthrough waves during SR were most frequently observed at the superior RA.[11] EEA indeed occurred most often in this area which also correlated to the highest amount of delayed activation and fractionation. The superior RA contains the sinus node within its fibrous case and the thickest part of the anisotropic terminal crest, which may underlie the proneness of this area to delays in activation, EEA and breakthrough waves.[9,12] The structural variability of the RA therefore influences epi-endocardial synchronicity and electrogram morphology. Electrical activity that remains undetected on one side may relate to thicker or more irregular parts of the RA.

The value of unipolar electrograms

Unipolar electrograms have the benefit over bipolar electrograms that their morphology carries additional information about the progression of the wavefront and remote activations. The ratio between the positive and negative component of a unipolar electrogram characterizes the start or end of a wavefront and possibly the curvature of the wavefront and conduction velocity.[13] Epicardial electrograms recorded during AF demonstrated an S-predominance which could not be strongly correlated to wavefront curvature or

anisotropy.[4] A tilted transmural stance of the wavefront resulting in an epicardial lead with constant epicardial to endocardial activation was proposed as theoretical explanation for S-predominance during AF which would present with more R-predominance at the endocardium. In this study, both epicardial and endocardial electrograms showed an S-predominance and endocardial electrograms did not have higher RS ratios than epicardial electrograms. Therefore, S-predominance during SR cannot be explained by epicardial to endocardial activation or vice versa. Previous studies demonstrated that endocardial unipolar electrogram voltage is more useful for detecting areas of scar at the epicardium than bipolar electrogram voltage because of their range of view.[14] We established that the view of unipolar electrograms can signify the presence of EEA and can reveal areas with intramural inhomogeneous conduction. Detecting EEA from the endocardium alone requires the atrial "farfield" potentials on unipolar electrograms that will be filtered out with standard bipolar recordings. Furthermore, the limitations of registering all atrial activity from throughout the atrial wall demonstrated by our high-density contact mapping approach will only increase with noncontact mapping systems. Therefore, current mapping approaches may be insufficient to detect transmural atrial activity.

Epi-endocardial electrograms during atrial arrhythmias

The incidence of local differences in epicardial and endocardial electrogram morphology and of electrogram fractionation due to EEA is relatively low during SR. According to the observations of Schuessler et al., epi-endocardial differences in activation were least prominent during SR and high-rate pacing, but were significantly increased with premature stimulation.[2] In a goat model of AF, the amount of EEA increased with AF persistence, which was also associated with more inhomogeneous conduction patterns and a shortening of fibrillation cycle length.[15] Our previous study in humans also demonstrated more EEA at the RA wall during AF with incidences between 0.9 and 55.9%.[3] EEA occurs more frequently in atrial arrhythmias because of the increase of inhomogeneous conduction and (functional) conduction disorders. Therefore, fractionation due to EEA and local differences in epi-endocardial electrogram fractionation are expected to increase during atrial arrhythmias. The RA appendage, which has the thickest wall of the whole atria, is especially susceptible to local differences in electrogram morphology and EEA. Nevertheless, breakthrough waves also occur frequently at the left atrium, indicating the presence of EEA, and with wavefronts decreasing in size during AF, electrogram amplitude will decrease causing local differences in fractionation more likely to occur in any area.[11,16] When fractionated electrograms are ablated only from the endocardial side, epicardial fractionated sites could be overlooked. However, more importantly, these fractionated sites have different pathophysiological origins, including EEA, and ablating all fractionated electrograms would only increase needless atrial scarring.

Study limitations

Intraoperative simultaneous endo-epicardial mapping in living humans can only be safely performed at the RA; therefore, we could not evaluate the relation of epicardial and endocardial electrograms at the structurally less complicated left atrium. However, epicardial breakthroughs also are often present at the left atrium, indicating the occurrence of EEA at the left atrium during SR as well.[11] The finite area of the mapping array and relatively low incidence of (complex) fractionation during SR limited the classification of fractionated deflections to those situated in the center of the array. The relatively small number of fractionated deflections classified to no corresponding local AT is probably still an overestimation.

CONCLUSIONS

In SR, EEA of the RA free wall occurs at >50 ms difference between epicardium and endocardium, which has never been described before. Electrograms on both sides demonstrate an S-predominance and the RS ratio cannot be used to identify the leading layer during SR. Fractionated potentials are not always identical on a high-resolution scale and can have local mismatches; however, these mismatches occur in a minority of cases. If a potential is fractionated during SR, most additional deflections can be explained by conduction disorders in the *same* plane and in a small percentage they represent EEA. The incidence of EEA and EEA-based fractionation is relatively low during SR, as was expected. However, during atrial arrhythmias the presence of (functional) conduction disorders and EEA will increase; therefore, epi-endocardial differences in electrogram morphology and EEA-based fractionation will likely increase as well. Particularly interesting, especially for clinical practice, is the observation that the morphology of unipolar electrograms can potentially be a tool to identify areas of EEA when electrograms are recorded on only one side of the wall.

REFERENCES

1. Lukas A, Antzelevitch C. Differences in the electrophysiological response of canine ventricular epicardium and endocardium to ischemia. Role of the transient outward current. Circulation. 1993;88:2903-2915.
2. Schuessler RB, Kawamoto T, Hand DE, Mitsuno M, Bromberg BI, Cox JL, Boineau JP. Simultaneous epicardial and endocardial activation sequence mapping in the isolated canine right atrium. Circulation. 1993;88:250-263.
3. de Groot N, van der Does L, Yaksh A, Lanters E, Teuwen C, Knops P, van de Woestijne P, Bekkers J, Kik C, Bogers A, Allessie M. Direct Proof of Endo-Epicardial Asynchrony of the Atrial Wall During Atrial Fibrillation in Humans. Circ Arrhythm Electrophysiol. 2016;9:e003648.
4. Houben RP, de Groot NM, Smeets JL, Becker AE, Lindemans FW, Allessie MA. S-wave predominance of epicardial electrograms during atrial fibrillation in humans: indirect evidence for a role of the thin subepicardial layer. Heart Rhythm. 2004;1:639-647.
5. Nademanee K, McKenzie J, Kosar E, Schwab M, Sunsaneewitayakul B, Vasavakul T, Khunnawat C, Ngarmukos T. A new approach for catheter ablation of atrial fibrillation: mapping of the electrophysiologic substrate. J Am Coll Cardiol. 2004;43:2044-2053.
6. van der Does LJ, de Groot NM. Inhomogeneity and complexity in defining fractionated electrograms. Heart Rhythm. 2017;14:616-624.
7. Knops P, Kik C, Bogers AJ, de Groot NM. Simultaneous endocardial and epicardial high-resolution mapping of the human right atrial wall. J Thorac Cardiovasc Surg. 2016;152:929-931.
8. Pathik B, Lee G, Sacher F, Haïssaguerre M, Jaïs P, Massoullie G, Derval N, Sanders P, Kistler P, Kalman JM. Epicardial-endocardial breakthrough during stable atrial macroreentry: Evidence from ultra-high-resolution 3-dimensional mapping. Heart Rhythm. 2017;14:1200-1207.
9. Sanchez-Quintana D, Anderson RH, Cabrera JA, Climent V, Martin R, Farre J, Ho SY. The terminal crest: morphological features relevant to electrophysiology. Heart. 2002;88:406-411.
10. Spach MS, Dolber PC. Relating extracellular potentials and their derivatives to anisotropic propagation at a microscopic level in human cardiac muscle. Evidence for electrical uncoupling of side-to-side fiber connections with increasing age. Circ Res. 1986;58:356-371.
11. Mouws E, Lanters E, Teuwen C, van der Does L, Kik C, Knops P, Bekkers J, Bogers A, de Groot N. Epicardial Breakthrough Waves during SR: Depiction of the Arrhythmogenic Substrate? Circ Arrhythm Electrophysiol. 2017:e005145.
12. Fedorov VV, Glukhov AV, Chang R, Kostecki G, Aferol H, Hucker WJ, Wuskell JP, Loew LM, Schuessler RB, Moazami N, Efimov IR. Optical mapping of the isolated coronary-perfused human sinus node. J Am Coll Cardiol. 2010;56:1386-1394.
13. Spach MS, Miller WT, 3rd, Miller-Jones E, Warren RB, Barr RC. Extracellular potentials related to intracellular action potentials during impulse conduction in anisotropic canine cardiac muscle. Circ Res. 1979;45:188-204.
14. Tokuda M, Tedrow UB, Inada K, Reichlin T, Michaud GF, John RM, Epstein LM, Stevenson WG. Direct comparison of adjacent endocardial and epicardial electrograms: implications for substrate mapping. J Am Heart Assoc. 2013;2:e000215.
15. Eckstein J, Zeemering S, Linz D, Maesen B, Verheule S, van Hunnik A, Crijns H, Allessie MA, Schotten U. Transmural conduction is the predominant mechanism of breakthrough during atrial fibrillation: evidence from simultaneous endo-epicardial high-density activation mapping. Circ Arrhythm Electrophysiol. 2013;6:334-341.

16. de Groot NMS, Houben RPM, Smeets JL, Boersma E, Schotten U, Schalij MJ, Crijns H, Allessie MA. Electropathological Substrate of Longstanding Persistent Atrial Fibrillation in Patients With Structural Heart Disease Epicardial Breakthrough. Circulation. 2010;122:1674-1682.

SUPPLEMENTAL MATERIAL CHAPTER 12: DATA ANALYSIS

Patient data inclusion

First activation was required to occur at the top or right atrial side of the mapping area of the superior or middle right atrial recording site, otherwise the rhythm was labelled as an ectopic atrial rhythm and the patient was not included for analysis. Patients required two included recording sites (see below) in order to qualify for study inclusion.

Electrogram exclusion criteria

Electrograms with injury potentials (that can appear due to firm contact with local tissue) were excluded for RS ratio analysis only or excluded for all analyses based on the following criteria:

RS ratio exclusion criteria:	elevation of the baseline after the local potential ≥1/3 and < total amplitude of local potential + concordant shift of potential
Total exclusion criteria:	elevation of the baseline after the local potential ≥1 mV and ≥ total amplitude of local potential

Examples are provided in Supplemental Figure 1.

Recording sites with 25% of missing or total excluded electrograms were excluded from further data analysis which included either a total number of missing/excluded electrograms ≥64 or a total of 32 electrodes from which the exact opposite electrode was missing/excluded. Excluded recording sites of patients are shown in Supplemental Table 2.

Signal marking

Deflections and peaks were marked by the criteria stated in the manuscript using MATLAB R2016a (The MathWorks Inc., Natick, MA). The signal-to-noise ratio was determined by the amplitude of the deflection in relation to the amplitude of the noise (Supplemental Figure 2, top). The peak-prominence of a new peak was used to evaluate the peak-to-noise ratio which defined a new deflection (Supplemental Figure 2, bottom). Noise levels were determined for each electrode separately. All signal markings were checked manually and markings of artifacts were corrected based on a consensus of two investigators.

Analysis of local epi-endocardial differences

Local epi-endocardial differences are analyzed by comparing each potential to the exact opposite potential and its 8 surrounding potentials; 9 potentials in total (=opposite square) and determined by the minimal difference of these 9 comparisons. If the opposite square consisted of 6 or less potentials the electrode was considered a border electrode and was excluded from analysis of local differences.

Supplemental Table 1. Clinical characteristics

Patient no.	Age (yr)	Gender	Structural heart disease	History of AF	RCA S1 stenosis	Dilated RA	Left ventricular function	HT	DM	HC	AAD
1	80	Male	IHD; MVD	Paroxysmal	No	No	Normal	Yes	No	Yes	Class 3
2	71	Male	IHD	None	No	No	Normal	Yes	No	No	Class 2
3	67	Male	IHD	None	Yes	Unknown	Normal	Yes	Yes	No	Class 2
4	70	Male	IHD	None	Yes	Unknown	Normal	Yes	Yes	Yes	Class 2
5	54	Female	IHD	None	No	Unknown	Normal	Yes	Yes	No	-
6	49	Female	IHD; MVD	None	No	Unknown	Mild impairment	No	No	No	-
7	79	Male	IHD; MVD	Persistent	No	Yes	Mild impairment	No	No	No	Class 2, digoxin
8	61	Male	IHD; MVD; PFO	None	No	No	Normal	No	No	No	Class 2
9	73	Male	AVD	None	No	No	Normal	No	No	No	-
10	59	Male	AVD	None	No	Unknown	Normal	Yes	No	No	Class 2
11	68	Male	IHD	Paroxysmal	No	No	Mild impairment	No	No	No	Class 2
12	53	Male	IHD	Paroxysmal	No	Unknown	Normal	No	No	No	Class 2
13	72	Male	IHD	None	No	No	Normal	Yes	Yes	Yes	Class 3
14	64	Female	AVD; MVD	None	No	No	Normal	No	Yes	No	Class 2
15	67	Male	AVD	None	No	Unknown	Normal	Yes	Yes	Yes	-
16	47	Male	IHD	None	No	Unknown	Normal	No	Yes	No	Class 2
17	85	Male	IHD	Paroxysmal	No	Unknown	Normal	Yes	No	No	Class 2, digoxin
18	65	Male	IHD	None	No	Unknown	Normal	Yes	No	No	Class 2
19	53	Male	IHD	Persistent	Yes	Yes	Severe impairment	No	No	No	Class 2, digoxin
20	71	Male	-	Paroxysmal	No	Unknown	Normal	Yes	No	No	Class 2+3
21	71	Male	IHD; MVD	Paroxysmal	Yes	No	Moderate impairment	Yes	No	Yes	Class 1+2
22	64	Male	IHD; AVD	Paroxysmal	No	No	Normal	Yes	No	Yes	Class 2

Supplemental Table 1. Clinical characteristics (continued)

Patient no.	Age (yr)	Gender	Structural heart disease	History of AF	RCA S1 stenosis	Dilated RA	Left ventricular function	HT	DM	HC	AAD
23	76	Female	MVD	Longstanding Persistent	No	Yes	Normal	Yes	Yes	No	Class 2, digoxin
24	64	Female	MVD; TVD	Longstanding Persistent	No	Unknown	Mild impairment	No	No	No	Class 4, digoxin
25	67	Male	IHD	None	No	No	Normal	No	Yes	Yes	Class 2
26	82	Male	IHD	None	No	Unknown	Normal	Yes	Yes	No	Class 2
Total/ mean	67±10	Male 21 (81%)	IHD 19 (73%) VHD 12 (46%)	11 (42%)	4 (15%)	3	Normal 20 (77%)	15 (58%)	10 (39%)	7 (27%)	-

IHD = ischemic heart disease; MVD = mitral valve disease; AVD = aortic valve disease; TVD = triscuspid valve disease; PFO = persistent foramen ovale; VHD = valvular heart disease; AF = atrial fibrillation; RCA S1 = right coronary artery segment 1 (proximal); HT = hypertension; DM = diabetes mellitus; HC = hypercholesterolemia; AAD = antiarrhythmic drugs.

Supplemental Table 2. Individual results of electrophysiological parameters and epi-endocardial electrogram morphology

Patientno.	Location	SRCL (ms)	DA (mm)		Voltage (mV)		RS ratio		Fractionation (%)		EEA (%)	Epi delay (%)	Endo delay (%)
			Epi	Endo	Epi	Endo	Epi	Endo	Epi	Endo			
1	inferior	1047	32	20	9.9	12.5	-0.24	-0.19	17	25	0	0	0
	mid	1171	8	12	7.5	9.5	-0.22	-0.32	16	25	0	0	0
	superior	563	24	36	7.6	7.4	0.19	0.07	35	37	0	0	0
2	inferior	1024	8	12	10.7	12.1	-0.41	-0.43	10	11	0	0	0
	mid	1008	72	36	6.3	6.6	-0.60	-0.61	56	55	6.2	4.6	1.6
	superior						excluded						
3	inferior	998	58	46	5.9	6.6	-0.20	-0.30	49	44	0.2	0	0.2
	mid						excluded						
	superior	1002	50	58	3.3	3.1	0.10	0.14	55	57	0	0	0
4	inferior	1088	2	8	9.5	11.3	-0.28	-0.24	19	12	0	0	0
	mid	1043	34	66	3.9	3.1	-0.80	-0.67	27	49	1.7	1.3	0.5
	superior	840	54	130	4.6	2.8	-0.68	-0.74	34	62	0.5	0.1	0.4
5	inferior	669	0	0	9.1	5.2	-0.47	-0.39	1	0	0	0	0
	mid	672	0	0	8.4	7.1	-0.31	-0.28	12	7	0	0	0
	superior	707	38	50	4.1	1.9	-0.65	-0.97	24	45	10.0	9.2	0.8
6	inferior	717	0	0	10.4	11.4	-0.21	-0.23	0	2	0	0	0
	mid	696	0	4	8.5	7.9	-0.32	-0.41	3	7	0	0	0
	superior	682	0	24	6.1	5.5	-0.76	-0.96	26	29	0.4	0	0.4
7	inferior	1577	8	2	8.9	7.8	-0.18	-0.20	14	11	0	0	0
	mid	1472	2	6	9.1	7.9	-0.17	-0.28	12	12	0	0	0
	superior						excluded						
8	inferior	729	0	0	9.1	7.5	-0.23	-0.17	5	4	0	0	0
	mid	718	8	24	8.9	6.3	-0.26	-0.34	14	19	0	0	0
	superior	705	18	44	7.1	5.9	-0.39	-0.41	23	24	0	0	0
9	inferior	793	22	44	5.9	3.6	-0.14	-0.28	39	49	0	0	0
	mid	793	12	38	6.0	3.9	-0.23	-0.33	39	43	0	0	0
	superior	895	66	68	4.0	3.4	-0.65	-0.87	51	49	2.6	0.3	2.3
10	inferior	895	4	6	11.5	7.6	-0.46	-0.43	12	4	0	0	0
	mid	1004	8	28	7.5	4.4	-0.73	-0.56	19	21	0	0	0
	superior	1005	22	60	4.3	4.1	-0.99	-0.83	36	72	1.5	0.5	1.1
11	inferior	954	0	0	9.7	9.6	-0.24	-0.20	4	5	0	0	0
	mid	1005	6	6	8.7	6.5	-0.26	-0.24	15	12	0	0	0
	superior	970	26	18	6.1	4.8	-0.26	-0.19	33	34	0.8	0	0.8
12	inferior	983	0	0	9.4	14.3	-0.49	-0.44	6	3	0	0	0
	mid	990	38	60	5.1	4.6	-0.63	-0.69	49	49	10.3	10.3	0

Supplemental Table 2. Individual results of electrophysiological parameters and epi-endocardial electrogram morphology (continued)

Patientno.	Location	SRCL (ms)	DA (mm)		Voltage (mV)		RS ratio		Fractionation (%)		EEA (%)	Epi delay (%)	Endo delay (%)
			Epi	Endo	Epi	Endo	Epi	Endo	Epi	Endo			
	superior	975	54	146	3.0	1.9	-0.77	-0.90	49	89	23.1	2.0	21.2
13	inferior	1014	0	22	5.1	6.0	-0.22	-0.18	22	28	0	0	0
	mid	962	14	24	5.7	5.8	0.05	-0.05	17	19	0	0	0
	superior	1005	16	12	4.6	4.6	-0.11	-0.09	32	23	0	0	0
14	inferior	677	36	34	5.7	3.3	0.44	0.44	30	25	2.8	0.0	2.8
	mid	820	24	16	3.7	3.2	-0.52	-0.57	26	11	0	0	0
	superior	689	62	72	1.9	1.9	-0.68	-0.84	35	16	6.6	0.4	6.3
15	inferior	849	0	0	16.9	16.9	0.19	0.25	2	5	0	0	0
	mid	720	0	0	17.8	14.5	-0.16	-0.22	3	9	0	0	0
	superior	571	0	0	16.3	13.4	-0.06	-0.17	3	9	0	0	0
16	inferior	1155	0	6	9.7	9.1	-0.25	-0.25	4	17	0	0	0
	mid	1135	0	0	11.2	6.0	-0.21	-0.18	4	4	0	0	0
	superior	1130	0	16	9.0	4.5	-0.41	-0.51	4	17	0	0	0
17	inferior	966	6	14	8.0	3.7	-0.39	-0.43	9	9	0	0	0
	mid	1053	50	34	3.6	2.3	-0.51	-0.49	29	31	0	0	0
	superior						excluded						
18	inferior	732	0	4	7.2	4.9	-0.36	-0.31	7	2	0	0	0
	mid	869	0	2	9.1	5.5	-0.32	-0.36	0	2	0	0	0
	superior						excluded						
19	inferior	1088	48	20	3.5	3.2	0.36	0.42	42	45	0	0	0
	mid	1067	14	12	8.1	6.8	0.10	0.23	12	10	0	0	0
	superior	974	24	50	8.0	6.9	-0.05	0.08	31	29	0	0	0
20	inferior	702	4	4	6.1	5.5	-0.11	-0.19	6	13	0	0	0
	mid	703	6	6	5.9	6.3	-0.44	-0.44	12	24	0	0	0
	superior	704	14	30	4.7	6.0	-0.66	-0.60	25	33	1.1	1.1	0
21	inferior	834	2	14	5.7	4.1	-0.24	-0.40	11	36	1.5	0	1.5
	mid	784	8	48	2.8	0.9	-0.65	-0.46	26	60	44.4	0	44.4
	superior	776	48	34	4.7	5.3	-0.32	-0.44	58	36	0	0	0
22	inferior	678	0	0	9.2	7.0	-0.12	-0.20	4	4	0	0	0
	mid	698	4	20	8.1	5.5	-0.47	-0.54	22	19	0	0	0
	superior	675	56	100	7.3	4.4	-0.69	-0.96	38	43	1.1	0.9	0.2
23	inferior	954	12	2	18.0	18.0	-0.07	-0.12	9	13	0	0	0
	mid	972	22	3	14.9	12.8	-0.26	-0.31	20	10	0	0	0
	superior	952	30	6	9.8	8.4	-0.35	-0.42	28	17	0	0	0
24	inferior	787	2	14	11.2	8.4	-0.22	-0.21	12	24	0	0	0

Supplemental Table 2. Individual results of electrophysiological parameters and epi-endocardial electrogram morphology (continued)

Patientno.	Location	SRCL (ms)	DA (mm)		Voltage (mV)		RS ratio		Fractionation (%)		EEA (%)	Epi delay (%)	Endo delay (%)
			Epi	Endo	Epi	Endo	Epi	Endo	Epi	Endo			
	mid	773	38	38	8.3	7.8	-0.11	-0.29	30	25	0	0	0
	superior						excluded						
25	inferior	728	72	32	3.7	2.8	-0.53	-0.60	45	37	0	0	0
	mid	770	60	22	4.7	4.4	-0.43	-0.25	23	5	7.2	7.2	0.0
	superior	750	50	34	5.2	3.8	-0.77	-0.56	39	40	16.1	15.1	1.0
26	inferior	802	20	24	11.5	10.7	-0.11	-0.16	19	18	0	0	0
	mid	800	26	32	9.5	6.8	-0.23	-0.22	28	31	0	0	0
	superior	794	14	48	7.7	6.2	-0.29	-0.40	28	38	0.6	0	0.6

SRCL = sinus rhythm cycle length; DA = delayed activation; EEA = endo-epicardial asynchrony.

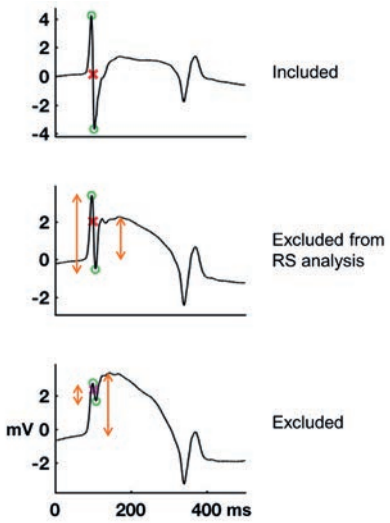

Supplemental Figure 1. Examples of potentials excluded from analysis.
The baseline after the potential in the middle is elevated > 1/3 of the total potential amplitude with a concordant shift of the potential to a positive dominance, this potential is excluded from RS analysis. The bottom potential is excluded from all analyses as the elevation of the baseline after the potential is larger than the total potential amplitude.

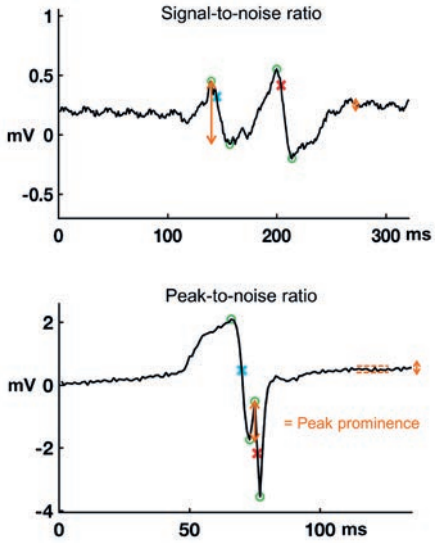

Supplemental Figure 2. Signal-to noise and peak-to-noise ratio.
Top: the ratio between the amplitude of the deflection and amplitude of the noise defined the signal-to-noise ratio. Bottom: the ratio between the peak prominence and the amplitude of the noise determined the detection of a new peak and the presence of a new deflection.

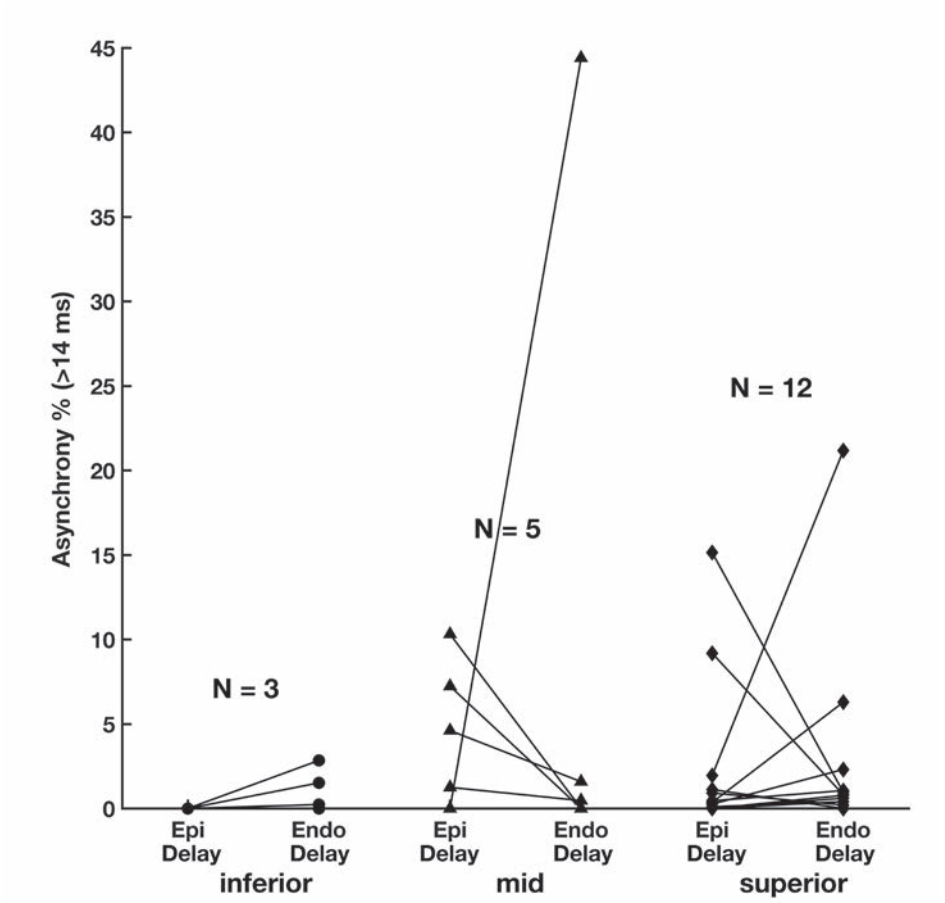

Supplemental Figure 3. Asynchrony in epi-endocardial activation.
Percentage of asynchrony (>14ms) with epicardial vs. endocardial delay per location for all patients with asynchrony. Asynchrony percentages are connected for each patient.

13

Endo-Epicardial Breakthrough: A Tale of Two Sides

Lisette van der Does
Natasja de Groot

Cardiac mapping has profoundly impacted diagnosis and treatments of focal and macro-re-entrant tachyarrhythmias. When the resolution of atrial mapping was increased, it revealed more specific patterns of activation during atrial fibrillation (AF) such as breakthrough waves. These breakthrough waves arose from circumscriptive areas from where they expand to a variable degree into the surrounding tissue. These breakthrough waves during AF were described as nonrepetitive events occurring scattered throughout both atria without any fixed pattern of activation.[1-3] Coupling intervals of breakthrough fibrillation waves were often longer than the dominant AF cycle lengths, so they were not a "driving source". Unlike the unipolar QS morphology at the origin of focal atrial tachycardia, most unipolar electrograms recorded from the initiation sites had a rS morphology. All these features suggested the presence of transmural propagating waves approaching the surface area from below.

As transmural conduction of fibrillation waves can only occur in the presence of endo-epicardial asynchrony, the hypothesis of asynchronous activation during AF was conceived. We subsequently provided the first direct proof of endo-epicardial asynchrony of the atrial wall during AF in humans by performing intraoperative simultaneous mapping of the endocardial and epicardial layer of the right atrial free wall. This study revealed not only the presence of endo-epicardial asynchrony, but also that breakthrough waves occur at both the endocardial and epicardial side.[3, 4]

The existence of asynchrony in activation between the epicardial and endocardial layer has been known for many years[5]; however, its importance in atrial arrhythmia pathophysiology has just recently started to be recognized. Simultaneous endo-epicardial mapping demonstrated that endo-epicardial asynchrony can be present up to 50% of the time during atrial fibrillation. For the majority of observed breakthrough waves, waves had passed by on the opposite side only a few moments before indicating that asynchronous fibrillation waves conducted through the atrial wall resulting in breakthrough waves.[2] The structural architecture of the atria is likely a key player in these phenomena. The first study of asynchrony performed by Schuessler et al. already associated endo-epicardial asynchrony with regions composed of pectinate muscles and cardiac fibers with different alignments.[5] Sites of breakthrough will presumably correspond to sites where intramural fibers connect the two layers. Although observations of asynchrony are limited to the right atrial wall for now, the variability in fiber orientation at the left atrial wall provides a suitable substrate for left atrial endo-epicardial asynchrony as well.[6]

Evidence that the concept of waves conducting from one side to the other is not only limited to atrial fibrillation has now been provided by Pathik et al.[7] Their elegant study demonstrated in a sample of 26 patients by using high-resolution endovascular mapping

that breakthrough waves occur at the right atrium during macro-re-entrant tachyarrhythmias as well. Breakthrough waves were present in about half of the cases, mostly at the posterior right atrium, situated near sites of slow or blocked conduction. Breakthrough sites were in a couple of cases verifiably embedded in the arrhythmia circuit and could even be critical in maintaining the circuit. In the latter case, the breakthrough site signified a shift of the circuit pathway after ablation to an alternative route consisting of a preserved pathway on the opposite side of the atrial wall and transmural conduction after the ablation line. The breakthrough sites near areas of conduction block demonstrate that barriers for conduction are not always transmural. Conduction can be preserved at the other side of the wall causing conduction to continue on only one side which results in asynchrony and consequently endo-epicardial breakthrough waves. These interesting findings underline the fact that the electrophysiology of the atria is not 2-dimensional and we should start seeing the atrial wall as a 3-dimensional structure where new waves can originate from cardiac fibers coursing on the other side of the wall. Although they are, unfortunately, not able to directly confirm an epicardial source for the breakthrough waves in this study due to technical limitations, supporting evidence was well provided by demonstrating unipolar rS electrogram morphology at breakthrough sites and stability of breakthrough sites during pacing.

The fact that asynchronous patterns of activation within the atrial wall can have such a key role in multiple arrhythmia pathophysiologies emphasizes the relevance of evaluating cardiac electrophysiology from more than one perspective. The two sides of the cardiac wall can clearly exhibit discrepancies in barriers for conduction, creating differences in timing and possibly patterns of activation between both sides. Disturbances in conduction on one side can greatly effect patterns of conduction on the other side and each can represent a continuous source for new breakthrough waves on the opposite side. Therefore, new techniques in order to accomplish mapping in all 3 dimensions of the atrial wall in clinical practice should be further explored. The interplay between the endo- and epicardial side can be critical in arrhythmia pathophysiology and to fully understand their hold on each other during arrhythmia requires representation of both sides during mapping in future investigations.

REFERENCES

1. de Groot NM, Houben RP, Smeets JL, Boersma E, Schotten U, Schalij MJ, Crijns H, Allessie MA. Electropathological substrate of longstanding persistent atrial fibrillation in patients with structural heart disease: epicardial breakthrough. Circulation. 2010;122:1674-1682.
2. de Groot NM, van der Does LJ, Yaksh A, Lanters EA, Teuwen CP, Knops P, van de Woestijne P, Bekkers JA, Kik C, Bogers AJ, Allessie MA. Direct Proof of Endo-Epicardial Asynchrony of the Atrial Wall During Atrial Fibrillation in Humans. Circ Arrhythm Electrophysiol 2016;9:e003648.
3. van der Does LJ, Kik C, Bogers AJ, Allessie MA, de Groot NM. Dynamics of Endo- and Epicardial Focal Fibrillation Waves at the Right Atrium in a Patient With Advanced Atrial Remodelling. Can J Cardiol. 2016;32:1260.e19-1260.e21.
4. Knops P, Kik C, Bogers AJ, de Groot NM. Simultaneous endocardial and epicardial high-resolution mapping of the human right atrial wall. J Thorac Cardiovasc Surg. 2016;152:929-931.
5. Schuessler RB, Kawamoto T, Hand DE, Mitsuno M, Bromberg BI, Cox JL, Boineau JP. Simultaneous epicardial and endocardial activation sequence mapping in the isolated canine right atrium. Circulation. 1993;88:250-263.
6. Ho SY, Sanchez-Quintana D, Cabrera JA, Anderson RH. Anatomy of the left atrium: implications for radiofrequency ablation of atrial fibrillation. J Cardiovasc Electrophysiol. 1999;10:1525-1533.
7. Pathik B, Lee G, Sacher F, Haïssaguerre M, Jaïs P, Massoullié G, Derval N, Sanders P, Kistler P, Kalman JM. Epicardial-Endocardial Breakthrough During Stable Atrial Macro-Reentry: Evidence from Ultra High-Resolution Three-Dimensional Mapping. Heart Rhythm. 2017;14:1200-1207.

14

Detection of Endo-Epicardial Asynchrony in the Atrial Wall using One-Sided Unipolar and Bipolar Electrograms

Lisette van der Does
Roeliene Starreveld
Rohit Kharbanda
Paul Knops
Charles Kik
Ad Bogers
Natasja de Groot

ABSTRACT

Background: Endo-epicardial asynchronous activation (EEA) is a new mechanism possibly maintaining atrial fibrillation. However, clinical electrophysiology studies can mostly record electrical activity at only one side of the atrial wall. EEA could be detected from one-sided electrograms by identifying farfield electrical activity (fractionation) reflecting EEA. We aimed to determine the sensitivity and best recording modus to detect EEA with use of electrogram fractionation.

Methods: Simultaneously obtained right atrial epicardial and endocardial multi-electrogram maps from 22 patients during cardiac surgery demonstrating EEA were selected. Unipolar electrograms were converted to bipolar electrograms in the horizontal (bi-x) and vertical (bi-y) direction. Unipolar electrograms and bipolar electrograms were analyzed by two investigators for presence and characteristics of unipolar and bipolar fractionation corresponding to EEA.

Results: Sensitivity of presence of fractionation corresponding to asynchronous activation was high in patients (86-96%) and moderately-high for the asynchronous surface area for both unipolar and bipolar electrograms equally (epi: 75% vs 65% (bi-x) and 69% (bi-y), endo: 72% vs 78% (bi-x) and 72% (bi-y)). Using the bipolar recording mode, signal-to-noise ratio of EEA corresponding fractionation decreased (from 11 (6-25) to 4 (2-7) in bi-y, $P<0.001$) and additional fractionation increased for electrograms recorded at the endocardium (53% (10-86) to 82% (52-100) in bi-x, $P=0.019$).

Conclusion: Sensitivity of fractionation corresponding to EEA is high for both unipolar and bipolar electrograms. However, unipolar electrograms are more suited for detection of EEA due to a larger signal-to-noise ratio and less disturbance of additional fractionation.

INTRODUCTION

The electrical pathophysiological mechanisms of persistent atrial fibrillation remain to this day largely unknown. Recent evidence suggests that dissociated electrical conduction between the layers of the atrial wall presenting as endo-epicardial asynchrony (EEA) in excitation is a potential significant mechanism for persistence of atrial fibrillation.[1,2] The asynchronous activation of epicardial and endocardial layers provide opportunity for waves of excitation to travel transmurally and cause new breakthrough waves on the opposite side of the wall. After canine and goat models, a new simultaneous endo-epicardial mapping approach finally allowed for documentation of EEA of the right atrial wall in patients as well.[1,3,4] However, this technique can only be applied in patients undergoing cardiac surgery and is limited to the right atrial appendage/free wall and occasionally the left atrial appendage.[5] A method to detect EEA during endovascular electrophysiological studies would greatly benefit research into the mechanisms of atrial fibrillation. Recently, we investigated simultaneously recorded unipolar endocardial and epicardial electrograms during sinus rhythm and discovered that EEA causes unipolar electrogram fractionation (additional deflections on the electrogram). By relating unipolar electrogram fractionation to spatial patterns of activation, fractionation could be attributed to EEA.[6] However, most electrophysiological studies use a bipolar recording mode for mapping to reduce farfield effects recorded by unipolar electrograms.[7] In case of EEA, remote activation on unipolar electrograms could be an important feature to detect EEA while recording on only one side of the atrial wall. We therefore hypothesized that unipolar electrograms are more sensitive in detection of atrial EEA than bipolar electrograms. Electrogram features of sites with EEA were analyzed in 22 patients and we compared the sensitivity of unipolar and bipolar electrograms for detection of EEA from only one side of the atrial wall.

METHODS

Study population

Twenty-two patients from the ongoing Epic End study in the Erasmus Medical Center were selected. The Epic End study is approved by the local medical ethics committee (MEC-2015-373) and includes patients over 18 years of age undergoing cardiac surgery for coronary artery disease, heart valve disease and/or congenital heart disease. Prior to participation all patients gave informed consent. Mean age of selected patients was 65±9 years and 15 of 22 patients were male. Cardiac surgery was performed for coronary artery disease (N=15) and/or valvular heart disease (N=12), ten patients had a history of atrial fibrillation of whom one had persistent atrial fibrillation.

Endo-epicardial mapping

Mapping during cardiac surgery was performed just before commencement of cardiopulmonary bypass and after arterial cannulation. Simultaneous endo-epicardial mapping was conducted by introducing one of two 128-electrode (8x16) arrays in the right atrium via the incision for venous cannulation for endocardial mapping. The other array was placed on top of the epicardium for epicardial mapping. Both electrode arrays (0.45 mm electrodes, 2 mm interelectrode spacing) were fixed on a steel spatula and bound together to ensure good contact and precise alignment of the two arrays. Unipolar electrograms of the right atrial wall were recorded for 5-10 seconds during sinus rhythm and pacing at the superior, middle and inferior right atrial free wall (Figure 1A-C). In one patient, endo-epicardial electrograms were recorded from the left atrial appendage before excision. Electrograms were sampled at 1000 Hz, filtered (0.5-400 Hz) and digitized (16-bits conversion) and, with a calibration signal of 2 mV, stored on hard disk for offline analysis. Details of the endo-epicardial mapping procedure were previously described.[5]

Data analysis

Electrogram selection, conversion and marking

Recorded data during sinus rhythm and pacing of all patients included in our study were analyzed for the presence of EEA (Figure 1D). Only patients demonstrating EEA were included and if multiple recording sites of a patient demonstrated EEA, only the recording site with the largest area of EEA was included. Local activation time (LAT) of unipolar electrograms was marked at the steepest negative slope (dV/dt) with a minimum of 0.05 mV/ms. Activation maps were constructed for both epicardium and endocardium. EEA was determined from these maps by calculating the differences between the local activation time at each electrode and the 9 opposite electrodes in the other plane; direct opposite and its 8 surrounding electrodes. Minimal time difference with these 9 opposite electrode sites determined the time difference for the electrode. EEA was defined as a difference between epicardial and endocardial local activation time of ≥15 ms. If unipolar asynchrony maps demonstrated EEA at ≥4 adjacent electrode sites that did not include border electrodes, the recording site was included for analysis. Border electrodes, defined as electrodes with <7 opposite local activation times, and electrodes missing the exact opposite electrogram were excluded from analysis. One electrode site corresponds to an area of 4 mm^2.

Unipolar electrograms were converted to bipolar electrograms by subtracting the unipolar electrogram from one electrode from the unipolar electrogram at the adjacent electrode of the array. Bipolar conversion was performed two times: in the horizontal (x) direction and in the vertical (y) direction. LAT of bipolar electrograms was marked at the largest (maximal or minimal) peak. EEA and electrode inclusion was then determined as described above with the exception that bipolar electrograms at the right or left border, in

case of x-direction conversion, and top or bottom border, in case of y-direction conversion, were also included for analysis (Figure 2). In addition, for the bipolar activation maps, only electrodes with EEA on similar sites of EEA on the unipolar activation maps were included. This assured only electrograms from the same EEA site were analyzed so there was no disagreement between the unipolar and bipolar EEA sites.

Included unipolar electrograms with EEA were then inspected for visual presence of additional (fractionated/farfield) deflections (Figure 1E), or additional peaks in case of bipolar electrograms. All markings were evaluated by two investigators independently. Bipolar fractionation peaks were marked by the investigators based on previous studies marking bipolar fractionated electrograms using the change in polarity of the depolarization slope to tag bipolar peaks.[8,9] Each additional marked peak on bipolar electrograms within baseline noise, defined as up to 120% of the noise, was excluded. Of each primary (=LAT) and fractionated unipolar deflection the following parameters were derived: amplitude (peak-to-peak voltage), the time of steepest slope (FT, fractionation time) and signal-to-noise ratio (SNR). Primary and fractionation peaks of bipolar electrograms were analyzed for voltage (peak-to-baseline), time of the peaks (LAT or FT) and SNR.

Corresponding fractionation analysis

At each EEA site, the primary epicardial deflection or peak and the endocardial primary deflection or peak were compared to the direct opposite electrogram for the presence of fractionation corresponding to the primary deflection/ peak. If the FT of a fractionation peak or deflection on the opposite side was ≤7 ms of the LAT, it was labelled as corresponding fractionation (to the primary deflection/ peak) (Figure 2). This cut-off was chosen based on our previous definitions of conduction delay and block.[10] In case of multiple deflections or peaks meeting this criterion, first the closest deflection/ peak, otherwise the largest deflection/ peak, was selected as fractionation corresponding to EEA. Parameters of the corresponding unipolar deflection or bipolar peak included voltage, SNR and voltage compared to the primary deflection/ peak on the same electrogram (in %). In addition, the time difference between the LAT and corresponding FT was analyzed to determine level of time accuracy.

Additional fractionation

Besides analysis of fractionation corresponding to EEA, each opposite electrogram was analyzed for the presence of fractionation in addition to the EEA corresponding fractionation with a FT ≥15 ms separated from the local AT. This fractionation can be confused for EEA and does not correspond to the primary deflection on the other side and could complicate determining presence of EEA.

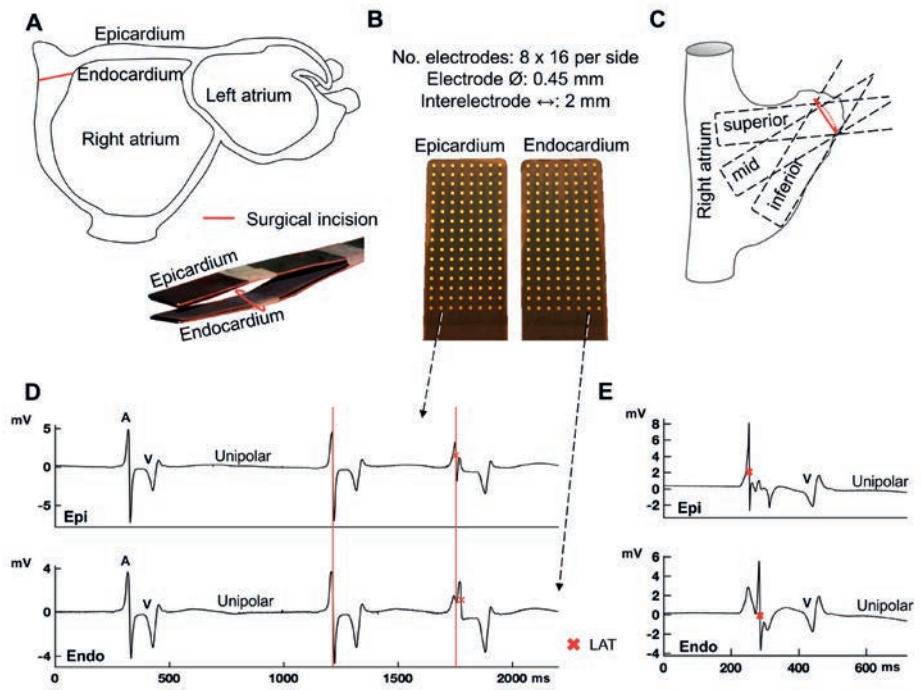

Figure 1. Simultaneous endo-epicardial mapping in patients during cardiac surgery.
A: The mapping tool consists of two identical electrode arrays fixed to each other. One leg (electrode array) of the mapping tool is introduced in the right atrium via a standard surgical incision for cardiopulmonary bypass. This allows to record electrograms from the epicardium (outside wall) and endocardium (inside wall) simultaneously. B: The properties of the electrode array. C: Mapping locations at the right atrium. D: Examples of directly opposite epicardial (epi) and endocardial (endo) unipolar electrograms. Endo-epicardial atrial activation (A) is in synchrony in the first two beats, the following atrial extrasystole demonstrates asynchronous endo-epicardial atrial activation. V, ventricular activation; LAT, local activation time. E: Example of atrial asynchrony and additional deflections next to the LAT-deflection on unipolar electrograms (=fractionation). One fractionation-deflection on each electrogram corresponds to the asynchronous activation on the opposite side.

Statistical analysis

Data with a normal distribution are presented as mean ±SD and skewed data are presented as median (p25-p75). To assess differences between unipolar and bipolar electrograms, Friedmans test was used in case of skewed data and ANOVA repeated measures was used in case of normally distributed data. Post hoc tests between 1) unipolar and bipolar-x and 2) unipolar and bipolar-y were performed with Wilcoxon signed rank test. Statistical significance was set at $P \leq 0.05$, post hoc test significance levels were adjusted according to Bonferroni at $P \leq 0.025$. Data of which outcomes of statistical significance were similar between observers is presented in the text as the mean of the two medians and percentiles and the highest *P*-value is presented.

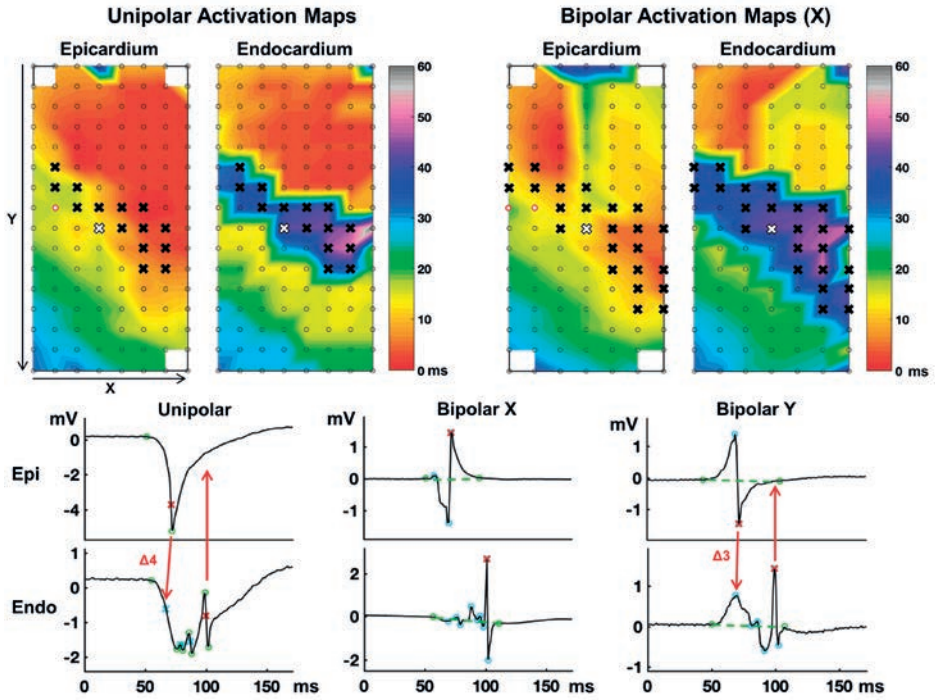

Figure 2. Data selection and analysis.

Top left: Epicardial and endocardial activation maps constructed from unipolar electrograms acquired from simultaneous endo-epicardial mapping. Top right: Epi-endocardial activation maps constructed after subtracting unipolar electrograms in the horizontal (X) direction creating bipolar electrograms. Crosses indicate electrogram sites with endo-epicardial asynchrony (EEA) that are included for the study. Red circles represent a broken electrode site and epicardial and endocardial electrograms at this site are excluded from the study. Bottom: Unipolar and bipolar epicardial and endocardial electrograms from the site marked with the white cross. Local activation time is marked at the steepest slope for unipolar electrograms and at the largest peak for bipolar electrograms (red crosses). Fractionation time (FT) is determined by marking the steepest slope of additional deflections for unipolar electrograms and by marking additional peaks for bipolar electrograms (blue markers). If the difference between a FT and the local activation time of the opposite electrogram is ≤7 ms, 4 ms in the unipolar electrogram example and 3 ms in the bipolar (Y) electrogram example, this fractionation is defined as fractionation corresponding to EEA. In this example, no fractionation corresponding to EEA (the endocardial local activation time) is present on the epicardial electrogram. Unipolar voltage of corresponding fractionation is measured as the difference between peaks (between green circles). Bipolar voltage of corresponding fractionation is measured as the difference between peak and baseline; baseline is virtually constructed as a straight line (green line) between the two green markers placed by the observers in bipolar electrograms (green circles) thereby correcting for baseline drift. Bipolar fractionation (blue circled peaks) within noise level of this virtual baseline are excluded from analysis, in this example the second blue circled peak on the y-bipolar endocardial electrogram is excluded. Fractionation (blue crosses or peaks) that does not correspond to EEA with a difference ≥15 ms of the local activation time in the same electrogram is counted to determine presence of additional fractionation.

RESULTS

Endo-epicardial asynchrony area and electrogram characteristics

Included EEA areas occurred during sinus rhythm in 14 patients, during an atrial extrasystole in 7 patients and during pacing at 240 bpm in one patient. EEA was present on a median surface of 52 (31-94) mm^2 in unipolar maps and no difference was observed between unipolar and bipolar maps (bipolar-x: 42 (22-87) mm^2, bipolar-y: 52 (32-94) mm^2, P=0.78, Table 1). Activation time differences between epicardium and endocardium in unipolar maps ranged from 16 to 96 ms per patient with a median delay of 26 (21-33) ms. Bipolar epi-endocardial delays were similar to unipolar epi-endocardial delays (P=0.37). Amplitudes of bipolar electrograms were lower compared to unipolar electrograms for both epicardial and endocardial electrograms (P<0.001). In addition, SNR of bipolar electrograms in the y-direction was lower compared to unipolar electrograms: 32 (16-62) vs 62 (32-114) for epicardial electrograms and 13 (5-35) vs 28 (18-52) for endocardial electrograms (P≤0.001).

Table 1. EEA and electrogram characteristics

			Epicardium		Endocardium	
	EEA area (mm^2)	EEA delay (ms)	Voltage* (mV)	SNR	Voltage* (mV)	SNR
Unipolar	52 (31-94)	26 (21-33)	3.4 (2.1-5.9)	62 (32-114)	1.8 (1.1-2.8)	28 (18-52)
Bipolar-x	42 (22-87)	25 (22-32)	1.1 (0.7-3.0)	73 (25-115)	0.5 (0.3-1.3)	29 (7-52)
Bipolar-y	52 (32-94)	24 (21-30)	1.4 (0.9-2.9)	32 (16-62)	0.8 (0.2-1.8)	13 (5-35)
P-value	0.78	0.37	<0.001	<0.001	<0.001	<0.001

* Maximal peak-to-peak voltage for unipolar and bipolar electrograms. EEA = endo-epicardial asynchrony; SNR = signal-to-noise ratio.

Endo-epicardial asynchrony corresponding fractionation

Both unipolar and bipolar electrograms demonstrated EEA related fractionation in equal amounts (Figure 3). Fractionation corresponding to EEA was present at 75% (34-96%) of the electrode sites per patient for epicardial unipolar electrograms and at 72% (41-96%) for endocardial unipolar electrograms. Bipolar epicardial electrograms showed fractionation corresponding to EEA at 64% (30-89%) of electrode sites per patient in the x-direction and 69% (24-92%) in the y-direction. Bipolar endocardial electrograms showed EEA corresponding fractionation in the x- and y-direction at respectively 78% (49-97%) and 72% (33-92%) of electrode sites. Complete absence of EEA fractionation occurred in one patient (<5%) for unipolar *epi*cardial electrograms and in maximal two patients (<10%) for bipolar *epi*cardial electrograms and in maximal three patients (<14%) for unipolar and bipolar *endo*cardial electrograms (Supplemental Table 1).

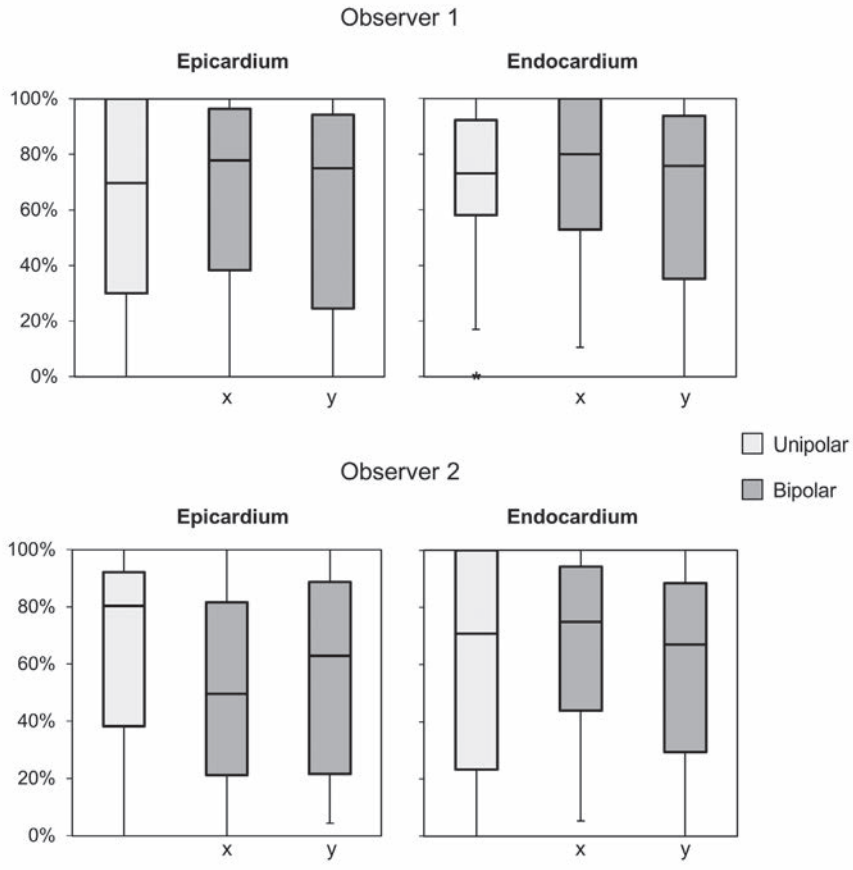

Figure 3. Presence of EEA corresponding fractionation on unipolar and bipolar electrograms.
Boxplots of the percentage of electrode-sites with EEA where the electrogram shows fractionation corresponding to EEA for observer 1 (top) and observer 2 (bottom). Outliers (>1.5 interquartile range) are presented as asterisks.

Absolute voltage of EEA corresponding fractionation was higher on unipolar electrograms than on bipolar electrograms (Table 2). However, relative size of EEA corresponding fractionation to the primary deflection or peak, representing the LAT, did not differ between unipolar and bipolar electrograms. The SNR of corresponding fractionation, or the ease in which the signal can be separated from the noise, was significantly decreased in bipolar electrograms created in the y-direction at the endocardium (unipolar SNR: 11 (6-25) vs bipolar-y SNR: 4 (2-7), $P<0.001$). Examples of SNR decrease in bipolar electrograms are shown in Figure 4A. Time accuracy of corresponding FT compared to the LAT was similar for unipolar and bipolar electrograms at an average of 2 to 3 ms.

Table 2. Characteristics of corresponding fractionation

	Observer 1							Observer 2						
	Unipolar		Bipolar-x		Bipolar-y		*P*-value	Unipolar		Bipolar-x		Bipolar-y		*P*-value
Epicardium														
Voltage (mV)	0.61	(0.27-1.38)	0.19	(0.08-0.31)	0.28	(0.14-0.48)	<0.001	0.57	(0.21-1.35)	0.22	(0.12-0.31)	0.31	(0.17-0.48)	<0.001
Relative to primary (%)	24	(13-37)	17	(9-31)	21	(16-32)	0.51	20	(12-43)	20	(11-39)	26	(17-42)	0.49
SNR	13	(4-22)	10	(4-13)	5	(3-12)	0.04	11	(4-23)	12	(5-16)	5	(4-11)	0.12
Time accuracy (ms)	2	±1.8	3	±1.3	3	±1.3	0.56	3	±1.6	3	±1.5	3	±1.6	0.60
Endocardium														
Voltage (mV)	0.56	(0.29-1.6)	0.17	(0.07-0.36)	0.18	(0.12-0.48)	<0.001	0.66	(0.27-1.74)	0.20	(0.09-0.37)	0.20	(0.11-0.45)	<0.001
Relative to primary (%)	49	(31-78)	34	(29-49)	34	(19-48)	0.14	50	(35-78)	39	(30-58)	35	(25-59)	0.37
SNR	11	(6-23)	9	(4-15)	4	(2-7)	<0.001	10	(6-26)	11	(3-18)	4	(2-7)	<0.001
Time accuracy (ms)	3	±1.6	2	±1.4	3	±1.1	0.53	3	±1.5	2	±1.6	3	±1.3	0.67

SNR = signal-to-noise ratio.

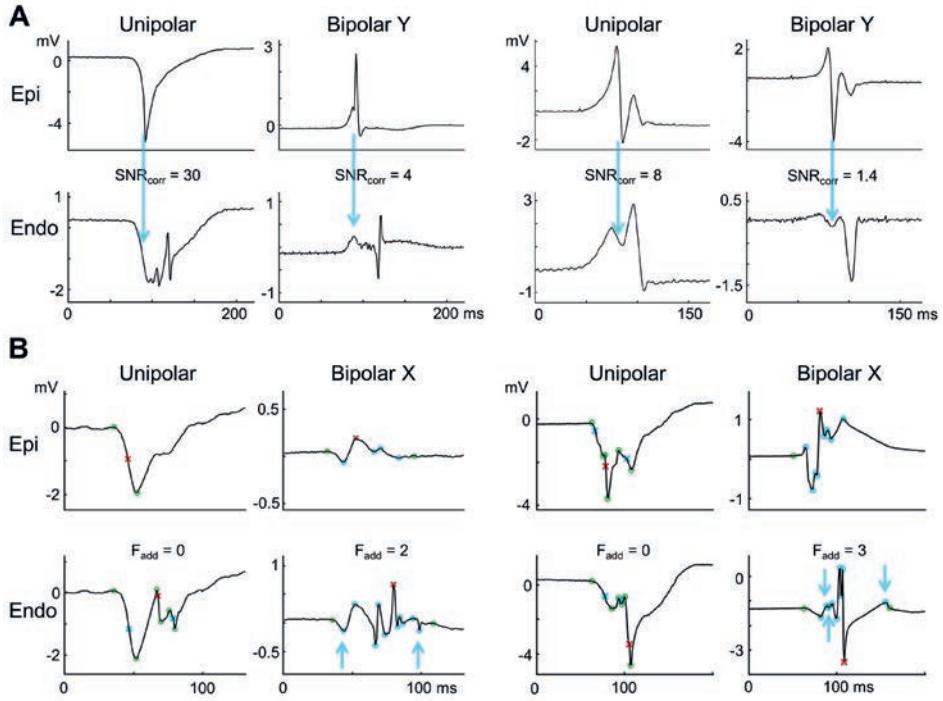

Figure 4. Unipolar versus bipolar electrograms.
A: Two electrogram examples demonstrating decrease of signal-to noise ratio of fractionation corresponding to EEA (SNRcorr) in bipolar endocardial electrograms in the y-direction. Blue arrow points to fractionation on the endocardial electrogram corresponding to the primary deflection/ peak of the local activation time on the epicardial electrogram. B: Two electrogram examples demonstrating increase of additional fractionation (Fadd) on the bipolar endocardial electrogram in the x-direction. Red cross indicates local activation time. Blue crosses or circles indicate fractionation. Blue arrows indicate fractionation which 1) does not correspond to EEA, 2) not within noise level of the baseline and 3) is ≥15 ms removed from the local activation time (= Fadd).

Additional fractionation

The presence of other fractionation that does not correspond to EEA, will complicate determining presence of EEA based on fractionation. Table 3 presents the percentage of electrograms that showed fractionation other than the EEA corresponding fractionation and the average number of additional deflections/ peaks per electrogram. At the endocardium, bipolar electrograms in the x-direction demonstrated more additional fractionation than unipolar electrograms: 82% (52-100) vs 53% (10-86) (*P*=0.019) of electrograms and 2 peaks (1-3) vs 1 (0-1) deflection per electrogram (*P*=0.004). Figure 4B shows examples of increase of additional fractionation on bipolar endocardial electrograms.

Table 3. Presence of additional fractionation.

	Unipolar		Bipolar-x		Bipolar-y		*P*-value
Epicardium							
electrogram %							
obs. 1	39	(0-79)	63	(24-100)	65	(29-87)	0.011
obs. 2	48	(2-66)	49	(19-100)	60	(23-77)	0.098
no. per electrogram							
obs. 1	0	(0-1)	1	(0-2)	1	(0-1)	0.002
obs. 2	1	(0-1)	1	(0-2)	1	(1-1)	0.056
Endocardium							
electrogram %							
obs. 1	59	(11-90)	85	(55-100)	68	(37-87)	0.006
obs. 2	46	(8-81)	79	(49-100)	63	(45-83)	0.002
no. per electrogram							
obs. 1	1	(0-1)	2	(1-2)	1	(0-2)	0.002
obs. 2	1	(0-1)	2	(1-3)	1	(1-1)	0.001

Interobserver differences

Results of each observer are shown in Supplemental tables 1-5. Differences between observers in the significant statistical outcomes of the presented results above included SNR of corresponding fractionation at the epicardium (*P*=0.04 vs *P*=0.12) and percentage and number of additional fractionation at the epicardium (*P*=0.011 vs *P*=0.098 and *P*=0.002 vs *P*=0.056). At the endocardium, the higher number of additional fractionation per electrogram reached significance in only one observer (*P*=0.023 vs *P*=0.027).

DISCUSSION

Previously, it was shown that most fractionation occurs due to inhomogeneous conduction patterns.[6, 11] Almost all fractionated deflections in unipolar electrograms can be traced to neighboring electrical activation sites including the opposite side of the atrial wall.[6] Most clinical studies that have investigated electrogram fractionation use bipolar electrograms because this is the preferred recording method in clinical practice.[7] This study has demonstrated that EEA is reflected equally on unipolar and bipolar electrograms. However, fractionation reflecting EEA is less easy to distinguish from noise on endocardial electrograms using the bipolar recording mode. Furthermore, bipolar electrograms from the endocardium demonstrate more additional fractionation compared to unipolar electrograms that could complicate detection of EEA. This study has also shown

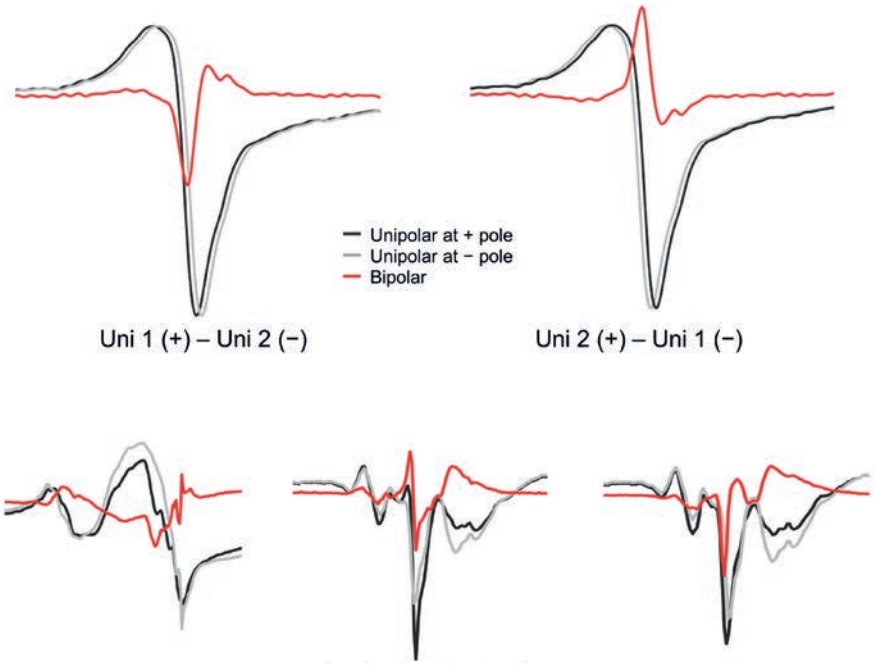

Figure 5. Peaks in bipolar electrograms.
Top left: A bipolar electrogram from two similar shaped signals with only one moved 1 sample on the time (x-)axis is the same as the derivative (Δ) of the signal. The minimum of the derivative is the steepest negative slope of the original signal. Top right: If the positive and negative poles are switched, the bipolar electrogram is the negative derivate (-Δ). The maximum of the bipolar electrogram is in this case the steepest negative slope of the signal. Bottom: Three examples of fractionated unipolar electrograms where the two unipolar electrograms switch in which is the leading electrogram between the different fractionated components. For example, for the electrograms on the left, the light grey unipolar electrogram deflects negatively before the dark unipolar electrogram. The bipolar electrogram shows a positive peak at this point. However, with the following deflection, the dark unipolar electrogram deflects before the lighter unipolar electrogram deflects. Here the bipolar electrogram shows a negative peak. Therefore, it is not possible in these bipolar electrograms to determine if a peak is a unipolar negative deflection (voltage decrease) or a rise (voltage increase) in the unipolar electrogram.

that EEA reflects well on electrograms, over 86% of patients have at least one site showing fractionation corresponding to EEA.

Factors influencing bipolar electrograms

Because a bipolar electrogram is the product of two unipolar electrograms, several factors influence the morphology of a bipolar electrogram. For one, the distance between the two poles of a bipolar electrogram effects degree of fractionation. A computer model, which was also validated in a clinical population of atrial fibrillation patients, demonstrated that a larger interelectrode distance increases electrogram fractionation in bipolar elec-

trograms in case of inhomogeneous activation patterns.[12] Also, increasing electrode size increases fractionation on both bipolar and unipolar electrograms.[12] Recordings of bipolar electrograms at scarred ventricular tissue representing a potential arrhythmogenic substrate in a study of Takigawa et al. confirmed the effect of orientation of the two poles on bipolar electrogram voltage and presence of abnormal electrograms of low voltage or with fractionation.[13] A parallel or transversal orientation of bipolar poles to the direction of activation resulted in differences in bipolar voltage of 50%. Sites with abnormal (fractionated) electrograms only matched in 57% between the different bipolar pole orientations and 30% of sites with abnormal (fractionated) electrograms were missed in the other pole orientation.[13] Therefore, the diverse morphology of bipolar electrograms based on electrode size, interelectrode spacing and catheter orientation, especially under conditions of complex activation patterns, complicates the use of bipolar electrogram morphology.

What do components of fractionated bipolar electrograms depict?

Components (deflections) of a unipolar fractionated electrogram relate to remote parts of dissociatively activated myocardium e.g. after a line of conduction block or to dissociation in activation of myocardial bundles underneath the electrode.[11,14] A bipolar electrogram is meant to present (an approximation to) the derivate of the unipolar electrograms and the maximal peak in the derivate (or bipolar electrogram) coincides with the negative steepest slope(s) of the unipolar electrogram. The timing of the two unipolar signals (signal at the negative pole is earlier vs later than the signal at the positive pole) determines if the peak on the bipolar electrogram is a maximum or a minimum (top of Figure 5). However, as seen in Figure 5, the bipolar electrogram also demonstrates peaks for the (steepest) positive slopes of the unipolar electrograms. Converting fractionated unipolar electrograms to bipolar electrograms makes distinguishing between bipolar peaks due to positive or negative components of the unipolar electrograms impossible. The electrograms at the bottom of Figure 5 demonstrate that peaks in bipolar electrograms can represent negative deflections as well as positive deflections in unipolar electrograms. This concept could explain why additional fractionation presented more frequently in bipolar electrograms in this study.

Endo-epicardial asynchrony detection with use of unipolar fractionation

EEA has been suggested as a pathophysiological mechanism for persistence of atrial fibrillation.[1] Unfortunately, simultaneous mapping of epicardium and endocardium is mostly limited to the right atrial free wall and only possible during cardiac surgery. Therefore, new techniques to identify EEA need to be developed in order to diversify research into the role of endo-epicardial asynchrony in arrhythmogenesis. Previously, we discovered that at least 95% of unipolar fractionation corresponds to remote activation by using automated detection of fractionation. In this study, fractionation was identified visually

by two investigators to maximize detection of EEA based fractionation and because automated signal detection in clinical practice is often evaluated by visual standards of the electrophysiologist. Outcome differences between the investigators were mainly limited to the epicardium. This may be explained by the larger SNR at the epicardium, making small additional peaks or deflections harder to detect visually. A positive finding is that a great majority (86%) of patients with EEA demonstrates fractionation corresponding to EEA on the other side of the atrial wall. This study did show that unipolar electrograms are better suited than bipolar electrograms for fractionation based EEA detection due to less interference of additional fractionation and because EEA corresponding signals are better distinguishable from the noise. During atrial fibrillation, activation waves are often much smaller and with more complex activation patterns with frequent wave break, wave collision and conduction block.[15] Unipolar voltage and SNR of fractionated components will be even smaller during atrial fibrillation than in this study emphasizing the use of unipolar over bipolar electrograms. The next steps in order to develop an EEA-detection tool would be to 1) label unipolar fractionated deflections corresponding to remote activation in the longitudinal plane and 2) find the most sensitive and specific signal parameters to diagnose fractionated deflections corresponding to asynchronous activation within the atrial wall.

Study limitations

Endo-epicardial mapping was mainly performed at the right atrial free wall as left atrial simultaneous endo-epicardial mapping can only be performed in very select cases. The differences between unipolar and bipolar electrograms may not apply to the thinner wall of the left atrium.

REFERENCES

1. de Groot N, van der Does L, Yaksh A, Lanters E, Teuwen C, Knops P, van de Woestijne P, Bekkers J, Kik C, Bogers A, Allessie M. Direct Proof of Endo-Epicardial Asynchrony of the Atrial Wall During Atrial Fibrillation in Humans. Circ Arrhythm Electrophysiol. 2016;9:e003648.
2. de Groot NMS, Houben RPM, Smeets JL, Boersma E, Schotten U, Schalij MJ, Crijns H, Allessie MA. Electropathological Substrate of Longstanding Persistent Atrial Fibrillation in Patients With Structural Heart Disease Epicardial Breakthrough. Circulation. 2010;122:1674-1682.
3. Schuessler RB, Kawamoto T, Hand DE, Mitsuno M, Bromberg BI, Cox JL, Boineau JP. Simultaneous epicardial and endocardial activation sequence mapping in the isolated canine right atrium. Circulation. 1993;88:250-263.
4. Eckstein J, Maesen B, Linz D, Zeemering S, van Hunnik A, Verheule S, Allessie M, Schotten U. Time course and mechanisms of endo-epicardial electrical dissociation during atrial fibrillation in the goat. Cardiovasc Res. 2011;4:816-824.
5. Knops P, Kik C, Bogers AJ, de Groot NM. Simultaneous endocardial and epicardial high-resolution mapping of the human right atrial wall. J Thorac Cardiovasc Surg. 2016;152:929-31.
6. van der Does L, Knops P, Teuwen CP, Serban C, Starreveld R, Lanters EAH, Mouws E, Kik C, Bogers A, de Groot NMS. Unipolar atrial electrogram morphology from an epicardial and endocardial perspective. Heart Rhythm. 2018;15:879-887.
7. van der Does LJ, de Groot NM. Inhomogeneity and complexity in defining fractionated electrograms. Heart Rhythm. 2017;14:616-624.
8. Yoshida K, Ulfarsson M, Tada H, Chugh A, Good E, Kuhne M, Crawford T, Sarrazin JF, Chalfoun N, Wells D, Jongnarangsin K, Pelosi F, Jr., Bogun F, Morady F, Oral H. Complex electrograms within the coronary sinus: time- and frequency-domain characteristics, effects of antral pulmonary vein isolation, and relationship to clinical outcome in patients with paroxysmal and persistent atrial fibrillation. J Cardiovasc Electrophysiol. 2008;19:1017-23.
9. Scherr D, Dalal D, Cheema A, Cheng A, Henrikson CA, Spragg D, Marine JE, Berger RD, Calkins H, Dong J. Automated detection and characterization of complex fractionated atrial electrograms in human left atrium during atrial fibrillation. Heart Rhythm. 2007;4:1013-20.
10. Teuwen CP, Yaksh A, Lanters EA, Kik C, van der Does LJ, Knops P, Taverne YJ, van de Woestijne PC, Oei FB, Bekkers JA, Bogers AJ, Allessie MA, de Groot NM. Relevance of Conduction Disorders in Bachmann's Bundle During Sinus Rhythm in Humans. Circ Arrhythm Electrophysiol. 2016;9:e003972.
11. Spach MS, Dolber PC. Relating extracellular potentials and their derivatives to anisotropic propagation at a microscopic level in human cardiac muscle. Evidence for electrical uncoupling of side-to-side fiber connections with increasing age. Circ Res. 1986;58:356-71.
12. Correa de Sa DD, Thompson N, Stinnett-Donnelly J, Znojkiewicz P, Habel N, Muller JG, Bates JH, Buzas JS, Spector PS. Electrogram fractionation: the relationship between spatiotemporal variation of tissue excitation and electrode spatial resolution. Circ Arrhythm Electrophysiol. 2011;4:909-16.
13. Takigawa M, Relan J, Martin R, Kim S, Kitamura T, Frontera A, Cheniti G, Vlachos K, Massoullie G, Martin CA, Thompson N, Wolf M, Bourier F, Lam A, Duchateau J, Klotz N, Pambrun T, Denis A, Derval N, Magat J, Naulin J, Merle M, Collot F, Quesson B, Cochet H, Hocini M, Haïssaguerre M, Sacher F, Jaïs P. Effect of bipolar electrode orientation on local electrogram properties. Heart Rhythm. 2018;15:1853-1861.
14. Konings KT, Smeets JL, Penn OC, Wellens HJ, Allessie MA. Configuration of unipolar atrial electrograms during electrically induced atrial fibrillation in humans. Circulation. 1997;95:1231-41.

15. Allessie MA, de Groot NM, Houben RP, Schotten U, Boersma E, Smeets JL, Crijns HJ. Electropathological substrate of long-standing persistent atrial fibrillation in patients with structural heart disease: longitudinal dissociation. Circ Arrhythm Electrophysiol. 2010;3:606-15.

SUPPLEMENTAL MATERIAL CHAPTER 14

Supplemental Table 1. Percentage of electrograms with EEA corresponding fractionation per patient

	Observer 1						Observer 2					
	Epicardium			Endocardium			Epicardium			Endocardium		
no.	uni	bi-x	bi-y	uni	bi-x	bi-y	uni	bi-x	bi-y	uni	bi-x	bi-y
1	75	78	92	50	89	77	75	67	92	25	89	77
2	100	100	75	88	100	38	88	100	25	100	100	38
3	56	95	67	70	71	87	56	81	63	70	62	77
4	67	85	100	89	100	100	100	54	88	100	92	50
5	73	22	43	34	33	74	32	13	15	18	22	66
6	11	85	23	100	100	100	44	69	38	100	100	100
7	20	86	14	100	100	100	40	71	14	100	86	100
8	100	100	50	86	73	60	100	45	60	71	73	50
9	40	83	75	100	100	100	60	83	63	100	100	100
10	33	100	100	17	80	0	33	90	100	0	80	0
11	3	44	25	73	54	68	3	38	20	70	26	30
12	100	50	88	100	100	88	86	25	88	100	100	88
13	100	100	100	89	13	92	100	100	100	89	25	92
14	16	16	22	60	11	4	16	16	22	0	5	4
15	100	78	100	0	89	0	86	22	100	0	100	0
16	67	50	86	100	75	100	89	25	64	100	75	93
17	0	4	0	67	75	87	0	8	4	67	67	87
18	65	0	80	88	50	87	65	0	27	82	50	87
19	100	100	100	0	100	0	100	100	100	17	50	0
20	91	48	86	70	97	73	91	30	82	70	82	68
21	97	20	20	72	14	28	95	18	12	74	22	28
22	86	60	71	71	80	57	86	55	79	64	75	36
median	70	78	75	73	80	76	80	50	63	71	75	67

Supplemental Table 2. Voltage and relative voltage of corresponding fractionation per patient

	Observer 1												Observer 2											
	Voltage (mV)						Relative voltage (%)						Voltage (mV)						Relative voltage (%)					
	Epicardium			Endocardium			Epicardium			Endocardium			Epicardium			Endocardium			Epicardium			Endocardium		
no.	uni	bi-x	bi-y	uni	bi-x	bi-y	uni	bi-x	bi-y	uni	bi-x	bi-y	uni	bi-x	bi-y	uni	bi-x	bi-y	uni	bi-x	bi-y	uni	bi-x	bi-y
1	1.27	0.29	0.96	1.60	0.33	0.60	23	4	26	30	7	8	1.24	0.31	1.04	2.15	0.32	0.63	23	5	30	54	9	10
2	0.95	0.23	0.20	0.29	0.09	0.09	25	22	13	31	69	50	1.15	0.22	0.30	0.27	0.09	0.10	29	21	27	27	65	71
3	0.69	0.31	0.25	1.64	0.36	0.30	35	40	20	44	32	19	0.57	0.30	0.25	1.74	0.37	0.37	29	39	20	45	35	22
4	0.63	0.18	0.30	0.56	0.17	0.18	21	10	21	35	49	16	0.56	0.19	0.32	0.57	0.20	0.18	13	9	21	35	58	18
5	0.41	0.15	0.10	0.46	0.11	0.13	28	26	12	77	42	19	0.45	0.10	0.06	1.24	0.17	0.13	58	39	17	70	48	35
6	0.23	0.07	0.15	1.57	0.32	0.48	25	41	40	172	38	64	0.15	0.11	0.18	1.57	0.30	0.52	12	47	28	172	38	65
7	0.33	0.48	1.15	1.99	0.52	0.48	2	12	62	107	29	27	0.17	0.57	1.14	1.99	0.40	0.58	2	10	61	107	26	25
8	1.42	0.06	0.61	0.12	0.07	0.14	44	14	41	10	23	35	1.38	0.09	0.41	0.17	0.08	0.17	44	19	43	14	21	70
9	0.19	0.39	0.50	1.77	0.48	0.49	6	50	31	78	38	34	0.16	0.37	0.68	1.77	0.51	0.45	3	58	37	78	40	29
10	2.28	0.76	0.77	0.23	0.17	-	107	25	28	21	41	-	2.28	0.79	0.71	-	0.20	-	107	24	21	-	71	-
11	0.25	0.17	0.23	0.51	0.09	0.12	9	9	11	19	7	9	0.25	0.19	0.33	0.46	0.09	0.14	9	14	15	18	7	26
12	0.94	0.09	0.16	0.66	0.28	0.17	27	8	19	36	63	24	0.92	0.06	0.17	0.66	0.25	0.27	31	6	15	36	58	31
13	1.55	0.30	0.42	1.12	0.40	0.25	16	6	15	40	90	23	1.55	0.29	0.49	1.12	0.61	0.21	16	6	17	40	87	25
14	0.21	0.12	0.09	0.18	0.03	0.07	13	60	32	50	56	74	0.20	0.14	0.10	-	0.04	0.07	12	73	43	-	80	59
15	0.59	0.08	0.33	-	0.05	-	37	10	34	-	69	-	0.67	0.29	0.41	-	0.05	-	39	18	50	-	73	-
16	0.07	0.04	0.08	0.27	0.04	0.06	13	32	32	66	40	41	0.06	0.04	0.12	0.27	0.04	0.07	13	44	49	66	39	50
17	-	0.19	-	2.27	0.23	0.31	-	59	-	163	27	40	-	0.15	0.11	2.29	0.34	0.29	-	45	30	163	35	38
18	0.73	-	0.16	0.44	0.10	0.16	16	-	5	49	33	63	0.62	-	0.18	0.45	0.12	0.11	14	-	7	48	44	50
19	5.91	0.85	0.14	-	0.51	-	84	19	2	-	34	-	5.91	0.84	0.17	0.07	0.62	-	84	18	3	1	39	
20	0.43	0.26	0.36	1.55	0.05	0.24	7	10	20	168	27	42	0.43	0.19	0.29	1.55	0.13	0.20	7	24	25	168	30	46
21	0.39	0.04	0.09	0.32	0.05	0.06	18	7	20	54	34	48	0.38	0.04	0.12	0.30	0.05	0.10	17	17	26	53	46	66
22	2.12	0.20	0.43	0.21	0.61	0.64	68	21	19	8	34	27	2.12	0.22	0.44	0.22	0.58	0.67	68	20	15	9	34	33
median	0.63	0.19	0.25	0.54	0.17	0.18	23	19	20	47	36	34	0.57	0.19	0.29	0.66	0.20	0.20	17	20	25	48	40	35

Supplemental Table 3. SNR and time accuracy of corresponding fractionation per patient

	Observer 1												Observer 2											
	SNR						Time accuracy (ms)						SNR						Time accuracy (ms)					
	Epicardium			Endocardium			Epicardium			Endocardium			Epicardium			Endocardium			Epicardium			Endocardium		
no.	uni	bi-x	bi-y	uni	bi-x	bi-y	uni	bi-x	bi-y	uni	bi-x	bi-y	uni	bi-x	bi-y	uni	bi-x	bi-y	uni	bi-x	bi-y	uni	bi-x	bi-y
1	31	13	20	28	17	11	2	3	1	5	4	3	31	16	23	45	15	12	2	3	1	4	3	3
2	22	8	4	8	4	2	0	1	2	1	0	4	24	8	6	7	3	3	0	1	1	1	0	4
3	13	19	4	25	15	4	1	2	4	3	2	3	10	19	4	26	19	4	1	1	3	3	1	3
4	5	8	4	6	9	3	4	2	3	4	3	3	5	8	4	6	11	3	3	3	3	3	3	4
5	17	12	6	20	10	7	1	5	2	2	5	3	20	9	3	60	13	7	0	5	1	3	5	3
6	3	3	3	16	14	9	4	3	2	0	1	0	2	5	4	16	13	9	3	2	5	0	1	0
7	3	12	17	15	15	10	0	4	4	0	1	1	1	15	16	15	11	10	3	4	4	0	2	1
8	20	2	10	2	2	2	1	3	2	1	1	2	20	3	7	2	2	2	1	3	2	1	1	2
9	3	13	14	34	17	11	5	2	3	4	2	1	3	14	17	34	18	10	4	2	2	4	2	1
10	12	21	4	2	4	-	5	3	3	2	4	-	12	20	4	-	5	-	5	3	3	-	3	-
11	8	10	7	17	4	3	6	5	3	5	5	3	8	11	9	15	4	4	6	6	5	5	5	5
12	13	2	3	10	6	3	2	2	3	2	2	2	13	1	3	10	6	5	3	3	3	2	2	2
13	16	12	6	10	12	2	3	1	2	2	1	3	16	12	7	10	18	2	3	1	2	2	4	3
14	3	4	2	3	1	1	1	6	4	2	4	2	3	5	2	-	2	1	1	6	4	-	6	2
15	30	9	18	-	4	-	4	2	3	-	2	-	32	27	23	-	4	-	4	2	4	-	2	-
16	2	4	2	7	3	2	2	3	0	4	1	3	1	4	4	7	3	2	3	3	0	4	1	4
17	-	7	-	47	14	5	-	1	-	5	2	3	-	7	2	47	27	5	-	2	2	5	2	3
18	28	-	5	11	5	5	0	-	3	3	2	2	22	-	7	10	6	3	0	-	4	3	2	2
19	202	71	4	-	47	-	3	3	3	-	1	-	202	69	7	5	86	-	3	3	2	0	1	-
20	9	21	13	23	4	6	3	3	2	3	3	4	9	16	11	23	10	4	3	2	2	3	3	4
21	5	1	2	4	1	1	1	4	6	4	3	4	5	1	2	4	1	2	1	5	6	4	3	5
22	33	10	5	3	23	7	1	2	1	1	2	2	33	9	4	3	24	7	1	2	2	1	1	3
median	13	10	5	11	8	4	2	3	3	3	2	3	12	9	5	10	10	4	3	3	3	3	2	3

Supplemental Table 4. Percentage of electrograms with additional fractionation per patient

	Observer 1						Observer 2					
	Epicardium			Endocardium			Epicardium			Endocardium		
no.	uni	bi-x	bi-y	uni	bi-x	bi-y	uni	bi-x	bi-y	uni	bi-x	bi-y
1	100	100	100	75	100	77	100	100	100	75	89	77
2	0	100	25	0	100	50	6	100	25	0	100	100
3	33	71	73	56	71	87	30	48	70	52	76	67
4	0	8	63	0	69	38	0	8	38	0	46	25
5	84	72	91	93	94	98	45	76	77	84	94	98
6	0	62	31	11	92	92	0	62	77	11	100	77
7	60	43	71	80	57	100	60	14	14	80	57	86
8	100	100	100	95	100	60	95	100	90	95	100	50
9	60	100	75	0	100	88	80	100	75	0	100	88
10	50	50	56	92	80	0	50	50	67	33	80	22
11	3	23	8	63	77	78	3	21	3	57	77	63
12	100	0	38	100	25	50	100	0	50	100	25	63
13	0	25	8	11	38	83	0	25	17	11	0	83
14	40	32	63	92	5	0	52	32	52	88	26	4
15	86	22	100	0	67	50	57	11	50	0	67	50
16	78	100	71	89	100	21	78	100	79	78	100	29
17	0	25	4	47	96	83	0	29	9	40	92	83
18	35	0	20	88	100	87	12	0	0	88	100	60
19	0	100	100	33	50	50	0	100	100	0	50	0
20	9	67	50	22	91	36	9	36	45	22	58	55
21	38	80	68	28	33	20	62	61	68	26	35	56
22	57	65	86	71	90	93	50	55	71	71	85	64
median	39	63	65	59	85	68	48	49	59	46	78	63

Supplemental Table 5. Average number of additional fractionation per electrogram per patient

	Observer 1						Observer 2					
	Epicardium			Endocardium			Epicardium			Endocardium		
no.	uni	bi-x	bi-y	uni	bi-x	bi-y	uni	bi-x	bi-y	uni	bi-x	bi-y
1	1	3	4	1	2	2	1	3	4	1	2	1
2	0	2	1	0	1	1	0	2	1	0	3	1
3	0	2	1	1	2	2	0	2	1	1	2	1
4	0	0	1	0	1	0	0	0	1	0	1	0
5	1	3	3	2	5	5	1	2	2	1	4	4
6	0	1	0	0	2	1	0	1	1	0	3	2
7	1	1	1	1	1	3	1	0	0	1	1	2
8	1	2	1	2	3	1	1	1	1	1	3	1
9	1	3	1	0	2	3	1	3	2	0	3	2
10	1	1	1	1	1	0	1	1	1	0	1	0
11	0	0	0	1	2	2	0	0	0	1	2	1
12	2	0	0	2	0	1	2	0	1	2	0	1
13	0	0	0	0	0	1	0	0	0	0	0	1
14	0	0	1	1	0	0	1	0	1	1	0	0
15	1	0	2	0	1	1	1	0	1	0	1	1
16	1	3	1	1	2	0	1	3	1	1	2	0
17	0	1	0	1	4	2	0	1	0	1	3	3
18	0	0	0	1	2	2	0	0	0	1	3	1
19	0	2	3	0	1	1	0	2	3	0	1	0
20	0	1	1	0	1	0	0	0	1	0	1	1
21	0	1	1	0	0	0	1	1	1	0	0	1
22	1	2	2	1	3	2	1	2	2	1	3	1
median	0	1	1	1	2	1	1	1	1	1	2	1

15

Atrial Ectopy Increases Asynchronous Activation of the Endo- and Epicardium at the Right Atrium

Lisette van der Does
Rohit Kharbanda
Christophe Teuwen
Paul Knops
Charles Kik
Ad Bogers
Natasja de Groot

ABSTRACT

Background: The predisposition of atrial extrasystoles (AES) to trigger arrhythmia may also arise from intramural conduction disorders causing endo-epicardial asynchrony (EEA). This study aimed to determine whether spontaneous AES disturb endo-epicardial conduction.

Methods: Simultaneous endo-epicardial mapping of the right atrium was performed in patients during cardiac surgery with two 128-electrode arrays. Sixty spontaneous AES were observed in 23 patients and were analyzed for incidence of conduction delay, conduction block and amount of EEA compared to the previous sinus rhythm beat.

Results: Both conduction delay and block occurred more often in AES compared to sinus rhythm. The difference in lines of conduction block between the epicardium and endocardium increased in AES causing a greater imbalance of conduction disorders between the layers. The incidence of EEA with differences ≥10 ms increased significantly in AES. AES caused delays between the epicardium and endocardium up to 130 ms and EEA to increase for up to half (47%) of the mapping area.

Conclusion: Conduction disturbances between the epicardial and endocardial layer giving rise to EEA increase during AES. Asynchronous activation of the atrial layers increases during AES which may be a mechanism for triggering cardiac tachyarrhythmias under the right conditions but EEA cannot be recognized by current mapping tools.

INTRODUCTION

Atrial extrasystoles (AES) are a common finding in the general population and usually the occurrence of AES is benign. However, frequent AES have been associated with increased risk of developing atrial fibrillation and paroxysmal episodes of atrial fibrillation are in more than 90% of the cases preceded by an AES.[1,2] The majority of AES triggering atrial fibrillation originate from the left atrium, most frequently the pulmonary veins.[3] Recently, high-resolution epicardial mapping demonstrated that atrial conduction disorders increase during spontaneous AES, which are caused by anisotropy due to their ectopic origin and/or refractoriness of myocardium due to their prematurity.[4] Slowing of conduction can in turn facilitate re-entry and initiate arrhythmia such as atrial fibrillation.

Conduction disorders are not limited to the 2-dimensions of the superficial layers of the atrial wall. During both atrial fibrillation and sinus rhythm conduction between epicardial and endocardial myocardium can be dissociated causing asynchronous activation of the epicardial and endocardial atrial wall.[5,6] Endo-epicardial asynchrony (EEA) and the ensuing breakthrough waves caused by endo-to-epicardial conduction or vice versa have been proposed as a possible mechanism sustaining atrial fibrillation.[5] Based on these previous findings, we hypothesized that during AES endo-epicardial conduction will become more disturbed than during SR and that EEA could be a potential mechanism triggering arrhythmia. Therefore, we investigated the difference of EEA in sinus rhythm beats and spontaneous AES by performing simultaneous endo-epicardial mapping in patients undergoing cardiac surgery.

METHODS

Study population

Patients participating in the Epic End study (NTR5370), an endo-epicardial mapping study in adult patients undergoing open-heart surgery, were included. This study was approved by the local ethics committee (MEC 2015-373) and all patients gave informed consent prior to inclusion. Twenty-three patients demonstrating AES during mapping were included of whom 17 (74%) underwent surgery for coronary artery disease and 11 (48%) had valvular heart disease. Nine patients (39%) had a history of atrial fibrillation. Clinical characteristics are presented in Table 1.

Table 1. Clinical characteristics

Total patients, N	23
Age, years	64 ±9
Male/ Female	18/5
Median number of AES (min-max)	2 (1-7)
Current heart disease, N (%)	
Coronary artery disease	17 (74)
Aortic valve disease	4 (17)
Mitral valve disease	7 (30)
Tricuspid valve disease	1 (4)
Patent foramen ovale	1 (4)
Left ventricular dysfunction	4 (17)*
Left atrial enlargement	7 (30)
Medical history, N (%)	
Hypertension	13 (57)
Hypercholesterolemia	10 (43)
Diabetes mellitus	8 (35)
Atrial Fibrillation	9 (39)
Paroxysmal	7 (30)
Persistent	2 (9)
Anti-arrhythmical medication, N (%)	
Class 1	0 (0)
Class 2	17 (74)
Class 3	1 (4)
Class 4	3 (13)
Digoxin	3 (13)

*3 mild and 1 moderate dysfunction. AES = atrial extra systole.

Endo-epicardial mapping procedure

Endo-epicardial mapping is performed during surgery prior to start of cardiopulmonary bypass and has been previously described in detail.[7] Two arrays containing 128 electrodes (16×8) with 2 mm interelectrode spacing were each fixed on a steel spatula and the spatulas were bound together at the end to preserve precise opposite alignment of the two arrays. After arterial cannulation, one array is introduced in the right atrium for endocardial mapping via the incision for venous cannulation. The second array remains on the outside to record from the epicardium. Simultaneous epicardial and endocardial unipolar electrogram recordings of the right atrial free wall were obtained for 5–10 s during sinus rhythm from three locations at the right free atrial wall (Figure 1A). In one case, endo-epicardial mapping was performed at the left atrial appendage before excision.

Data analysis

Electrogram analysis was performed in MATLAB R2016a (The MathWorks Inc, Natick, MA, USA). Electrograms with injury potentials (baseline elevation after the atrial potential larger than the amplitude of the atrial potential) were excluded from analysis.[6] Recording sites with ≥25% missing or excluded electrograms were not included in this study. Local activation times were marked at the steepest negative slope with a minimal slope of 0.05 mV/ms and a signal-to-noise ratio >2.[6] Local endo-epicardial time differences were determined for each electrode and consisted of the shortest activation time difference between the electrode and the 9 electrodes on the opposite side (exact opposite electrode and its 8 surrounding electrodes; Figure 1C). Border electrodes (<7 opposite local activation times present) were excluded from analysis. Previously, we defined EEA as activation time difference between epicardium and endocardium of ≥15 ms.[5] As atrial wall thickness is very diverse within the atria, we not only analyzed EEA of ≥15 ms (large EEA) but also moderate EEA between 10–15 ms. EEA in AES is expressed as a percentage of the total electrodes during the AES demonstrating EEA (equaling the area of the array with EEA). Conduction disorders in the superficial epicardial and endocardial planes were defined as the incidence of 1) conduction block with interelectrode difference >11 ms and 2) conduction delay with interelectrode difference of 7–11 ms. Conduction disorders are expressed in mm, translating to the total length of all interelectrode lines of conduction delay and block in the activation maps.

Atrial extrasystoles

AES were defined as beats during sinus rhythm with either a shortening in cycle length ≥25% to the previous sinus-beat and/or an aberrant activation pattern compared to sinus-beats.[4] Prematurity compared to the sinus-beat (the prematurity index) could not be determined for 1) AES that were the first or second beat of the recording, or 2) AES following another AES, or 3) in case of AES in bigeminy. AES were labelled for their degree of aberrancy from sinus rhythm, for example, shift in direction of the main wavefront trajectory (wave covering the largest area of the mapping area) (Figure 1B, 1D). Based on our previous study[4] that demonstrated increased conduction disorders for wavefront shifts of 90°, breakthrough and complex patterns during AES, the following categories for aberrancy of AES were defined: 1) no aberrancy (only premature AES) or mild to moderate shift of the main wavefront trajectory in AES (0–45° or 135°–180° shift), 2) severe shift of the main wavefront trajectory in AES (90° shift), breakthrough or complex pattern of activation of AES (and sinus rhythm) and 3) breakthrough or complex pattern of activation in sinus rhythm only. When degree of aberrancy differed between epicardium and endocardium, the severest degree of aberrancy of the two determined the aberrancy category.

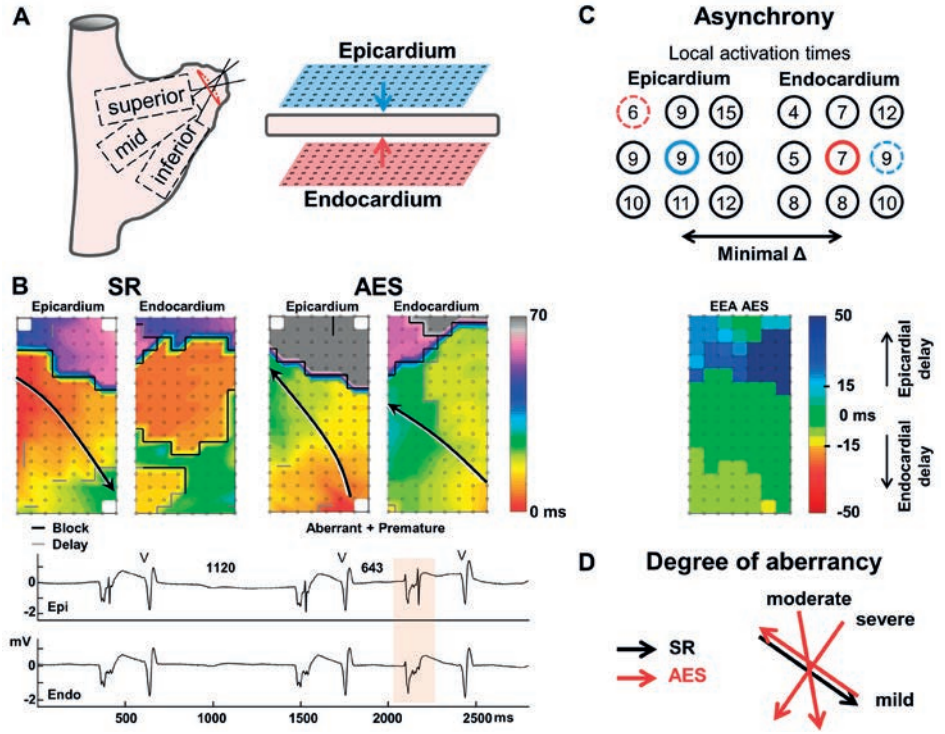

Figure 1. Endo-epicardial mapping and data analysis.
A: Endo-epicardial mapping was performed with two 128-electrode arrays, one placed on the epicardium and one on the endocardium. Recording locations included 1) the superior right atrium (RA), 2) the mid-RA and 3) the inferior RA. B: Endo-epicardial activation maps of a sinus rhythm (SR) beat and an atrial extrasystole (AES) show the aberrant activation pattern of the AES, at the epicardium there is mild aberrancy (180° shift of the main wavefront trajectory), at the endocardium there is a complex pattern of activation during sinus rhythm without a main trajectory. Conduction block (Δ > 11 ms) or delay (7–11 ms) between two electrodes represents a line of 2 mm. The total length of all lines represents the amount of conduction block and delay. Epi- and endocardial electrograms demonstrate the AES is premature as well, with a 57% shortening of the cycle length. V, ventricular activation. C: Endo-epicardial asynchrony (EEA) is determined by the minimal local activation time difference between the nine opposite electrodes and the index electrode (center). Electrodes at the border of the array only have ≤ 6 opposite electrodes and are excluded. At the epicardium the minimal difference is 0 ms (blue), in this example, at the endocardium the minimal difference is -1 ms (red). The maximal difference of two opposite electrodes is shown in the EEA map. Positive values represent an epicardial delay in activation and negatives values an endocardial delay in activation. D: Degree of aberrancy is categorized based on the rotational shift of the main trajectory of the AES wavefront; mild 180°, moderate 45°/135°, severe 90°.

Statistical analysis

Normally distributed data are presented as mean ± SD and skewed data are presented as median (interquartile range). AES mapping data consists of clustered measurements (multiple AES recorded within a patient). Therefore, the associations of sinus rhythm and AES with conduction delay, conduction block and EEA were evaluated using Generalized Estimated Equations. The skewed distributions of conduction delay, conduction block and EEA could not be transformed to a normal distribution and thus, were converted to a binary distribution by setting cutoff values that represented a possible shift in occurrence between AES and sinus rhythm as observed in the histograms. The number of positive cases required at least 25% of the data; otherwise, the cutoff value was set at the top quartile. All cutoff values are presented after the *P*-value. A binary logistic model was used to assess the effect of AES on conduction delay, conduction block and EEA. Correlation structure was chosen based on the goodness of fit in the quasi-likelihood function. In all cases an independent correlation structure was chosen. Statistical analyses were performed with IBM SPSS Statistics version 21 (IBM corp., Armonk, NY, USA).

RESULTS

Atrial extrasystole characteristics

Twenty-three patients demonstrated 60 AES, per patient a median AES of 2 (min–max: 1–7), and most were recorded at the inferior right atrial free wall (31 at the inferior right atrium vs 12 at the middle and 16 at the superior right atrium and 1 at the left atrium). Ten AES were only aberrant and 9 AES were only premature, the remainder was both aberrant and premature or aberrant with unknown prematurity. The prematurity index could not be determined for 29 AES of the 50 (possibly) premature AES, the remaining 21 premature AES had a prematurity of 45% ± 10%. All premature and/or aberrant AES had a mean interval after the previous beat of 560 ± 135 ms (min–max: 340–920 ms). Twenty-five AES (42%) had no to moderate aberrancy, 29 AES (48%) had severe/ complex aberrancy and 6 AES (10%) had a complex pattern of activation on one or both sides during SR only. The majority of AES (37/60) were the second to seventh AES recorded in the same patient. Most of these AES likely originated from the same location within the atria as a previous AES in that same patient, because 26 AES had the same degree of aberrancy as one of those previous AES.

Conduction delay and block

During sinus rhythm, the endocardium contained more extensive conduction disorders than the epicardium as total length of conduction block lines was longer at the endocardium (P=0.015, ≥20 mm). Total length of lines with conduction delay was similar for both the epicardium and endocardium. AES increased the total length of these lines of conduction

block and delay (Table 2). Conduction block increased during AES from 8 (0–48) mm to 20 (6–41) mm (*P*=0.020, ≥10 mm). Comparable to conduction block, conduction delay increased as well during AES from 24 (12.5-36) mm to 38 (18.5–50) mm (*P*=0.014, ≥30 mm). At the epicardium, conduction delay increased from 11 (4–19.5) mm to 16 (8–27.5) mm in AES (*P*=0.030, CD ≥10 mm) whereas conduction block did not change (*P*=0.639, >16 mm). Total length of conduction block (*P*=0.113, ≥10 mm) rather than conduction delay (*P*=0.276, ≥24 mm) tended to increase in AES at the endocardium. The difference between the epicardial and endocardial layer in the total length of conduction disorders was also analyzed. The endo-epicardial difference in total length of conduction block increased from 2 (0–8) mm in SR to 10 (2–18) mm during AES (*P*=0.037, Δ≥14 mm). Endo-epicardial difference of total conduction delay did not change during AES (*P*=0.102, Δ≥14 mm).

Table 2. Conduction disorders during sinus rhythm vs atrial extrasystole

	Sinus rhythm		Atrial extrasystole		*P*-value
Overall					
CB (mm)	8	(0–48)	20	(6–41)	0.020
CD (mm)	24	(12.5–36)	38	(18.5–50)	0.014
Epicardium					
CB (mm)	2	(0–16)	4	(0–15.5)	0.639
CD (mm)	11	(4–19.5)	16	(8–27.5)	0.030
Endocardium					
CB (mm)	4	(0–26)	14	(5–23.5)	0.113
CD (mm)	12	(6–22)	16	(8–26)	0.276
Endo- vs. epicardium					
ΔCB (mm)	2	(0–8)	10	(2–17.5)	0.037
ΔCD (mm)	6	(2–11.5)	7	(4–14)	0.102
Endo-epicardial asynchrony					
EEA ≥ 10 ms (%)	0	(0–2.3)	0.7	(0–6.0)	0.023
EEA ≥ 15 ms (%)	0	(0–0.6)	0	(0–3.0)	0.053

CB = conduction block; CD = conduction delay; EEA = endo-epicardial asynchrony.

Endo-epicardial asynchrony

During AES, an increase of EEA occurred almost twice as much as a decrease of EEA. An increase in EEA ≥15 ms occurred in 17 AES (28%) presenting in 8 patients, which included the AES recorded at the left atrium (Figure 2). These AES resulted in EEA with a median delay of 20 ms per AES and 23 ms per patient (min–max: 16–81 ms). The largest endo-epicardial time delay observed at a site during an AES was 130 ms. In 9 AES (15%) recorded from 8 patients EEA decreased compared to sinus rhythm. These AES had EEA during sinus rhythm with a median delay of 16 ms per AES and patient (min–max: 15–26 ms). In the remaining 34 AES (57%), EEA did not change.

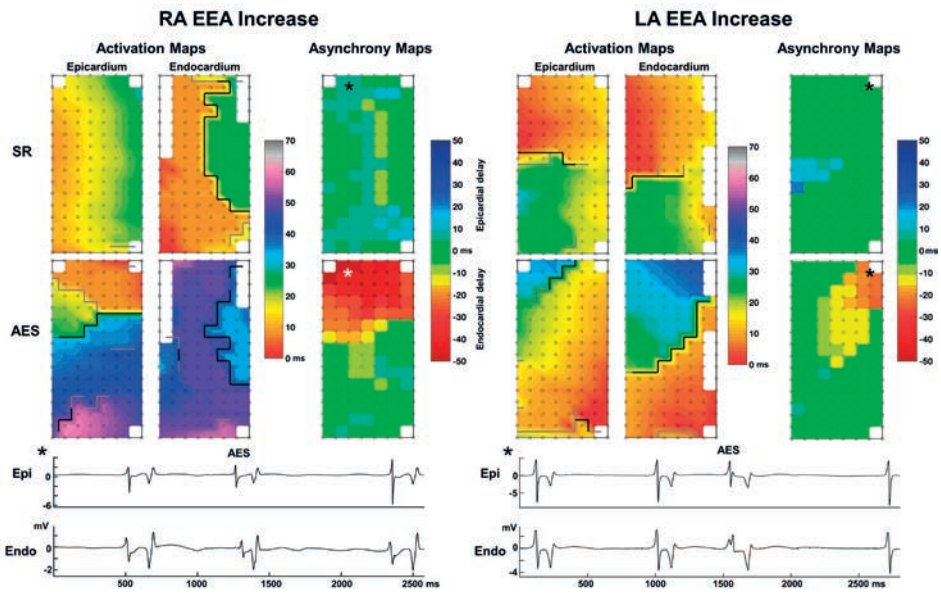

Figure 2. Examples of an increase of endo-epicardial asynchrony (EEA) during atrial extrasystoles at the right (RA) and left atrium (LA).
Color-coded activation maps of epicardial and endocardial local activation times and asynchrony maps are presented for sinus rhythm (SR, top) and atrial extra systole (AES, middle). Grey and black lines represent interelectrode conduction delay and block. Bottom: Electrogram examples from the location where EEA increases during the AES (asterisks).

Besides EEA of ≥15 ms, also endo-epicardial time differences between 10-15 ms were analyzed. Figure 3A shows the number of sinus-beats and AES demonstrating areas of large EEA (≥15 ms) and moderate and large EEA combined (≥10 ms). Incidences for both EEA groups increased during AES for EEA areas >5%. The changes in EEA during each AES for every individual patient are presented in Figure 3B. The top panel includes large EEA (≥15 ms) only and the middle panel includes both moderate and large EEA (≥10 ms). The increase of large EEA during AES almost reached a significant result (*P*=0.053, EEA area >5%). The most extensive increase of EEA area observed during AES involved 47% of the mapped area. When both moderate and large EEA were included, almost half of all AES (47%) demonstrated an increase in EEA during AES. Incidence of EEA ≥10 ms increased during AES (*P*=0.023, EEA area >5%).

There was no clear preference for either epicardium or endocardium to lag during AES. However in AES with the most increase of EEA (>20% of the array), the endocardial side was delayed relative to the epicardium (Figure 4). The same side was often delayed in case of EEA during multiple AES within one patient. One of the patients demonstrated a change from endocardial to epicardial delay in two consecutive AES (Figure 5). The first AES of this

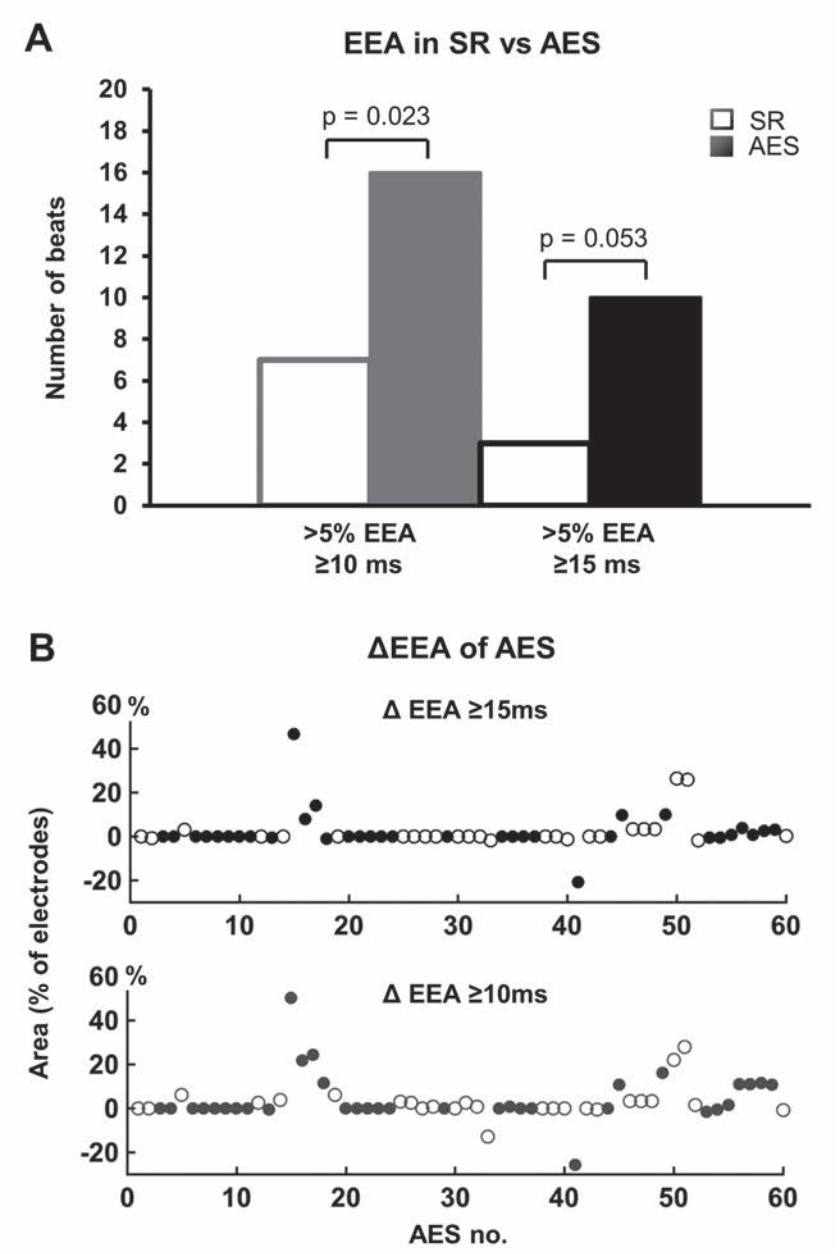

Figure 3. Change in endo-epicardial asynchrony (EEA) during atrial extra systoles (AES).
A: Frequency histograms of EEA between 10–15 ms and ≥15 ms during sinus rhythm (SR) and AES. Areas of EEA covering >5% of electrodes increase during AES. For EEA ≥10 ms, binary logistic analysis using Generalized Estimated Equations demonstrated a significant association between >5% EEA and AES (P=0.023).
B: Difference in EEA of AES compared to SR for EEA ≥10 ms and EEA ≥15 ms. Positive values represent an increase of EEA in AES, negative values represent a decrease of EEA in AES. Multiple AES in one patient are clustered and a change from an open (white) to a filled (dark) marker represents a different patient.

patient also had the longest increase in EEA of all AES of all patients; the endocardium was delayed by up to 130 ms compared to the epicardium during AES. There was no effect of a history of atrial fibrillation on the degree of EEA during sinus rhythm or AES.

Impact of prematurity and aberrancy

There was no correlation observed between prematurity and EEA increase. AES with the largest increases in EEA had severe or complex aberrancy (Supplemental Figure 1). Median ΔEEA for AES with the mildest aberrancy was 0 (0–0)%, for AES with severe and complex aberrancy 0 (0–2.8)% and for AES with complex sinus rhythm activation pattern 0.7 (-1.9–+3.6)%. No difference was observed for ΔEEA in AES between aberrancy categories.

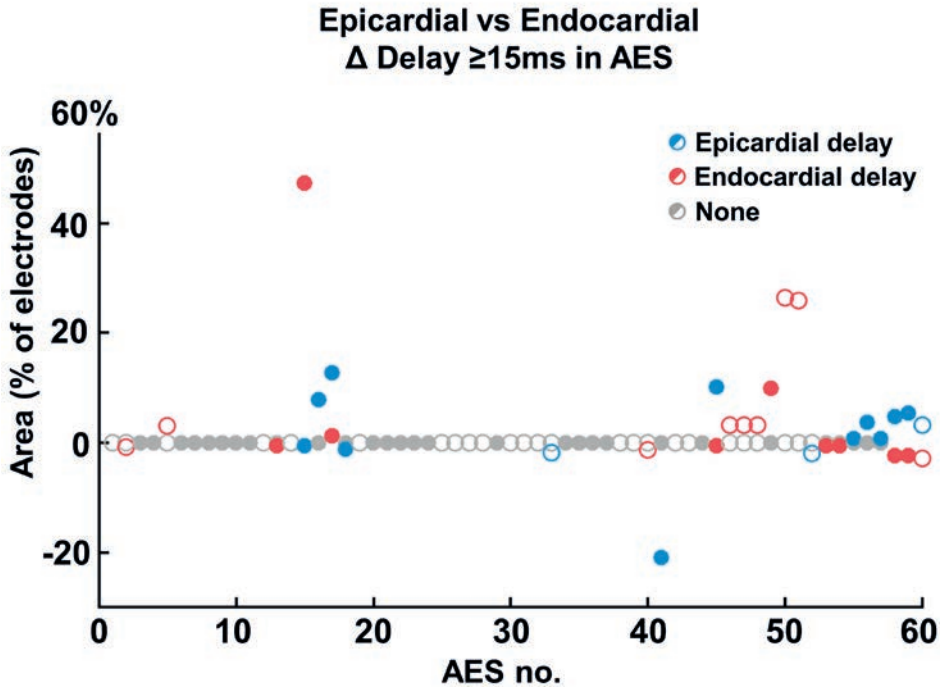

Figure 4. Epicardial vs. endocardial delay in atrial extrasystoles.
Scatterplot presenting the amount of decrease or increase of endocardial and epicardial delays ≥15 ms per atrial extrasystole (AES) compared to sinus rhythm. Multiple AES in one patient are clustered and a change from an open to a filled marker represents a different patient. For example, in the 8th patient the first AES has a 47% increase in endocardial delays and an 0.5% decrease in epicardial delays. The second AES in this patient demonstrates a 7.8% increase in epicardial delay and no change in endocardial delay.

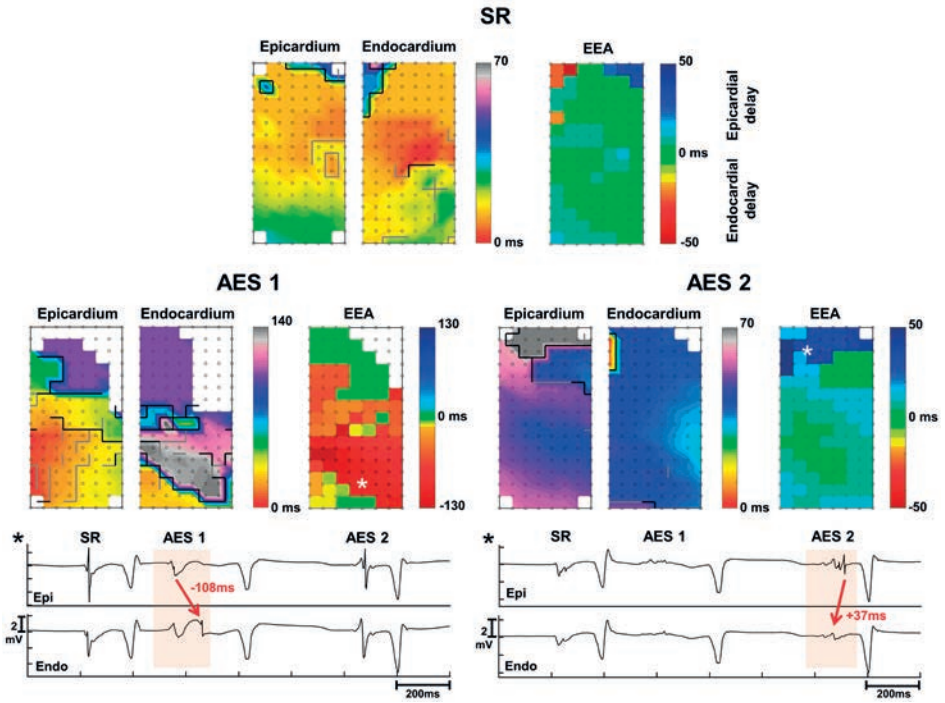

Figure 5. Presentation of severe endocardial delays during atrial extra systoles (AES).
Delays reach up to 130 ms at the lower part and the upper part is refractory. However, with the second immediately following AES the delay shifts to the epicardium (epi) with delays up to 50 ms at the upper part. Electrogram examples demonstrate the severe delays at the endocardium (endo) for the first AES and at the epicardium for the second AES. Asterisks refer to the site of the electrograms in the corresponding maps. SR, sinus rhythm.

DISCUSSION

Main findings

The main finding of this study is that spontaneous AES demonstrate more EEA than sinus-beats. Maximal increase in EEA-delay observed with AES was 130 ms and maximal EEA-area increase was 47%. A possible cause for increased EEA during AES was an increase in the imbalance of epicardial versus endocardial conduction disorders. Both conduction delay and block increased during AES; conduction delay increased mainly at the epicardium whereas conduction block likely increases mainly at the endocardium.

Conduction disorders in atrial extrasystoles

The increase of high-resolution conduction disorders in AES especially for aberrant AES was previously reported.[4] The current study demonstrated that these conduction disorders also become more unequally distributed between the epicardium and endocardium

in AES which may be one of the causes of increased EEA in AES. If conduction is delayed unevenly at epicardial and endocardial layers, this creates or enhances a substrate for asynchronous endo-epicardial activation. Studies have shown that conduction in AES mainly slows in the transverse direction, perpendicular to the myocardial fibers, thereby increasing the anisotropic behavior of the tissue.[8–10] This was underlined by our previous finding that aberrancy had an important role in aggravating conduction disorders during AES.[4] The severity of transverse conduction disorders in diseased myocardium was related to the fibrosis architecture. Myocardium with clustered fibrotic areas demonstrated more AES induced conduction disorders than those with diffuse fibrosis.[8,9] Distribution between sub-epicardial and sub-endocardial atrial fibrosis has not been described so far, however, is possibly very heterogeneously in nature. Nonetheless, the right atrial anatomy may favor endocardial conduction delays due to naturally limited transverse connections of the pectinate bundles making them vulnerable for conduction disorder in case of transversely traveling waves. In this study, there was no clear dominance of endocardial delay. Although, the AES with the largest increases in areas of EEA did have endocardial delay.

Arrhythmogenic potential of AES and effect of EEA

AES interrupt the stable rhythm originating from the sinus node by exciting the atria prematurely and/or from a site distant to the sinus node. As a result, at the time of the AES, recovery of myocardial cells can still be heterogeneously distributed in case of a premature AES. In the case of a different activation site during AES, the direction of activation changes leading to different conduction velocities due to anisotropy. Both of these concepts are able to result in re-entry in which an electrical pathway sustains itself, like a dog chasing its tail, causing a tachyarrhythmia.[11,12] The two prerequisites for re-entry are 1) unidirectional block and 2) a cycle length longer than the longest refractory (recovery) period. When unidirectional block occurs from the epicardium to the endocardium or vice versa, this will, in the best case, result in EEA only or it could result in an intramural re-entry circuit. This study demonstrated that either unidirectional or bidirectional conduction block between the layers occurs only during AES in patients.

Schuessler et al. have investigated endo-epicardial conduction at the right atrial appendage of dogs during sinus rhythm, pacing, extra-stimuli and induced tachyarrhythmias.[13] EEA increased with premature stimulation close to the refractory period and increased most with aberrant premature stimulation. Maximal recorded difference in excitation between epicardium and endocardium during premature stimulation was 30 ms. They then induced tachyarrhythmias in the presence of high-dose acetylcholine with a single extra-stimulus and demonstrated an intramural re-entry pattern during tachyarrhythmia with a very short cycle length of approximately 60 ms and EEA up to 31 ms. In our study, we recorded a much larger endo-epicardial excitation difference of 130 ms in a spontane-

ous AES in a patient with aortic valve disease. Functional right atrial refractoriness has been measured at around 270 ± 30 ms during electrophysiological studies in patients with or without a history of atrial fibrillation at cycle lengths of 600 ms.[14] In human right atrial bundles perfused with pinacidil, intramural re-entry patterns with cycle lengths of 57 to 210 ms and maximal EEA of about half the re-entry cycle length (22–105 ms) were observed.[15] During atrial fibrillation, EEA >50 ms was demonstrated at the right atrium in patients with atrial fibrillation cycle lengths between 140–246 ms and at the left atrium in a goat-model of atrial fibrillation with cycle lengths around 120–140 ms.[5,16] In both studies, the majority of the frequent focal waves were most likely caused by transmural conduction as a result of EEA. These findings suggest that EEA of 130 ms could create an intramural pathway of long enough delay for atrial tissue to recover from refractoriness, thereby promoting re-entry. Besides re-entry around an unexcitable core, EEA could also result in spiral wave re-entry: if conduction between the layers is slowed down to an extent that the intramural wavefront curve starts to spiral.

Multifactorial conditions for AES to trigger tachyarrhythmias

Multiple conditions can either contribute or counteract tachyarrhythmias initiation under different circumstances. One important factor is the refractory period, as it determines excitability of myocardial cells. Prematurity of AES close to the refractory period favors conduction disorders and inhomogeneous conduction due to uncompleted repolarization. However, the refractory period of myocardial cells is not a fixed time period and may vary under the influence of different factors. For example, the refractory period is rate-dependent and between atrial sites and within myocardial bundles differences in refractory duration also exist.[12] Furthermore, conduction velocity depends on anatomical factors such as anisotropy and source-to-sink principles. Anisotropy is that impulses travel slower along the transverse direction of myocardial bundles than the longitudinal direction. The source-to-sink principle is that conduction slows down when a small bundle has to excite a relatively large myocardial area.[17] Therefore, the direction of the wavefront in the heterogeneous atrial architecture determines conduction velocity.

Next to the previously mentioned conditions for re-entry, a third one is required: the existence of a pathway for re-entry. If there are no connecting myocardial bundles between epicardium and endocardium at the site of EEA, there is no pathway for intramural re-entry. Finally, the atrial architecture can be disrupted in all three dimensions by underlying heart diseases or aging causing fibrosis or the conduction properties of myocardial cells change due to tachyarrhythmia induced electrical remodeling.[8,9,18] Atrial structural and electrical remodeling thereby influences conduction velocity and continuity. All these factors combined determine atrial sensitivity for an AES to initiate a tachyarrhythmia. Although in our study the AES did not initiate tachyarrhythmias, the increase of epi-endocardial con-

duction disorders observed in AES add to arrhythmogenic tissue properties that underlie arrhythmias.

Clinical impact

This study demonstrated that EEA aggravates during AES, which thereby increases the arrhythmogenic properties of AES. Importance of EEA therefore seems not confined to atrial fibrillation alone. EEA has also been suggested as a mechanism during atrial flutter.[19] Clinicians need to be aware that current mapping technologies in patients are limited to diagnosing conduction disturbances on only one side of the atrial wall. There is a whole black box of atrial activation on the other side, especially during arrhythmia and arrhythmia prone conditions such as AES.

Study limitations

No atrial tachyarrhythmia was initiated by the AES in this study, as is the case for most AES, and most patients also did not have a history of atrial arrhythmias. Multiple factors contribute to tachyarrhythmia initiation. Due to the limited size of our study group and frequent occurrence of multiple AES in a short recording time period, this study could not substantially determine the effect of prematurity or aberrancy on increase of EEA during AES. Endo-epicardial mapping with performance of pacing protocols including premature stimulation could elucidate the contribution of AES characteristics on EEA occurrence. Furthermore, endo-epicardial mapping during cardiac surgery is mostly restricted to the right atrium; therefore, left atrial data is limited.

CONCLUSIONS

Atrial ectopic activation interrupting sinus rhythm provokes more conduction disorders between the epicardium and endocardium which creates or aggravates EEA. An imbalance in the degree of conduction disorders at the epicardium versus the endocardium could attribute to the occurrence of EEA in AES. Asynchrony between the layers in AES reached up to 130 ms which could be enough to initiate an intramural re-entry pathway under the right conditions. Current mapping tools in patients are not equipped to recognize arrhythmogenic properties between epicardium and endocardium.

REFERENCES

1. Johnson LS, Juhlin T, Juul-Moller S, Hedblad B, Nilsson PM, Engstrom G. A prospective study of supraventricular activity and incidence of atrial fibrillation. Heart Rhythm. 2015;12:1898-1904.
2. Vincenti A, Brambilla R, Fumagalli MG, Merola R, Pedretti S. Onset mechanism of paroxysmal atrial fibrillation detected by ambulatory Holter monitoring. Europace 2006;8:204-210.
3. Haïssaguerre M, Jaïs P, Shah DC, Takahashi A, Hocini M, Quiniou G, Garrigue S, Le Mouroux A, Le Métayer P, Clémenty J. Spontaneous initiation of atrial fibrillation by ectopic beats originating in the pulmonary veins. N Engl J Med. 1998;339:659-666.
4. Teuwen CP, Kik C, van der Does LJME, Lanters EAH, Knops P, Mouws EMJP, Bogers AJJC, de Groot NMS. Quantification of the Arrhythmogenic Effects of Spontaneous Atrial Extrasystole Using High-Resolution Epicardial Mapping. Circ Arrhythm Electrophysiol. 2018;11:e005745.
5. de Groot N, van der Does L, Yaksh A, Lanters E, Teuwen C, Knops P, van de Woestijne P, Bekkers J, Kik C, Bogers A, Allessie M. Direct Proof of Endo-Epicardial Asynchrony of the Atrial Wall During Atrial Fibrillation in Humans. Circ Arrhythm Electrophysiol. 2016;9:e003648.
6. van der Does LJME, Knops P, Teuwen CP, Serban C, Starreveld R, Lanters EAH, Mouws EMJP, Kik C, Bogers AJJC, de Groot NMS. Unipolar atrial electrogram morphology from an epicardial and endocardial perspective. Heart Rhythm. 2018;15:879-887.
7. Knops P, Kik C, Bogers AJ, de Groot NM. Simultaneous endocardial and epicardial high-resolution mapping of the human right atrial wall. J Thorac Cardiovasc Surg 2016;152:929-931.
8. Angel N, Li LI, Macleod RS, Marrouche N, Ranjan R, Dosdall DJ. Diverse Fibrosis Architecture and Premature Stimulation Facilitate Initiation of Reentrant Activity Following Chronic Atrial Fibrillation. J Cardiovasc Electrophysiol. 2015;26:1352-1360.
9. Kawara T, Derksen R, de Groot JR, Coronel R, Tasseron S, Linnenbank AC, Hauer RN, Kirkels H, Janse MJ, de Bakker JM. Activation delay after premature stimulation in chronically diseased human myocardium relates to the architecture of interstitial fibrosis. Circulation. 2001;104:3069-3075.
10. Spach MS, Heidlage JF, Dolber PC, Barr RC. Mechanism of origin of conduction disturbances in aging human atrial bundles: experimental and model study. Heart Rhythm. 2007;4:175-185.
11. Spach MS, Dolber PC, Heidlage JF. Influence of the passive anisotropic properties on directional differences in propagation following modification of the sodium conductance in human atrial muscle. A model of reentry based on anisotropic discontinuous propagation. Circ Res. 1988;62:811-832.
12. Spach MS, Dolber PC, Heidlage JF. Interaction of inhomogeneities of repolarization with anisotropic propagation in dog atria. A mechanism for both preventing and initiating reentry. Circ Res. 1989;65:1612-1631.
13. Schuessler RB, Kawamoto T, Hand DE, Mitsuno M, Bromberg BI, Cox JL, Boineau JP. Simultaneous epicardial and endocardial activation sequence mapping in the isolated canine right atrium. Circulation. 1993;88:250-263.
14. De Sisti A, Attuel P, Manot S, Fiorello P, Halimi F, Leclercq JF. Electrophysiological determinants of atrial fibrillation in sinus node dysfunction despite atrial pacing. Europace. 2000;2:304-311.
15. Hansen BJ, Zhao J, Csepe TA, Moore BT, Li N, Jayne LA, Kalyanasundaram A, Lim P, Bratasz A, Powell KA, Simonetti OP, Higgins RS, Kilic A, Mohler PJ, Janssen PM, Weiss R, Hummel JD, Fedorov VV. Atrial fibrillation driven by micro-anatomic intramural re-entry revealed by simultaneous sub-epicardial and sub-endocardial optical mapping in explanted human hearts. Eur Heart J. 2015;36:2390-2401.
16. Eckstein J, Zeemering S, Linz D, Maesen B, Verheule S, van Hunnik A, Crijns H, Allessie MA, Schotten U. Transmural conduction is the predominant mechanism of breakthrough during atrial fibrillation:

evidence from simultaneous endo-epicardial high-density activation mapping. Circ Arrhythm Electrophysiol. 2013;6:334-341.

17. Spach MS, Miller WT, Dolber PC, Kootsey JM, Sommer JR, Mosher CE. The functional role of structural complexities in the propagation of depolarization in the atrium of the dog. Cardiac conduction disturbances due to discontinuities of effective axial resistivity. Circ. Res. 1982, 50, 175–191.
18. Allessie M, Ausma J, Schotten U. Electrical, contractile and structural remodeling during atrial fibrillation. Cardiovasc. Res. 2002, 54, 230–246.
19. Pathik B, Lee G, Sacher F, Haïssaguerre M, Jaïs P, Massoullié G, Derval N, Sanders P, Kistler P, Kalman JM. Epicardial-endocardial breakthrough during stable atrial macroreentry: Evidence from ultra-high-resolution 3-dimensional mapping. Heart Rhythm. 2017;8:1200-1207.

SUPPLEMENTAL MATERIAL CHAPTER 15

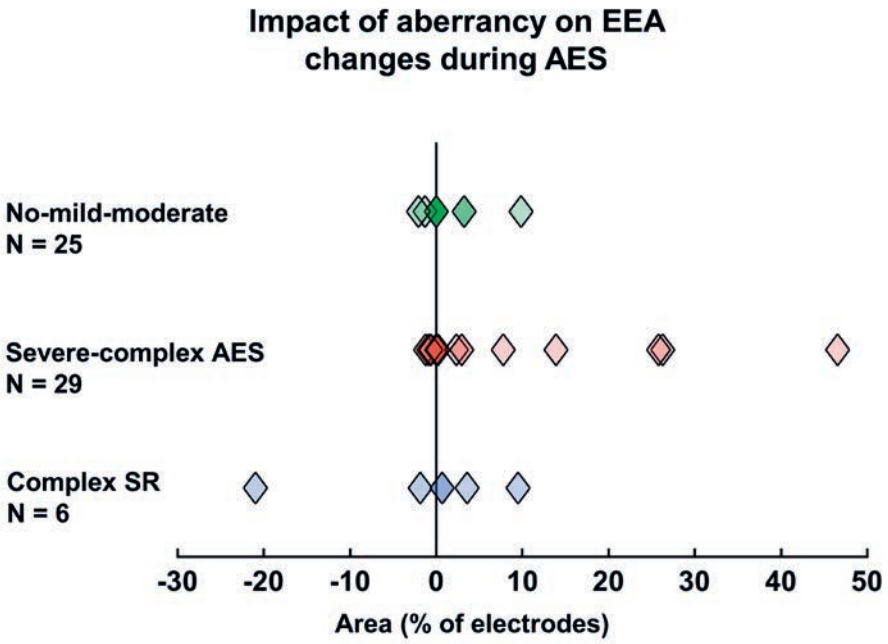

Supplemental Figure 1. Endo-epicardial asynchrony difference for AES compared to SR per aberrancy category.
Aberrancy categories include AES with no, mild or moderate aberrancy vs AES with severe or complex activation patterns during AES vs AES with complex activation patterns during SR only. Largest increases in EEA occurred in AES with severe/ complex activation patterns. A complex pattern during only SR decreased EEA by 21% in one patient.

16

General Discussion

Lisette van der Does

GENERAL DISCUSSION

Controversy in mechanisms underlying atrial fibrillation

For most atrial tachyarrhythmias the mechanism, i.e., pathological electrical pathway is known and therefore ablative procedures for these tachyarrhythmias are very effective. On the other hand, the mechanism underlying atrial fibrillation (AF) remains uncertain and controversy exists between researchers studying AF. What *is* known is that paroxysmal AF is in most cases triggered by electrical activity from the pulmonary veins.[1] Many theories have been proposed for persistence of AF and the two main positions taken over the last years were researchers supporting the concept of rotors or focal activity driving AF vs researchers supporting the multiple wavelet theory.[2-5] Evidence for both sides has been published and this raises the question: why do results between AF studies differ so significantly?[2-4, 6, 7] In 2014, both positions were argued in a crosstalk and the important argument was made that the mapping resolution and signal processing technologies are fundamentally different.[8-11] Mapping, i.e., the representation of electrical activity pathways is based on, first, recording of local electrical activity on electrograms, and then determining the local activation time of each signal recorded on the electrogram. Mapping outcomes are determined by recording modus, quality of electrograms, density and surface area of electrogram recordings. The next paragraphs will discuss which previous mapping studies and mapping approaches have been performed and which mechanism they supported, which resolution is required for AF mapping, the effect of recording modus, and will argue the added complexity in AF mapping caused by endo-epicardial asynchrony.

Mapping studies of atrial fibrillation

Studies that have mapped AF activation patterns in patients with persistent AF to find the underlying mechanism, and have used direct contact mapping with different resolution or recording mode have been summarized in Table 1. In the last column the dominant supporting theory is shown, meaning which pattern of activation is seen in most patients/most of the recording time. Table 2 specifies also the other activation patterns that were observed in these studies. Rotors have been mostly detected during mapping with a very low resolution (0.6-1/cm^2) and in these studies rotors were present in >88% of patients.[5, 12-14] There was one high-resolution mapping that showed (mostly) transient rotors during only 12% of the recording time with a median of 3 rotations. In one case, a relatively stable rotor (presence >95% of the time) was seen.[7] The studies with the highest resolution of 19 and 21-24/cm^2 mainly supported the multiple wavelets theory because drivers were not or only sparsely observed.[2-4, 7] Earlier studies with a low to medium resolution (0.8-8.5/cm^2) often attributed their findings to micro- or macro-re-entry, however, often it was based on a theoretical explanation of either a focal pattern of activation or regular repetitive activation pattern without demonstration of a re-entry pathway (Table 2).[15-18] Important is to not

Table 1. Human mapping studies of atrial fibrillation

Study	Electrode size (mm)	Resolution (electrodes/ cm^2)*	Total area (cm^2)	Recording modus (IES,mm)	Location	Side	AF type	Dominant supporting theory
Harada et al. 1996[15]	2	0.8	71.6	Unipolar	RA + LA	Epicardium	PsAF/ LsPAF	Micro-reentry or ectopic focus (LA)
Holm et al. 1997[16]	1	7 / 14	17	Bipolar (3)	RA	Epicardium	LsPAF (+PsAF)	Micro or macro-reentry
Wu et al. 2002[17]	-	8.5 / 17	26.4	Bipolar (3)	RA + LA (s)	Epicardium	LsPAF (+PsAF)	Ectopic focus (PV) or micro-reentry (LA)
Yamauchi et al. 2002[18]	2	1.7	71.5	Unipolar	RA + LA	Epicardium	LsPAF	Ectopic focus or micro-reentry (LA)
Nitta et al. 2004[27]	-	3	91.1	Unipolar	RA + LA (s)	Epicardium	LsPAF	Ectopic focus (PV/LA)
Takahashi et al. 2006[6]	1	1.0 / 2.1	96	Bipolar (2)	RA + LA	Endocardium	PAF (+ LsPAF + PsAF)	Multiple wavelets
De Groot/ Allessie et al. 2010[2, 3]	0.3	24 + 21	23.4	Unipolar	RA + LA	Epicardium	LsPAF	Multiple wavelets
Narayan et al. 2012-2019[5, 13, 14]	1	1 + 0.6	128-226†	Unipolar/ Bipolar (4-5) → MAP	RA + LA (s)	Endocardium	PsAF (+PAF)	Rotors
Lee/ Walters et al. 2014[4, 7]	0.7	19	27	Bipolar (2.5)	RA + LA	Epicardium	PsAF	Multiple wavelets
Lee et al. 2015/2017[28, 29]	-	2.2 / 5.5	92.9	Bipolar (1.2)	RA + LA + BB (s)	Epicardium	LsPAF (+PsAF)	Ectopic foci
Honarbakhsh et al. 2018[12]	1	0.8 + 0.6	78.5†	Unipolar	LA	Endocardium	PsAF/ LsPAF	Rotors

* For bipolar recording the number of recording sites (electrode pairs) and / total electrodes are shown. † Calculated from the diameter of the balloon, real surface area is smaller due to absence of electrically active tissue at the location of the atrioventricular valve. IES = interelectrode spacing; MAP = monophasic action potentials; s = simultaneous recordings; RA = right atrium; LA = left atrium; AF = atrial fibrillation; PAF = paroxysmal AF; PsAF = persistent AF; LsPAF = longstanding persistent AF; PV = pulmonary veins.

Table 2. Observed activation patterns during atrial fibrillation

Study	Regular repetitive activation	Stable repetitive focal waves	Transient repetitive focal waves	Random focal waves	Reentry	Stable rotor	Transient rotor	Multiple wavelets
Harada et al. 1996[15]	x		x					x
Holm et al. 1997[16]			x		x			x
Wu et al. 2002[17]	x							x
Yamauchi et al. 2002[18]	x				x			x
Nitta et al. 2004[27]	x	x		x	x			x
Takahashi et al. 2006[6]			x					x
De Groot/ Allessie et al. 2010[2, 3]				x				x
Narayan et al. 2012-2019[5, 13, 14]		x				x	x	
Lee/ Walters et al. 2014[4, 7]			x				x	x
Lee et al. 2015/2017[28, 29]		x	x					
Honarbakhsh et al. 2018[12]			x				x	

exclude the multiple wavelets theory only based on transient regular repetitive activities or activation patterns at certain atrial parts. This theory does not imply that all waves have to be random at all time, based on local functional or anatomical features, predilection for certain activation patterns may exist.

Moreover, the definition used for a rotor in human mapping studies is very debatable. On a basic level, the difference between normal re-entry and a rotor is the electrically active core (phase singularity) of a rotor in comparison to the electrically inactive center of re-entry around an obstacle.[19] However, human mapping studies define rotors only as rotational activity around a center which was, in the beginning, required to remain sustained for >50 or >1000 cycles, but later also >10 cycles or >2-3 cycles was defined as a rotor.[4, 5, 7, 12, 14, 20] Core electrical activity of rotational activation patterns in these studies cannot be determined due to the low resolution. Currently, due to technological limitations, *endo*cardial mapping is of low resolution and high-resolution mapping with multi-electrode arrays can only be performed *epi*cardially. Therefore, it is unknown if there is an association between the atrial side of mapping (endocardium vs epicardium) and the fact that rotors are mainly found in endocardial mapping studies. One advantage of low-resolution mapping is that a large area can be mapped simultaneously providing a total overview of the atrial activation pattern.

Chapters 4 and 5 introduced a new epicardial mapping approach covering both atria and Bachmann's bundle with a resolution higher than in the studies of Table 1. At 9 atrial areas, 192 electrograms were recorded simultaneously with a density of 30/cm^2 (total surface 58 cm^2) in order to identify small conduction disturbances and to create a detailed map of activation patterns during sinus rhythm, pacing and AF. This technique can also be applied during minimally invasive surgery, although for complete left atrial mapping additional incision sites would then be required. Also, in Chapter 9 another new mapping technique was introduced of simultaneous epicardial and endocardial high-resolution mapping that provided a new possible mechanism expanding on the multiple wavelets theory.

The resolution required for atrial fibrillation

To determine the required resolution for mapping of AF, it is necessary to have an understanding of the resolution of AF itself. Sizes of waves in human AF have been described in two previous studies that performed high-resolution mapping. Lee et al. defined narrow AF wavelets as waves between 5-15 mm and observed a mean wave size of 20.9±15 mm and median wave size of 15 mm (interquartile range: 15-35 mm).[4] AF waves in the figures of studies by Allessie et al. and De Groot et al.[2, 3] were as narrow as a single electrode row translating to a wave diameter of ±2.5 mm. In patients with longstanding persistent AF the number of waves per cm^2 was 4.5 (4.1-5.1) compared to the 2.3 (1.7-2.9) waves/cm^2 in

Figure 1. Low-resolution pictures.

patients without AF in whom AF was induced.[2] The focal waves observed in Chapter 9, were defined to have a minimal size of 4 electrodes. Smallest focal waves with sizes of 4, 5 and 6 electrodes comprised, respectively, 5.3%, 4.9% and 4.2% of all focal waves. Sizes of focal waves therefore range in 15% between 16-24 mm^2. Mapping approaches with a low resolution will not be able to detect these small AF wavelets because it would require a minimum resolution of unipolar electrodes or bipolar electrode pairs of 7 per cm^2 to be able to register these AF waves on one electrode alone. From the 11 mapping studies presented in Table 1, 4 studies meet these requirements. When comparing the resolution of high-resolution electrode arrays to the resolution of the basket catheter used in the studies of Narayan et al[5, 13, 14] and Honarbakhsh et al[12], the resolution of the latter is 30 to 50 times lower (0.6 or 1 electrode/cm^2 vs 30 electrodes/cm^2). A high-resolution during mapping of AF will decrease the chance of under-detection of AF waves and of incorrect interpretation of atrial activation patterns.

Why are current mapping technologies sufficient for most atrial arrhythmias, but not AF? The required resolution of mapping depends on the level of complexity of the arrhythmia. For example, in Figure 1 two pictures with the same low resolution are shown. The top picture is simple and even with a very low resolution you will be able to determine its

content. However, the bottom picture is much more complex and the low resolution here can easily result in a false interpretation of the actual picture (the high-resolution versions are shown in Figure 2). Similar with regular tachyarrhythmias and AF; regular tachyarrhythmias are mostly easy to identify even with a low resolution, however, the chaotic patterns of activation and small wavelets during AF require a high resolution. The challenge with current high-resolution mapping is that due to the relatively small size of the arrays, atrial areas need to be mapped sequentially. This can be explained as having to take several small pictures of one large picture in order to cover the entire object (black square in Figure 2). You will still be able to correctly deduce the object, but if the situation changes between pictures, for example a few balls are taken away or moved, this may not be noticed. Although studies have shown that patterns of activation remain stable in areas during 10 minutes of AF[7], a more panoramic high-resolution view will help to identify and understand the mechanisms underlying AF even better.

Endo-epicardial asynchrony: a new mechanism during atrial fibrillation

Focal waves observed in the study of De Groot et al. in 2010 led to the concept of asynchrony between epicardial and endocardial activation being the origin of focal waves.[3] The evidence for this theory was provided in the study presented in Chapter 9. This was the first study to perform simultaneous epicardial *and* endocardial mapping in living human subjects to investigate differences in electrical activation. Because mapping on both sides simultaneously is technically very challenging, it can only be consistently performed at the right atrial free wall. The right atrial appendage is the only location where an incision in the atrium is standardly made during cardiac surgery *before* induced cardiac arrest. Endo-epicardial asynchrony (EEA) occurred in patients at 0.9-55.9% of the sites during 10 seconds of AF. EEA was especially observed in patients with longstanding persistent AF; all patients with longstanding AF demonstrated EEA in over 20% of the sites. Focal waves were preceded by a wave of activation on the opposite side in 65% which means that the majority of focal waves could be attributed to transmural electrical conduction. These findings constitute an important new mechanism during AF. The electrical dissociation between the layers provides an opportunity for waves to travel from one side to the other and create new (focal) waves by conducting through the atrial wall. The possibilities for waves to encounter excitable tissue thereby increase substantially. Focal activation observed in previous studies may actually represent transmural conduction of AF waves.

Significance of EEA is not limited to AF alone, EEA also increases in atrial extrasystoles which can act as triggers for AF (Chapter 15) and EEA has also been significant in some cases of atrial flutter.[21] The presence and likely important role of EEA during arrhythmia further complicates mapping of AF. Current technologies can only record electrograms from one side of the atrial wall and therefore lack information about electrical activation

on the other side. This presents a great challenge as the incidence of EEA is high and there are no simple technical solutions to record the entire atria on both sides simultaneously. However, in Chapter 12 the morphology of epicardial and endocardial electrograms was compared during sinus rhythm. A possible solution was provided by the discovery that EEA can be reflected on the electrogram by fractionation. Analyzing fractionation of the electrogram could be the key to indirectly detect EEA. This possibility was explored further in Chapter 14. Areas at the right atrial free wall demonstrating EEA in patients during sinus rhythm, pacing or atrial extrasystoles were analyzed to determine how sensitive fractionation is in identifying EEA. In 86% of patients, EEA was visible on the epicardial or endocardial electrogram at a median of 75% and 72% electrode sites with EEA, respectively. EEA was easier to identify on unipolar electrograms than on bipolar electrograms.

Electrograms: unipolar vs bipolar and functionality of fractionation

As explained, bipolar electrograms are the difference between two unipolar electrograms and therefore farfield electrical activity is mostly cancelled. The disadvantage of bipolar electrograms is that they are affected by wave orientation.[22, 23] When the activation direction is parallel to the two poles or in case of simultaneous activation, timing of the signals are similar and electrogram voltage can decrease to very low values making it more difficult to determine the local activation time. Especially during AF, where AF waves travel in chaotic patterns constantly changing direction, bipolar electrograms are likely much more often affected than during other atrial tachyarrhythmias. Furthermore, technical properties such as a larger electrode size and larger electrode spacing increase the amount of electrogram fractionation on the bipolar electrogram.[24] The foundation for unipolar fractionation was elegantly demonstrated a long time ago by Spach and co-workers. On a microscopic level it was seen that each component of a fractionated electrogram could be traced to activation of a specific muscle bundle.[25] Although in Chapter 11 other possible factors contributing to fractionation were discussed, the conclusion in Chapter 12 was that 95% of fractionation on unipolar high-resolution electrograms could be attributed to remote atrial activation. It was also demonstrated that EEA causes fractionation of unipolar electrograms. It was then theorized that EEA based electrogram fractionation would be largely removed from bipolar electrograms as farfield electrical activity is substracted. In actuality, EEA remote electrical activity proved to be local enough to appear on bipolar electrograms as well. However, fractionation corresponding to EEA was less distinguishable from the noise on bipolar electrograms and more additional fractionation will make it more difficult to identify fractionated deflections based on EEA (Chapter 14). These observations indicate that unipolar electrograms are better suited for mapping of AF than bipolar electrograms.

Figure 2. High-resolution pictures.

In some AF mapping studies of Table 1, a different type of electrogram analysis was performed to map AF. In the endocardial electrophysiology studies by Narayan et al. unipolar or bipolar electrograms are converted to monophasic action potentials from which activation maps are created.[5, 14] Recently, the effects of mapping using monophasic action potentials (phase mapping) were demonstrated by direct comparison of activation mapping from unipolar electrograms to mapping based on phase analysis of unipolar electrograms.[26] Mapping in this study was performed with a very high resolution of 50 electrodes/cm^2. The specificity of rotor waves by phase mapping was only 10%, and false-positive cases were mostly localized at lines of conduction block with waves traveling opposite to each other in unipolar activation maps.[26]

Limitations of high-resolution mapping

Currently, there are still several limitations of high-resolution mapping. First, high-resolution arrays can only be placed on the epicardium due to their size, thereby certain atrial areas such as the septum cannot be mapped. Secondly, the arrays can, due to its epicardial application, only be used during cardiac surgery. Endovascular electrophysiological procedures are much less invasive and therefore available to a larger AF population. Finally, to cover the entire atrial surface, mapping is performed sequentially in high-resolution

mapping, whereas low-resolution mapping studies can map the entire surface simultaneously. As mentioned, the entire activation pattern of both atria cannot yet be visualized by high-resolution mapping. Both low-resolution and high-resolution mapping have certain advantages and disadvantages; however, these differences also lead to differences in study outcomes of AF mechanisms. It is plausible that different mechanisms of AF are involved in different patients. Because of the complexity of AF, high-resolution mapping is necessary in order to find the individual arrhythmogenic substrates and to not make false assumptions based on an undetailed map. This way, the optimal treatment course can be determined for each AF patient. To this end, technical advancements need to follow in order to further unravel mechanisms underlying AF.

CONCLUSIONS AND FUTURE PERSPECTIVES: BACK TO THE DRAWING BOARD

Mapping of AF requires a high resolution of electrogram recording sites that is able to spot detailed conduction disorders and thereby identify the arrhythmogenic substrate in individual patients. Asynchrony in activation between the epicardial and endocardial layers is a potential substrate for AF and a new mechanism explaining perpetuation of AF. Although current mapping tools are unable to identify EEA, it was discovered here that EEA is reflected on the electrogram as fractionation in most patients. To detect EEA on the electrogram, unipolar electrograms are superior to bipolar electrograms due to less disturbances and a better signal-to-noise ratio of EEA based fractionation. As the frequent occurrence of EEA demonstrated, AF is even more complex than previously thought and current technologies for AF mapping are insufficient. To actually understand mechanisms involved in AF, we need to go back to the drawing board and start to critically review mapping techniques that may lead to false interpretation of AF and develop new high-resolution tools and software.

The most optimal AF mapping tool will require the following features:

1. A high resolution/ electrode density
2. Cover the entire surface of both atria
3. Simultaneous recordings of all electrograms
4. Use unipolar electrograms
5. Be able to detect asynchrony between epicardium and endocardium
6. A high sample rate (to increase accuracy of fractionation)
7. Preferably record from the endocardium

The technical side of developing a system of high-resolution than can be placed within small catheters but still cover the entire atrium will be extremely challenging. It will require experts in electrical engineering to design and develop such an advanced mapping system. Development of feature 5 can be continued based on findings in this thesis. It would require software that is able to relate fractionation to activation patterns and identify fractionation caused by EEA. Therefore, future studies will need to characterize fractionated unipolar deflections which identify EEA and determine features that provide the best sensitivity and specificity for EEA.

Finally, to overcome current controversies in AF mechanisms, besides upgrading mapping tools, research into AF would greatly benefit from exchanging electrogram data between research groups to discover the differences in annotation and analysis of electrograms resulting in activation maps. If a consensus is made over how to analyze and interpret electrograms based on (previous) experimental data, study outcomes will likely become more in agreement.

REFERENCES

1. Haïssaguerre M, Jaïs P, Shah DC, Takahashi A, Hocini M, Quiniou G, Garrigue S, Le Mouroux A, Le Metayer P, Clementy J. Spontaneous initiation of atrial fibrillation by ectopic beats originating in the pulmonary veins. N Engl J Med. 1998;339:659-666.
2. Allessie MA, de Groot NM, Houben RP, Schotten U, Boersma E, Smeets JL, Crijns HJ. Electropathological substrate of long-standing persistent atrial fibrillation in patients with structural heart disease: longitudinal dissociation. Circ Arrhythm Electrophysiol. 2010;3:606-615.
3. de Groot NMS, Houben RPM, Smeets JL, Boersma E, Schotten U, Schalij MJ, Crijns H, Allessie MA. Electropathological Substrate of Longstanding Persistent Atrial Fibrillation in Patients With Structural Heart Disease Epicardial Breakthrough. Circulation. 2010;122:1674-1682.
4. Lee G, Kumar S, Teh A, Madry A, Spence S, Larobina M, Goldblatt J, Brown R, Atkinson V, Moten S, Morton JB, Sanders P, Kistler PM, Kalman JM. Epicardial wave mapping in human long-lasting persistent atrial fibrillation: transient rotational circuits, complex wavefronts, and disorganized activity. Eur Heart J. 2014;35:86-97.
5. Narayan SM, Krummen DE, Rappel WJ. Clinical mapping approach to diagnose electrical rotors and focal impulse sources for human atrial fibrillation. J Cardiovasc Electrophysiol. 2012;23:447-454.
6. Takahashi Y, Hocini M, O'Neill MD, Sanders P, Rotter M, Rostock T, Jonsson A, Sacher F, Clementy J, Jaïs P, Haïssaguerre M. Sites of focal atrial activity characterized by endocardial mapping during atrial fibrillation. J Am Coll Cardiol. 2006;47:2005-2012.
7. Walters TE, Lee G, Morris G, Spence S, Larobina M, Atkinson V, Antippa P, Goldblatt J, Royse A, O'Keefe M, Sanders P, Morton JB, Kistler PM, Kalman JM. Temporal Stability of Rotors and Atrial Activation Patterns in Persistent Human Atrial Fibrillation: A High-Density Epicardial Mapping Study of Prolonged Recordings. JACC Clin Electrophysiol. 2015;1:14-24.
8. Allessie M, de Groot N. CrossTalk opposing view: Rotors have not been demonstrated to be the drivers of atrial fibrillation. J Physiol. 2014;592:3167-3170.
9. Allessie M, de Groot N. Rebuttal from Maurits Allessie and Natasja de Groot. J Physiol. 2014;592:3173.
10. Narayan SM, Jalife J. CrossTalk proposal: Rotors have been demonstrated to drive human atrial fibrillation. J Physiol. 2014;592:3163-3166.
11. Narayan SM, Jalife J. Rebuttal from Sanjiv M. Narayan and Jose Jalife. J Physiol. 2014;592:3171.
12. Honarbakhsh S, Schilling RJ, Dhillon G, Ullah W, Keating E, Providencia R, Chow A, Earley MJ, Hunter RJ. A Novel Mapping System for Panoramic Mapping of the Left Atrium: Application to Detect and Characterize Localized Sources Maintaining Atrial Fibrillation. JACC Clin Electrophysiol. 2018;4:124-134.
13. Leef G, Shenasa F, Bhatia NK, Rogers AJ, Sauer W, Miller JM, Swerdlow M, Tamboli M, Alhusseini MI, Armenia E, Baykaner T, Brachmann J, Turakhia MP, Atienza F, Rappel WJ, Wang PJ, Narayan SM. Wavefront Field Mapping Reveals a Physiologic Network Between Drivers Where Ablation Terminates Atrial Fibrillation. Circ Arrhythm Electrophysiol. 2019;12:e006835.
14. Narayan SM, Krummen DE, Shivkumar K, Clopton P, Rappel WJ, Miller JM. Treatment of atrial fibrillation by the ablation of localized sources: CONFIRM (Conventional Ablation for Atrial Fibrillation With or Without Focal Impulse and Rotor Modulation) trial. J Am Coll Cardiol. 2012;60:628-636.
15. Harada A, Sasaki K, Fukushima T, Ikeshita M, Asano T, Yamauchi S, Tanaka S, Shoji T. Atrial activation during chronic atrial fibrillation in patients with isolated mitral valve disease. Ann Thorac Surg. 1996;61:104-111; discussion 111-102.

16. Holm M, Johansson R, Brandt J, Luhrs C, Olsson SB. Epicardial right atrial free wall mapping in chronic atrial fibrillation. Documentation of repetitive activation with a focal spread--a hitherto unrecognised phenomenon in man. Eur Heart J. 1997;18:290-310.
17. Wu TJ, Doshi RN, Huang HL, Blanche C, Kass RM, Trento A, Cheng W, Karagueuzian HS, Peter CT, Chen PS. Simultaneous biatrial computerized mapping during permanent atrial fibrillation in patients with organic heart disease. J Cardiovasc Electrophysiol. 2002;13:571-577.
18. Yamauchi S, Ogasawara H, Saji Y, Bessho R, Miyagi Y, Fujii M. Efficacy of intraoperative mapping to optimize the surgical ablation of atrial fibrillation in cardiac surgery. Ann Thorac Surg. 2002;74:450-457.
19. Vaquero M, Calvo D, Jalife J. Cardiac fibrillation: from ion channels to rotors in the human heart. Heart Rhythm. 2008;5:872-879.
20. Alhusseini M, Vidmar D, Meckler GL, Kowalewski CA, Shenasa F, Wang PJ, Narayan SM, Rappel WJ. Two Independent Mapping Techniques Identify Rotational Activity Patterns at Sites of Local Termination During Persistent Atrial Fibrillation. J Cardiovasc Electrophysiol. 2017;28:615-622.
21. Pathik B, Lee G, Sacher F, Haïssaguerre M, Jaïs P, Massoullie G, Derval N, Sanders P, Kistler P, Kalman JM. Epicardial-endocardial breakthrough during stable atrial macroreentry: Evidence from ultra-high-resolution 3-dimensional mapping. Heart Rhythm. 2017;14:1200-1207.
22. Takigawa M, Relan J, Martin R, Kim S, Kitamura T, Frontera A, Cheniti G, Vlachos K, Massoullié G, Martin CA, Thompson N, Wolf M, Bourier F, Lam A, Duchateau J, Klotz N, Pambrun T, Denis A, Derval N, Magat J, Naulin J, Merle M, Collot F, Quesson B, Cochet H, Hocini M, Haïssaguerre M, Sacher F, Jaïs P. Effect of bipolar electrode orientation on local electrogram properties. Heart Rhythm. 2018;15:1853-1861.
23. Brunckhorst CB, Delacretaz E, Soejima K, Maisel WH, Friedman PL, Stevenson WG. Impact of changing activation sequence on bipolar electrogram amplitude for voltage mapping of left ventricular infarcts causing ventricular tachycardia. J Interv Card Electrophysiol. 2005;12:137-141.
24. Correa de Sa DD, Thompson N, Stinnett-Donnelly J, Znojkiewicz P, Habel N, Muller JG, Bates JH, Buzas JS, Spector PS. Electrogram fractionation: the relationship between spatiotemporal variation of tissue excitation and electrode spatial resolution. Circ Arrhythm Electrophysiol. 2011;4:909-916.
25. Spach MS, Dolber PC. Relating extracellular potentials and their derivatives to anisotropic propagation at a microscopic level in human cardiac muscle. Evidence for electrical uncoupling of side-to-side fiber connections with increasing age. Circ Res. 1986;58:356-371.
26. Podziemski P, Zeemering S, Kuklik P, van Hunnik A, Maesen B, Maessen J, Crijns HJ, Verheule S, Schotten U. Rotors Detected by Phase Analysis of Filtered, Epicardial Atrial Fibrillation Electrograms Colocalize With Regions of Conduction Block. Circ Arrhythm Electrophysiol. 2018;11:e005858.
27. Nitta T, Ishii Y, Miyagi Y, Ohmori H, Sakamoto S, Tanaka S. Concurrent multiple left atrial focal activations with fibrillatory conduction and right atrial focal or reentrant activation as the mechanism in atrial fibrillation. J Thorac Cardiovasc Surg. 2004;127:770-778.
28. Lee S, Sahadevan J, Khrestian CM, Cakulev I, Markowitz A, Waldo AL. Simultaneous Biatrial High-Density (510-512 Electrodes) Epicardial Mapping of Persistent and Long-Standing Persistent Atrial Fibrillation in Patients: New Insights Into the Mechanism of Its Maintenance. Circulation. 2015;132:2108-2117.
29. Lee S, Sahadevan J, Khrestian CM, Markowitz A, Waldo AL. Characterization of Foci and Breakthrough Sites During Persistent and Long-Standing Persistent Atrial Fibrillation in Patients: Studies Using High-Density (510-512 Electrodes) Biatrial Epicardial Mapping. J Am Heart Assoc. 2017;6:e005274.

17

English Summary

Chapter 1 introduces atrial fibrillation which is the most common heart rhythm disorder in the world that is associated with life-threatening long-term complications. Treatment strategies for atrial fibrillation often fail and atrial fibrillation runs a progressive course in a quarter of patients. One important cause is the inability to determine the electrophysiological mechanism in individual patients. This thesis focusses on 1) new techniques to identify conduction disorders of the heart with a high resolution, 2) the presence of differences in electrical conduction during a normal heart rhythm between different patient groups and areas of the atria, 3) the implication and value of complex electrical signals, and 4) asynchronous activation of the inner and outer layers of the atrial wall and the role it potentially has in the pathophysiology of atrial fibrillation.

In **Chapter 2** is explained that currently the only curative treatment for atrial fibrillation is electrical isolation of the pulmonary veins. However, a single ablative treatment is often not successful and in many cases conduction from the pulmonary veins recovers. New ablation techniques are being developed to prevent reconduction such as visualization of the treated area during ablation as outlined by the commented article of Chapter 2. In some patients, despite optimal isolation of the pulmonary veins, atrial fibrillation still recurs. At this time, there is no proven effective subsequent therapy when isolation of the pulmonary veins has been achieved. In order to effectively treat these patients, research into the underlying mechanism of atrial fibrillation is required.

To take the first step towards an individualized diagnosis and treatment plan for patients with atrial fibrillation, a new study was proposed in **Chapter 3**. There is a diversity of other heart diseases among patients with atrial fibrillation. Heart diseases such as coronary artery disease, valvular heart disease and congenital heart disease can all contribute to the occurrence of atrial fibrillation. Atrial myocardial scarring could occur in different predisposed locations of the atria depending on the underlying heart disease. Therefore, the cause and mechanism of atrial fibrillation could originate from different areas in the atria. In our research proposal, we use a high-resolution epicardial mapping approach to record atrial electrical conduction in patients during standard cardiac operation procedures. These patients are divided into 12 subgroups based on their underlying heart disorder and if they have a history of atrial fibrillation. Characteristics of electrical conduction and morphology of signals will be compared between these groups to find the differences that may lead to atrial fibrillation. A postoperative follow-up of five years will demonstrate early or late development of atrial fibrillation after surgery.

The mapping technique used for this study is a unique new approach of mapping. In **Chapter 4** the execution and experiences with this mapping approach are described in detail. In adult patients undergoing open-heart surgery a ribbon-shaped electrode-array is placed

on the atria during surgery just before cardiopulmonary bypass is started. This electrode array consists of 192 electrodes of 0.45 mm diameter and an interelectrode distance of 2 mm. The flexible array is fixed to a bendable steel spatula for stability. Then the array is placed on all accessible areas of the right and left atrium among which Bachmann's bundle. The areas are mapped following a schedule and anatomical landmarks. Unipolar electrograms are recorded from 192 spots at the atrium simultaneously during 5-10 seconds. When recordings are made of all areas of both atria, there are a minimal of 1728 unipolar electrograms recorded. Epicardial mapping is performed during sinus rhythm and atrial fibrillation. In case a patient is in sinus rhythm, atrial fibrillation is induced by high-rate atrial burst pacing using a pacemaker. In case a patient is in atrial fibrillation, sinus rhythm is restored by electrical cardioversion after mapping of atrial fibrillation. In 168 patients, the mapping procedure and preparations took 9±2 minutes and no complications were observed.

The surgical techniques for patients requiring cardiac surgery are still in development and cardiac surgical procedures are increasingly performed with minimally invasive techniques. Minimally invasive cardiac surgery uses small openings between the ribs instead of a long incision and a sternotomy. Patients with mitral valve disease are nowadays more often operated minimally invasively and are known to have a high incidence of atrial fibrillation. In **Chapter 5** we present three cases in which we performed our high-resolution mapping approach who underwent minimally invasive mitral valve surgery. The electrode array fixed on the steel spatula was introduced via a lateral mini-thoracotomy incision of 4-5 cm in the intercostal space on the right side of the chest. The right atrium and Bachmann's bundle were easily accessible for mapping. The left atrium was more challenging to reach and not all areas were able to be reached. The left atrial appendage was accessed by sliding the array past Bachmann's bundle. The posterior left atrium beneath the inferior pulmonary veins was reached in one patient. An additional incision on the left chest side could possibly offer better access to the left atrium for epicardial mapping during minimally invasive surgery. This study has shown that epicardial high-resolution mapping with good quality electrograms can also be performed during minimally invasive cardiac surgery. Epicardial mapping via minimally invasive procedures offers future possibilities for patients with atrial fibrillation who do not require cardiac surgery for other heart diseases.

The incidence of atrial fibrillation in patients with mitral valve disease is between 25-50% and much more frequent than in patients with aortic valve disease. Atrial fibrillation incidence in patients with aortic valve disease is around 12%. The stretch of the left atrium is larger in mitral valve insufficiency than in patients with an aortic valve insufficiency or stenosis. Likely, this causes more damage of atrial tissue which leads to atrial fibrillation. Therefore, we analyzed in **Chapter 6** if patients with mitral valve disease have more areas

of conduction delay and block during sinus rhythm than patients with aortic valve disease and if there were predilection areas for conduction disorders. The extent of conduction disorders on the right and left atrium and Bachmann's bundle was studied in 85 patients with aorta valve stenosis or insufficiency and 54 patients with mitral valve insufficiency. We used our high-resolution mapping approach to quantify conduction disorders. Both groups demonstrated various degrees of conduction disorders throughout the atria. Most conduction disorders were observed at the superior right atrium, the area of the sinus node. Patients with mitral valve disease more often presented with conduction disorders at the lateral left atrium and left atrial appendage. The 38 patients with a history of atrial fibrillation, however, had more conduction disorders at Bachmann's bundle.

Conduction disorders at Bachmann's bundle during sinus rhythm are further explored in **Chapter 7**. In 304 patients, of which 193 with coronary artery disease and 11 with valvular heart disease, activation patterns were analyzed and the length of lines with conduction disorders were quantified. No differences were observed in conducting disorders at Bachmann's bundle between patients with coronary artery disease and valvular heart disease. Patients in whom Bachmann's bundle was (also) activated from the center of the bundle more often had a history of atrial fibrillation. In addition, the absence of both central activation and long lines ≥12 mm with interrupted electrical conduction was highly sensitive for the absence of atrial fibrillation. Therefore, conduction disorders and activation patterns at Bachmann's bundle were not associated with the underlying heart disease but with atrial fibrillation.

The pulmonary vein area is also known as a potential arrhythmogenic area for atrial fibrillation. Scarring of the posterior wall of the left atrium where the pulmonary veins exit is associated with recurrence of atrial fibrillation after isolation of the pulmonary veins. The conduction disorders in this area during sinus rhythm and the relation to persistent atrial fibrillation were analyzed in **Chapter 8**. High-resolution epicardial mapping of the posterior left wall was performed in 268 patients with coronary artery disease or valvular heart disease. The 49 patients with a history of atrial fibrillation had more uninterrupted lines and long lines >6 mm of conduction disorders between the pulmonary veins. The extent and distribution of conduction disorders did not differ between patients with paroxysmal or persistent atrial fibrillation. Although conduction disorders are more frequently present during sinus rhythm in patients with atrial fibrillation, the relation to atrial fibrillation, whether they are a symptom or a contributor, remains unclear.

Spontaneous electrical impulses originating from the pulmonary veins are known as the most important cause for triggering paroxysmal atrial fibrillation. However, the underlying mechanism for persistent atrial fibrillation remains unclear. A new discovery in **Chapter 9**

is a potential mechanism for persistence of atrial fibrillation. It was demonstrated in 14 patients that the atrial wall is asynchronously activated during atrial fibrillation. Electrograms were recorded on both the epicardial (outer) and endocardial (inner) side during surgery for this study. One of two identical electrode-arrays was introduced in the right atrium and placed on the endocardial wall via the incision made for cardiopulmonary bypass. All patients had atrial fibrillation during recording, either spontaneous or induced with a pacemaker. The activation times between 128 opposite electrograms were compared. Endo-epicardial asynchrony of the right atrial wall varied between 0.9-55.9% during atrial fibrillation. Patients with longstanding persistent atrial fibrillation all had asynchrony of >20%. Focal waves, waves originating in the middle of the mapping area, were observed frequently on both sides. Those focal waves were in 65% preceded by a wave passing by on the other side. The majority of focal waves could thus be attributed to transmural conduction of a wave traveling on the other side. Asynchronous activation of the epicardial and endocardial atrial layers give opportunity for waves to travel from one side to the other and creating new breakthrough waves causing atrial fibrillation to persist.

In **Chapter 10** a case is presented demonstrating the dynamic of focal waves during atrial fibrillation. Simultaneous endo-epicardial mapping was performed in a 63-year-old patient with mitral valve and tricuspid valve insufficiency and longstanding persistent atrial fibrillation. Focal waves appeared equally frequent on both the epicardial and endocardial side, respectively 59 and 53 times, during 10 seconds of atrial fibrillation. Most focal waves appeared on a random location without a fixed pattern or timing between the focal waves. This observation decreases the likelihood of focal waves being caused by a rotor or ectopic focus. This random behavior of focal waves better suits the theory of endo-epicardial asynchrony and transmural conduction of atrial fibrillation waves being the source for focal waves as described in chapter 9.

One of the additional treatments developed for persistent atrial fibrillation after isolation of the pulmonary veins is ablation of complex fractionated atrial electrograms (CFAEs). These electrograms consist of signals with multiple deflections that could represent areas with conduction disorders. However, there are also other pathophysiological causes for these electrograms and definitions used for CFAE differ between studies. **Chapter 11** describes a literary search, firstly, to provide an overview of the pathophysiological causes of electrogram fractionation. Both pathological and non-pathological causes of fractionation of electrograms have been identified. Secondly, a systemic literature search was performed to the definitions for CFAE that have been used over the years. Large differences existed between studies: 11 visual definitions for CFAE, 3 automatic detection programs for CFAE and 7 different parameters to describe CFAE. Because fractionation does not always have

a pathological origin, a clear method to identify pathological fractionation needs to be developed before CFAE locations are (unnecessarily) targeted during ablation.

The morphologic properties of electrograms such as fractionation are thus being used to identify areas to target during ablation. However, in chapter 9 the asynchronicity between the epicardial and endocardial atrial side was described signifying that differences in epicardial and endocardial electrograms occur regularly. The morphology of epicardial and endocardial electrograms were compared during sinus rhythm in **Chapter 12**. Furthermore, asynchronous activation of the atrial wall as cause for fractionation was analyzed. Most fractionation during sinus rhythm was similar between both sides, incidentally signals up to 4 mV were absent at the opposite electrogram. The large majority (95%) of additional deflections (fractionation) observed on unipolar electrograms could be attributed to remote electrical activation. Asynchronous activation was the cause in 4% of those additional deflections. Although differences in epicardial and endocardial fractionation occur only incidentally during sinus rhythm, they will likely increase during atrial fibrillation due to increase of asynchrony and smaller waves. An important finding in this study is that endo-epicardial asynchrony can reflect on the electrogram on the opposite side.

In **Chapter 13**, the consequences of endo-epicardial asynchrony during atrial fibrillation are described and a study is reviewed that demonstrated that asynchrony can also be important in the persistence of an atrial flutter. The significance of endo-epicardial asynchrony in the pathophysiology of heart rhythm disorders requires further investigation, however, there is a major limitation. During most electrophysiological procedures electrograms can only be recorded from one side of the atrial wall. Fortunately, it was discovered in chapter 12 that the morphology of unipolar electrograms contain information about the state of the neighboring tissue and with that the presence of asynchrony. This is a possible method to indirectly measure asynchrony when only recording from one side.

However, bipolar electrograms are mostly used in current clinical practice. If bipolar electrograms are equally suitable for identifying asynchrony via fractionation is studied in **Chapter 14**. Unipolar electrograms of areas with endo-epicardial asynchrony were converted to bipolar electrograms in two directions of the array (x and y). Two investigators independently labelled all fractionation on the unipolar and bipolar electrograms. Presence of fractionation corresponding to atrial activation on the opposite side (asynchrony) was identified. Fractionation corresponding to asynchrony was equally present on both unipolar as bipolar electrograms. Nineteen of 22 patients demonstrated fractionation based on asynchrony. However, this fractionation was easier to distinguish from the noise on unipolar electrograms than on bipolar electrograms in the y-direction. In addition, more additional fractionation was observed on bipolar electrograms in the x-direction

than on unipolar electrograms which makes it harder to identify fractionation caused by asynchrony. Unipolar electrograms are therefore more suited to detect endo-epicardial asynchrony based on fractionation.

Endo-epicardial asynchrony does not only have a possible role in persistent atrial fibrillation, but also in triggering atrial fibrillation which is investigated in **Chapter 15**. Most atrial fibrillation episodes are preceded by an atrial extrasystole. These arise spontaneously in the atria, mostly the pulmonary veins, and result in increased conduction disorders due to their prematurity or different atrial origin. Sixty atrial extrasystoles from 23 patients were examined for differences in degree of endo-epicardial asynchrony compared to sinus rhythm. Endo-epicardial asynchrony increased in atrial extra systoles. One of the possible causes is increased inequality in the total amount of conduction disorders in the epicardial vs endocardial plane. Maximal time difference between the epicardial and endocardial layers during an atrial extrasystole was 130 ms. Under the right circumstances, this extent of asynchrony could trigger an arrhythmia.

18

Nederlandse Samenvatting

De achtergrond van het ziektebeeld atriumfibrilleren (boezemfibrilleren) wordt ingeleid in **Hoofdstuk 1**. Hier wordt toegelicht dat atriumfibrilleren de meest voorkomende hartritmestoornis is die ook ernstige complicaties op de lange termijn kan hebben. De behandelmogelijkheden falen regelmatig en de ziekte heeft in een kwart van de patiënten een progressief beloop. Een belangrijke oorzaak is dat het mechanisme van atriumfibrilleren nog niet goed vastgesteld kan worden bij de individuele patiënt. Dit proefschrift richt zich op 1) nieuwe technieken om geleidingsstoornissen van het hart vast te kunnen stellen met een hoge resolutie, 2) aanwezigheid van verschillen in elektrische geleiding tijdens het normale hartritme tussen patiëntgroepen en gebieden van de hartboezems, 3) de betekenis en waarde van complexe elektrische signalen en 4) asynchrone activatie van de binnenste en buitenste laag van de boezemwand en de rol die dit mogelijk heeft in de pathofysiologie van atriumfibrilleren.

In **Hoofdstuk 2** wordt beschreven dat op dit moment de enige mogelijkheid voor het curatief behandelen van atriumfibrilleren bestaat uit het elektrisch isoleren van de pulmonaal venen door middel van ablatie. Vaak is één behandeling echter niet genoeg en komt het regelmatig voor dat de geleiding vanaf de pulmonaal venen zich hersteld. Er worden nog steeds nieuwe ablatie technieken voor de pulmonaal venen ontwikkeld zoals het visualiseren van het behandelde gebied tijdens de ablatie om te voorkomen dat de geleiding zich hersteld. Echter bij een deel van de patiënten komt atriumfibrilleren toch terug ondanks dat de pulmonaal venen goed zijn geïsoleerd. Op dit moment bestaat voor deze patiënten nog geen bewezen effectieve vervolg behandeling na pulmonaal venen isolatie. Hiervoor moet eerst worden onderzocht wat het onderliggende mechanisme van atriumfibrilleren is bij deze patiënten.

Om de eerste stap te zetten voor de individualisering van de diagnose en behandeling voor patiënten met atriumfibrilleren, wordt in **Hoofdstuk 3** een nieuw onderzoeksvoorstel gedaan. Patiënten met atriumfibrilleren kunnen een diversiteit van andere onderliggende hartziekten hebben. Hartziekten zoals kransslagaderlijden, hartklepafwijkingen en aangeboren hartaandoeningen kunnen allen bijdragen aan het ontstaan van boezemfibrilleren. De schade aan het hartweefsel zou bij deze verschillende hartaandoeningen op andere (voorkeurs)plaatsen in de boezems kunnen optreden. Hierdoor kan de oorzaak en mechanisme van atriumfibrilleren op andere plekken in de boezems liggen. In dit onderzoeksvoorstel wordt gebruik gemaakt van een hoge resolutie epicardiale mapping methode om bij patiënten die een hartoperatie ondergaan de elektrische geleiding van de boezems te meten tijdens de operatie. Deze patiënten worden in 12 groepen verdeeld op basis van hun onderliggende hartziekte(n) en of zij in hun voorgeschiedenis atriumfibrilleren hebben gehad. Deze groepen worden met elkaar vergeleken om zo te zien waar de verschillen zitten in de elektrische geleiding en de morfologie van de elektrische signalen

die mogelijk in verband kunnen worden gebracht met het ontstaan van atriumfibrilleren. Na de operatie worden de patiënten 5 jaar opgevolgd om te zien of zij vroeg of laat na de operatie atriumfibrilleren ontwikkelen.

De epicardiale mapping techniek die voor deze studie wordt toegepast is een unieke, nieuwe methode van mapping. In **Hoofdstuk 4** wordt de uitvoering en onze ervaringen met het gebruik van deze techniek in detail beschreven. Bij volwassen patiënten die een openhartoperatie ondergaan wordt tijdens de operatie, net voordat zij aan de hartlong-machine gaan, een lint-elektrode op de boezems gelegd. Deze lint-elektrode bestaat uit een array van totaal 192 elektrodes van 0.45 mm groot met een afstand van 2 mm tussen de elektrodes. De flexibele lint-elektrode wordt gebonden op een stalen buigzame spatel voor stevigheid. Vervolgens wordt de elektrode op alle bereikbare plekken van de linker- en rechterboezem gelegd, waaronder ook de bundel van Bachmann. Dit wordt gedaan volgens een vast schema met anatomische oriëntatiepunten. Gedurende 5 tot 10 seconden worden op 192-plaatsen gelijktijdig unipolaire elektrische signalen (elektrogrammen) van de boezem gemeten. Als de elektrode op alle plaatsen van beide boezems is gelegd, zijn er op minimaal 1728 plekken unipolaire elektrogrammen met boezemsignalen opgenomen. Epicardiale mapping wordt tijdens sinusritme en atriumfibrilleren uitgevoerd. Indien nodig wordt met behulp van een pacemaker die met hoge frequentie de boezems stimuleert atriumfibrilleren geïnduceerd tijdens de operatie. Patiënten die atriumfibrilleren hebben bij aanvang van de operatie worden elektrisch gecardioverteerd naar sinusritme na mapping van atriumfibrilleren. In de 168 patiënten waarbij deze techniek is uitgevoerd in dit hoofdstuk duurde de gehele epicardiale mapping procedure inclusief voorbereidingen 9±2 minuten en waren er geen complicaties.

De chirurgische technieken voor hartpatiënten zijn volop in ontwikkeling en steeds meer operaties worden niet meer via een ‘openhart’ procedure uitgevoerd maar via minimaal invasieve technieken. Hierbij wordt, zoals bij een kijkoperatie, gebruik gemaakt van kleine openingen in de borstkas om de operatie uit te voeren in plaats van het openzagen van het borstbeen. Een patiëntengroep waarbij veel atriumfibrilleren voorkomt die steeds vaker minimaal invasief worden geopereerd zijn patiënten met mitraliskleplijden. Dat ook tijdens deze operaties onze epicardiale mapping techniek kan worden toegepast wordt gedemonstreerd bij 3 patiënten in **Hoofdstuk 5.** De elektrode gebonden op de spatel wordt ingebracht via de laterale mini-thoracotomie snede van 4-5 cm tussen de ribben aan de rechterzijde van de borstkas. De rechterboezem en de bundel van Bachmann zijn vanuit hier goed bereikbaar, maar de linkerboezem was niet geheel bereikbaar. Het linkerhartoor was wel bereikbaar door de elektrode voorbij de bundel van Bachmann door te schuiven. De achterwand van de linkerboezem onder de pulmonaal venen was in één patiënt bereikbaar. Een extra toegang via de borstkas aan de linkerzijde zou mogelijk een

uitkomst bieden voor het bereiken van de linkerboezem in de toekomst. De studie heeft laten zien dat ook bij minimaal invasieve operaties epicardiale mapping met een hoge resolutie en hoge signaalkwaliteit haalbaar is. Daarnaast is epicardiale hoge resolutie mapping via minimaal invasieve methoden ook in de toekomst toegankelijker voor de vele patiënten met atriumfibrilleren die geen openhartoperatie hoeven ondergaan.

De incidentie van atriumfibrilleren bij patiënten met mitraliskleplijden ligt tussen de 25-50%. Dit is ruim hoger dan bij patiënten met aortakleplijden, de andere meest voorkomende hartklepafwijking. Bij aortaklepafwijkingen komt atriumfibrilleren voor bij ongeveer 12% van de patiënten. De rek op de linkerboezem is bij een lekkende mitralisklep groter dan bij patiënten met een lekkende of vernauwde aortaklep. Hierdoor ontstaat waarschijnlijk meer schade in het hartspierweefsel van de boezems wat kan leiden tot atriumfibrilleren. In **Hoofdstuk 6** werd onderzocht of patiënten met mitraliskleplijden meer vertraging van de elektrische geleiding hebben tijdens sinusritme dan patiënten met aortakleplijden en of er voorkeurslocaties waren voor geleidingsstoornissen. In 85 patiënten met aortaklepstenose of –insufficiëntie en 54 patiënten met mitralisklep insufficiëntie werd de mate van geleidingsstoornissen op de hele oppervlakte van beide boezems onderzocht. Hierbij werd opnieuw gebruik gemaakt van de epicardiale mapping techniek met een hoge resolutie welke kleine geleidingsstoornissen kan opsporen. Tijdens sinusritme waren er in beide groepen in verschillende mate geleidingsstoornissen aanwezig verspreid over de hele boezems. De meeste geleidingsstoornissen zaten in het bovenste deel van de rechterboezem, in het gebied van de sinusknoop. Patiënten met mitraliskleplijden hadden vaker geleidingsstoornissen aan de zijkant van de linkerboezem waaronder het linker hartoor. Bij de 38 patiënten uit beide groepen met een voorgeschiedenis van atriumfibrilleren werden juist vaker geleidingsstoornissen gezien op de bundel van Bachmann.

In **Hoofdstuk 7** is de geleiding op de bundel van Bachmann tijdens sinusritme verder geanalyseerd bij patiënten met kransslagaderlijden en/of hartklepafwijkingen en het verband op de aanwezigheid van atriumfibrilleren. Bij 304 patiënten waarvan 193 met ischemische hartziekte en 111 met hartklepafwijkingen werd gekeken naar het activatiepatroon van de bundel van Bachmann en de lengte en aantal lijnen die de elektrische geleiding verstoorden. Geleidingsstoornissen op de bundel van Bachmann kwamen bij patiënten met kransslagaderlijden en hartklepafwijkingen evenveel voor. Patiënten waarbij de bundel van Bachmann (ook) vanuit het midden van de bundel werd geactiveerd hadden vaker een voorgeschiedenis van atriumfibrilleren. In dit onderzoek bleek dat de afwezigheid van activatie vanuit het midden en een lange lijn ≥12 mm met onderbroken geleiding erg voorspellend (90%) was voor de afwezigheid van atriumfibrilleren. Geleidingstoornissen

en het activatiepatroon op de bundel van Bachmann zijn dus niet geassocieerd met de onderliggende hartziekte maar wel met aanwezigheid van atriumfibrilleren.

Naast de bundel van Bachmann staat ook het pulmonaal venen gebied als een potentieel belangrijk gebied voor atriumfibrilleren. Verlittekening van de achterwand van de linkerboezem waar de pulmonaalvenen uitmonden is geassocieerd met een hogere recidief kans van atriumfibrilleren na ablatie van de pulmonaalvenen zelf. In **Hoofdstuk 8** hebben we de geleidingsstoornissen in dit gebied onderzocht en de relatie tot persistentie van het atriumfibrilleren. Hiervoor is er tijdens sinusritme hoge resolutie mapping verricht van de achterwand tussen de pulmonaal venen bij 268 patiënten met kransslagaderlijden en/of hartklepafwijkingen. Van deze patiënten waren er 49 bekend met atriumfibrilleren. Deze patiënten met atriumfibrilleren hadden meer aaneengesloten lijnen van geleidingsstoornissen en meer lange lijnen >6 mm van gestoorde geleiding tussen de pulmonaalvenen. Er werd geen verschil gezien in de mate of verdeling van geleidingsstoornissen tussen patiënten met paroxismaal of persistent atriumfibrilleren. Hoewel er dus duidelijk meer geleidingsstoornissen aanwezig zijn tijdens sinusritme bij patiënten met atriumfibrilleren, is het nog onduidelijk wat het verband is met atriumfibrilleren. Het kan slechts een uiting zijn van de ziekte of een mede-veroorzaker.

De spontane elektrische impulsen die ontstaan *in* de pulmonaalvenen staan al enkele jaren bekend als de belangrijkste oorzaak achter het opstarten van paroxismaal atriumfibrilleren. Maar het elektrische mechanisme die het persisteren van atriumfibrilleren veroorzaakt is nog niet precies bekend. In **Hoofdstuk 9** wordt een nieuwe bevinding beschreven die een mogelijke verklaring hiervoor biedt. Bij 14 patiënten is aangetoond dat tijdens (geïnduceerd) atriumfibrilleren de boezemwand asynchroon wordt geactiveerd. Om dit te kunnen doen zijn tijdens de operatie elektrische signalen van de rechterboezem aan de epicardiale (buiten-) zijde en de endocardiale (binnen-) zijde tegelijkertijd gemeten. Eén van twee identieke elektrode-arrays werd tegen de binnenzijde van de rechterboezem gelegd via een snede in het rechterhartoor die werd gemaakt voor het aansluiten van de hartlongmachine. De activatietijden tussen de 128 paar tegenoverliggende epicardiale en endocardiale elektrogrammen werden met elkaar vergeleken. De mate van endo-epicardiale asynchrone activatie van de rechterboezem tijdens atriumfibrilleren varieerde tussen de 0.9-55.9%. Patiënten met langdurig persisterend atriumfibrilleren hadden allen >20% asynchrone activatie. Er werden ook frequent focale golven gezien aan beide kanten; golven die middenin het mapping-gebied ontstaan. In 65% van de gevallen werd gezien dat een focale golf aan de ene zijde vooraf werd gegaan door een golf die voorbij kwam aan de andere zijde. Focale golven konden dus in de meerderheid worden verklaard door transmurale geleiding van een golf van de ene naar de andere zijde. De asynchrone activatie van de epicardiale en endocardiale laag van de boezems geeft ruimte voor golven om

van de ene naar de andere zijde te geleiden en daar nieuwe golven te creëren, waardoor atriumfibrilleren kan blijven doorgaan.

In **Hoofdstuk 10** wordt een casus gepresenteerd waarbij de dynamiek van focale golven tijdens atriumfibrilleren wordt gedemonstreerd. Er was endo-epicardiale mapping verricht in een 63-jarige patiënte met mitralis- en tricuspidalisinsufficiëntie en langdurig persisterend atriumfibrilleren. Focale golven verschenen even vaak aan zowel de epicardiale als endocardiale zijde, respectievelijk 59 en 53 keer, gedurende 10 seconden atriumfibrilleren. Daarbij verschenen de meeste op een willekeurige locatie zonder vast patroon of vaste tijdsduur tussen de focale golven. Deze bevinding maakt het minder waarschijnlijk dat focale golven worden veroorzaakt door een mechanisme zoals een rotor of een ectopisch focus. Het willekeurig verschijnen van deze golven past beter bij het mechanisme van endo-epicardiale asynchronie en transmurale geleiding van atriumfibrillatie-golven zoals beschreven in hoofdstuk 9.

Eén van de behandelingen die is toegepast als aanvulling op pulmonaalvenen isolatie ter voorkomen van recidieven van atriumfibrilleren, is het ableren van complex gefractioneerde atriale elektrogrammen (CFAEs). Deze elektrogrammen bestaan uit signalen met meerdere deflecties die kunnen wijzen op gebieden met geleidingsstoornissen. Alleen zijn er ook andere pathofysiologische oorzaken voor deze elektrogrammen en de definities gebruikt voor CFAE verschillen tussen studies. Er is daarom in **Hoofdstuk 11** een literatuurstudie gedaan waarin eerst een overzicht is geven van de oorzaken van elektrogram fractionatie. Er wordt beschreven dat er zowel pathologische als niet-pathologische oorzaken zijn voor fractionatie van elektrogrammen. Daarnaast is er op een systematische wijze gezocht naar de definities voor CFAE die de afgelopen jaren zijn gebruikt. Er werden grote verschillen onder studies gevonden voor het bepalen van fractionatie: 11 visuele definities voor CFAE, 3 verschillende automatische detectie programma's voor CFAE en 7 verschillende parameters om CFAE te omschrijven. Voordat er (onnodig) op plaatsen van CFAE een ablatie behandeling wordt toepassen, moet eerst duidelijk worden hoe we pathologische fractionatie kunnen identificeren.

De morfologische eigenschappen van elektrogrammen zoals fractionatie (CFAE) worden dus gebruikt voor het identificeren van gebieden om te ableren. Echter in hoofdstuk 9 is gezien dat de activatie van het epicardiale en endocardiale zijde van de boezem niet altijd synchroon plaatsvindt. Er zijn dus verschillen tussen meten van electrogrammen aan de binnenzijde en buitenzijde van het hart. In **Hoofdstuk 12** is de epicardiale en endocardiale morfologie van atriale signalen op 16.954 unipolaire elektrogrammen van 26 patiënten met elkaar vergeleken tijdens sinusritme. Ook is er onderzocht of asynchrone activatie van de boezemwand fractionatie kan veroorzaken. Voor het grootste deel kwam fractionatie

aan beide zijde overeen tijdens sinusritme, in incidentele gevallen waren er signalen tot 4 mV die niet werden gezien op dezelfde plek aan de andere zijde. De grote meerderheid (95%) van de extra deflecties (fractionatie) gezien op unipolaire elektrogrammen kon worden toegeschreven aan elektrische activatie in de omgeving. Hiervan bestond 4% uit asynchrone activatie aan de tegenoverliggende zijde. Hoewel verschillen in fractionatie tussen de epicardiale en endocardiale zijde dus maar weinig voorkomen tijdens sinusritme, zullen deze waarschijnlijk toenemen tijdens atriumfibrilleren door de toename van asynchronie en kleinere golven. Een belangrijke bevinding in deze studie is dat asynchronie weerspiegeld kan zijn op het electrogram aan de andere zijde.

De gevolgen die endo-epicardiale asynchronie kan hebben tijdens atriumfibrilleren wordt verder toegelicht in **Hoofdstuk 13**. Er wordt ook een studie besproken waarin is aangetoond dat asynchronie ook een rol kan hebben bij het onderhouden van een andere hartritmestoornis; een atriumflutter. Het is daarom van belang de betekenis van endo-epicardiale asynchronie in de pathofysiologie van hartritmestoornissen verder te onderzoeken. Maar is er ook een grote hindernis: tijdens de meeste elektrofysiologische onderzoeken kan er maar aan één kant van het hart worden gemeten. In hoofdstuk 12 is echter gezien dat de morfologie van unipolaire elektrogrammen informatie bevat over wat er gebeurd in de omgeving en daarbij de aanwezigheid van asynchronie. Dit is een mogelijke methode om asynchronie indirect te meten wanneer er maar aan één zijde signalen worden gemeten.

In de klinische praktijk wordt er daarentegen voornamelijk gebruik gemaakt van bipolaire elektrogrammen. Of bipolaire elektrogrammen even geschikt zijn voor het aantonen van asynchronie door middel van fractionatie als unipolaire elektrogrammen is onderzocht in **Hoofdstuk 14**. Unipolaire elektrogrammen van gebieden met endo-epicardiale asynchronie werden omgezet naar bipolaire elektrogrammen in twee verschillende richtingen (x en y). Twee onderzoekers markeerde onafhankelijk van elkaar handmatig alle fractionatie op de unipolaire en bipolaire elektrogrammen. Vervolgens werd gezocht naar fractionatie die overeenkwam met het moment van activatie aan de andere zijde (asynchronie). Fractionatie overeenkomend met asynchronie kwam even vaak voor op unipolaire als bipolaire elektrogrammen. Bij 19 van de 20 patiënten was fractionatie gebaseerd op asynchronie aanwezig. Alleen was deze fractionatie op bipolaire elektrogrammen in de y-richting aan de endocardiale zijde minder goed te onderscheiden van de ruis dan op unipolaire elektrogrammen. Daarnaast was er meer extra fractionatie aanwezig op bipolaire elektrogrammen in de x-richting dan op unipolaire elektrogrammen, waardoor het onderscheiden van fractionatie door asynchronie lastiger wordt. Unipolaire elektrogrammen zijn hierdoor meer geschikt voor het detecteren van endo-epicardiale asynchronie op basis van fractionatie.

Naast een rol bij het persisteren van atriumfibrilleren is endo-epicardiale asynchronie ook een mogelijk mechanisme voor het opstarten van atriumfibrilleren, dit wordt onderzocht in **Hoofdstuk 15**. De meeste episodes van atriumfibrilleren worden voorafgegaan door een atriale extra slag. Deze ontstaan spontaan in de boezems, meestal in de pulmonaal venen, en zorgen voor meer geleidingsstoornissen doordat ze vroeger komen of vanuit een andere plek dan bij sinusritme. In deze studie werden in 23 patiënten 60 atriale extra slagen onderzocht op de mate van endo-epicardiale asynchronie in vergelijking tot sinusritme. Tijdens atriale extra slagen was er meer endo-epicardiale asynchronie aanwezig was dan tijdens sinusritme slagen. Eén van de mogelijke oorzaken hiervoor was dat er een grotere ongelijkheid was in het aantal geleidingsstoornissen in het endocardiale vlak ten opzichte van het epicardiale vlak tijdens atriale extra slagen. Het maximale tijdsverschil tussen de epicardiale en endocardiale laag dat werd geobserveerd tijdens een atriale extra slag was 130 ms. Onder de juiste omstandigheden zou deze mate van asynchronie tijdens een atriale extra slag kunnen leiden tot het opstarten van een hartritmestoornis.

19

Appendices

ENDO–EPICARDIAL DISSOCIATION IN CONDUCTION

Lisette van der Does, Charles Kik, Maurits Allessie, Natasja de Groot

Cardiovascular Flashlight. Eur Heart J. 2016;38:1775.

The online video* shows 40 successive, simultaneous epicardial (left) and endocardial (right) wavemaps of the right atrial free wall constructed during 5 s (40 times slowed down) of longstanding persistent atrial fibrillation (LSPAF) obtained from a 70-year-old female patient who underwent cardiac surgery for severe tricuspid and mitral valve insufficiency. Mapping was performed with a high-resolution endo–epicardial clamp consisting of two identical rectangular electrode arrays of 8 × 16 electrodes (interelectrode distance 2 mm) precisely positioned opposite to each other. Wavemaps are generated by previously described computer algorithms and show areas activated by individual fibrillation waves; the territories of the waves are demarcated by colors according to their sequence of appearance. Fibrillation waves do not only enter the mapping area from the border of the electrode array, but they also emerge frequently in the middle. Significant differences in endocardial and epicardial activation time are present throughout the entire recording period. In map 14, for example, activation time differences in the lower part of the mapping area vary between 41 and 71 ms. In addition, the direction of activation can also be different between the endocardial and epicardial layer. In Figure 1, the middle part of the epicardial mapping area is activated by a wave front propagating from the right to the left, whereas the same area on the endocardial surface was earlier activated by a fibrillation wave traversing from the bottom to the top of the mapping array. Hence, this video clearly shows the presence of endo–epicardial dissociation during LSPAF.

*https://doi.org/10.1093/eurheartj/ehw245

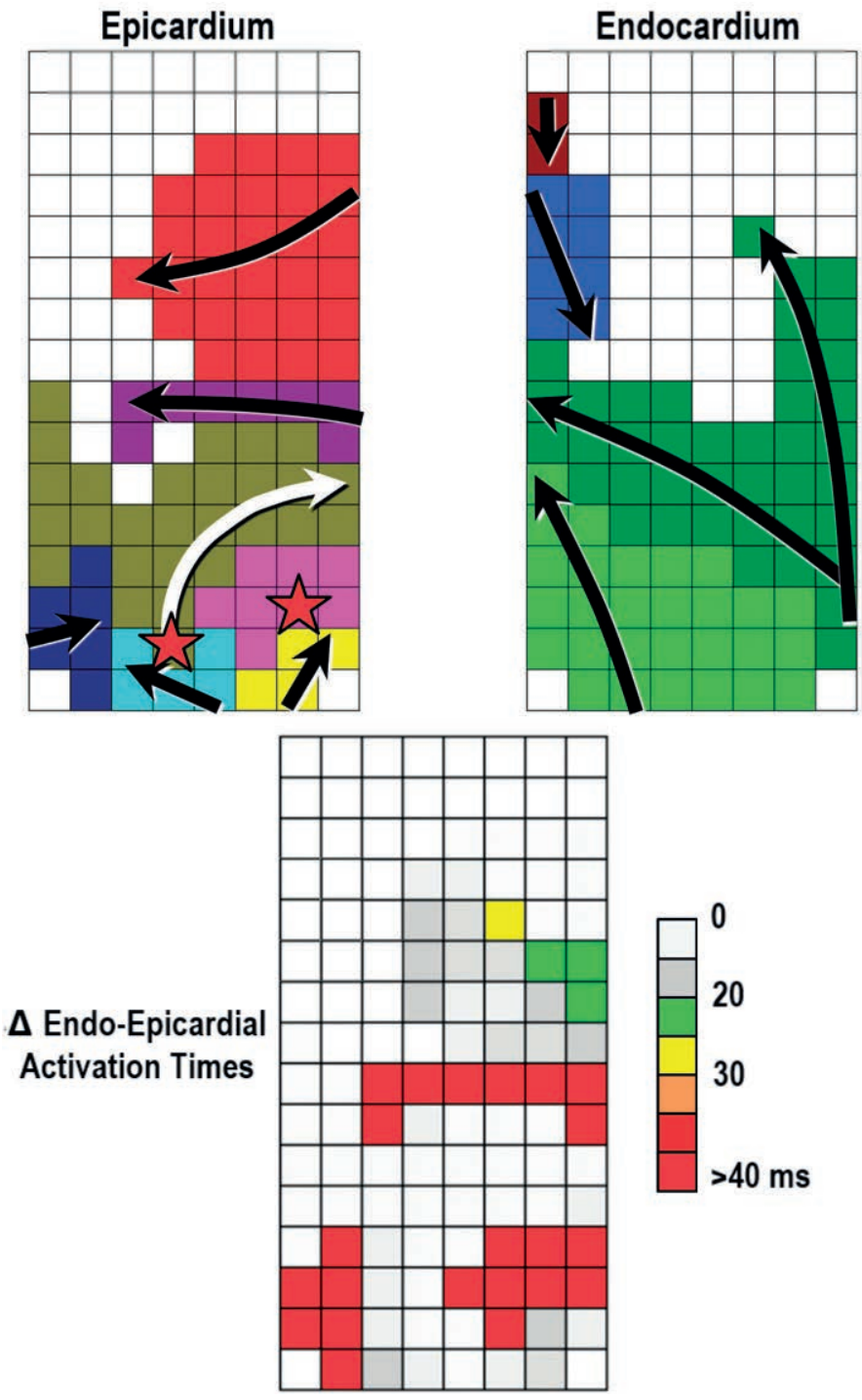

Figure 1. Black arrows illustrate the main direction of conduction. Red stars indicate focal fibrillation waves.

LIST OF ABBREVIATIONS

AAD	Antiarrhythmic Drugs
AF	Atrial Fibrillation
AFCL	Atrial Fibrillation Cycle Length
AV	Aortic Valve
BB	Bachmann's Bundle
CABG	Coronary Artery Bypass Grafting
CA	Conduction Abnormalities
CB	Conduction Block
CD	Conduction Delay
CFAE	Complex Fractionated Atrial Electrograms
CHD	Congenital Heart Disease
EAS	Endoscopic laser balloon Ablation System
ECG	Electrocardiogram
EEA	Endo-Epicardial Asynchrony
EEB	Endo-Epicardial Breakthrough
FU	Follow Up
ICI	InterCaval Inferior
ICF	Informed Consent Form
ICS	InterCaval Superior
IHD	Ischemic Heart Disease
IQR	Inter Quartile Range
LA	Left Atrium
LAA	Left Atrial Appendage
LLA	Lateral Left Atrium
LVF	Left Ventricular Function
MV	Mitral Valve
PLA	Posterior Left Atrium
PV	Pulmonary Veins
PVI	Pulmonary Vein Isolation
PVL	Left Pulmonary Veins
PVR	Right Pulmonary Veins
RA	Right Atrium
RAA	Right Atrial Appendage
RAI	Right Appendage Inferior
RAS	Right Appendage Superior
RV	Right Ventricle
SR	Sinus Rhythm

VCI	Vena Cava Inferior
VCS	Vena Cava Superior
VHD	Valvular Heart Disease

LIST OF PUBLICATIONS

* co-first authorship

1. Atrial Ectopy Increases Asynchronous Activation of the Endo- and Epicardium at the Right Atrium.
   van der Does LJME, Kharbanda RK, Teuwen CP, Knops P, Kik C, Bogers AJJC, de Groot NMS. J Clin Med. 2020;18:E558.

2. The Effects of Valvular Heart Disease on Atrial Conduction during Sinus Rhythm
   van der Does LJME, Lanters EAH, Teuwen CP, Mouws EJMP, Yaksh A, Knops P, Kik C, Bogers AJJC, de Groot NMS. J Cardiovasc Transl Res. 2020;13:632-639.

3. Unipolar atrial electrogram morphology from an epicardial and endocardial perspective.
   van der Does LJME, Knops P, Teuwen CP, Serban C, Starreveld R, Lanters EAH, Mouws EMJP, Kik C, Bogers AJJC, de Groot NMS. Heart Rhythm. 2018;15:879-887.

4. Epicardial atrial mapping during minimally invasive cardiothoracic surgery.
   van der Does LJME, Oei FBS, Knops P, Bogers AJJC, de Groot NMS. Interact Cardiovasc Thorac Surg. 2019;28:108-111.

5. Endo-epicardial breakthrough: A tale of 2 sides.
   van der Does LJME, de Groot NM. Heart Rhythm. 2017;14:1208-1209.

6. Inhomogeneity and complexity in defining fractionated electrograms.
   van der Does LJME, de Groot NM. Heart Rhythm. 2017;14:616-624.

7. Endo-epicardial dissociation in conduction.
   van der Does LJME, Kik C, Allessie MA, de Groot NMS. Eur Heart J. 2016;38:1775.

8. Direct Proof of Endo-Epicardial Asynchrony of the Atrial Wall During Atrial Fibrillation in Humans.
   de Groot NMS*, **van der Does LJME***, Yaksh A, Lanters EAH, Teuwen CP, Knops P, van de Woestijne PC, Bekkers JA, Kik C, Bogers AJJC, Allessie MA. Circ Arrhythm Electrophysiol. 2016;9:e003648.

9. QUest for the Arrhythmogenic Substrate of Atrial fibRillation in patients undergoing cardiac surgery (QUASAR study): rationale and design.
   van der Does LJME, Yaksh A, Kik C, Oei F, van de Woestijne P, Knops P, Lanters EAH, Teuwen CP, Bogers AJJC, Allessie MA, de groot NMS. J Cardiovasc Transl Res. 2016;9:194-201.

10. Dynamics of Endo- and Epicardial Focal Fibrillation Waves at the Right Atrium in a Patient with Advanced Atrial Remodelling.
    van der Does LJME, Kik C, Bogers AJJC, Allessie MA, de groot NMS. Can J Cardiol. 2016;32:1260.e19-1260.e21

11. A Novel Intra-Operative, High-Resolution Atrial Mapping Approach.
    Yaksh A*, **van der Does LJME***, Kik C, Knops P, Oei F, van de Woestijne PC, Bogers AJJC, Allessie MA, de groot NMS. J Interventional Card Electrophysiol. 2015;44:221-225.

12. A Genetic Predisposition for Lethal Arrhythmias: No Need for Preventive Treatment?
    van der Does LJME, Burghouwt DE, de Groot NMS. Am J Med Sci. 2015;350:340-341.

13. What's to come after isolation of the pulmonary veins?
    van der Does LJME, de Groot NM. Neth Heart J. 2015;23:94-5.

14. Anatomical hotspots of fractionated electrograms in the left and right atrium: do they exist?
    Starreveld R, **van der Does LJME**, de Groot NMS. Europace. 2019;21:60-72.

15. Pharmacological Therapy of Tachyarrhythmias During Pregnancy.
    Yaksh A, **van der Does LJME**, Lanters EAH, de Groot NMS. Arrhythm Electrophysiol Rev. 2016;5:41-44.

16. Right versus left atrial pacing in patients with sick sinus syndrome and paroxysmal atrial fibrillation (Riverleft study): study protocol for randomized controlled trial.
    Ramdjan TT, **van der Does LJME**, Knops P, Res JC, de Groot NMS. Trials. 2014;15:445.

17. A Rare Case of the Digenic Inheritance of Long QT Syndrome Type 2 and Type 6.
    Heida A, **van der Does LJME**, Ragab AAY, de Groot NMS. Case Rep Med. 2019:1384139.

18. Impact of the Arrhythmogenic Potential of Long Lines of Conduction Slowing at the Pulmonary Vein Area.
    Mouws EMJP, **van der Does LJME**, Kik C, Lanters EAH, Teuwen CP, Knops P, Bogers AJJC, de Groot NMS. Heart Rhythm. 2019;16:511-519.

19. Sinus Rhythm Conduction Properties Across Bachmann's Bundle: Impact of Underlying Heart Disease and Atrial Fibrillation.
    Teuwen CP, **van der Does LJME**, Kik C, Mouws EMJP, Lanters EAH, Knops P, Taverne Y, Bogers AJJC, de Groot NMS. J Clin Med. 2020;16;9:E1875.

20. Simultaneous Endo-Epicardial Mapping of the Human Right Atrium: Unraveling Atrial Excitation.
    Kharbanda RK, Knops P, **van der Does LJME**, Kik C, Taverne YJHJ, Roos-Serote MC, Heida A, Oei FBS, Bogers AJJC, de Groot NMS. J Am Heart Assoc. 2020;9:e017069.

21. Atrial Programmed Electrical Stimulation Techniques on Unipolar Electrogram Morphology.
    Knops P, Schram-Serban C, **van der Does LJME**, Croes M, Houben R, de Groot NMS. J Cardiovasc Electrophysiol. 2020;31:943-951.

22. Novel Insights in the Activation Patterns at the Pulmonary Vein Area.
    Mouws EMJP, Kik C, **van der Does LJME**, Lanters EAH, Teuwen CP, Knops P, Bogers AJJC, de Groot NMS. Circulation: Arrhythmia and Electrophysiology. 2018;11:e006720

23. Impact of Ischemic and Valvular Heart Disease on Atrial Excitation: A High-Resolution Epicardial Mapping Study.
    Mouws EMJP, Lanters EAH, Teuwen CP, **van der Does LJME**, Kik C, Knops P, Yaksh A, Bekkers JA, Bogers AJJC, de Groot NMS. J Am Heart Assoc. 2018;7: e008331.

24. Spatial Distribution of Conduction Disorders during Sinus Rhythm.
    Lanters EAH, Yaksh A, Teuwen CP, **van der Does LJME**, Kik C, Knops P, van Marion DMS, Brundel BJJM, Bogers AJJC, Allessie MA, de Groot NMS. Int J Cardiol. 2017;249:220-225.

25. Intraoperative Inducibility of Atrial Fibrillation Does Not Predict Early Postoperative Atrial Fibrillation.
    Lanters EAH, Teuwen CP, Yaksh A, Kik C, **van der Does LJME**, Mouws EMJP, Knops P, van Groningen NJ, Hokken T, Bogers AJJC, de Groot NMS. J Am Heart Assoc. 2018;7:e007879.

26. Epicardial Breakthrough Waves during Sinus Rhythm: Depiction of the Arrhythmogenic Substrate?
Mouws EMJP, Lanter EAH, Teuwen CP, **van der Does LJME**, Kik C, Knops P, Bekkers JA, Bogers AJJC, de Groot NMS. Circ Arrhythm Electrophysiol. 2017;10:e005145.

27. Quantification of the Arrhythmogenic Effects of Spontaneous Atrial Extrasystole Using High-Resolution Epicardial Mapping.
Teuwen CP, Kik C, **van der Does LJME**, Lanters EAH, Knops P, Mouws EMJP, Bogers AJJC, de Groot NMS. Circ Arrhythm Electrophysiol. 2018;11:e005745.

28. Relevance of Conduction Disorders in Bachmann's Bundle During Sinus Rhythm in Humans.
Teuwen CP, Yaksh A, Lanter EAH, Kik C, **van der Does LJME**, Knops P, Taverne YJ, van de Woestijne PC, Oei FB, Bekkers JA, Bogers AJJC, Allessie MA, de Groot NMS. Circ Arrhythm Electrophysiol. 2016;9:e003972.

29. Impact of Supraventricular Tachyarrhythmia in Patients With Inherited Cardiac Arrhythmia.
Ragab AAY, Houck CA, **van der Does LJME**, Lanters EAH, Muskens AJQM, de Groot NMS. Am J Cardiol. 2017;120:1985-1989.

30. Prediction of ventricular tachyarrhythmia in Brugada syndrome by right ventricular outflow tract conduction delay signs.
Ragab AAY, Houck CA, **van der Does LJME**, Lanters EAH, Muskens AJQM, de Groot NMS. J Cardiovasc Electrophysiol. 2018;29:998-1003.

31. Usefulness of the R-Wave Sign as a Predictor for Ventricular Tachyarrhythmia in Patients With Brugada Syndrome.
Ragab AAY, Houck CA, **van der Does LJME**, Lanters EAH, Burghouwt DE, Muskens AJQM, de Groot NMS. Am J Cardiol. 2017;120:428-434.

32. Effects of visual processing and congenital nystagmus on visually guided ocular motor behavior.
Pel JJ, **van der Does LJME**, Boot FH, de Faber T, van der Steen-Kant S, Willemsen S, van der Steen H. Developmental Medicine & Child Neurology. 2011;53:344–349.

33. Orienting Responses to Various Visual Stimuli in Children With Visual Processing Impairments or Infantile Nystagmus Syndrome.
    Pel JJ, Kooiker MJ, **van der Does LJME**, Boot FH, de Faber T, van der Steen-Kant S, van der Steen H. Journal of child neurology. 2014;29:1632-1637.

Book chapters

1. Cardiac Mapping, 5th edition. M Shenasa, G Hindricks, DJ Callans, JM Miller, ME Josephson. Hoboken (New Yersey). Wiley-Blackwell. 2019.
   Chapter 26 Atrial Fibrillation from a Unipolar, High-resolution Perspective.
   NMS de Groot, MA Allessie, **LJME van der Does**, AJJC Bogers.

Submitted

1. Detection of Endo-Epicardial Asynchrony in the Atrial Wall using One-Sided Unipolar and Bipolar Electrograms.
   van der Does LJME, Starreveld R, Kharbanda R, Knops P, Kik C, Bogers AJJC, de Groot NMS

PHD PORTFOLIO

Summary of PhD training and teaching activities

Name PhD student:	Lisette (JME) van der Does
Erasmus MC Department:	Cardiology
Research School:	Cardiovascular Research School (COEUR)
PhD period:	2014-2020
Title thesis:	Mapping of Atrial Fibrillation: Back to the Drawing Board
Promotors:	Prof. dr. N.M.S. de Groot
	Prof. dr. F. Zijlstra

1. PhD training		
	Year	**Workload (ECTS)**
General academic skills		
- Research Integrity	2015	0.3
- Basiscursus Regelgeving en Organisatie voor Klinisch Onderzoekers	2016	1.5
In-depth courses (e.g. Research school, Medical Training)		
- Research master Neuroscience	2008-2010	120
- Summer school Neuroscience	2008	1.5
Presentations		
- AAV wetenschapsmiddag, oral	2015	0.5
- American Heart Association, poster	2015	0.3
- AF symposium, poster	2016	0.3
- NVVC Unlimited, oral	2016	0.5
- ECAS, oral	2016	0.5
- Hearth Rhythm, oral	2016	0.5
- Cardiostim, poster	2017	0.3
(Inter)national conferences		
- NVVC Spoed Congress	2014	0.3
- NVVC Cardiologie in Beweging	2015	0.3
- American Heart Association	2015	1.5
- AF Symposium	2016	0.9
- NVVC Unlimited	2016	0.3
- ECAS	2016	0.9
- Heart Rhythm	2016	1.5
- ECAS	2017	0.9
- Cardiostim	2017	1.0
- NVVC recept	2017	0.3
Seminars and workshops		

- Elektrocardiografie, CVOI	2012	0.3
- Pacemaker cursus	2014	0.6
- COEUR seminar: imaging of cardiac arrhythmias	2014	0.2
- COEUR seminar: role of biomarkers in pathophysiology of AF	2015	0.4
- COEUR PhD course Arrhythmia Research	2016	1.5
- SVT Workshop Biotronik	2016	0.6
- Cardiac Arrhythmias: from biology & technology to electrophysiology	2019	0.2
Didactic skills		
- BKO Teaching the Teacher I	2015	0.6
- BKO workshop Omgaan met Groepen	2015	0.2
- BKO workshop Individuele Begeleiding	2015	0.2
Other		
- Advanced Life Support	2017	1.0
- Fundamental Critical Care Support	2017	1.0
2. Teaching activities		
	Year	**Workload (Hours/ECTS)**
Lecturing		
- Continuing Nursing Education	2016	0.5
Supervising practicals and excursions		
- VO patient met hartritmestoornissen	2015	0.1
- VO Interpretatie van het ECG	2015	0.1
- ICK	2015	0.2
Supervising Master's theses		
- Medical students	2014-2015	1.0
TOTAL		140.4

Did you **see** and un**cover** AF?

Financial support for the publication of this thesis was generously provided by:

Erasmus Medisch Centrum
Afdeling Cardiologie, Erasmus Medisch Centrum
Stichting BeroepsOpleiding Huisartsen